

**LOCAL AND REGIONAL CONTRIBUTIONS TO NITROGEN  
DIOXIDE CONCENTRATIONS IN URBAN AREAS OF THE UK**

**EMILY WESTMORELAND  
PHD**

**UNIVERSITY OF YORK  
ENVIRONMENT DEPARTMENT**

**JUNE 2008**

## ABSTRACT

This study examines in detail the NO<sub>x</sub> and NO<sub>2</sub> concentrations across the City of York using the monitoring data collected by the City of York Council's Air Quality Department. It tailors the traffic emissions contained within the York emissions inventory specific to the York area by comparing local traffic survey results with national transport statistics.

Annual mean and median NO<sub>x</sub> and NO<sub>2</sub> concentrations have fallen over the period 1999 to 2006. In all cases the NO<sub>x</sub> concentrations have fallen at a faster rate than NO<sub>2</sub>. The largest decline in NO<sub>x</sub> concentration occurred at the roadside site of Fishergate, with a 1.94 ppb ( $p > 0.01$ ) reduction per year for the period 1999 to 2006. The NO<sub>2</sub> concentrations at this site fell by 0.14 ppb a year (trend not significant).

Generalised additive models consistently identified background NO<sub>x</sub>/NO<sub>2</sub> as being important in explaining the variability in observed NO<sub>x</sub> and NO<sub>2</sub> concentrations (explaining around 33 % to 62 % of the total variability in NO<sub>2</sub> concentrations depending on site). Such evidence suggests that a large proportion of the NO<sub>x</sub> and NO<sub>2</sub> concentrations at York are beyond the management control of the City of York Council and instead are a consequence of air pollution from other areas of the UK.

Examination of the trends in NO<sub>x</sub> and NO<sub>2</sub> concentrations revealed a departure in agreement between modelled (ADMS-Urban) and observed concentrations towards the end of the study years. This departure is most likely a consequence of observed emissions differing from modelled.

This work provides a useful contribution to the scientific understanding of NO<sub>x</sub> and NO<sub>2</sub> concentrations in smaller provincial cities in the UK since hitherto the majority of detailed studies have focused on the larger urban areas, such as London.



# TABLE OF CONTENTS

1.	Introduction .....	12
	General introduction .....	12
	Focus on NO <sub>2</sub> .....	12
	Focus on York.....	13
	Research objectives.....	14
2.	Literature review .....	17
	2.1. Historical context .....	17
	2.2. Current legislation.....	18
	2.3. Troposphere: structure and nature.....	21
	2.4. NO <sub>x</sub> chemistry .....	26
	2.5. Health effects of air pollution .....	36
	2.6. Chapter summary .....	38
3.	Experimental .....	39
	3.1. Introduction.....	39
	3.2. Ambient NO <sub>x</sub> measurements .....	39
	3.3. Ambient O <sub>3</sub> measurement .....	40
	3.4. Air quality monitoring stations in York.....	40
	3.5. Meteorological data.....	53
4.	ADMS-Urban validation.....	54
	4.1. Background and introduction.....	54
	4.2. Emissions inventory and emissions calculations .....	54
	4.3. ADMS-Urban.....	61
	4.4. Aims.....	62
	4.5. Update of traffic emissions for the York area.....	62
	4.6. ADMS-Urban input sensitivity .....	80
	4.8. Chapter summary .....	88
5.	NO <sub>x</sub> and NO <sub>2</sub> in York.....	91
	5.1. Chapter preview .....	91
	5.2. Air Quality Objectives .....	91
	5.3. Spatial trends.....	93
	5.4. Temporal trends .....	101
	5.5. Chapter summary .....	132
6.	Long-term generalised additive modelling analysis.....	134
	6.1. Chapter preview .....	134
	6.2. Introduction and literature review.....	134
	6.3. Aims.....	137
	6.4. Data.....	137
	6.5. Statistical model methodology.....	143

6.6. Results.....	150
6.7. Discussion and conclusion.....	172
6.8. Chapter summary.....	173
7. A case study: Comparison of ADMS-Urban and generalised additive modelling.....	175
7.1. Chapter preview.....	175
7.2. Introduction.....	175
7.3. Methodology.....	175
7.4. Results and discussion.....	179
7.5. Chapter summary.....	186
8. Conclusions.....	189
9. References.....	195

## LIST OF FIGURES

<b>Figure 1:</b> The relationship between wind speed and NO <sub>2</sub> concentration..	22
<b>Figure 2:</b> Ground level NO <sub>x</sub> predictions for an elevated emission source for both unstable (blue line) and stable (green line) boundary layer conditions.....	25
<b>Figure 3:</b> Ground level NO <sub>x</sub> predictions for a ground level emission source for both unstable (blue line) and stable (green line) boundary layer conditions. ....	25
<b>Figure 4:</b> The partitioning of NO <sub>x</sub> in different environments.....	33
<b>Figure 5:</b> Mean diurnal profile for NO and NO <sub>2</sub> concentrations from a roadside site in York city centre. ....	34
<b>Figure 6:</b> Mean diurnal profile for NO, NO <sub>2</sub> and O <sub>3</sub> concentrations during the SOAPEX-2 campaign at the Cape Grim Baseline Air Pollution Station in north-western Tasmania, Australia in 1999. ....	35
<b>Figure 7:</b> A schematic of atmospheric chemistry in urban environments..	36
<b>Figure 8:</b> The chemiluminescence analyser sites around the City of York. Bootham, City Centre, Fishergate Rawcliffe and Dunnington are the original five sites.....	41
<b>Figure 9:</b> Location of Bootham monitoring station.....	45
<b>Figure 10:</b> Location of City Centre monitoring station.....	46
<b>Figure 11:</b> Location of Dunnington monitoring station. ....	47
<b>Figure 12:</b> Location of Fishergate monitoring station.....	48
<b>Figure 13:</b> Location of Gillygate monitoring station.....	49
<b>Figure 14:</b> Location of Holgate Road monitoring station. ....	50
<b>Figure 15:</b> Location of Lawrence Street monitoring station. ....	51
<b>Figure 16:</b> Location of Nunnery Lane monitoring station. ....	52
<b>Figure 17:</b> A schematic of the various input and reference data needed when calculating emissions from road sources.....	59
<b>Figure 18:</b> Illustration of emission source types in York..	60
<b>Figure 19:</b> Breakdown of vehicle counts into the different survey periods by survey locations	66



**Figure 20:** Breakdown of engine type (petrol/diesel) for each vehicle classification. .... 68

**Figure 21:** Percentage breakdown of rigid and articulated HGVs into the various categories contained with the emissions factors. .... 70

**Figure 22:** Percentage breakdown of cars into the various categories used by the model to calculate traffic emissions. .... 71

**Figure 23:** A schematic of the York road network..... 73

**Figure 24:** Annual mean NO<sub>2</sub> predictions for the five receptor sites as a result of varying the average speed of all vehicles An average speed is assumed in the model for each road link. .... 77

**Figure 25:** Average speeds recorded at the five specific sites. Error bars are standard deviations. .... 78

**Figure 26:** ADMS-Urban predicted annual mean NO<sub>2</sub> concentration for the years 2002 to 2006 for the five different study sites. .... 84

**Figure 27:** ADMS-Urban predicted annual mean NO<sub>2</sub> concentrations and 95% confidence intervals for the for the five different study sites..... 87

**Figure 28:** ADMS-Urban predicted annual mean NO<sub>x</sub> concentrations and 95% confidence intervals for the for the five different study sites..... 87

**Figure 29:** Mean hourly ratios of NO<sub>x</sub> (i), NO<sub>2</sub> (ii) and the NO<sub>2</sub>: NO<sub>x</sub> ratio (iii) for each hour of the day. .... 96

**Figure 30:** Mean hourly traffic counts from the automatic traffic counter for the inbound lane of traffic at Gillygate..... 97

**Figure 31:** Diurnal profile of NO<sub>x</sub> and NO<sub>2</sub> concentration for the roadside monitoring site at Marlybone Road, London (a); the suburban site at Hillingdon, London (b) and Haringey, London (c). .... 98

**Figure 32:** Mean NO<sub>x</sub> (a) and NO<sub>2</sub> (b) concentrations for the two-year period (2004 to 2005) for the sites of Dunnington, Bootham and City Centre, York..... 99

**Figure 33:** Mean NO<sub>x</sub> (a) and NO<sub>2</sub> (b) concentrations for the urban background site of Bootham and the various roadside sites. .... 100

**Figure 34:** Annual mean NO<sub>x</sub> (a) and NO<sub>2</sub> (b) concentration for the Dunnington, Bootham, City Centre and Fishergate sites (from left to right)..... 105

**Figure 35:** Slope coefficient with 95% confidence intervals for long-term monitoring sites of a) Bootham NO<sub>2</sub>, b) Bootham NO<sub>x</sub>, c) City centre NO<sub>2</sub>, d) City Centre NO<sub>x</sub>,..... 108

**Figure 36:** Annual maximum NO<sub>x</sub> concentration at City Centre monitoring site for the period 1999 to 2006. .... 110

**Figure 37:** Annual mean NO<sub>2</sub>: NO<sub>x</sub> ratio for the sites Dunnington, Bootham, City Centre and Fishergate (from left to right). .... 112

**Figure 38:** Annual mean O<sub>3</sub> concentrations observed at Dunnington background site..... 114

**Figure 39:** NO<sub>2</sub> (a) and NO<sub>x</sub> (b) slope coefficients and 95% confidence intervals for the other cities chosen for inclusion within this study..... 118



<b>Figure 40:</b> Estimated annual change in NO <sub>x</sub> for the period 1999 to 2006 for the cities included in Table 29.....	119
<b>Figure 41:</b> Estimated annual change in NO <sub>x</sub> for the period 1999 to 2006 for the Cities included in Table 29.....	120
<b>Figure 42:</b> Scatterplot of the estimated NO <sub>x</sub> and NO <sub>2</sub> linear regression slope coefficient (a) and annual percentage change (b) for the various sites (includes York sites).....	123
<b>Figure 43:</b> Monthly mean NO <sub>2</sub> concentrations for Bootham (a), Dunnington (b), City Centre (c) and Fishergate (d) for the period 1999 to 2006. ....	125
<b>Figure 44:</b> Monthly mean NO <sub>x</sub> concentrations for Bootham (a), Dunnington (b), City Centre (c) and Fishergate (d) for the period 1999 to 2006. ....	126
<b>Figure 45:</b> Monthly mean O <sub>3</sub> concentrations for Dunnington for the period 1999 to 2006....	126
<b>Figure 46:</b> The calculated slope coefficients for the change in monthly mean NO <sub>2</sub> concentrations for the period 1999 to 2006. Plot a) is for Bootham, b) Dunnington, c) City Centre and d) for Fishergate.....	127
<b>Figure 47:</b> The calculated slope coefficients for the change in monthly mean NO <sub>x</sub> concentrations for the period 1999 to 2006. Plot a) is for Bootham, b) Dunnington, c) City Centre and d) for Fishergate.....	128
<b>Figure 48:</b> Estimated O <sub>3</sub> slope coefficients for each month of the year for Dunnington (1999 to 2006).....	130
<b>Figure 49:</b> Time series plots of the various meteorological variables recorded at the Meteorological Office station at Church Fenton. d) wind direction (degrees); e) precipitation (mm); cloud cover (oktas) .....	139
<b>Figure 50:</b> Time series of 24-h mean NO <sub>x</sub> concentrations at the monitoring sites in York (a) Bootham, (b) City Centre, (c) Fishergate, (d) Gillygate, (e) Holgate, (f) Lawrence, (g) Nunnery. ....	141
<b>Figure 51:</b> Time series of 24-h mean NO <sub>2</sub> concentrations at the monitoring sites in York (a) Bootham, (b) City Centre, (c) Fishergate, (d) Gillygate, (e) Holgate, (f) Lawrence, (g) Nunnery. ....	142
<b>Figure 52:</b> Fitted smooth curve for NO <sub>x</sub> and temperature at the background site of Dunnington. ....	145
<b>Figure 53:</b> Smooth plots of NO <sub>x</sub> concentration as a function of time (days since monitoring began), for the NO <sub>x</sub> concentrations at Bootham urban background monitoring site. ....	147
<b>Figure 54:</b> Fitted components of the Fishergate NO <sub>2</sub> model:.....	155
<b>Figure 55:</b> Perspective plot (a) and polar plot (b) of the interactive wind speed – wind direction smooth curve for the Fishergate NO <sub>2</sub> concentrations. ....	156
<b>Figure 56:</b> Map of Fishergate monitoring site.....	157
<b>Figure 57:</b> ‘u,v’ response curves for observed NO <sub>2</sub> concentrations for each of the monitoring sites in York.....	159



**Figure 58:** Fitted  $s(\text{year})$  smooth curves for  $\text{NO}_2$  concentrations for the three long-term monitoring sites to the time variable (year). ..... 162

**Figure 59:** Fitted  $s(\text{year})$  smooth curves for  $\text{NO}_x$  concentrations for the three long-term monitoring sites to the time variable (year)..... 163

**Figure 60:** Regression diagnostics for the  $\text{NO}_x$  GAM at the Fishergate monitoring site..... 165

**Figure 61:** Fitted components of the ADMS-Urban  $\text{NO}_2$  concentrations..... 168

**Figure 62:** ‘u,v’ response curves for  $\text{NO}_2$  concentrations predicted with ADMS-Urban for each of the monitoring sites in York..... 170

**Figure 63:** Response curves for monitored (a) and modelled (b)  $\text{NO}_2$  concentrations at Fishergate. .... 171

**Figure 64:** Fitted  $s(\text{year})$  smooth curves for monitored (a) and ADMS-Urban predicted (b)  $\text{NO}_x$  concentrations for the site of Fishergate..... 172

**Figure 65:** Smoothed bivariate wind-pollution roses for measured and predicted  $\text{NO}_x$  and  $\text{NO}_2$  concentrations at Gillygate. .... 180

**Figure 66:** Diurnal profile of  $\text{NO}_x$  (a) and  $\text{NO}_2$  (b) concentrations for wind speeds greater than  $3 \text{ m s}^{-1}$  and between  $0^\circ$  and  $50^\circ$ ..... 181

**Figure 67:** Bivariate wind-pollution rose for measured  $\text{NO}_x$  concentrations at the Marylebone Road, London.. .... 182

**Figure 68:** Observed 24-hr mean (a)  $\text{NO}_2$  and (b)  $\text{NO}_x$  concentrations recorded at Gillygate for the year 2005.. .... 188

### LIST OF TABLES

**Table 1:** The national air quality objectives for  $\text{NO}_2$ ..... 20

**Table 2:** Typical concentrations of  $\text{NO}_x$ ,  $\text{NO}_2$  and  $\text{O}_3$  in clean and polluted environments. .... 32

**Table 3:** The air pollution monitoring site categories and their descriptions. (AQEG, 2004).... 42

**Table 4:** Descriptions of the eight permanent air quality monitoring stations around the City of York. .... 43

**Table 5:** The status of air quality monitoring sites in York over the period 1999 to 2007..... 53

**Table 6:** Emission factors for  $\text{NO}_x$  for the various vehicle sub-categories for petrol cars travelling at 40km/hr from the NAEI. .... 57

**Table 7:** The LAEI 11-category vehicle classification system..... 58

**Table 8:** Breakdown of total emissions (tonnes/year) of the various sources included in the emissions inventory for York. .... 61

**Table 9:** Description and location of the six traffic survey sites. .... 64

**Table 10:** Dates of the detailed traffic surveys ..... 65

**Table 11:** Breakdown (%) of the vehicle count into the 11-category-LAEI-system..... 67

**Table 12:** EURO standards and dates of introduction ..... 69

**Table 13:**Background concentrations in ppb (annual means).  $\text{NO}_x$ ,  $\text{NO}_2$  and  $\text{SO}_2$  concentrations from Bootham,  $\text{O}_3$  from Dunnington..... 73



<b>Table 14:</b> Meteorological data (annual mean values) recorded by the UK Meteorological Office at Church Fenton for 2005 (latitude 53.8, longitude-1.2).....	74
<b>Table 15:</b> Values of the various ADMS-Urban input requirements for the base case model scenario.....	75
<b>Table 16:</b> Base case emissions (tonnes for the year 2005) and annual mean predictions (2005) of NO <sub>x</sub> and NO <sub>2</sub> .....	76
<b>Table 17:</b> Estimated traffic emissions (tonnes for the year 2005) and annual mean predictions (2005) of NO <sub>x</sub> and NO <sub>2</sub> for the model scenario using the York specific transport data to calculate traffic emissions. ....	76
<b>Table 18:</b> Annual mean predictions (2005) of NO <sub>x</sub> and NO <sub>2</sub> for the model scenario using the new average speeds recorded from traffic surveys. ....	79
<b>Table 19:</b> Emissions (tonnes per 2005) and annual mean predictions (2005) of NO <sub>x</sub> and NO <sub>2</sub> concentration for the new traffic emissions (York tailored) scenario.....	80
<b>Table 20:</b> Annual mean (2005) NO <sub>2</sub> and NO <sub>x</sub> concentrations for the various sensitivity scenarios. ....	83
<b>Table 21:</b> Summary (annual mean and maximum) of meteorological data for the various years	85
<b>Table 22:</b> Observed and predicted annual mean (2005) NO <sub>2</sub> and NO <sub>x</sub> concentrations for the five technical breach sites in York.....	89
<b>Table 23:</b> Annual mean NO <sub>2</sub> concentration recorded at the various monitoring sites in the City of York.....	92
<b>Table 24:</b> The 18 <sup>th</sup> highest hourly NO <sub>2</sub> concentration for each calendar year for the various monitoring sites in the urban area of York. ....	92
<b>Table 25:</b> Mean concentrations of NO <sub>x</sub> , NO <sub>2</sub> and the NO <sub>2</sub> : NO <sub>x</sub> ratio recorded at the various monitoring sites in York for the period 1/1/2004 to 31/12/2005; percentage data captures for the air quality data, plus AADT estimate from the emission inventory for York .....	94
<b>Table 26:</b> Descriptive statistics for NO <sub>x</sub> (a) and NO <sub>2</sub> (b) concentrations (ppb) for the periods 1999 to 2006 and 2005 to 2006 for sites with long-term concentration records. ....	101
<b>Table 27:</b> Estimated annual change in NO <sub>x</sub> and NO <sub>2</sub> concentrations for the period 1999 to 2006 for different descriptive statistics.....	106
<b>Table 28:</b> Estimated slope coefficient for the change in NO <sub>2</sub> : NO <sub>x</sub> ratio over the period 1999-2006. ....	111
<b>Table 29:</b> Estimated trend in annual mean NO <sub>x</sub> and NO <sub>2</sub> concentration for a range of monitoring sites across the UK for the years 1999 to 2006.. ....	116
<b>Table 30:</b> Stepwise selection procedure for the development of the Fishergate NO <sub>x</sub> GAM....	149
<b>Table 31:</b> Pearson's correlation for the various covariates considered for inclusion in the GAMs. ....	151
<b>Table 32:</b> Terms included in the NO <sub>x</sub> GAMs for the seven monitoring sites.....	152
<b>Table 33:</b> Terms included in the NO <sub>2</sub> GAMs for the seven monitoring sites.....	152



**Table 34:** The contributions to percentage deviance explained for the various explanatory variables calculated by removing the term of interest from the fully fitted model and comparing the difference in explained deviance.. ..... 154

**Table 35:** Relative contributions of the various explanatory variables included in the final fitted models..... 167

**Table 36:** The contributions to percentage deviance explained for GAMs containing solely the background pollutant data as an explanatory term. .... 174

**Table 37:** Measured and predicted NO<sub>x</sub> and NO<sub>2</sub> concentrations (ppb) at Gillygate for 2005 and the root mean square error of the hourly deviance ..... 179

**Table 38:** Annual mean predictions (2005) of NO<sub>x</sub> and NO<sub>2</sub> concentrations for various scenarios. .... 183

### LIST OF REACTIONS

$\text{N}_2 + \text{O}_2 \rightarrow 2\text{NO}$                     1 ..... 26

$2\text{NO} + \text{O}_2 \rightarrow 2\text{NO}_2$                 2 ..... 27

$\text{NO} + \text{O}_3 \rightarrow \text{NO}_2 + \text{O}_2$             3 ..... 27

$\text{NO}_2 + h\nu \rightarrow \text{NO} + \text{O}({}^3\text{P})$             4 ..... 27

$\text{O}({}^3\text{P}) + \text{O}_2 + \text{M} \rightarrow \text{O}_3 + \text{M}$             5 ..... 27

$\text{O}_3 + h\nu (\lambda < 320 \text{ nm}) \rightarrow \text{O}({}^1\text{D}) + \text{O}_2$             6 ..... 28

$\text{O}({}^1\text{D}) + \text{H}_2\text{O} \rightarrow 2\text{OH}$             7 ..... 28

$\text{HONO} + h\nu (\lambda < 370 \text{ nm}) \rightarrow \text{OH} + \text{NO}$             8 ..... 28

$\text{HOOH} + h\nu (\lambda < 370 \text{ nm}) \rightarrow 2\text{OH}$             9 ..... 28

$\text{CH}_4 + \text{OH} \rightarrow \text{CH}_3. + \text{H}_2\text{O}$             10 ..... 29

$\text{CH}_3. + \text{O}_2 \rightarrow \text{CH}_3\text{O}_2$             11 ..... 29

$\text{CH}_3\text{O}_2 + \text{NO} \rightarrow \text{CH}_3\text{O} + \text{NO}_2^*$             12 ..... 29

$\text{CH}_3\text{O} + \text{O}_2 \rightarrow \text{HO}_2 + \text{HCHO}$             13 ..... 29

$\text{HCHO} + h\nu + (\text{O}_2) \rightarrow 2\text{HO}_2 + \text{CO}$             14 ..... 29

$\text{HCHO} + \text{OH} + (\text{O}_2) \rightarrow \text{HO}_2 + \text{CO} + \text{H}_2\text{O}$             15 ..... 29

$\text{HO}_2 + \text{NO} \rightarrow \text{OH} + \text{NO}_2^*$             16 ..... 29

$\text{NO}_2 + h\nu \rightarrow \text{NO} + \text{O}({}^3\text{P})$             17 ..... 29

$\text{O}({}^3\text{P}) + \text{O}_2 + \text{M} \rightarrow \text{O}_3 + \text{M}$             18 ..... 29

$\text{NO}_2 + \text{O}_3 \rightarrow \text{NO}_3 + \text{O}_2$             19 ..... 30

$\text{NO}_3 + \text{NO}_2 + \text{M} \leftrightarrow \text{N}_2\text{O}_5 + \text{M}$             20 ..... 30

$\text{HO}_2 + \text{NO}_3 \rightarrow \text{OH} + \text{NO}_2 + \text{O}_2$             21 ..... 30

$\text{OH} + \text{NO}_2 + \text{M} \rightarrow \text{HNO}_3 + \text{M}$             22 ..... 31

$\text{N}_2\text{O}_5 + \text{H}_2\text{O} \rightarrow 2 \text{HNO}_3$             23 ..... 31

$\text{NO} + \text{OH} + \text{M} \rightarrow \text{HONO} + \text{M}$             24 ..... 31

HONO + $h\nu \rightarrow$ OH + NO	25 .....	31
OH + O <sub>3</sub> $\rightarrow$ HO <sub>2</sub> + O <sub>2</sub>	26 .....	34
HO <sub>2</sub> + O <sub>3</sub> $\rightarrow$ 2O <sub>2</sub> + OH	27 .....	34
HO <sub>2</sub> + HO <sub>2</sub> $\rightarrow$ H <sub>2</sub> O <sub>2</sub> + O <sub>2</sub>	28 .....	35
NO + O <sub>3</sub> $\rightarrow$ NO <sub>2</sub> * + O <sub>2</sub>	29 .....	39
NO <sub>2</sub> * $\rightarrow$ NO <sub>2</sub> + $h\nu$	30 .....	39
ROC + $h\nu \rightarrow$ RP + ROC	31 .....	81
RP + NO $\rightarrow$ NO <sub>2</sub>	32 .....	81
NO <sub>2</sub> + $h\nu \rightarrow$ NO + O <sub>3</sub>	33 .....	81
NO + O <sub>3</sub> $\rightarrow$ NO <sub>2</sub>	34 .....	81
RP + RP $\rightarrow$ RP	35 .....	81
RP + NO <sub>2</sub> $\rightarrow$ SGN	36 .....	81
RP + NO <sub>2</sub> $\rightarrow$ SNGN	37 .....	81
2NO + O <sub>2</sub> $\rightarrow$ 2NO <sub>2</sub>	38 .....	81
NO + O <sub>3</sub> $\rightarrow$ NO <sub>2</sub> + O <sub>2</sub>	39 .....	94

## ABBREVIATIONS

PPB    Parts per billion (1,000,000,000)  
PPT    Parts per trillion

## DECLARATION

I declare that all the work contained within this thesis is my own unless otherwise stated.

The work of Chapter 7 has been published in the scientific journal Atmospheric Environment, volume 42, for which I was the principal author.

## ACKNOWLEDGEMENTS

Firstly I would like to thank my supervisor Nicola Carslaw for her constant help and support throughout my undergraduate and doctorate degrees. She managed to put up with my regular crises of confidence and despite her extremely busy life she always made time for me. Not many supervisors would share their office with one of their students!

The financial support of the Natural Environment Research Council (NERC) and the City of York Council was greatly appreciated. The CASE-studentship allowed my PhD to have a more practical edge and this helped enormously when applying for jobs.

I would also like to thank the members of the Air Quality Section at the City of York Council for being friendly and approachable throughout my four years' acquaintance with them. Firstly, Elizabeth Bates was a great help during my doctorate study. It was from her that the project came about in the first place and for this I am extremely grateful. Secondly, my thanks go to Andrew Gillah for putting up with endless emails. He was a real help with the ADMS-Urban modelling side of my project. Last but not least, I would also like to thank Chris Parkinson for taking me out on site visits. I have also not forgotten all the help Chris gave me and all the driving he did for me during my undergraduate dissertation fieldwork.

David Carslaw was also extremely kind in giving his comments, suggestions and R codes for use in Chapter 7 of this thesis. The guidance and enthusiasm provided by Mark Bulling over the three years was also greatly appreciated.

I would also like to thank everyone at the Environment Department for making my time there enjoyable. I made good friends there, and for this I think the stress of three years of PhD study was definitely worth it.

Finally, I thank my family for their constant love and support.



# 1. Introduction

## General introduction

Public attitudes to air quality have changed dramatically over the past century. Air pollution, once unthinkingly accepted as a necessary by-product of urban expansion and economic development ('Where there's muck, there's brass'), has now come to be understood as having a direct impact on human health as well as a range of ecosystems. Even though air quality issues have become increasingly important in the UK, Europe and the rest of the world, and a large improvement in air quality has been achieved (i.e. the eradication of urban smogs (smoke + fog) following the clean air act of 1957), it is by no means the case that the problem has been solved.

The majority of urban air pollution is nowadays associated with road traffic. During the period from 1950 to 2000, the number of vehicles registered in Britain increased by around 24 million, or 600 % (NSCA, 2002). Although technological improvements have helped to decrease total road traffic emissions by 38 % since 1989 (AQEG, 2004), the rate of increase in vehicles now outstrips the population growth rate (Fenger, 1999), and the current issues regarding urban air quality look set to remain.

Moreover, in addition to the serious health implications and costs (increased hospital admissions, extra medication and working days lost), air pollution is also responsible for less quantifiable damage to the environment, such as acidification of ecosystems and damage to crops and forests (DEFRA, 2006).

In recent times, the topic of climate change has pushed other air quality issues aside, with the attention becoming increasingly focused on the rising levels of carbon dioxide (CO<sub>2</sub>) in the atmosphere. However, with eighty percent of the UK's population currently living and/or working in urban areas and the associated public health implications of poor air quality, adequate attention must be paid to the problem of urban air quality.

## Focus on NO<sub>2</sub>

Nitrogen dioxide (NO<sub>2</sub>) poses a direct threat to the health of many people in the UK and a range of ecosystems. It is therefore important that appropriate and effective control strategies are aimed at reducing the concentrations of NO<sub>2</sub> in those areas where people are exposed on a regular basis. Indeed, NO<sub>2</sub> is included in the National Air Quality Strategy with objectives covering this pollutant on both a short and long term exposure basis. It has also been recognised by NCAS as one of three airborne pollutants where future research should be focused.

Over the period from 1990 to 2000, UK emissions of nitrogen oxides (NO<sub>x</sub> (NO<sub>x</sub> = NO + NO<sub>2</sub>)) have fallen by roughly 37 % (AQEG, 2004). This reduction is mainly attributable to improvements in emission abatement technologies for road transport and industry (i.e. catalytic converters in vehicles, for example). It was thought that a reduction in NO<sub>x</sub> would result in corresponding reductions in ambient NO<sub>2</sub> concentrations. However, over the past decade the



reduction in NO<sub>2</sub> concentration has not occurred as quickly as expected. Indeed, the ratio of NO<sub>2</sub>: NO<sub>x</sub> concentrations has increased at many urban monitoring sites (AQEG, 2004; AQEG, 2006).

NO<sub>2</sub> is currently the biggest single cause of air quality problems in urban areas of the UK; a total of 92 % of Air Quality Management Areas (AQMAs) have been declared by local authorities as a result of this pollutant exceeding the annual guideline concentration (Carslaw, 2005). Therefore out of all the air pollutants included in domestic air quality legislation, NO<sub>2</sub> is posing the greatest challenge to public health in terms of exceeding the national air quality objectives. Additionally, more recent monitoring data from the London area have suggested that the hourly NO<sub>2</sub> target in 2007 will be breached at some urban roadside and background sites across the capital. It is likely, therefore, that both the annual and hourly NO<sub>2</sub> objectives will continue to pose a significant air quality challenge in future years.

### **Focus on York**

The City of York is located in North Yorkshire, England. It sits at the confluence of the Rivers Ouse and Foss and is contained within an area known as the Vale of York. York is not a particularly large city either in terms of population (181 000) or land coverage (272 km<sup>2</sup>), though it is the largest urban area inside the Vale of York. There are however a number of large cities located to the south west of York, i.e. Leeds (population 726 400) and Bradford (population 485 000) and to the east, i.e. Hull (population 249 100) (National Statistics online).

Traditionally, the flat arable land of the Vale of York allowed a successful agricultural economy to develop. Over time agriculture gave way to industry, with the establishment of several large firms such as Rowntrees, Nestlé and Terrys in the area. The economy of York today however, is heavily dominated by the service sector (both tourism and other service-related industries). In 2003 around 76 % of York's economy was attributable to the service sector, just under 24 % to industry and less than 1% to agriculture (<http://www.statistics.gov.uk>).

Despite York being a relatively small city, a substantial area of the city centre has been identified as having NO<sub>2</sub> concentrations in excess of the annual objective. Indeed a large area of the city centre was declared an AQMA in 2002 after a series of monitoring and modelling work carried out by the City of York Council (CYC) and lengthy public consultations. Traffic is a major contributor to the high NO<sub>2</sub> concentrations seen in the City of York. Indeed source apportionment studies have indicated that as much as 60 % of the ambient NO<sub>x</sub> in the City of York is a result of traffic emissions. However, little is known about the various pathways by which this pollutant becomes elevated in the city centre.

York is an interesting study area because it has a dense collection of roads that become heavily congested at peak periods. The congestion commonly found on the inner ring road is to some extent a result of the old medieval streets not being able to cope with increasing traffic demands. Further congestion problems arise as a result of bottlenecks around the three bridges crossing the River Ouse. Additionally, the narrowness of some streets in York (canyonisation)



enables the accumulation of pollutants since ‘normal’ dispersion levels are suppressed. One street in particular (Gillygate, located to the north of the city) has already been the subject of investigation in the two part study by Boddy et al. (2005a, 2005b), where the influence of background winds and traffic characteristics were used to explain the spatial variation in carbon monoxide concentrations. The CYC also records the hourly traffic counts of certain streets around the city; such information is useful when modelling air quality in the city.

The CYC has established a relatively high number of air quality monitoring sites throughout the city. The exact location of the monitoring sites will be detailed in Chapter 3, but include five roadside, one urban centre, one urban background and one background site. All these sites contain NO<sub>x</sub> monitors, however, three also jointly record PM<sub>10</sub> concentrations. The relatively high density of monitoring sites in York again makes York an interesting city in which to study air quality.

The CYC has established a number of traffic and air quality control strategies since the declaration of the AQMA. Indeed, the latest Air Quality Action Plan (AQAP) is now combined with the Local Transport Plan (LTP) to allow for a more coherent approach in reducing traffic and its associated negative impacts. Several existing strategies include: the control of traffic light timings (SCOOT), variable messenger boards indicating car parking availability, Park and Ride systems and the promotion of cycling, for example.

The majority of urban air quality research to date has focused on large urban areas, such as London. It is therefore desirable, and novel, to investigate urban air quality in smaller, provincial, cities around the UK. The combination of air quality and traffic monitors, coupled with the proactive nature of the CYC (in terms of abatement strategies), therefore make the City of York a suitable urban area in which to study urban air quality.

## **Research objectives**

It has long been known that air pollution is not a local issue and thus it is impossible for any local authority to tackle air pollution effectively without cooperation from neighbouring authorities. However, given this interconnectedness, one would think neighbouring authorities and governments would work collectively towards the solution. However, it is in fact the opposite that occurs since it is difficult to establish blanket policies that are relevant for all areas. For this reason, the local air quality management (LAQM) process, (Chapter 2, section 2.2.2) was established in the hope that smaller, more localised, management would foster novel and locally relevant solutions.

This thesis is essentially borne out of the LAQM process, since the CYC is keen to establish a greater understanding of air quality within their region. The successive Chapters will investigate NO<sub>x</sub> and NO<sub>2</sub> concentrations in the city, analysing spatial and temporal trends, in the hope that more comprehensive management strategies can be implemented to tackle the air quality issue in the historic City of York.



The specific objectives of this dissertation are:

1. To highlight temporal trends in  $\text{NO}_x$  and  $\text{NO}_2$  concentrations in and around York using the existing monitoring framework established by the CYC
2. To develop new statistical models that can reproduce  $\text{NO}_x$  and  $\text{NO}_2$  concentrations in the City of York.
3. To investigate the sensitivity of the dispersion model, ADMS-Urban, to its various input parameters, thus maximising the potential of this model in terms of understanding air pollution in the City of York.
4. To compare and contrast ADMS-Urban with the statistical models developed as part of the second objective and to use the various modelling techniques to reproduce and analyse the long-term temporal trends in the  $\text{NO}_x$  and  $\text{NO}_2$  concentrations recorded at the various monitoring sites in and around York.
5. To implement the statistical techniques so that a more detailed understanding of the important processes that control/influence the ambient  $\text{NO}_x$  and  $\text{NO}_2$  concentrations can be gained. Such information is important for the CYC in the development of localised air quality management strategies.

The structure of this thesis is as follows:

**Chapter 2.** This Chapter will provide an introduction and review of the relevant literature for this dissertation. It will begin with a brief overview of the history of air pollution and past air quality events. Next, a review of the relevant air quality legislation will set out the requirements currently faced by local authorities. This Chapter also provides an introduction to  $\text{NO}_x$  chemistry for both urban and clean environments, and also the influence of meteorology on air quality. Finally, the Chapter concludes by examining the health implications of  $\text{NO}_x$  and  $\text{NO}_2$ .

**Chapter 3:** This Chapter sets out the techniques used to make routine  $\text{NO}_x$ ,  $\text{NO}_2$  and  $\text{O}_3$  measurements, along with site descriptions for each site included in the study.

**Chapter 4:** This Chapter investigates the sensitivity of the dispersion model, ADMS-Urban, in terms of the input parameters, tailoring the model for York. The results of the sensitivity studies are compared against real time measurements made at the various monitoring sites across the city.

**Chapter 5:** This Chapter provides an overview of air quality in York between 1999 – 2006. Air quality data, along with meteorological and traffic data, from the various permanent stations have been analysed, providing an overview of temporal trends in air quality across the City of York.

**Chapter 6:** Chapter 6 investigates further the temporal trends in  $\text{NO}_x$  and  $\text{NO}_2$  concentrations across York. The statistical framework of generalised additive models (GAMs) are used to analyse non-linear, long-term fluctuations in ambient  $\text{NO}_x$  and  $\text{NO}_2$  concentrations at the various monitoring sites. The statistical models have also been compared to predictions made with ADMS-Urban.

**Chapter 7:** This Chapter focuses specifically on the  $\text{NO}_x$  and  $\text{NO}_2$  concentrations recorded in the canyonised street of Gillygate. Generalised additive modelling and ADMS-Urban are used to reproduce the ambient  $\text{NO}_x$  and  $\text{NO}_2$  concentrations at the monitoring station for a single year of measurement. The model predictions from the two modelling techniques are compared and contrasted.

**Chapter 8:** This Chapter considers the wider implications of this study and suggests areas of further research.



## 2. Literature review

### 2.1. Historical context

The problem of air pollution is not new and has existed in one form or another from the earliest days of civilisation e.g. as soon as man used fire to cook (Brimblecombe, 1988). However, it has only been relatively recently that the air pollution problem has been recognised and attempts have been made to control emissions.

There are a number of early documented cases of air quality complaints; for example in 1273 complaints led to a royal proclamation banning coal burning in London as it was seen as damaging to health. Much later in 1661 John Evelyn published '*Fumifugium or the smoake of London dissipated: Practical schemes to reduce smoke/air over London*' (NSCA, 1999).

Interestingly, and of particular reference to this study, there are early references to air pollution in York. For example, a local poet who, in 1778, had been arrested and was held in York Castle prison wrote about how the emissions from the adjacent Castle Mills were '*a punishment to which the unfortunate inhabitants of this place are doomed without the authority of judge or jury*' (Brimblecombe and Bowler, 2002). There are also a number of documented cases regarding the effect that air pollution was having on the exterior of York Minister. It was noted that many of the ornaments and figures were so badly damaged that they were either in danger of falling off or had become shapeless (Brimblecombe and Bowler, 2002).

The first national attempts at controlling air pollution occurred during the onset of the industrial revolution where the co-location of industry and housing meant the public could clearly see, and feel, the effects of air pollution. The 'Alkalis Act' (1863), later updated in 1874, was among the first national attempts at controlling emissions (NSCA, 2002). These Acts were passed to control hydrogen chloride emissions from alkali works that produced sodium carbonate from salt (Greater London Authority, 2002). The Acts required a 95 % reduction in the offensive emissions and the use of 'best practical means', a principle that is still in use today (NSCA, 1999).

Some time later, air quality legislation became focused on the control of smoke and particulates from combustion processes. The increased use of coal combined with calm stagnant conditions, led to the formation of smog, which soon became a London Characteristic or 'Particular' (NSCA, 2002). The sulphur contained in coal is converted to sulphur dioxide ( $\text{SO}_2$ ) following combustion and then to sulphuric acid ( $\text{H}_2\text{SO}_4$ ) through a series of chemical reactions (Carslaw and Carslaw, 2001). These 'peasouper' smogs were commonplace across the UK and Europe and were immortalised in fiction by authors such as Sir Arthur Conan Doyle in Sherlock Holmes (NSCA, 2002) and also in paintings by artists such as Monet in the 1904 painting 'Sun breaking through the fog'.

One air pollution event in particular, the infamous smog of 1952, caused over 4700 deaths (Department of Health, 1997) and triggered a radical rethink in air pollution control. This



event (December 5<sup>th</sup> – 8<sup>th</sup>) occurred as a direct result of domestic and industrial emissions coupled with stagnant meteorological conditions (low wind speeds and an inversion layer of less than 100 metres) (NSCA, 2002). This event forced the government to take action. The Beaver Committee was established and the first Clean Air Act (1956) developed. This Act introduced 'smoke control areas' and provided grants to convert fireplaces to use alternative fuels (Department of the Environment, 1995). It became illegal to burn any fuel in any chimney in these smoke control areas with the exception of smokeless fuels. The Clean Air Act of 1956 and its subsequent revisions regulated the burning of fuels and controlled smoke and SO<sub>2</sub> emissions from both domestic and industrial sources (Bower et al., 1994). Subsequently, the passing of these Acts, coupled with the declining popularity of coal in the domestic and industrial sectors, led to a great improvement in urban air quality. The Clean Air Act of 1993 still remains the principle piece of legislation for the control of emissions from domestic premises.

More recently air quality legislation has become focused on traffic related emissions. High emissions of NO<sub>x</sub> and volatile organic compounds (VOC) coupled with hot, sunny and poorly ventilated environments can lead to the formation of ground level ozone (O<sub>3</sub>) (Finlayson-Pitts and Pitts 2000). This type of air pollution event is known as a photochemical smog. It was first noticed in the Los Angeles Basin, California in the 1940s; however this phenomenon is now known to exist in many other locations across the globe e.g. Athens (Klemm et al., 1998), Grenoble (Ferrari et al., 1998) and Sao Paulo (Guardani et al., 1999). Additionally, the 1991 winter smog in London highlighted the effects that increased traffic emissions can have on air quality. During this event the stable and stratified atmosphere coupled with the high traffic emissions enabled NO<sub>2</sub> concentrations to reach 423 ppb - the highest ever recorded concentration in the UK (Bower et al., 1994). It was not long after this episode that the current UK air quality legislation, the National Air Quality Strategy (NAQS), was released.

## **2.2. Current legislation**

Air quality legislation has developed in a slow and piecemeal fashion, mirroring the increased understanding of air pollution and the associated health implications. The current legislation regarding air quality derives from both national and international policies.

### **2.2.1. European legislation**

Since joining the European Union (EU) in the 1970s the UK is subject to European policies, and air quality is one area where the EU has been extremely proactive. For example the 6<sup>th</sup> Environment Action Programme 'Environment 2010: Our future, our choice' identifies air pollution as a key area for further research (<http://ec.europa.eu/environment/newprg/index.htm>).

The main air quality legislation with which the UK needs to comply is the 1996 Air Quality Framework Directive 96/62/EC and its subsequent Daughter Directives. This legislation provides a comprehensive list of air pollutants, legally binding limit concentrations and dates by which



they are to be achieved. The pollutants include: SO<sub>2</sub>, NO<sub>2</sub>, lead, particulate matter (PM<sub>10</sub>), benzene, carbon monoxide, ozone (O<sub>3</sub>), arsenic, cadmium, mercury, nickel and polycyclic aromatic hydrocarbons (PAH). The first and third Air Quality Directives (1999/30/EC and 2002/3/EC), under the larger umbrella framework of the Air Quality Framework Directive 96/62/EC, are concerned with the control and monitoring of ambient NO<sub>2</sub> concentrations. The first daughter directive sets a limit value for annual mean NO<sub>2</sub> concentration to be achieved by 1 January 2010. The third daughter directive is concerned primarily with O<sub>3</sub>, although also requires the monitoring of NO<sub>2</sub> and other O<sub>3</sub> precursors.

Each member state is also subject to the National Emissions Ceilings Directive (2001/81/EC) and the Large Combustion Plant Directive (2001/80/EC), both of which make specific reference to NO<sub>x</sub> emissions.

### **2.2.2. Domestic legislation**

In response to European legislation, the UK has developed its own domestic approach. Prompted by the 1995 UK Government White Paper and Part IV of the Environment Act, which identified the need for an integrated management system and a framework of air quality standards and objectives, the NAQS was designed to help control and manage air quality in the UK. It integrated closely the European limit values included in the Framework Directive 96/62/EC as well as introducing new and tighter domestic air quality objectives. The NAQS was first published in 1997, later reviewed and re-released in 2000, and has subsequently become known as the Air Quality Strategy for England, Scotland, Wales and Northern Ireland (DETR, 2000). A revised NAQS was released in 2007. This new report places greater emphasis on the health problems associated with the airborne pollutants; this is especially true of particulates whereby a new concept called the exposure reduction approach has been established. In terms of NO<sub>2</sub> however both the hourly and annual mean objectives remain the same as those set out in the 2000 version.

The NAQS contains a series of standards and objectives. Standards represent a target concentration for a specific averaging time e.g. 20 ppb for one hour. The actual target concentration represents a specific level set in response to the associated impacts the pollutant has on human health and/or the potential damage to the environment (AQEG, 2004). Standards are based on the latest scientific and medical evidence from the Expert Panel on Air Quality Standards (EPAQS) or the World Health Organisation (WHO) (DETR, 2000). Objectives set a date for which the air quality standards must be achieved. Objectives take into consideration the costs and benefits, feasibility and practicality of achieving the standards (DETR, 2000). In many circumstances they allow a number of exceedences per year to accommodate for those uncontrollable circumstances, such as traditional events (e.g. bonfire night) or abnormal weather etc. The NAQS contains standards and objectives for benzene, 1,3-butadiene, carbon monoxide,

lead, NO<sub>2</sub>, SO<sub>2</sub>, PM<sub>10</sub> and O<sub>3</sub>. An addendum in February 2003 introduced PAH to this list of pollutants (DEFRA, 2003).

The EU and UK standards and objectives for NO<sub>2</sub> (with which this research is concerned) are shown in Table 1 (note: the hourly objective is not to be exceeded more than 18 times in one year).

**Table 1:** The national air quality objectives for NO<sub>2</sub>

	Hourly Objective µg/m <sup>3</sup>	Annual Objective µg/m <sup>3</sup>	Date to be achieved by
EU limits	200 (105 ppb)	40 (21 ppb)	2010
UK air quality standards	200 (105 ppb)	40 (21 ppb)	2005

In addition, Part IV of the Environment Act (1995) also suggested developing the role of local air quality management in controlling UK air quality. The NAQS in accordance with section 82 of the Environment Act (1995) therefore placed a statutory obligation on local authorities to periodically review and assess air quality in their region. This process occurred in a series of stages. The first stage, compulsory for all local authorities, was known as a ‘screening stage’, and its aim was for local authorities to understand the extent of air quality problems in their own areas. If a pollutant was found unlikely to meet the national objectives then the local authority progressed to a stage two ‘Review and Assessment’. Stage two required a more detailed investigation of air quality. The successive stages became more detailed so that hotspot areas were identified with respect to the different pollutants in question. Local authorities who found ambient concentrations in their area unlikely to exceed the objectives left the review and assessment programme.

An authority declared an AQMA if any ambient concentration of any of the seven out of the eight target pollutants were found to exceed the national objectives (DETR, 2000). Once an AQMA was declared a local authority had twelve months to draw up an ‘Action Plan’ suggesting air pollution reductions measures (DETR, 2000). Action plans are then subject to review every two years. O<sub>3</sub> is not included in the local authority review and assessment procedure as it is recognised as trans-boundary in nature and beyond the control of local authorities. O<sub>3</sub> concentrations and other climate change pollutants (i.e. CO<sub>2</sub>) are, however, considered by local authorities on a voluntary basis. In total 218 local authorities have declared AQMAs as a result of the local air quality management process (see <http://www.airquality.co.uk/archive/laqm/list.php> for the list of local authorities with an AQMA).

Since the introduction of the NAQS, there has been a marked improvement in air quality in the UK and its associated impact on health, with the numbers of premature deaths and hospital admissions associated with air quality falling each year (DEFRA, 2006). Additionally, it is believed that the number of people exposed to ambient NO<sub>2</sub> in excess of the annual objective by



2010 will have been reduced by 98 % (compared to no abatement) (DEFRA, 2004). However a continued effort is needed if air quality is to be successfully managed in the longer term.

Ambient pollutant concentrations depend on both physical and chemical processes. For example, the formation of photochemical smogs, highlighted in section 2.1, were both a response of the high level of emissions, the meteorological conditions present at the time and also the complex chemical reactions. The present section has outlined the current situation in terms of legislation. The sections that follow will provide details of the theory behind the physical (section 2.3) and chemical (section 2.4) processes that influence urban air quality, with a specific focus on  $\text{NO}_x$  and  $\text{NO}_2$  concentrations.

## **2.3.Troposphere: structure and nature**

The troposphere is the lowest layer of the atmosphere and is highly influenced by human activities at the surface. It is in this region of the atmosphere where most anthropogenic emissions are released and so is important in terms of resultant pollutant concentrations.

### **2.3.1. Introduction**

The height of the tropopause (the barrier between the troposphere and the stratosphere) varies across the globe as a result of the varying degrees of heat released from the earth. The mean height is therefore generally greater at the equator (~ 18 km) compared to the poles (~ 8 km) (Harrison, 2001). The temperature of the troposphere also generally declines with altitude. The rate of temperature reduction with height (lapse rate) is generally considered to be around  $9.8 \text{ K km}^{-1}$  or  $1^\circ\text{C}$  for every 100 m (Harrison, 2001) but can vary substantially in the presence of water vapour. The height and temperature of the troposphere changes on an almost continuous basis. Additionally, the troposphere is subject to weather (i.e. 95 % of total cloud formation and precipitation occurs within it), which in turn substantially affects the concentrations of trace gases (i.e., wet and dry deposition and dispersion).

The troposphere can be sub-divided into two further sections: the boundary layer and the free troposphere. The boundary layer is the part of the troposphere closest to, and most affected by, the earth's surface. The free troposphere is the part that lies above the boundary layer.

Pollutants emitted at, or near, the earth's surface are subject to dispersion. The height of the boundary layer determines the volume of air in which pollutant concentrations will be mixed. Similarly to the overall depth of the troposphere, the height of the boundary layer is not fixed. Its depth, a result of solar radiation and ground level heat, varies diurnally and varies roughly from 100 m at night to around 1000 m during the day (Harrison, 2001). With all other things remaining constant, a boundary layer of 100 m in height would lead to higher ground level concentrations than a height of 1000 m as pollutants are subject to a smaller volume of air close to the surface. The height of the boundary layer therefore strongly influences the ground level pollutant concentrations.

### 2.3.2. Turbulence and air movements

The air in the troposphere is well mixed. This mixing can vary from extremely local movements driven by localised winds to large scale, global, influences such as the Coriolis force and solar radiation. This section will highlight and explain the various influences that pollutants are subjected to, so that the dynamic nature of the troposphere can be understood.

#### 2.3.2.1 Atmospheric stability: mechanical turbulence

Mechanical turbulence is driven by the horizontal movement of air (winds) over the surface of the ground. The amount of resistance offered by the earth's surface strongly influences mechanical turbulence. For example, there will be less mechanical turbulence over a smooth surface compared to a surface littered with obstacles e.g. trees, building etc. The smoothness of the ground's surface for a particular area is known as the surface roughness. Subsequently, the surface roughness of a city will be higher compared to a field of crops, and indeed a field of crops will have a greater surface roughness compared to a field of bare earth. Naturally the level of mechanical turbulence generally decreases with height.

Generally speaking a higher amount of mechanical turbulence will result in lower ground level concentrations, as the amount of turbulence will affect the dilution and dispersion of pollutants. This relationship can be illustrated by plotting observed  $\text{NO}_2$  concentrations against wind speed (see Figure 1); here wind speed is a proxy for mechanical turbulence.

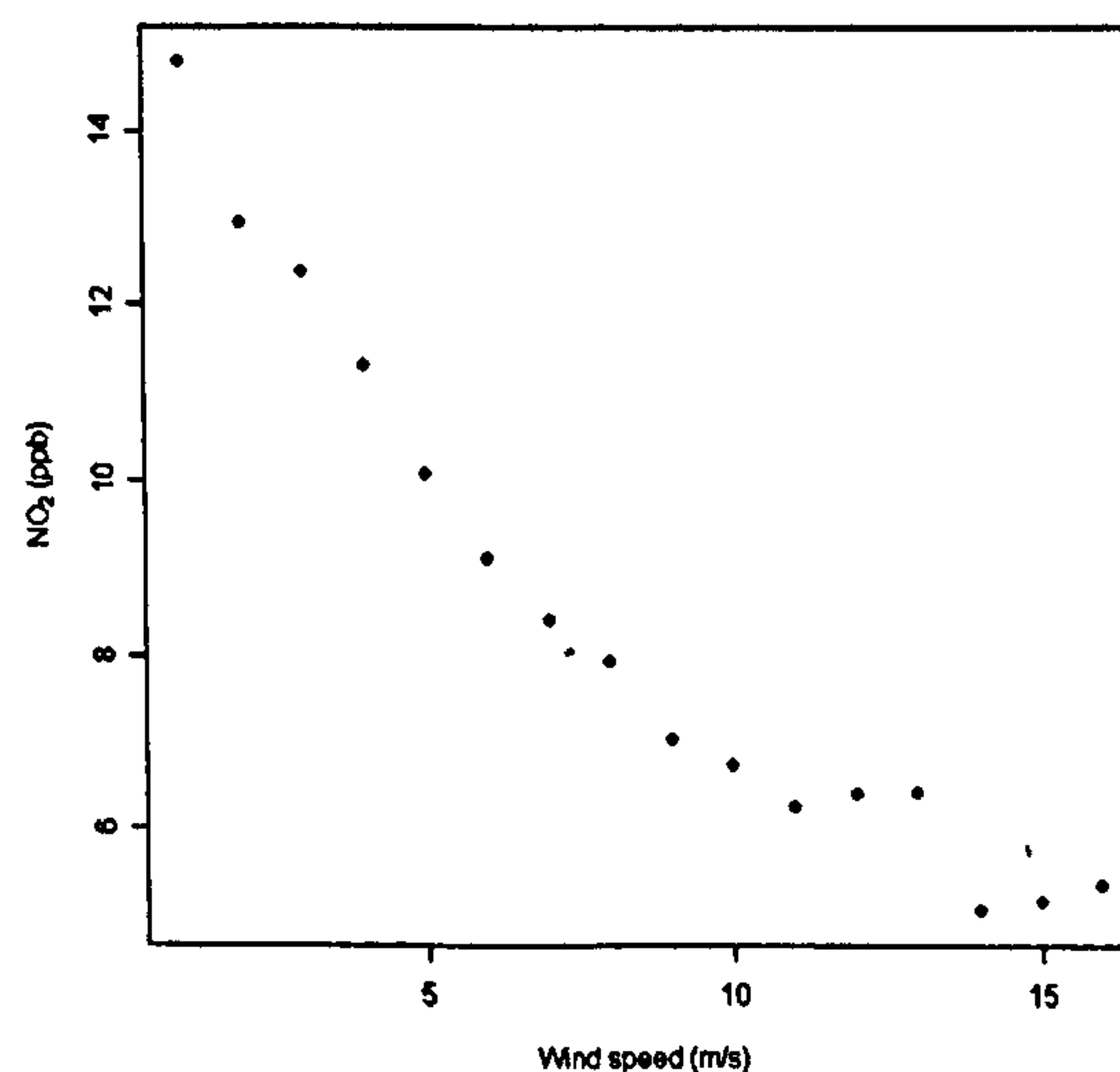


**Figure 1:** The relationship between wind speed and  $\text{NO}_2$  concentration. The mean  $\text{NO}_2$  concentration has been calculated for different wind speed 'bins', i.e.  $0 - 1 \text{ ms}^{-1}$ ,  $1 - 2 \text{ ms}^{-1}$  etc.  $\text{NO}_2$  data are from the urban background site in York, the wind speed data are from Church Fenton, the Meteorological Office site for York for the year 2005.



### **2.3.2.2 Atmospheric stability: convective turbulence and stability**

Convective turbulence is driven by the heat released from the earth's surface heating the lowest layers of the atmosphere causing an upward movement of air (vertical mixing). Generally speaking the stronger the heat flux, the greater the amount of convective mixing. Convective mixing is important in determining the stability of the atmosphere and, in turn, atmospheric stability is an important factor in determining ground level pollutant concentrations.

As an air parcel is displaced to an area with lower pressure, its volume will increase and its temperature will subsequently decrease. This concept is illustrated by the general decrease in air temperature with increasing height in the boundary layer (section 2.3.1). This type of temperature change, caused purely by the movement of the air parcel, is known as adiabatic. Adiabatic temperature change can be illustrated by the pumping of air into a bicycle tyre (Finlayson-Pitts and Pitts, 2000). The pumping action forces air from a relatively large area (the pump) into a smaller area (bicycle tyre) and subsequently results in an increase in air temperature felt by the warming of the pump tubing; the associated temperature increase of the air has occurred purely as a result of the movement of air. Conversely, the temperature change associated with the addition of an external force is known as diabatic; for example, the heating of water in a saucepan on the stove is diabatic. In the case of an air parcel, the temperature change associated with the mixture of two air parcels is diabatic. Diabatic temperature changes are usually associated with horizontal movements of air, whereas adiabatic temperature changes usually occur during vertical air movements.

Atmospheric stability can be roughly split into three categories: unstable, stable and neutral. Firstly, where the temperature of an air parcel is greater than its surroundings it will become buoyant and rise. The air parcel will continue to rise so long as its temperature remains higher than its surroundings (i.e., its rate of cooling does not exceed that of the remaining atmosphere). Such conditions are common on hot sunny days, where the earth's surface leads to the temperature of the lower layers of air becoming elevated and buoyant. These types of atmospheric conditions are considered unstable and the associated movement of air encourages the rapid dispersal of pollutants.

Secondly, a stable atmosphere occurs when there is little difference between an air parcel and its surroundings i.e., the temperature of an air parcel becomes similar to its surroundings and its buoyancy is lost. This equality between a particular air parcel and its surroundings causes the vertical movement (convective turbulence) to stop and so the boundary layer is deemed stable. A lack of convective turbulence (or mixing) is associated with low rates of pollutant dispersion. Such conditions are usually associated with a lack of sunshine i.e. night time. Inversions (section 2.3.2.4.) are also common under stable conditions.

Neutral conditions occur when mechanical turbulence dominates over convective turbulence. Mechanical turbulence becomes overriding at wind speeds of around  $6 - 8 \text{ m s}^{-1}$  (Harrison, 2001) irrespective of the level of heat flux. Dawn and dusk tend to be associated with neutral conditions.

Discrete Pasquill-Gifford categories (A to G) have been traditionally used to distinguish between varying levels of atmospheric stability (AQEG, 2004). A is the most unstable (convective) class, D is associated with neutral conditions, and finally the most stable conditions are represented by G. However, in reality, conditions will vary throughout the boundary layer i.e. the atmosphere may appear neutral at the surface but become convective in nature at higher levels. The Monin Obukhov length (MO) length is a measure of the relative importance of mechanical and convective mixing. The MO length is the height in the boundary layer at which the contributions of mechanical and convective turbulence are equal (Harrison, 2001). It is a relatively new measure of atmospheric stability, which has replaced the old Pasquill-Gifford categories.

#### **2.3.2.3 Atmospheric stability: dispersion**

The dispersal of a pollution plume depends strongly on the emission source and the type of atmospheric conditions present. Figure 2 illustrates the release of emissions under the different atmospheric stability conditions highlighted above for an elevated source i.e., chimneystack. It can be seen that under **unstable** atmospheric conditions (blue line) the ground level concentrations reach their peak (i.e. the plume becomes grounded) much closer to the emissions source compared to stable or neutral boundary layer conditions (green line). This close proximity in plume grounding is a result of the pollution plume becoming mixed with the surrounding air (vertically and horizontally) in the unstable atmospheric conditions and so the plume is brought down to ground level quickly. Conversely, a stable atmosphere results in little vertical movement of air and so the pollution plume may travel for some distance without being brought down to ground level. The eventual ground level peak concentration for elevated emission sources is generally much lower under stable conditions than unstable conditions, since the pollution plume will be subject to dispersal whilst aloft.

The situation is very different for ground level emission sources (Figure 3). Note in Figure 3 all the features of the elevated emission source of Figure 2 have been retained with the exception of the stack height, which has been reset to zero. Stable atmospheric conditions (green line) prevent dispersal (mixing) of ground level emissions causing elevation of ground level concentrations that remain high at large distances from the source. Such conditions are often associated with inversion layers. For unstable conditions (blue line), the emissions released at ground level will be subject to rapid vertical mixing and so the ground level concentrations fall off quickly with increasing distance from the source. It should be noted that the high initial ground level concentrations shown in Figure 3 are a result of the high exit velocity effectively increasing the release height of the plume.



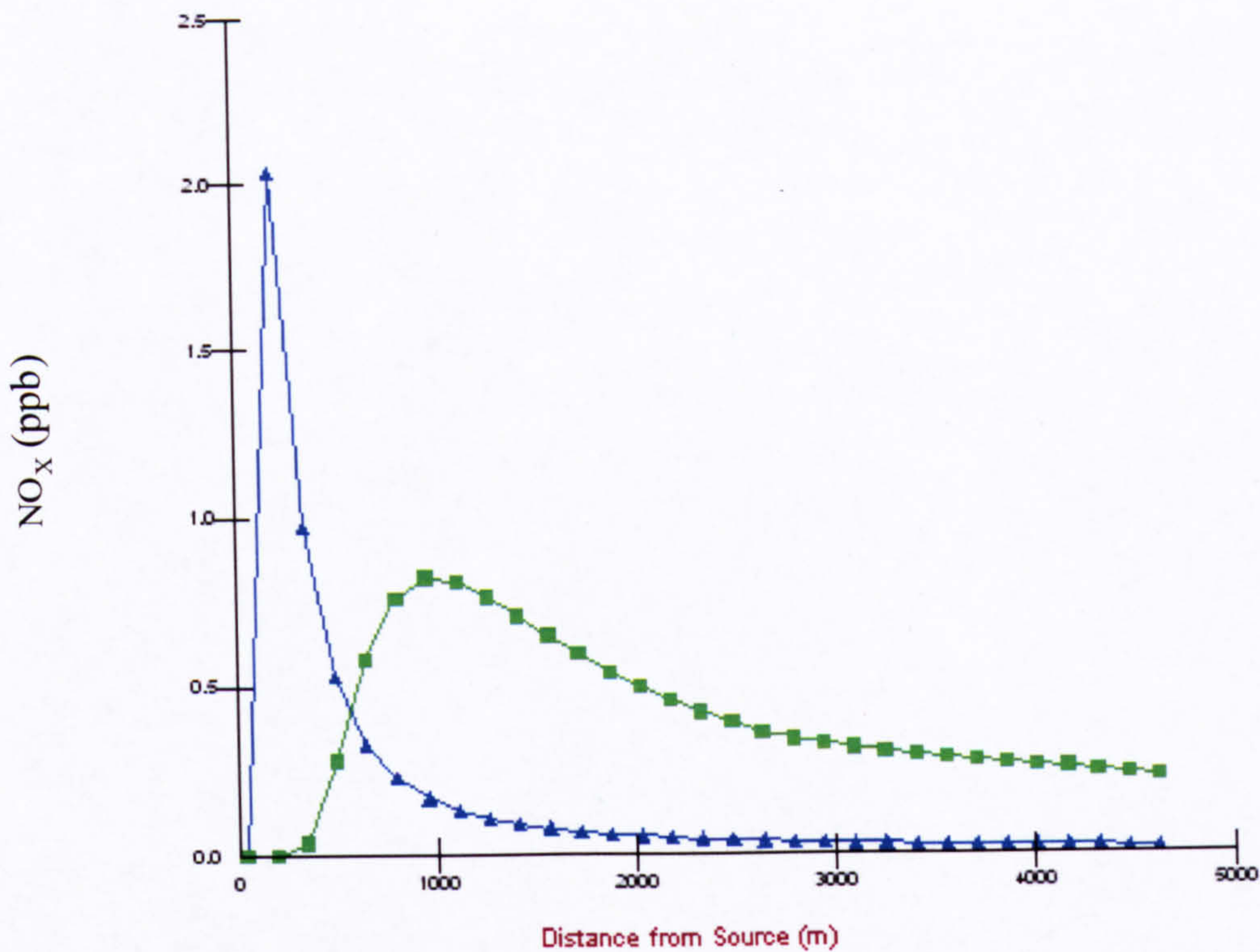


**Figure 2:** Ground level  $\text{NO}_x$  predictions for an elevated emission source for both unstable (blue line) and stable (green line) boundary layer conditions. Emission source is the University of York boiler, release height = 58.4 m,  $x = 462700$ ,  $y = 450700$ ,  $\text{NO}_x$  emissions = 3.45 g/s, stack diameter = 0.55 m, release velocity = 20 m/s, release temperature = 200 °C.

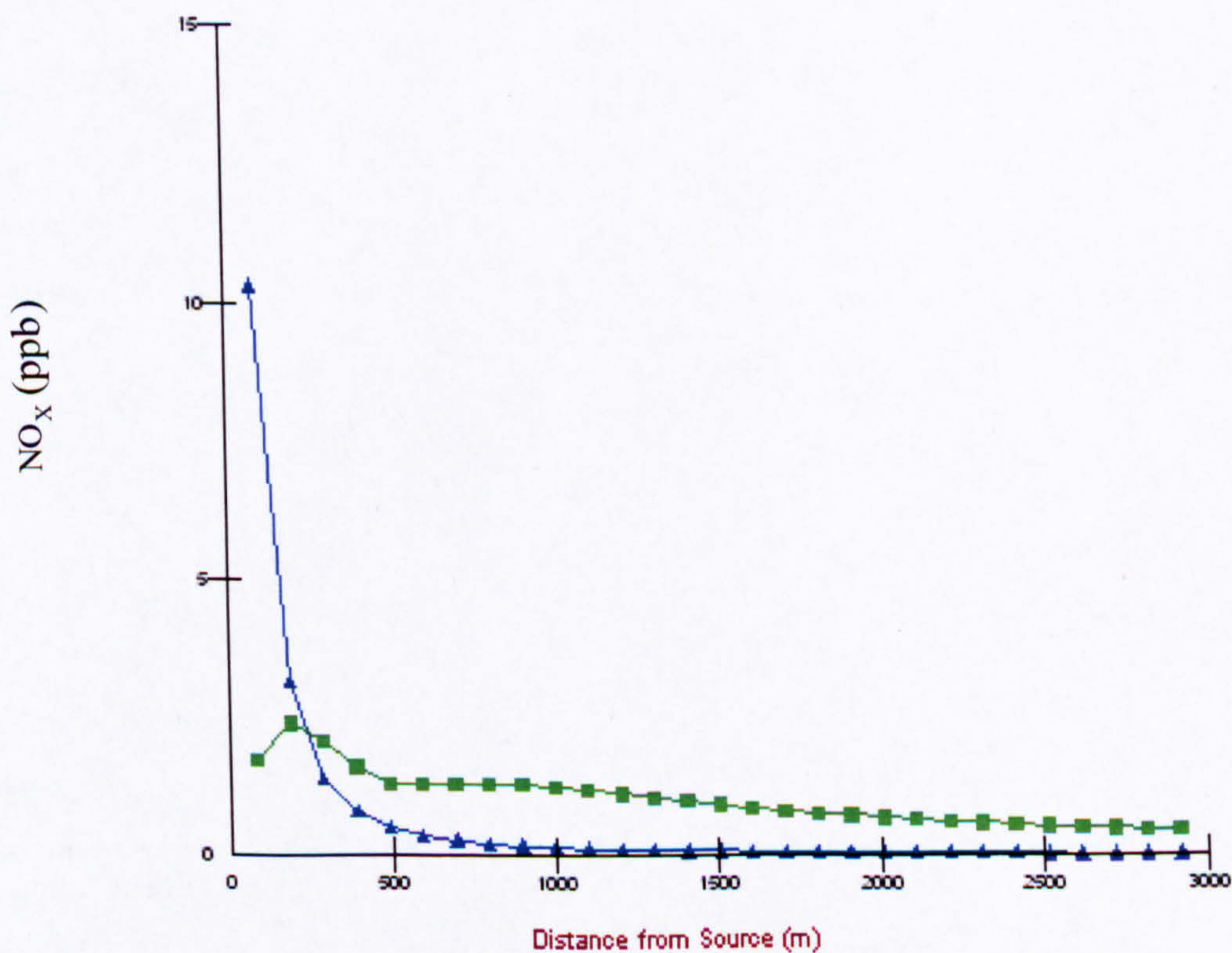


**Figure 3:** Ground level  $\text{NO}_x$  predictions for a ground level emission source for both unstable (blue line) and stable (green line) boundary layer conditions. Emission source is the University of York boiler but with the release height set to zero,  $x = 462700$ ,  $y = 450700$ ,  $\text{NO}_x$  emissions = 3.45 g/s, stack diameter = 0.55 m, release velocity = 20 m/s, release temperature = 200 °C.



#### 2.3.2.4 Atmospheric stability: inversions

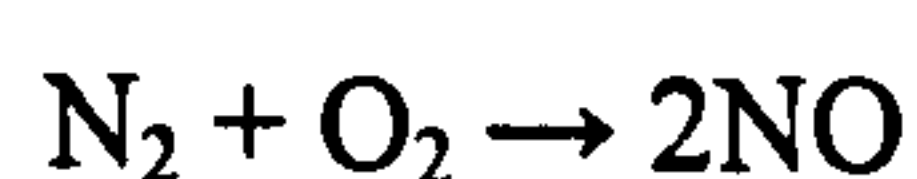
A temperature inversion can occur when a layer of warm air overlays a layer of cooler air, effectively trapping the cool air at ground level. In terms of the temperature profile, an inversion occurs when the temperature of the troposphere increases with height before reversing itself again (Harrison, 2006). The volume of air that ground level sources are released into is therefore much lower than would otherwise be the case, and so ground level concentrations become elevated. Emissions released above the inversion layer are effectively subject to a different set of atmospheric conditions and so will not affect the ground level concentrations. It will not be until the inversion layer has broken down that the two layers of atmosphere will be mixed.

There are two main types of inversions: radiation (ground based) and overhead (subsidence) (Finlayson-Pitts and Pitts, 2000). Radiation inversions usually occur at night where rapid cooling of the earth's surface leads to a rapid cooling of the air directly above it. This ground level cooling exceeds the rate of cooling in the rest of the troposphere and so a layer of cold air is trapped by warmer conditions above. Such inversions usually last until morning with the onset of solar radiation. Fogs are commonly associated with this type of inversion layer and prolong the effects by reflecting sunlight e.g. the 1952 London smog. Overhead inversions are caused by downward movement of air masses moving over continents where the air becomes compressed and so leads to an increase in temperature (Finlayson-Pitts and Pitts, 2000). Local topography can also promote the occurrence of inversion layers e.g. valleys where cool air flows down the valley sides and covers warmer air close the valley bottom.

### 2.4. NO<sub>x</sub> chemistry

#### 2.4.1. Introduction to NO<sub>x</sub>, NO and NO<sub>2</sub>

Nitric oxide (NO) and NO<sub>2</sub> together are known as NO<sub>x</sub>. NO<sub>x</sub> is produced in high temperature combustion processes, for example gas fired power stations, vehicle engines, aircraft etc. The majority of NO<sub>x</sub> emissions are released as the colourless gas, NO. The main route for NO production through combustion processes (reaction 1) occurs as a result of the N<sub>2</sub> and O<sub>2</sub> in air being converted to NO (thermal-NO<sub>x</sub>). However, a small amount of NO can also be produced as a result of nitrogen contained in the fuel (fuel-NO<sub>x</sub>) (Harrison, 2006).



1

There are also natural sources of NO. For example the high temperatures associated with shockwaves from lightning strikes can also fix atmospheric N<sub>2</sub> producing NO (Brimblecombe, 1986). In addition, substantial amounts are produced as a result of biomass burning, plus a further release from soil and animals.



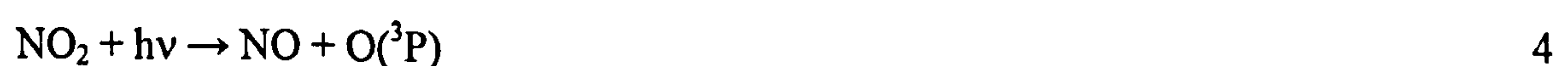
NO<sub>2</sub> is a brown gas. It is mainly considered a secondary pollutant, formed through chemical reaction in the atmosphere (see following section). Some NO<sub>2</sub> can be released directly from combustion sources and this fraction is known as ‘primary NO<sub>2</sub>’. For over thirty years the fraction of NO<sub>2</sub> believed to be primary in origin has been assumed to be ~5 % of NO<sub>x</sub> (0 - 10 %) (AQEG, 2006; PORG, 1997). However, there is now increasing evidence that this fraction may grossly under-estimate the true extent of primary NO<sub>2</sub> emissions. Jenkin (2004a, 2004b) suggested that the fraction of primary NO<sub>2</sub> from diesel vehicles is in the region of 11.8 ± 1.2 % and around 3 % for petrol vehicles. A subsequent study focusing specifically in London suggested the fraction of primary NO<sub>2</sub> actually ranges from 3.2 % to 23.5 %, the median value being 10.6 % (Carslaw and Beevers, 2005a). Such evidence is important, since emission inventories and dispersion models often use a general proportion to represent the NO-NO<sub>2</sub> split from combustion sources across the whole urban area.

#### 2.4.2. Photostationary state

Once NO is produced it can be converted to NO<sub>2</sub> via reaction with O<sub>2</sub> (reaction 2). This reaction, often known as the thermal (or non photochemical) reaction, is only important at high concentrations of NO. For example, it was believed to contribute to the high wintertime NO<sub>2</sub> concentrations (reaching 423 ppb) during the 1991 pollution episode in London (Bower et al., 1994). It can also occur close to the release site of industrial emissions, leaving a visible brown pollution plume e.g. the emission release from typical flue gas concentrations for industrial coal burning power stations (Harrison, 2001).



NO<sub>2</sub> can also be produced by reaction of NO with O<sub>3</sub>, (reaction 3). This reaction rate is much quicker than the self reaction of NO with O<sub>2</sub> (reaction 2) and under ambient conditions is considered the main production route of NO<sub>2</sub> in the atmosphere. Once NO<sub>2</sub> is formed, it is subject to photolysis which reforms NO and produces a ground state oxygen atom (O(<sup>3</sup>P)), reaction 4. The major fate of the oxygen atom is to produce O<sub>3</sub> by combining with O<sub>2</sub> (reaction 5). The production of NO<sub>2</sub> is therefore indirectly linked to the production of tropospheric O<sub>3</sub>. The M in reaction 5 is a third body that takes away excess energy; it is usually nitrogen or oxygen.



These three reactions (3 – 5) represent a null cycle in isolation. This steady state is known as the photo-stationary state (Leighton, 1961) and the O<sub>3</sub> concentration can be represented by the following equation:

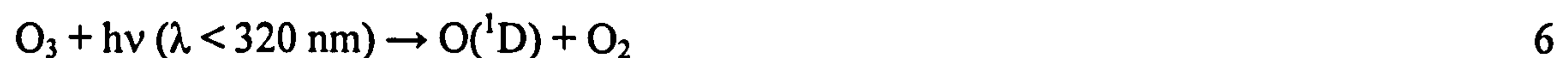
$$[\text{O}_3] = J_1[\text{NO}_2]/k_1[\text{NO}] \quad \text{Equation 1}$$

where  $J_1$  is the photolysis coefficient for NO<sub>2</sub> and  $k_1$  is the rate coefficient for the reaction of NO with O<sub>3</sub>.

### 2.4.3. OH radical

The OH radical, only present in extremely small quantities ( $2\text{--}3 \times 10^6$  molecule cm<sup>-3</sup>) owing to its particularly short lifetime, has a large impact on the chemistry of the atmosphere. It is often referred to as the atmospheric cleanser as it reacts with, and controls, the concentrations of many important trace gases in the atmosphere.

A source of OH in the clean (and polluted) environment is through the photolysis of O<sub>3</sub> which produces the excited O(<sup>1</sup>D) atom. The O(<sup>1</sup>D) atom then goes on to react with water and produce the OH radical (reactions 6 and 7).



In a polluted environment the OH radical can also be produced by the photodissociation of nitrous acid (HONO) (reaction 8) and hydrogen peroxide (HOOH) (reaction 9):



### 2.4.4. Polluted atmospheres and the breakdown of the photostationary state

In urban environments, anthropogenic emissions (namely, NO<sub>x</sub> and VOC) are high, and include releases from a variety of sources e.g. fuel combustion, industrial operations, domestic heaters, hazardous waste etc. The anthropogenic emissions are additional to those released naturally, including some hydrocarbons, often referred to as biogenic species.

In urban environments, the focus of this thesis, O<sub>3</sub> concentrations generally increase throughout the day rather than stay steady as predicted by the steady-state argument and so there must be alternative routes for its production. This deviation from the stationary state results from the



reactions of the OH radical with the suite of VOCs present in polluted environments. The VOCs, such as non methane hydrocarbons, aldehydes and ketones, are attacked by the OH radical, and lead to the formation of NO<sub>2</sub> without the consumption of O<sub>3</sub>, via the production of intermediate peroxy radicals (RO<sub>2</sub> and HO<sub>2</sub>). The OH radical is therefore an extremely important species in polluted environments and the presence of VOCs and NO<sub>x</sub> promotes the production of O<sub>3</sub>.

To illustrate this formation of NO<sub>2</sub> without the consumption of O<sub>3</sub>, the oxidation of methane (CH<sub>4</sub>) is illustrated by reactions 10 to 18. This sequence of reactions illustrates the complexity inherent in polluted atmospheric chemistry.

**Step 1:** the methyl radical (CH<sub>3</sub>) is produced



**Step 2:** the methyl peroxy radical (CH<sub>3</sub>O<sub>2</sub>) is produced



**Step 3:** formation of NO<sub>2</sub> and methoxy radical (CH<sub>3</sub>O)



**Step 4:** formaldehyde (HCHO) and the hydroperoxy radical (HO<sub>2</sub>) are produced:



**Step 5:** more HO<sub>2</sub> radicals produced from HCHO breakdown



**Step 6:** destruction of HO<sub>2</sub> resulting in the formation of NO<sub>2</sub>, alongside the regeneration of the OH radical:



**Step 7:** formation of O<sub>3</sub> through NO<sub>2</sub> photolysis



The sequence of reactions shows the production of two NO<sub>2</sub> molecules from two NO, molecules without the destruction of O<sub>3</sub>, the latter of which can therefore accumulate. Additionally, the formation of the hydroperoxy radical HO<sub>2</sub> during the HCHO destruction (step 5, reactions 14 and 15) and its subsequent destruction (reaction 16) results in the regeneration of the OH radical. This regenerated OH radical will go on to attack further hydrocarbons, restarting this whole process, and so the overall number of NO<sub>2</sub> molecules produced will be much higher than that initially created from the reaction sequence 10 -18.

Polluted environments generally contain hundreds of VOCs, and many of these hydrocarbons have the potential to generate much more O<sub>3</sub> than methane. The importance of various VOC in producing O<sub>3</sub> has been categorised by the Photochemical Ozone Creation Potential (POCP) system (Derwent et al., 1996). Methane has the lowest value owing to its low reactivity despite its high abundance and 1,3,5-trimethylbenzene the highest (Carslaw and Carslaw, 2001). The presence of VOCs in polluted environments can thus significantly complicate atmospheric chemistry.

#### 2.4.5. Night time chemistry

The chemistry described in the previous section is driven by photolysis (i.e. sunlight) and is confined to daylight. However, the absence of photolysis at night allows photo-sensitive species to accumulate to significant levels e.g. NO<sub>3</sub> (reaction 19) and N<sub>2</sub>O<sub>5</sub> (reaction 20). The nitrate radical (NO<sub>3</sub>) becomes a significant scavenger at night (Smith et al., 1995; Carslaw et al., 1997). It reacts with VOCs present in a polluted environment forming, among other things, HO<sub>2</sub> and NO<sub>2</sub> and thus leads to an overall depletion of VOCs during the night (Jenkin and Clemitshaw, 2000). The formation of HO<sub>2</sub> and thus OH (through reaction 21) means that the oxidative capacity of the night time environment is increased (Carslaw and Carslaw, 2001) as OH can oxidise many VOCs rapidly once formed through this 'dark' route. The lifetime of NO<sub>2</sub> with respect to reaction 19 is around 3.5 hours (Finlayson-Pitts and Pitts, 2000).



NO<sub>3</sub> and N<sub>2</sub>O<sub>5</sub> exist in equilibrium, and thus sinks of N<sub>2</sub>O<sub>5</sub> (i.e. wet deposition) also become sinks for NO<sub>3</sub> (this is discussed further in the following section).

#### 2.4.6. Removal of NO<sub>x</sub>

For gases to remain at constant concentrations in the atmosphere it is necessary that removal processes balance the production processes. Wet and dry deposition are important removal



mechanisms for the atmospheric system. Wet deposition is the removal of substances dissolved in rainfall, whereas dry deposition is the direct transfer of gases and aerosols to the Earth's surface. Dry deposition can also include transference onto wet surfaces e.g. oceans or dew covered vegetation, indeed this often speeds up the removal process. Dry deposition will also vary depending on the surface in question, for example a field of crops will result in a greater rate of transfer than bare soil. Also, this process is faster at night-time owing to the reduced height of the boundary layer.

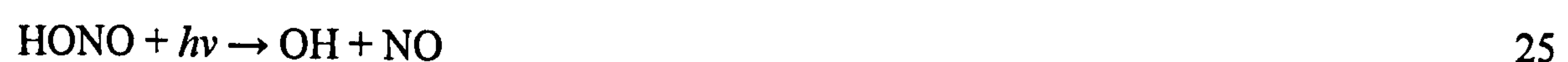
NO<sub>x</sub> is mainly removed from the atmospheric system by wet or dry deposition of the 'sticky' nitric acid (HNO<sub>3</sub>). The formation of HNO<sub>3</sub> occurs either by reaction of NO<sub>2</sub> with the OH radical (22), or through the reaction of N<sub>2</sub>O<sub>5</sub> with water (23).



The rate of reaction 22 can be sufficiently high in polluted environments (NO<sub>2</sub> lifetime of 16 hours with respect to this reaction at OH concentrations of  $2 \times 10^6$  radicals cm<sup>-3</sup>) so that significant amounts of HNO<sub>3</sub> are formed and subsequently removed from the atmosphere (Finlayson-Pitts and Pitts, 2000). Reactions 22 and 23 generally lead to the formation HNO<sub>3</sub> in its gaseous form, which is quickly scavenged by raindrops or deposited onto surfaces. There is also a loss of NO<sub>2</sub> by direct dry deposition; however the rate of loss by this method is very slow and so not considered a major NO<sub>x</sub> sink (AQEG, 2004).

There are also two types of temporary NO<sub>x</sub> loss where the reactions are reversible. These are often referred to as NO<sub>x</sub> reservoirs and include peroxy acetyl nitrate or PAN (CH<sub>3</sub>C(O)O<sub>2</sub>NO<sub>2</sub>) and nitrous acid (HONO). PAN, the known eye irritant, is formed when NO<sub>2</sub> and acetylperoxy radicals (CH<sub>3</sub>CO<sub>3</sub>) combine. PAN is thermally unstable and so its ambient concentration is determined largely by temperature. It is possible for PAN to be formed and transported with a relatively cool air mass and then thermally degraded back to NO<sub>2</sub> as it reaches a warmer area, thus providing the potential for NO<sub>2</sub> release a long way from sources.

HONO is formed by reaction of NO and OH (reaction 24) and can easily be reversed through photolysis (reaction 25). HONO can accumulate at night and lead to a sharp peak in OH at dawn due to rapid photolysis (Finlayson-Pitts and Pitts, 1997).



Additionally, the HONO production rate can be enhanced by the reaction of NO<sub>2</sub> with H<sub>2</sub>O on surfaces (Kurtenbach, et al., 2001). The influence of this alternative HONO production pathway on the concentrations of OH and HO<sub>2</sub> has been highlighted in the Emmerson et al. (2005) study.

**2.4.7. Clean vs. Polluted environment**

There are noticeable differences in NO, NO<sub>2</sub> and O<sub>3</sub> concentrations in clean and polluted environments. Firstly, the magnitude of NO and NO<sub>2</sub> concentrations are much greater in urban environments (polluted), reaching a few ppm in some cases; whereas in cleaner, more rural environments NO<sub>x</sub> is usually only present at a few ppt (Jacobson, 1999). This difference in magnitude is illustrated in Table 2.

**Table 2:** Typical concentrations of NO<sub>x</sub>, NO<sub>2</sub> and O<sub>3</sub> in clean and polluted environments. Data are taken from Jacobson (1999)

Mixing ratios	Clean environment	Urban environment
NO	5 ppt	100 ppb
NO <sub>2</sub>	20 – 50 ppt	100 – 250 ppb
O <sub>3</sub>	20 – 40 ppb	10 – 350 ppb

A second important distinction between clean and polluted environments is the ratio of NO to NO<sub>2</sub> concentrations. At locations close to an emission source as much as 90% of NO<sub>x</sub> will be in the form of NO (Shi and Harrison, 1997). However at locations further from the emission source, NO is destroyed by reaction with O<sub>3</sub> (reaction 3) producing NO<sub>2</sub>, therefore allowing NO<sub>2</sub> to make up a greater fraction of NO<sub>x</sub>. The varying scale of the NO: NO<sub>2</sub> ratio was illustrated in the article by Carslaw and Carslaw (2001) and is shown in Figure 4.



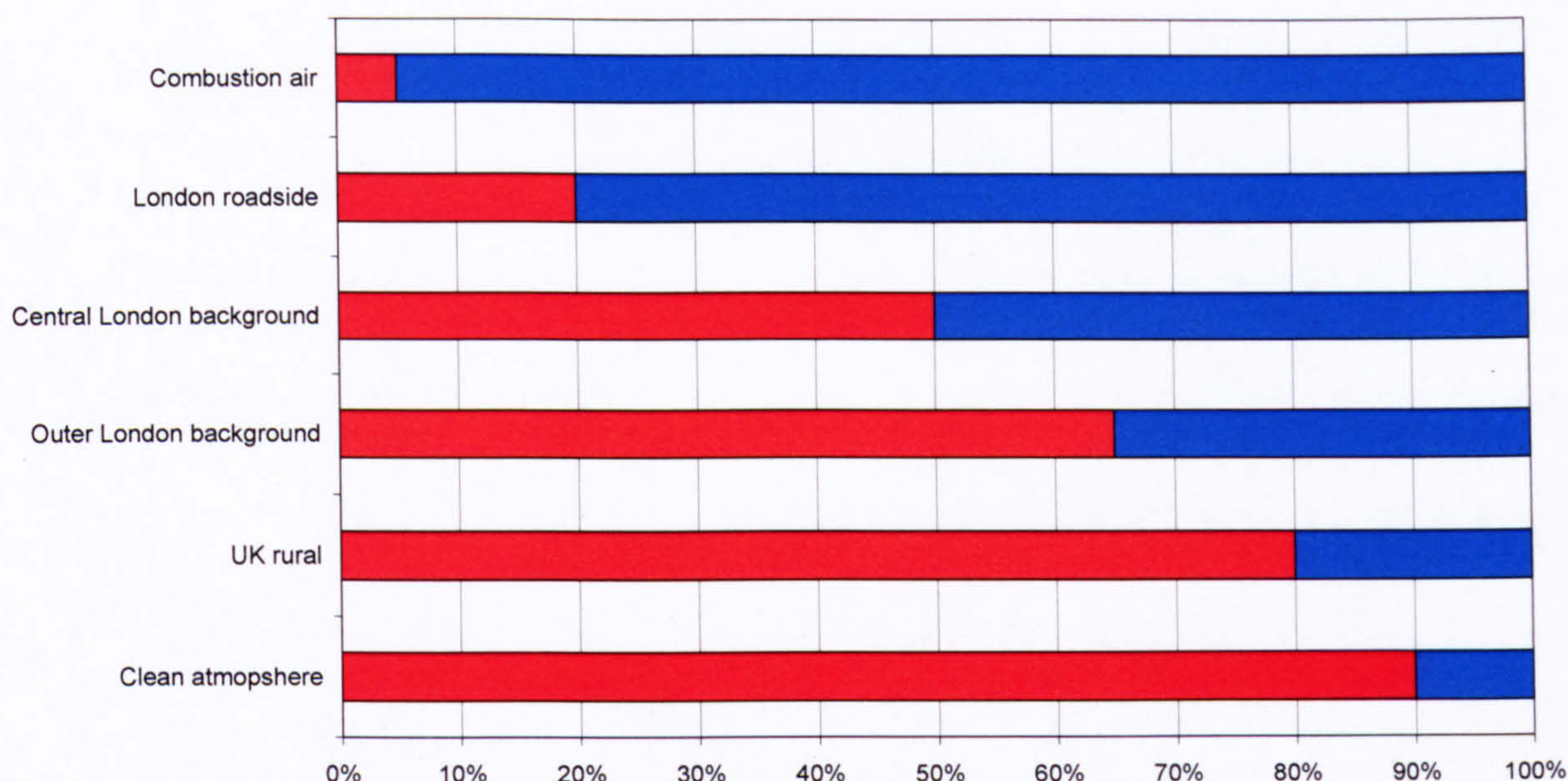


**Figure 4:** The partitioning of NO<sub>x</sub> in different environments. Red bars represent the fraction of NO<sub>2</sub> and blue represent NO. After Carslaw and Carslaw (2001)

Figure 5 depicts the typical diurnal profiles of NO, NO<sub>2</sub> and O<sub>3</sub> concentrations at a roadside location in York and are typical of polluted environments.

Typical night time NO<sub>2</sub> concentrations exceed those of NO, due to the relatively low NO emissions during these hours. The general decline in NO<sub>x</sub> through the night seen in Figure 5 illustrates the loss by dry and wet deposition of NO<sub>2</sub> and HNO<sub>3</sub>. During the morning rush hour period (~ 06:00 – 10:00) the fresh traffic emissions lead to an increase of ambient NO concentrations (NO > NO<sub>2</sub>). Some NO at this time will also be a result of NO<sub>2</sub> photolysis at dawn. The high NO concentration suppresses O<sub>3</sub> formation during this period as any O<sub>3</sub> is rapidly converted to NO<sub>2</sub> (reaction 3). The main production pathway for OH concentrations initially at dawn is through HONO photolysis (Fujita et al., 2003), followed by O<sub>3</sub> photolysis as the UV component of sunlight becomes stronger. NO<sub>2</sub> is formed through the conversion of NO via the suite of reactions involving peroxy radicals (reactions 10 to 18) and this, in turn, leads to an accumulation in O<sub>3</sub> concentrations during the early afternoon. Note the peak in O<sub>3</sub> concentration coincides with a dip in the ambient concentrations of NO since these two pollutants cannot co-exist at high concentrations for reasons explained in section 2.4.2.



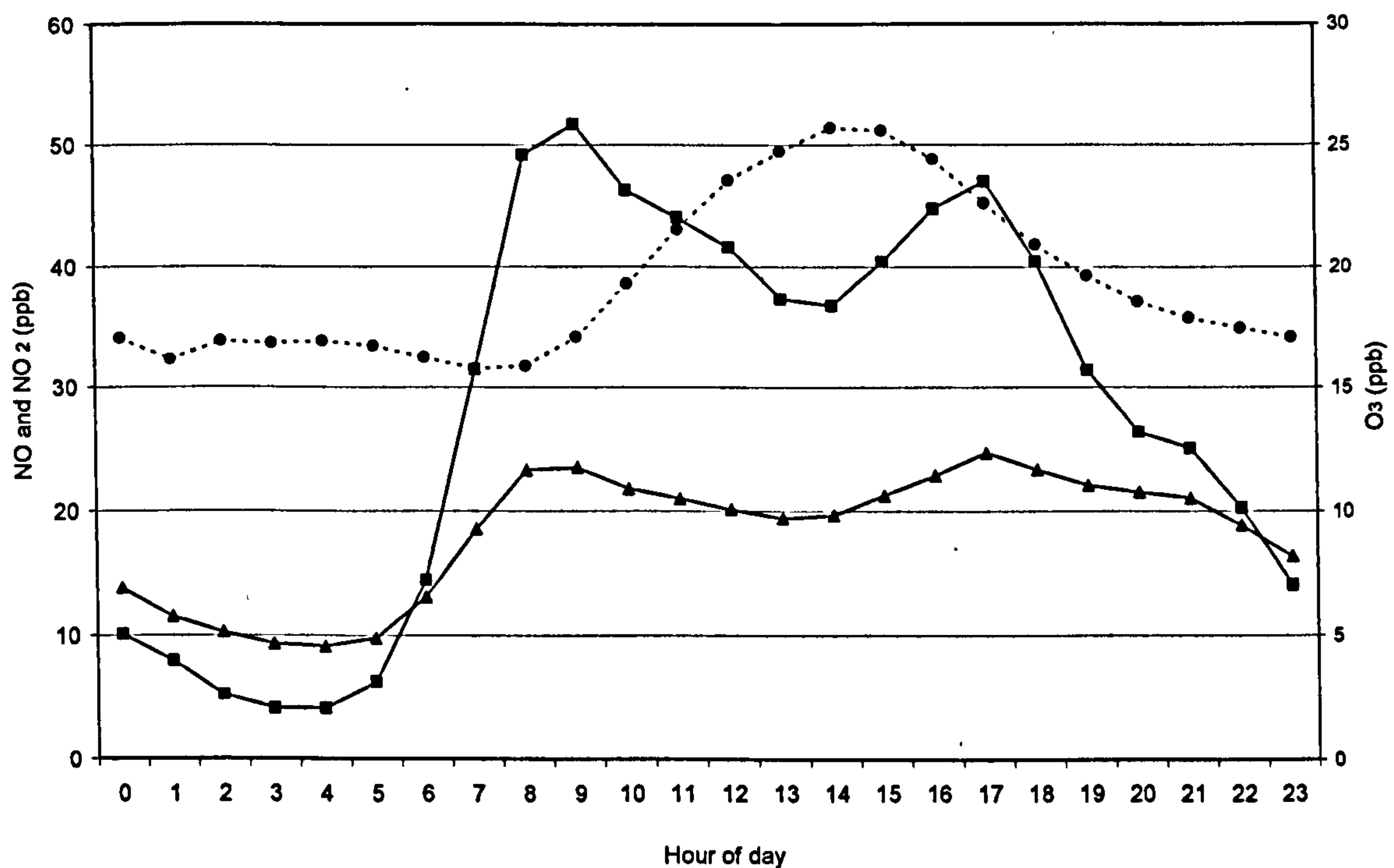


**Figure 5:** Mean diurnal profile for NO (solid line with squares) and NO<sub>2</sub> (solid line with triangles) concentrations from a roadside site in York city centre. The O<sub>3</sub> (dashed lines with diamonds) concentrations are from a background station located outside the city centre (as this is the only site where O<sub>3</sub> concentrations are measured in York). Data are averaged for the year 2000.

There are a number of studies that focus specifically on the chemistry of clean atmospheres (Carpenter et al., 1998 for example). One such location is the Cape Grim monitoring site on the northwest tip of Tasmania, Australia. This area has been studied as part of the Southern Ocean Atmospheric Photochemistry Experiment, or SOAPEX, as it is more commonly known.

In clean environments there is an overall net loss of O<sub>3</sub> throughout the day. This net loss is mainly attributable to the substantially lower amount of hydrocarbons (or VOCs) and NO<sub>x</sub> concentrations in clean environments as opposed to more polluted environments. The majority of VOCs present are a result of biogenic releases or have been transported from urban environments.

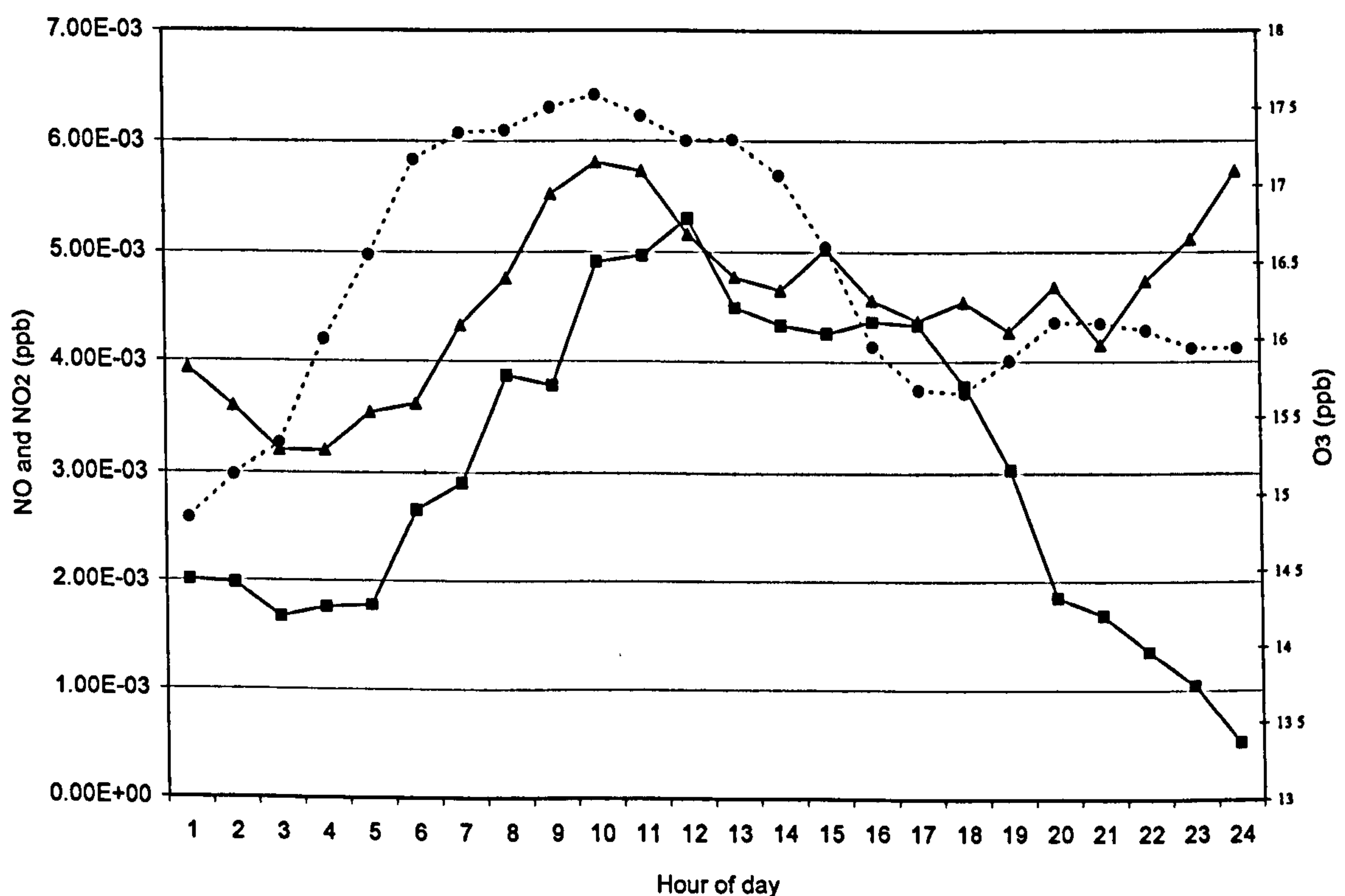
The O<sub>3</sub> present in a clean atmosphere is subject to reaction with OH (reaction 26) and HO<sub>2</sub> (reaction 27). As there is no means to reform O<sub>3</sub>, the O<sub>3</sub> is gradually destroyed. In the absence of NO<sub>x</sub>, peroxy radicals also enter reaction with other peroxy radicals (reaction 28), subsequently reducing the potential to create more O<sub>3</sub>.





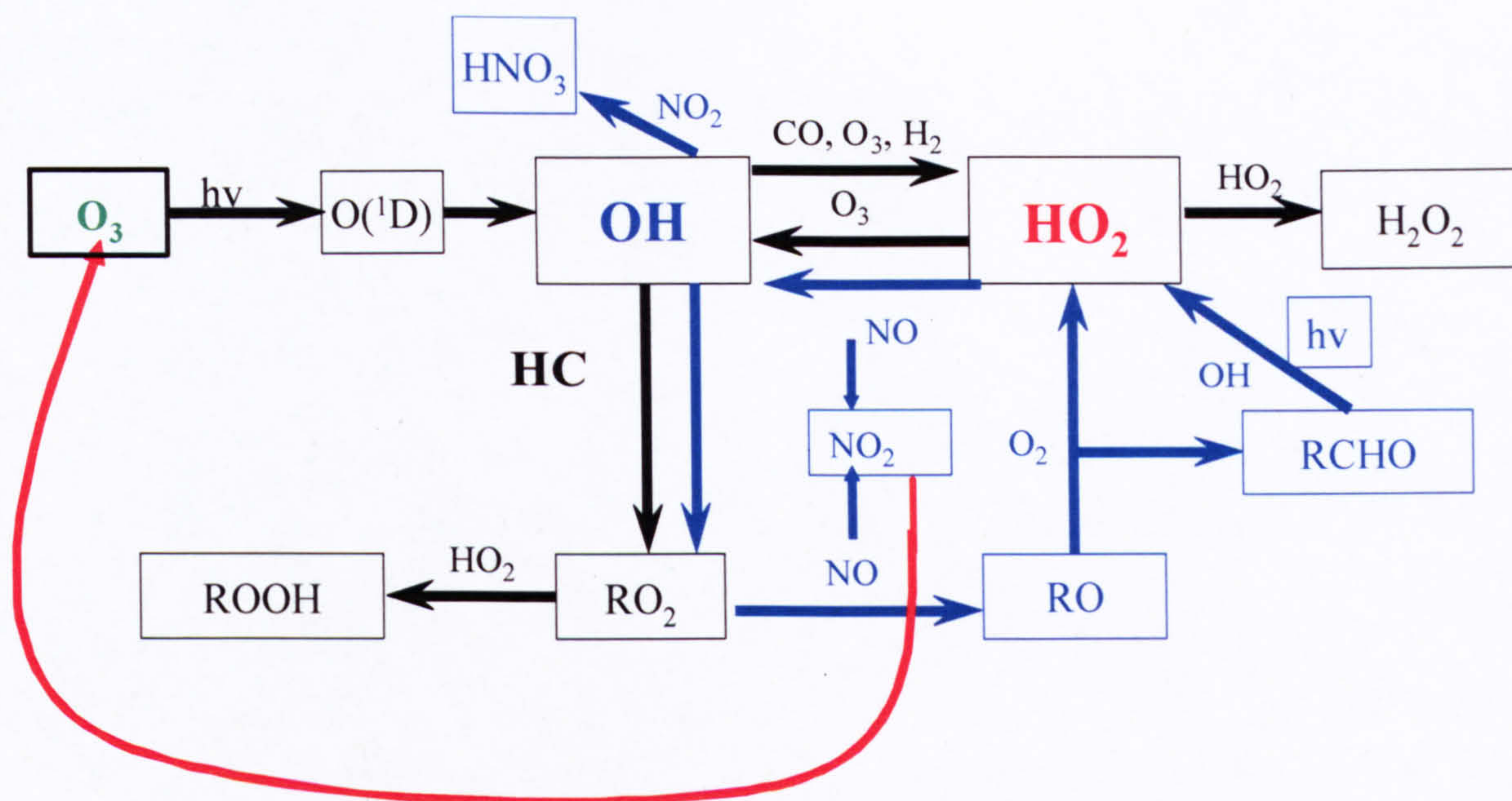
The peroxy radicals formed through PR –PR reactions (e.g. reaction 28) are removed from the atmosphere through dry and wet deposition and constitute a radical sink. Figure 6 depicts the typical diurnal profiles of NO, NO<sub>2</sub> and O<sub>3</sub> concentrations at Cape Grim (measurements recorded as part of the SOAPEX campaign). It can be seen that the concentrations of NO<sub>x</sub> and NO<sub>2</sub> for the clean atmosphere are much lower than those seen in the polluted atmosphere (Figure 5). Additionally, the diurnal profiles are also very different in Figure 6 than those in Figure 5. Firstly, the concentration of NO is not influenced directly by traffic emissions; instead there is a steady build up of NO as NO<sub>2</sub> is photolysed during the day. O<sub>3</sub> generally decreases throughout the day through its reaction with HO<sub>2</sub> (reaction 27): At night there is a general loss of NO<sub>x</sub> due to dry and wet deposition. The conditions shown in Figure 6 will be much closer to the photo-stationary state outlined in the section 2.4.2, than that seen in Figure 5.

Figure 7 depicts a schematic diagram of the chemistry of clean and polluted environments. The black lines depict the chemistry inherent in clean atmospheres. The blue lines show the added complexity seen in the chemistry of polluted environments i.e., through addition of NO<sub>x</sub>. The red line highlights the pathway to O<sub>3</sub> creation in polluted environments. This red line is not present in clean environments.



**Figure 6:** Mean diurnal profile for NO (solid line with squares), NO<sub>2</sub> (solid line with triangles) and O<sub>3</sub> (dashed line with diamonds) concentrations during the SOAPEX-2 campaign at the Cape Grim Baseline Air Pollution Station in north-western Tasmania, Australia in 1999. The data are a mean of four days of clean southern ocean marine boundary layer air. (Source: Sommariva et al., 2004)





**Figure 7:** A schematic of atmospheric chemistry in urban environments. HC represents hydrocarbons,  $\text{RO}_2$  are organic peroxy radicals, RCHO are aldehyde species and  $\text{ROOH}$  peroxide species. Blue arrows indicate polluted chemistry, black indicate clean chemistry. The red line shows the route to  $\text{O}_3$  production in polluted atmospheres.

## 2.5. Health effects of air pollution

There are a wide number of scientific studies that have investigated the link between air pollution (chiefly those pollutants included in air quality objectives) and health. For example, the 1994 study by Schwartz investigated the daily counts of hospital admissions (for the symptoms of pneumonia, asthma, chronic obstructive pulmonary disease) in Detroit, USA for individuals over the age of 65. The study discovered a statistically significant positive association between  $\text{PM}_{10}$  and pneumonia and COPD hospital admissions.

Larrieu et al. (2007) investigated the short-term association between cardiovascular disease hospitalisation and pollutant concentrations ( $\text{PM}_{10}$ ,  $\text{NO}_2$  and  $\text{O}_3$ ) for 8 French cities. The study found a statistically significant association between  $\text{PM}_{10}$  and  $\text{NO}_2$  concentrations with cardiovascular disease hospitalisation. Larrieu et al. (2007) also found that these associations were stronger in the sampled population that were over 65.

Also as part of the large consortium study, European APHEA project (Air Pollution and Health, a European Approach), Samoli et al. (2006) investigated the short-term effect of  $\text{NO}_2$  concentration on total, cardiovascular and respiratory mortality in 30 European cities. The study reported a significant association of  $\text{NO}_2$  with total, cardiovascular and respiratory mortality and found segregation between different sectors of Europe and population dynamics. For example, the association between  $\text{NO}_2$  and cardiovascular mortality was found mainly in western and southern Europe. Additionally, cities with a relatively greater proportion of elderly people showed a stronger association between  $\text{NO}_2$  and respiratory mortality. However, the authors of



the 2006 paper concluded that the effects of other pollutant concentrations, namely black smoke and SO<sub>2</sub>, could not be ruled out as causal factors (due to their high correlation).

Moreover, a paper that investigated the effects of winter air pollution on infants (younger than 3 years) bronchiolitis in Paris, found significant association between NO<sub>2</sub>, SO<sub>2</sub> and PM<sub>10</sub> concentrations and hospital admissions (Segala et al., 2008). The authors suggested that air pollution might act as a trigger for the occurrence of acute bronchiolitis cases. Other recent examples of epidemiological studies that have reported positive correlations between air pollutant concentrations and adverse health effects include: O'Neil et al., 2004; Naess et al., 2006; Schlink et al., 2006; Kan et al., 2007; Qian et al., 2007).

The health effects of traffic related pollutants has become a popular area of research (Clench-Aas et al., 2000; Kunzli et al., 2000; Brauer et al., 2002; Hoek et al., 2002; Paramesh, 2002; Pope et al., 2002; Solomon and Balmes, 2003). For example, Hoek et al. (2002) investigated the health impacts associated with living in close proximity to main roads. This study used an 8-year dataset of cardiopulmonary mortality, air quality and other confounding factors to investigate whether long term exposure to traffic pollution in individuals living at varying distances from a main road would result in significant health impacts. Indeed, the study concluded that living within 100 m of a main road results in a significant increase in cardiopulmonary mortality at a population level as a result of the increase in black smoke and NO<sub>2</sub> concentrations. The authors concluded that long-term exposure to traffic-related air pollution might shorten life expectancy. Additionally, the prevalence of childhood asthma has been shown to increase in children living in close proximity to roads (Paramesh, 2002).

It should however be noted that epidemiological studies should be interpreted with caution since the strong correlation between different air pollutants makes it difficult to separate the associated health effects (i.e., it is difficult to determine whether the negative health effect was a consequence of NO<sub>2</sub> or some other airborne pollutant).

Additionally, the statistical methods used to analyse the time series data of epidemiological studies cannot, with any degree of confidence, establish a causal effect. The results indicate that an association between health complaints and air pollution exists but there is no way for sure of determining whether this association is causal. The air pollutant concentration could merely be a surrogate for other factors not included in the model. However, with both these limitations in mind, epidemiological studies provide a valuable insight into the likely health consequences of air pollution in general and in the main the cocktail of pollutants associated with traffic is generally accepted as being damaging to health.

It should also be noted that some individuals of a population are more susceptible to the problems of air pollution than others. For example, children in particular are believed at risk since they take more breaths per unit body weight and have immature immune systems. Indeed, there are links between increased infant mortality and traffic-related pollutants (WHO, 1997). The elderly, and those individuals who are already suffering from poor health, are also extremely vulnerable in terms of the effects of air pollutants. In fact, a recent epidemiological study in Oslo,

Norway, which investigated the relationship between  $\text{NO}_2$  and  $\text{PM}_{10}$  exposures with cause-specific mortality, discovered those persons with a pre-existing medical condition, e.g. chronic pulmonary disease, to be more susceptible to air pollution at lower levels than the general population (Naess et al., 2006). This same study, found an increase in cause-specific deaths in the elderly (aged 50 - 90) above a threshold of  $40 \mu\text{g}/\text{m}^3$  concentration of  $\text{NO}_2$ , with the relationship increasing in severity for those individuals aged 71 -90.

## **2.6. Chapter summary**

The importance of urban air quality has been highlighted in the preceding sections. First, a brief history of air quality legislation was provided in section 2.1. This section highlighted changing public perceptions regarding air pollution plus its negative effects on human health and the environment. Next, the influence of physical properties, such as turbulence and meteorology, on ambient air pollutant concentration was explored in section 2.3. Finally, the chemistry involved in air quality is also important and section 2.4 outlined the basic chemical reactions controlling clean and polluted atmospheres.

The remaining Chapters of this thesis will draw upon the concepts outlined in this introductory Chapter to provide explanations as to the trends and behaviour of  $\text{NO}_x$  and  $\text{NO}_2$  concentrations recorded in the urban area of York.



## 3. Experimental

### 3.1. Introduction

This Chapter will outline the techniques used to measure ambient NO<sub>x</sub>, NO<sub>2</sub> and O<sub>3</sub> concentrations at the various monitoring stations in and around the City of York. A detailed description of the locations of the air quality monitors from which data have been used in this thesis is also provided. Finally, this Chapter provides details of the Meteorological Office site location at Church Fenton from which all meteorological data used in this thesis have been sourced.

### 3.2. Ambient NO<sub>x</sub> measurements

Chemiluminescence, the EU reference method for the measurement of ambient NO<sub>x</sub> concentration, is used in all NO<sub>x</sub> analysers included in York's air quality network. The technique has a low detection limit of around 1 µg/m<sup>3</sup>, and is accurate to within +/- 5% and precise to within 1% (PORG, 1997; AQEG, 2004).

Chemiluminescence works on the principal that light emitted from excited molecules (formed as a result of chemical reaction) can be used to measure the concentration of a gaseous species. The emitted light intensity is proportional to the concentration of the reactants and so by holding one of the reactants constant it is possible to measure the concentration of the other (Finlayson-Pitts et al., 2000).

The system works by continuously drawing samples of air into the analyzer. The air samples are then split into two sub-samples or streams. The first stream passes directly into a reaction chamber where O<sub>3</sub> is released. Any NO in the air sample reacts with the released O<sub>3</sub> to form excited NO<sub>2</sub> via reaction 29. The excited NO<sub>2</sub>, produced as a result of the reaction of NO and O<sub>3</sub> (reaction 30), emits light at wavelengths between 590 nm and 2800 nm. The amount of NO<sub>2</sub> in the reaction chamber is therefore directly indicative of the amount of NO in the sub-sample of air (Finlayson-Pitts et al., 2000), and allows the latter to be measured.



The second stream passes into a molybdenum catalyst that converts any NO<sub>2</sub> in the air sub-sample to NO. This is necessary because NO<sub>2</sub> does not undergo a chemiluminescent reaction with O<sub>3</sub>. The air sample (with the newly formed NO) then enters a reaction chamber and undergoes the same chemiluminescence process as described in reactions 29 and 30. The total NO<sub>x</sub> is then calculated by adding the NO concentration of the two air streams (namely, the NO and NO<sub>2</sub> from the air samples). The concentration of NO<sub>2</sub> is therefore not measured directly, but



is instead calculated from the difference between the measurements of total NO and total NO<sub>x</sub> ( $\text{NO}_2 = \text{NO}_x - \text{NO}$ ) (AQEG, 2004)

One problem with the chemiluminescence technique is the interference that results from other nitrogen containing species e.g. HNO<sub>3</sub>, HONO, PAN, alkyl nitrates etc. These other species can be reduced to NO by the molybdenum converter and consequently recorded as NO<sub>2</sub>. The AQEG (2004) conclude (based on the findings of other studies: Winor et al., 1974; Grosjean and Harrison, 1985; Gerboles et al., 2002) that the interference can be quite substantial at background locations, and for PAN and HONO, around 2% and 5% of the NO<sub>2</sub> concentrations recorded at background sites may be attributed to these two compounds, respectively. It is therefore possible that the measured NO<sub>2</sub> concentrations at the various sites across York could be slightly over estimated as a result of this interference from other compounds. However, the CYC follow a strict QA-QC procedure during the measurement of NO<sub>x</sub> and NO<sub>2</sub> concentrations at their various sites. For example, in addition to the manual calibrations carried out by a CYC officer every two weeks, the consultants NETCEN also check, calibrate, and validate the air quality measurements on a six monthly basis. The services of NETCEN ensure that the NO<sub>x</sub> and NO<sub>2</sub> measurements made at the automatic analyzers undergo a strict QA-QC procedure independent from the CYC and thus reduce the uncertainty associated with the measurement data. The QA-QC procedure is fully detailed in the Technical Annex 2: Air Pollution Monitoring in York' which was submitted with the Second and Third Stage Review and Assessment of Air Quality in York.

There are other NO<sub>x</sub> and NO<sub>2</sub> measurement techniques available, such as electrochemical cells, thick film sensors, diffusion tubes and DOAS (differential optical absorption spectroscopy). With the exception of diffusion tubes, none of these alternative techniques are deployed by the CYC in the measurement of NO<sub>x</sub> and NO<sub>2</sub> in York. Therefore, these methods shall not be considered further here. For a thorough outline of such techniques refer to the AQEG report of NO<sub>2</sub> (AQEG, 2004).

### **3.3. Ambient O<sub>3</sub> measurement**

Ambient O<sub>3</sub> concentration is measured by a UV photometric analyser at a single site in York (site fully described in following section). A UV photometric analyser works by exploiting the ability of O<sub>3</sub> to absorb light. A UV lamp emits radiation of wavelength 254 nm which is absorbed by the O<sub>3</sub> contained within the sample, at a rate proportional to the [O<sub>3</sub>] within it.

### **3.4. Air quality monitoring stations in York**

The review and assessment process of LAQM outlined in Chapter 2 (section 2.2.2) requires detailed information regarding the state of air quality across urban areas and so has driven the monitoring of ambient air pollutants throughout the UK. The proactive nature of the CYC's Air Quality Department has resulted in the purchase of nine permanent NO<sub>x</sub> monitors. These monitors are strategically located at various sites of interest around York (Figure 8).





**Figure 8:** The chemiluminescence analyser sites around the City of York. Bootham, City Centre, Fishergate Rawcliffe and Dunnington are the original five sites. Gillygate, Nunnery Lane, Holgate Road and Lawrence Street are the four newer ‘hotspot’ sites.

The LAQM process requires monitors to be located with regards to a classification system (Table 3). This system groups together sites of similar characteristics. However, the specific locations of each individual site may not fully represent all aspects of the classification system and so direct inter-city comparisons of sites contained within a single group can only be made with caution.

The CYC has given consideration to these different site types, in addition to public exposure risk and practical monitoring aspects, when locating each air quality monitor and diffusion tube.



**Table 3:** The air pollution monitoring site categories and their descriptions. (AQEG, 2004).

Type of site	Description
Kerbside	1 m from road edge. Representative of fresh traffic emissions.
Roadside	1 m to 5 or 15 m from road edge (depending on pavement width). Representative of local traffic emissions
Urban Centre	Non-roadside or kerbside. Representative of typical population exposure in town or city centre areas e.g. pedestrian precincts and shopping areas. Source influences include vehicle emissions and other general urban pollution sources.
Urban background	Distanced from emission sources but representative of general urban area pollutant concentrations e.g. parks and urban residential areas.
Urban Industrial	Located within close proximity to industrial activity.
Suburban	Representative of residential areas on the outskirts of a town or city. Source influences include traffic emission, domestic heating etc.
Rural	Representative of open country or locations away from large population centres, roads and industrial areas. Concentrations indicative of long range transport and urban plumes.
Remote	Representative of isolated rural areas (open country). Concentrations indicative of regional background pollution levels.

Despite York being relatively small compared to other cities, the air pollutant concentrations vary considerably from site to site. Data from all of the air quality stations are included in this thesis, save those from Rawcliffe. The Rawcliffe site had poor data capture and was relocated in 2001, resulting in an insufficient period of continuous data for analysis. Brief site descriptions of each of the eight remaining monitoring sites are provided in Table 4, along with their site types and a list of the pollutants monitored. Photographs of the eight sites are provided in Figure 9 to Figure 16.



**Table 4:** Descriptions of the eight permanent air quality monitoring stations around the City of York.

<b>Location</b>	<b>Site type</b>	<b>Pollutants monitored</b>	<b>Site description</b>
Bootham Hospital	Urban background	NO <sub>x</sub> , NO, NO <sub>2</sub> , SO <sub>2</sub> , PM <sub>10</sub>	The hospital ground represents one of the few open areas which are in close proximity to the City Centre but in a location away from main roads. The presence of the residential care unit and the outdoor sports facility make this a relevant location for the purpose of long term and short-term air quality objectives, respectively (Figure 9).
City Centre	Urban centre	NO <sub>x</sub> , NO, NO <sub>2</sub> , SO <sub>2</sub>	Located in the City Centre Manager's office on Parliament Street at the heart of the busy pedestrianised shopping area. As well as being a busy shopping area, the space outside the office is often used for outside events attracting large crowds of people. During the hours of 11:00 to 16:00 h vehicles are not allowed into the pedestrianised area. Outside these hours, delivery vehicles are permitted to use the road at the side of the office. The inlet point for the air pollution station is approximately 11 m from the side of this road (Figure 10).
Dunnington Village	sub-urban/ background	NO <sub>x</sub> , NO, NO <sub>2</sub> , SO <sub>2</sub> , O <sub>3</sub>	Dunnington is located 6 km to the east of York City Centre. National Power established the site for the purpose of monitoring potential emissions from the power stations of Drax, Ferrybridge and Eggborough. It is housed within a water pumping station and meets all the necessary criteria for a background-monitoring site. The site is approximately 30 m from the nearest houses and is adjacent to a children's playground. It is therefore a relevant location for both short term and long term air quality objectives (Figure 11).



Location	Site type	Pollutants monitored	Site description
Fishergate	Roadside	NO <sub>x</sub> , NO, NO <sub>2</sub> , PM <sub>10</sub>	This site is located adjacent (3 m) to the busy main road of Fishergate. This is to the south east of the city centre close to where the busy A19 arterial route meets the Inner Ring Road. The station is located on a large triangular shaped traffic island in the centre of the road. The monitoring site is located close to the entrance of a primary school and a number of houses, from which parents and residents have raised concerns about air pollution. The area also experiences severe congestion during rush hour periods (Figure 12).
Gillygate	Roadside	NO <sub>x</sub> , NO, NO <sub>2</sub>	This street is located to the north of the city close to where the A19 arterial route meets the inner ring road. Gillygate is a narrow canyonised street with poor dispersion of traffic pollutants. During a considerable period of the day there is queuing traffic along Gillygate. The majority of premises along this road are small businesses and shops that have residential properties above. However, there are a number of residential properties at street level on the west side of the street (Figure 13).
Holgate Road	Roadside	NO <sub>x</sub> , NO, NO <sub>2</sub>	Holgate Road (A59) is located to the south west of the city centre close to where the A59 and the A1036 meet the inner ring road. Traffic lights on this road cause standing traffic throughout the day. Holgate Road is primarily a residential area but also contains a few small shops and business premises (Figure 14).
Lawrence Street	Roadside	NO <sub>x</sub> , NO, NO <sub>2</sub> , PM <sub>10</sub>	Lawrence Street is located to the east of the city centre, on the A1079 that leads towards the A64 outer ring road. There is substantial queuing throughout the day owing to the traffic lights at the junction of the Lawrence Street with the A1079. There is a mixture of residential, business and light industry along this road. It is also the main access point for the James Street Industrial Park. Recent redevelopment has introduced a greater proportion of residential properties along Lawrence Street (Figure 15).
Nunnery Lane	Roadside	NO <sub>x</sub> , NO, NO <sub>2</sub> , PM <sub>10</sub>	Nunnery Lane is located to the south west of the city centre and forms a one-way gyratory system. This area experiences severe congestion during rush hour periods and is busy throughout the day. There is a high proportion of residential properties and a large school and car park to the north (Figure 16).



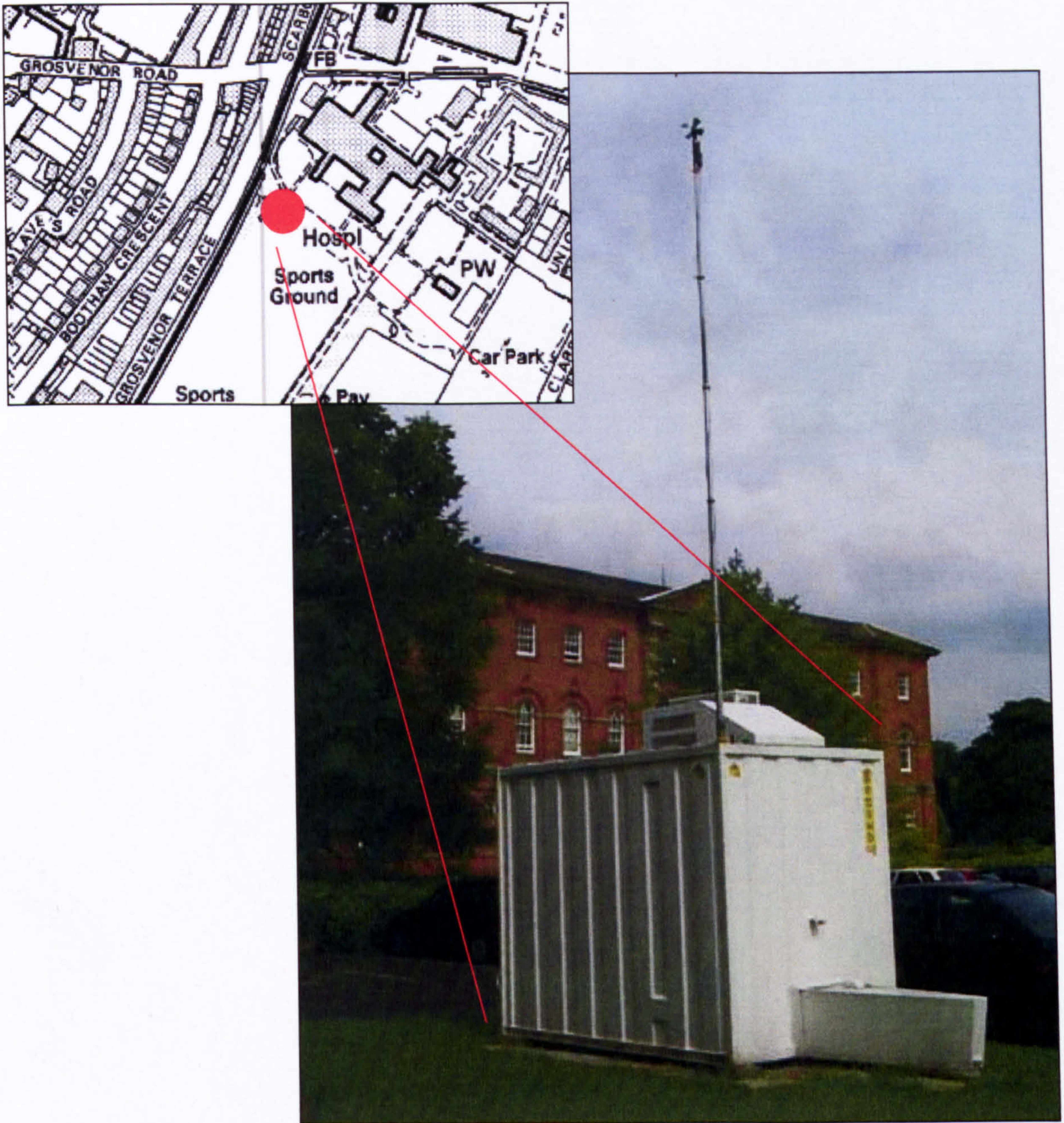


**Figure 9:** Location of Bootham monitoring station. Image taken from the City of York Council's website (Yorair.co.uk ). Coordinates: 460 022, 452 777.





**Figure 10:** Location of City Centre monitoring station. Image taken from the City of York Council’s website (Yorair.co.uk ). Coordinates: 460 427, 451 768



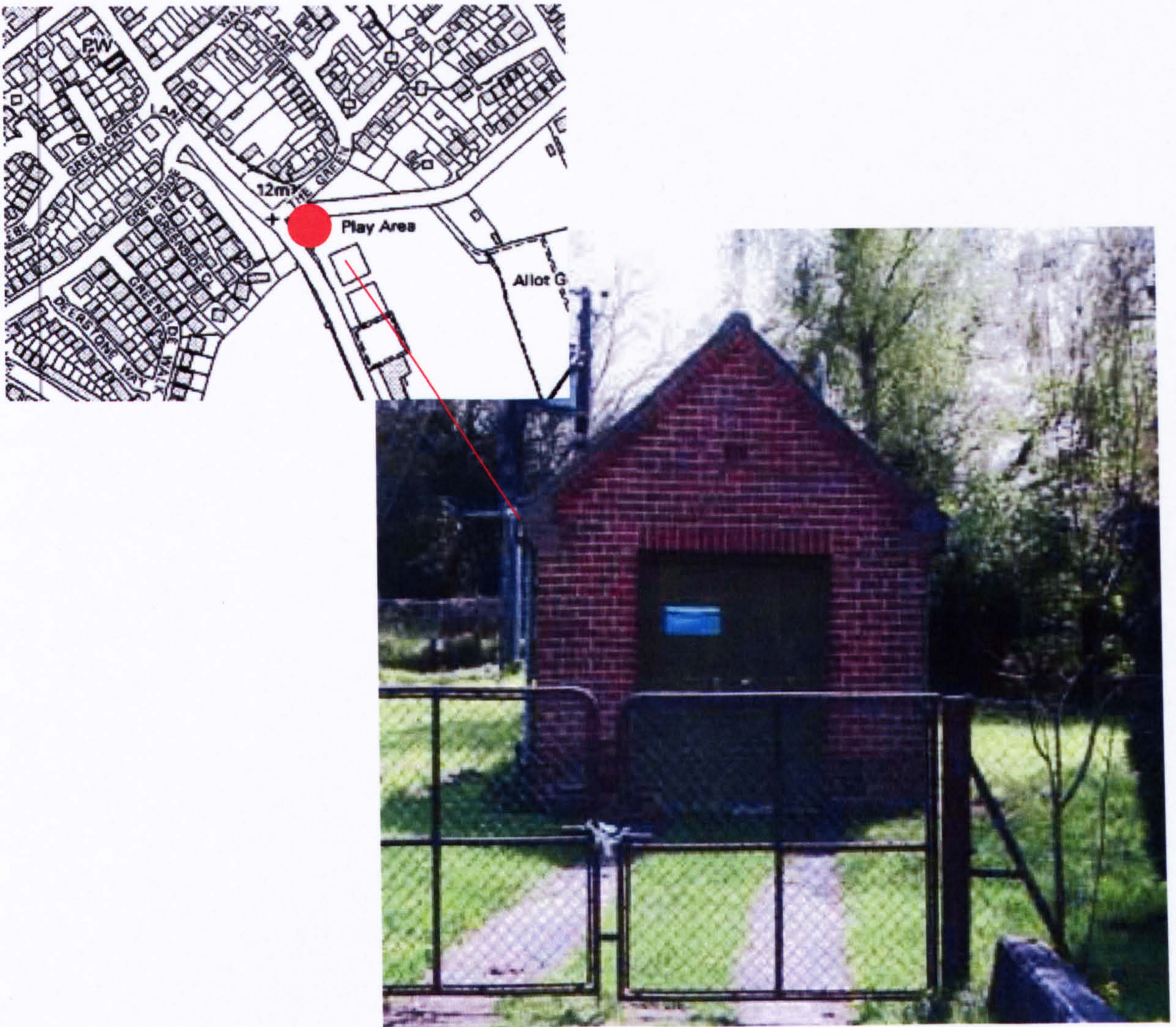


**Figure 11:** Location of Dunnington monitoring station. Image taken from the City of York Council's website (Yorair.co.uk ). Coordinates: 467 275, 452 355



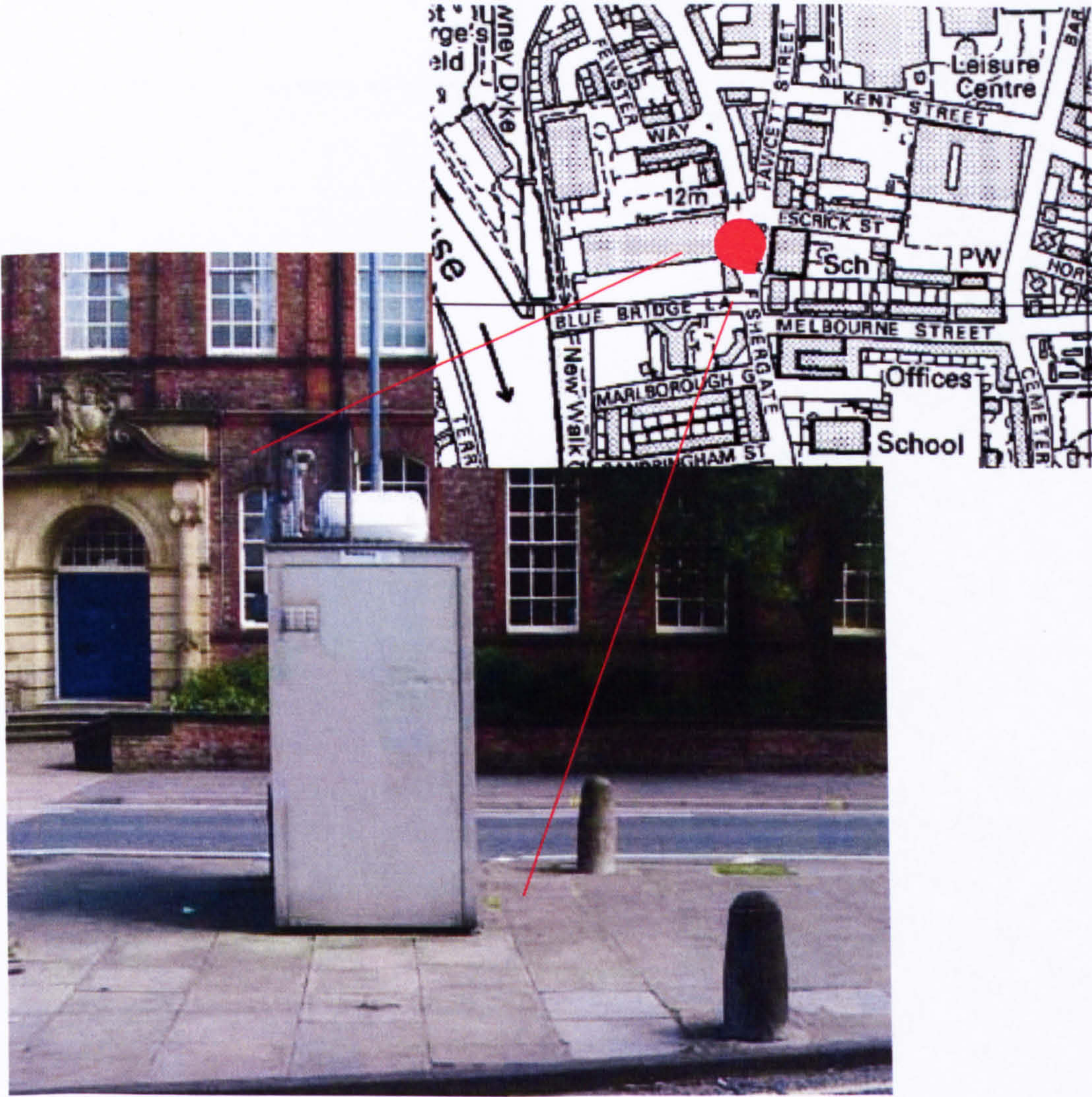


**Figure 12:** Location of Fishergate monitoring station. Image taken from the City of York Council's website (Yorair.co.uk ). Coordinates: 460 746, 451 638





**Figure 13:** Location of Gillygate monitoring station. Image taken from the City of York Council's website (Yorair.co.uk ). Coordinates: 460 147, 452 345





**Figure 14:** Location of Holgate Road monitoring station. Image taken from the City of York Council's website (Yorair.co.uk ). Coordinates: 459 512, 451 282



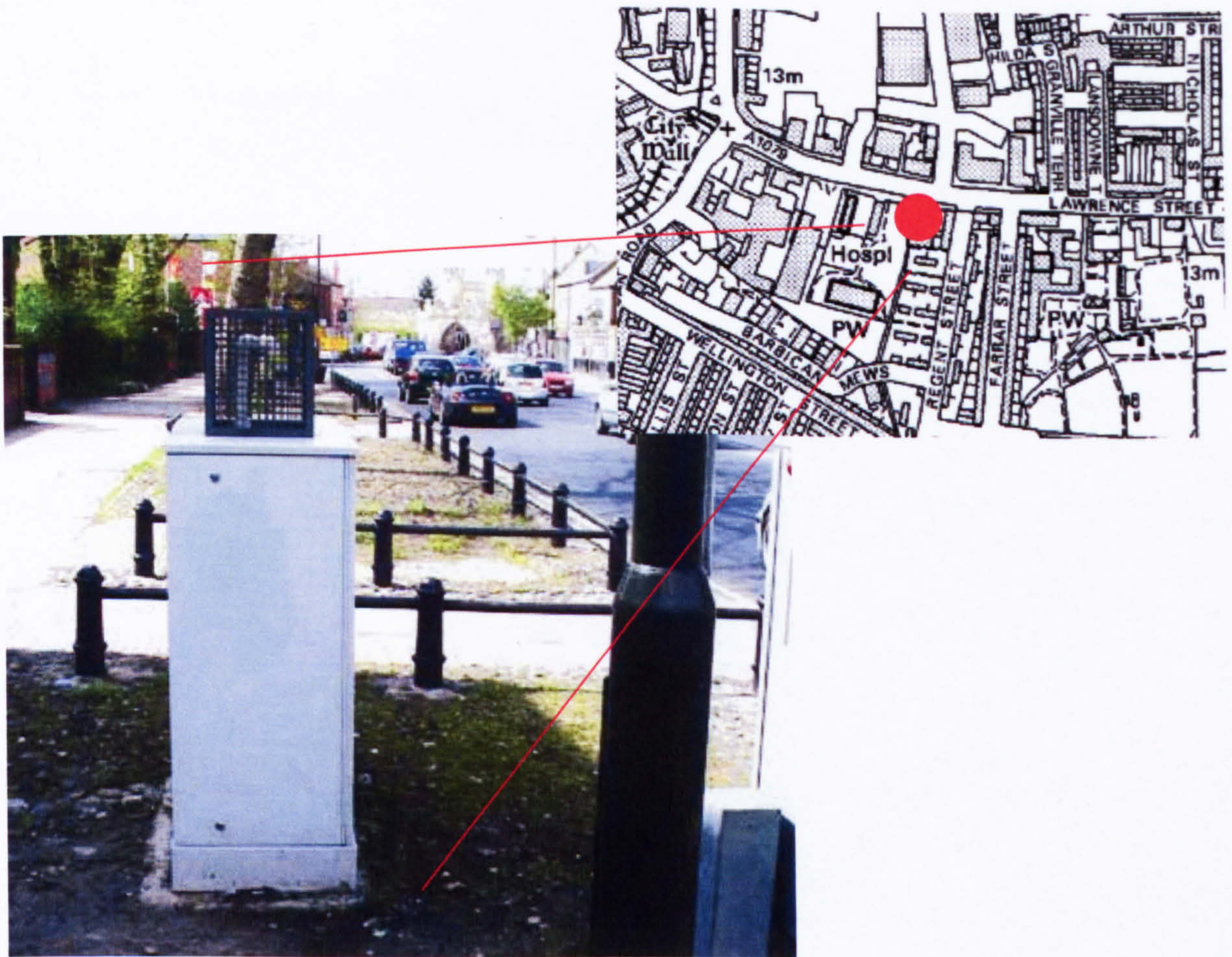


**Figure 15:** Location of Lawrence Street monitoring station. Image taken from the City of York Council's website (Yorair.co.uk ). Coordinates: 461 256, 451 340





**Figure 16:** Location of Nunnery Lane monitoring station. Image taken from the City of York Council's website (Yorair.co.uk ). Coordinates: 460 068, 451 199

The air quality monitoring network in York has undergone many changes over the 8 year period of monitoring and these changes are summarised in Table 5. The sites of Bootham, Fishergate, Dunnington and Fishergate (referred to as long-term sites) were the first established in York in 1999. Dunnington is also the only location in which ambient  $O_3$  concentrations are made in York. The  $O_3$  monitor was established in 1999 and measurements continue to the present day. Towards the end of 2003 the sites of Gillygate, Holgate Road, Lawrence Street and Nunnery Lane were introduced to provide information regarding pollution hotspots in York.

There have been several instances where monitors have been removed or relocated, for instance the chemiluminescence analyser at Dunnington was removed during the second half of 2006. Therefore, only  $NO_x$  and  $NO_2$  data for the period shown in Table 5 are included in this thesis (note,  $O_3$  data from Dunnington are available for the full year of 2006). Additionally, the chemiluminescence analyser at the City Centre site was relocated after 2005 from one end of Parliament Square to the other. For the purpose of this thesis only data from the City Centre original location have been included in the analysis.



**Table 5:** The status of air quality monitoring sites in York over the period 1999 to 2007. Note only the sites which monitor NO<sub>x</sub> and NO<sub>2</sub> are included. Shaded areas illustrate periods when a site was in full operation.

Site name	1999				2000				2001				2002				2003				2004				2005				2006				2007			
	s	s	a	w	s	s	a	w	s	s	a	w	s	s	a	w	s	s	a	w	s	s	a	w	s	s	a	w	s	s	a	w	s	s	a	w
Bootham																																				
Dunnington																																				
Fishergate																																				
City centre																																				
Gillygate																																				
Lawrence St																																				
Nunnery La																																				
Holgate Rd																																				

### 3.5. Meteorological data

Data from a single Meteorological Office station have been included in this study. Church Fenton (station id number 03355) is located around 20 km to the south west of York (53, 48 N; 001, 33 W) and is believed to give a good representation of the wind speeds and direction in York (Meteorological Office). This station is at a height of 10 m.

The following parameters are recorded on an hourly basis: temperature (degrees), humidity (%), cloud cover (Oktas), precipitation (mm), wind speed (m/s), wind direction (degrees) and pressure (mbar).



## **4. ADMS-Urban validation**

### **4.1. Background and introduction**

Air quality monitoring is often constrained by budget costs. In addition, measurements are confined to sites with monitoring equipment, with the air quality at interim locations being a largely unknown quantity. For these reasons, the importance of emission inventories and dispersion models in the air quality management process has been highlighted by government bodies (DETR, 2000); they are considered complementary to air quality monitoring.

ADMS-Urban is an atmospheric dispersion model. The development of ADMS-Urban was driven by the Cambridge Environmental Research consultants (CERC) in response to the release of the National Air Quality Strategy in 1997. The Government helped fund the project, along with a consortium of organisations including the Meteorological Office and National Power (Hanna et al., 1999). The current version of ADMS-Urban stems from the original industrial pollution model, ADMS 3, which specialised in mapping the distribution of pollutants from industrial point sources. ADMS-Urban has evolved through a series of revisions and re-releases the most recent of which, version 2.2, was released in January 2006.

As the name suggests, ADMS-Urban is a dispersion model used to reconstruct the urban environment and track the dispersion of pollutants from their origin. The model can be used both to predict future pollutant concentrations in response to policy changes, and to predict present day concentrations at a variety of spatial locations. The model can also be used in conjunction with GIS or SURFER to produce pollution contour plots for an urban area.

ADMS-Urban is used widely by local authorities to assist in their air quality management processes; the modelling work can be carried out in-house or the local authority can hire CERC (or other air quality consultants) to carry out the work on their behalf. ADMS-Urban is now used widely across the UK.

### **4.2. Emissions inventory and emissions calculations**

#### **4.2.1. Emissions introduction**

A fundamental input requirement for dispersion models is a list of emission sources with their relevant locations (emission inventory). Emissions inventories can range from a simple summary of estimated emissions to a comprehensive database of geographically referenced emission sources (including the rate and quantity of pollutants released). They are essentially a complete list of all emission sources for a given area. It is important that emission inventories contain the most detailed information possible and are updated continuously, since any uncertainties will be inherent within dispersion model results and, in turn, management decisions.



It is often necessary to calculate the level of pollutant emissions from a particular source since exact emission levels are not fully known; this is often the case with road traffic emissions. Emission levels can be estimated from activity data and emissions factors. Activity data are a measure of consumption or use. In the case of transport, the required activity data are traffic counts, preferably categorised by vehicle type. For industrial sources the activity data usually describe the amount of fuel consumed or the amount of end product produced. Emissions from domestic sources can also be estimated using the number of dwellings in a particular area.

Emissions factors are calculated by specialist organisations (e.g. Department for Environment Food and Rural Affairs (DEFRA)) from laboratory and field tests. They characterise the rate at which emissions are released per unit activity i.e. miles travelled or fuel consumed etc.

The total emissions from a particular source are then calculated using Equation 2, where  $E$  is total emission rate (tonnes/year),  $A$  is the activity (unit activity/year) and  $E_f$  is the emissions factor (tonnes of pollutant/unit activity).

$$E = A * E_f$$

Equation 2

#### 4.2.2. Calculation of traffic emissions

Transport emissions are an important source of airborne pollution. It is necessary, and desirable, to calculate the volume of traffic emissions for a range of different pollutants, so that a more complete understanding of air pollution can be gained.

##### 4.2.2.1. Traffic emission factors

The amount of emissions produced from transport can vary quite substantially from vehicle to vehicle and is dependent on fuel type, vehicle type, speed, acceleration and age of vehicle (CERC, 2006b). There are, therefore, a great number of emissions factors associated with the particular type of vehicle (e.g. car/HGV/LGV etc.), the speed the vehicle travels (e.g. 10 mph, 20 mph etc.) and also the age of the vehicle (e.g., EURO 1, EURO 4 etc.). Emissions factors are designed to take into consideration all these factors and essentially quantify the volume of emissions of a particular pollutant per unit travelled. Table 6 highlights the detail employed by emission factor datasets. Note that Table 6 only shows the  $\text{NO}_x$  emissions factors; emissions factors for other pollutants are available but are not shown. It can be seen that for petrol cars alone, there are 30 different sub-categories; each of which has its own unique emission factor.

A number of organisations attempt to classify and quantify the volume of emissions associated with transport sources. These emissions factors are contained in comprehensive databases and are available on the internet (e.g., [http://www.naei.org.uk/data\\_warehouse.php](http://www.naei.org.uk/data_warehouse.php) contains a number of different emissions factors available for use when calculating transport emissions).



ADMS-Urban utilises a number of different databases, containing emission factors from a variety of different sources: DEFRA, National Atmospheric Emission Inventory (NAEI), and the UK Highways Agency. These emissions factors are not editable and the user needs to decide upon which set of emissions factors to use when calculating traffic emissions for the road network in question.

#### **4.2.2.2. Activity data**

Activity data are source specific (i.e., vary from road to road). The required elements include: vehicle count, vehicle type, and the length of road.

Traffic counts can be obtained either from observations, that is, traffic surveys, or they can be estimated from traffic models, such as in the case of the CYC and the SATURN traffic model. Traffic counts are commonly expressed as the total number of vehicles per day on a particular road, and are referred to as AADTs (annual average daily traffic). It is usual to have a unique AADT estimate for each road link in the area under examination.

Traffic type, or the fleet component, is the breakdown of the road-specific AADT estimate into a number of different categories representing the different types of traffic e.g. cars, buses, LGVs etc. There are two classification systems used in ADMS-Urban; the first system splits vehicles into three types: light, heavy and motorcycles; the second splits vehicles into 11 different categories, see Table 7, and is based on the London Atmosphere Emissions Inventory (LAEI) system. Again, the fleet components for various road links can either be obtained by local observations, or from national statistics from sources such as the DVLA (Driver and vehicle License authority) or Department of Transport. Note, the vehicle classification systems exist at a much broader resolution compared to those used in the emission factor databases due to sampling limitations.



**Table 6:** Emission factors for NO<sub>x</sub> for the various vehicle sub-categories for petrol cars travelling at 40km/hr from the NAEI (In ADMS-Urban it is known as EURO SCALED 03). This set of emission factors is supplied in ADMS-Urban.

<b>EURO standard</b>	<b>Engine size</b>	<b>Emission factor (g/km)</b>
Pre- ECE	< 1.4 l	1.849
	1.4 - 2.0 l	2.164
	> 2.0 l	2.860
ECE 15.00	< 1.4 l	1.849
	1.4 - 2.0 l	2.164
	> 2.0 l	2.860
ECE 15.01	< 1.4 l	1.849
	1.4 - 2.0 l	2.164
	> 2.0 l	2.860
ECE 15.02	< 1.4 l	1.619
	1.4 - 2.0 l	1.831
	> 2.0 l	2.066
ECE 15.03	< 1.4 l	1.680
	1.4 - 2.0 l	1.917
	> 2.0 l	2.806
ECE 15.04	< 1.4 l	1.382
	1.4 - 2.0 l	1.742
	> 2.0 l	2.090
Euro I	< 1.4 l	0.258
	1.4 - 2.0 l	0.227
	> 2.0 l	0.302
Euro II	< 1.4 l	0.152
	1.4 - 2.0 l	0.315
	> 2.0 l	0.176
Euro III	< 1.4 l	0.091
	1.4 - 2.0 l	0.189
	> 2.0 l	0.105
Euro IV	< 1.4 l	0.049
	1.4 - 2.0 l	0.101
	> 2.0 l	0.056



**Table 7: The LAEI 11-category vehicle classification system**

Vehicle type	Description
Motor cycles	Including scooters.
Cars	Including saloon, small car, estate, people carrier, car towing caravan (counted as one vehicle), 3-wheeler cars, Land rover/ Range rovers and Jeeps. Includes light vans with side windows to the rear of the drivers seat e.g. camper vans
Taxis	Black cabs and private license vehicles
LGVs	Includes all vehicles up to 3.5 tonnes. All car delivery vans and transit vans. Small pick up trucks, milk floats, ambulances. Also includes three wheeled goods vehicles.
Buses and coaches	Including work buses but not mini-buses
Rigid HGVs 2 axles	Includes rigid vehicles over 5 tonnes with two axles. (Axles = set of wheels). Tractors, road rollers, box vans and similar large vans. Usually less than 17 tonnes
Rigid HGVs 3 axles	Includes all non-articulated goods vehicles with three axles irrespective of the position of the axles.
Rigid HGVs 4+ axles	Includes all non-articulated goods vehicles with four plus axles, regardless of the position of the axles.
Articulated HGVs 3&4 axles	Includes all articulated vehicles with three or four axles regardless of the position of the axles.
Articulated HGVs 5 axles	This includes all articulated vehicles with a total of five axles regardless of the position of the axles.
Articulated HGVs 6+ axles	This includes all articulated vehicles with a total of six or more axles regardless of the position of the axles.

#### 4.2.2.3. Route types

A translator or bridging mechanism is needed to bridge the gap between the broad activity data categories (i.e., the 11 category system outlined in Table 7) and those of the finer resolution emission factors required by the model (i.e., the 30 category system outlined in Table 6; note this was for cars only, there are many more categories for each of the other vehicles types). Route types therefore breakdown the fleet components into the various vehicle sub-categories used by emission factors. They in effect split the AADT from the 3 or 11 category systems into the more detailed categories used to calculate the emission factors. This splitting process represents the various proportions of vehicles for the sub-categories that would be found on the road network in question and is illustrated in Figure 17.



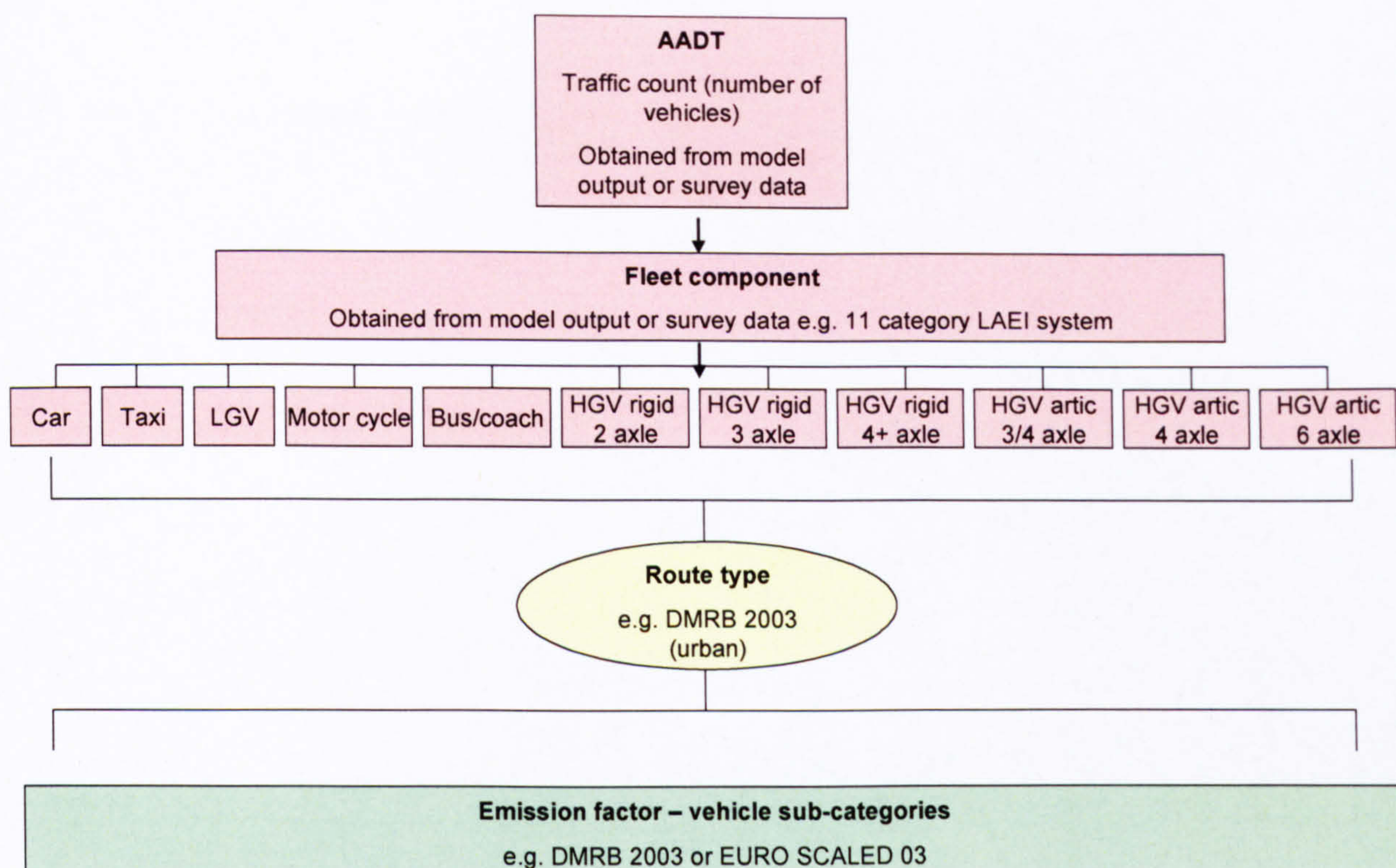


**Figure 17:** A schematic of the various input and reference data needed when calculating emissions from road sources. Activity data are in pink, emission factors in green and the route type in yellow.

A number of pre-defined route types, based on national average traffic data (transport statistics), are supplied for use in EMIT and ADMS-Urban. The data contained in these pre-defined route types are calculated from national transport information collected by various organisations, such as the DVLA and represent the general composition of traffic seen on a national scale.

### 4.2.3. York emission inventory

The CYC maintains and operates an emissions inventory for the City of York. It contains emissions for all major sources found in the urban area of York and includes all main roads (line sources), industrial practices (point sources), minor roads (grid sources), domestic emissions (grid sources) and major railway lines (line sources). The various emission sources included in the York emissions inventory are shown in Figure 18.





**Figure 18:** Illustration of emission source types in York. Green lines indicate railways, blue lines are major roads, red circles are point sources in York, and orange grids are minor roads, blue grids are commercial and domestic grid sources.

The 11 point sources include major power stations such as Drax and Ferrybridge, but also smaller point sources such as British Sugar and the York District Hospital. The volume of emissions for the various point sources is estimated from activity data (i.e., fuel consumed).

The AADT and average speed of traffic are calculated using the traffic model, SATURN. This model produces information for all 921 road links in the network (Figure 18). The breakdown of vehicles into the various emission factor sub-categories is based on national transport statistics. The remaining traffic and road data (i.e. vertices, width, canyon height etc.) were put together by survey work carried out by the CYC. This information is then used to calculate the total emissions for the major road links in York.

Minor (background) roads are those considered too small to be included explicitly in the emissions inventory (i.e., many are small residential roads) and are thus modelled by a grid system. Grid modelling reduces the complexity of models and so model run times are shortened. A further 401 grid sources are also included in the emission inventory to represent the emissions associated with commercial and domestic emissions (i.e., central heating). Again, it would be extremely difficult to include the emissions associated with every single building in an urban environment and so total emissions from this source type are lumped together and calculated on a 1 km by 1 km grid basis.

The volume of emissions from the various source types highlighted in Figure 18 are categorised in Table 8. The greatest source of NO<sub>x</sub> emissions contained in the York emissions inventory are those from the major roads with over 800 tonnes a year. The commercial and domestic (C and D) sources constitute the next highest source of emissions in the urban area of



York. However both industrial and minor road emissions contribute to a substantial fraction of the total emissions contained in the York emissions inventory.

**Table 8:** Breakdown of total NO<sub>x</sub> and NO<sub>2</sub> emissions (tonnes/year) of the various sources included in the emissions inventory for York. For the year 2005 only as these are the most up to date emissions available.

<b>Emission source</b>	<b>NO<sub>2</sub></b>	<b>NO<sub>x</sub></b>
Commercial and domestic sources (grids)	32.8	328.6
Industrial point sources	32.7	326.5
Minor roads (grids)	30.5	304.8
Rail	10.4	104
Major roads	82.0	819.5
<b>TOTAL</b>	<b>188.4</b>	<b>1883.4</b>

### 4.3. ADMS-Urban

The dispersion model, ADMS-Urban, uses a Gaussian approach to model atmospheric dispersion. This is a simple method of modelling the release of emissions from a particular point source and projecting the dispersion pathway of the pollutants. Complex mathematical formulas are used to describe the lateral and vertical spread in an emissions plume.

Dispersion modelling originates from pioneering research by Pasquill in the 1950s (AQEG, 2004), which investigated the stability of the atmospheric boundary layer. The work was later built on by Gifford, and resulted in the discrete stability classifications of the atmosphere. The old generation dispersion models are therefore based on the assumptions that the boundary layer falls into these 8 discrete categories (Carruthers et al., 1994; Hanna et al., 1999). These old models do not allow for differences in atmospheric conditions with increasing height i.e. the atmosphere may appear neutral at the surface, but in fact becomes convective in nature at higher levels.

However, since the 1950s and 60s there has been substantial research in this area that has led to a new generation of dispersion models. These new generation models assume a continuous scale by which the boundary layer is categorised (Hall et al., 2000). These new models parameterise the boundary layer in terms of boundary layer depth and Monin-Obukhov length (Carruthers et al., 1998) and allow for a more realistic representation of the vertical variations in turbulence (Carruthers et al., 1997).

Additionally, there are two schemes of chemistry included in the ADMS-Urban framework. The first scheme is based on the semi-empirical photochemical model developed by Venkatram et al. (1994). The Generic Reaction Set (GRS), which attempts to consider the key chemical reactions involving NO<sub>x</sub> and VOC in a set of 7 reactions. The second chemical scheme



in ADMS-Urban is based on the work by Derwent and Middleton (1996) in London. This second scheme does not treat chemistry explicitly and instead, approximates the production of  $\text{NO}_2$  from the 'mean weighted plume age' at the site in question.

Finally, ADMS-Urban incorporates the street canyon model, OSPM, to describe the dispersion of pollutants in street canyon environments (Berkowicz, 2000). The presence of street canyons can have a profound affect on the dispersion of pollutants in such environments as an across canyon vortex can be established when the wind flow is blowing perpendicular to the canyon. The presence of these eddies leads to a recirculation of air inside the canyon, and thus circulation of emissions. The highest ambient pollutant concentrations in such streets therefore tend to occur when the wind is blowing away from the point in question towards the road, the exact opposite of what would usually occur in a non street canyon environment.

#### **4.4. Aims**

Traffic emissions are an important aspect of the air quality in urban areas. Indeed, the breakdown of emissions contained within the York emissions inventory shown in Table 8 highlight this importance. At present the traffic emissions estimated for York are not based on local activity data and so potentially represent a source of uncertainty in the predictions made with ADMS-Urban. Other local authorities, however, have fine-tuned their transport emissions calculations to more accurately represent the traffic fleet using their road network; indeed, the London Atmospheric Emissions Inventory (LAEI) uses a combination of automatic traffic counters and manual surveys to produce a comprehensive database of London transport emissions. Therefore, an important aim of this thesis and the primary aim of this Chapter was to design and execute a study to provide information to 'update' the York traffic emissions contained within the York emissions inventory.

Secondly, a series of model scenarios will be created so that the input sensitivities of ADMS-Urban can be characterised. This will include investigating the impact that changing the meteorological data can have on the  $\text{NO}_x$  and  $\text{NO}_2$  predictions. Also, adjustments regarding the fraction of primary  $\text{NO}_2$  will be investigated.

### **4.5. Update of traffic emissions for the York area**

#### **4.5.1. Introduction**

As already outlined, the traffic model SATURN provides an estimate of traffic volume for the main road links in the York area (i.e., those that would be modelled explicitly in ADMS-Urban). This model also provides an estimation of the average vehicle speed for each road link based on the national speed limit. Additionally, the CYC recently carried out a comprehensive survey of road length, road width and canyon height of each road link included in the emissions inventory.



However, the fleet compositions used to calculate traffic emissions are currently based on national transport statistics. Essentially there are no locally relevant data available regarding the breakdown of vehicle types using the road network in York. Since transport emissions are highly dependent on vehicle type (among other factors) it was considered necessary to undertake a comprehensive assessment of vehicle composition across the York road network so that a better understanding of vehicle fleet could be gained. It was therefore decided that a systematic series of traffic surveys should be carried out in York to provide detailed and locally relevant traffic information which could then be used to ‘fine-tune’ the calculation of traffic emissions for the York area and so enhance the air quality modelling process.

#### **4.5.2. Traffic survey methodology**

In an attempt to collect information relating to the traffic composition of the York traffic fleet a detailed traffic survey was designed and implemented in 2006. A total of six sites was surveyed at various locations across the city: three sites on main arterial routes, two sites on the inner ring road and finally a single site representing background/minor roads. The location of Park and Ride bus routes, the proximity to schools, businesses, residential properties and whether the sites were inside the AQMA were also taken into consideration when locating the survey sites.

Table 9 provides the names and a description of each of the six sites. The traffic survey focused on three main aspects: vehicle age, vehicle type and fuel type. Age was determined from the registration plates. The type of vehicle was recorded according to the 11-category LAEI system already discussed (section 4.2.2.2). Finally, fuel type was determined from observation of the vehicles, for instance many diesel vehicles display a small ‘D’ on their rear, or the exhaust pipe is pointed downwards or the engine makes a deeper sound. It was important that these different aspects of information were collected simultaneously for each vehicle.



**Table 9: Description and location of the six traffic survey sites.**

<b>Name of site</b>	<b>Road number</b>	<b>Description</b>
Foss Island Road	A1079/ A1036	This is a busy street that is part of the inner ring road system. It is located to the east of the city and is adjacent to large businesses and offices. This site is included as part of the AQMA.
Field Lane		This is a minor road located to the south east of the city. It is situated close to the University of York, near to Hull Road. It is within a residential area.
Shipton Road	A19	This is a busy arterial route linking the inner and outer ring road. It is part of the Park and Ride system, with the Rawcliffe station located adjacent to the outer ring road junction. Shipton road is located to the north west of the city.
Wiggington Road	B1363	This is an arterial route that links the inner and outer ring roads. It is located to the north of the city and is not part of the Park and Ride system. This site is located near to the Nestle factory, a railway crossing and York District Hospital.
Tadcaster Road	A1036	This is a busy arterial route located to the south west of the city. This road is part of the Askham bar Park and Ride system. This site is also close to a busy supermarket and York sixth form college.
Gillygate		This is a busy street that forms part of the inner ring road. It is a 'technical breach' site and therefore forms part of the AQMA of York. It is a residential and small business area.

The surveys were duplicated at each site three times so that a more representative sample of traffic was collected. The six sites were usually sampled in a consecutive three day period (two teams surveying two sites a day). The three survey periods were carried out in August/early September (school holidays), October and November of 2005 (Table 10 gives the exact dates of each survey). Each site was surveyed for three hours between the hours of 07:00 – 10:00. Two people were present in each team, thus allowing a continuous three-hour survey.



**Table 10: Dates of the detailed traffic surveys**

Site	Period 1	Period 2	Period 3
Foss Island	30/08/06	17/10/06	21/11/06
Field Lane	04/09/06	17/10/06	21/11/06
Shipton Rd	31/09/06	18/10/06	22/11/06
Gillygate	31/09/06	07/11/06	23/11/06
Tadcaster Rd	01/09/06	19/10/06	22/11/06
Wiggington Rd	01/09/06	19/10/06	23/11/06

The information was recorded by a Norsonic (sophisticated recording equipment usually used by the Environmental Protection team at the council when assessing noisy neighbours). Norsonics keep a time record or 'time stamp' and so lend themselves perfectly to traffic surveys.

The Norsonics were left recording throughout the three hours and the survey teams dictated the relevant information into the microphone as each vehicle went past i.e. "car petrol N registration" or "car diesel 02 registration". The data were then transcribed from the surveys tapes at a later date. When transcribing the data from the Norsonic the time (to the nearest minute) the information was recorded was also noted.

#### **4.5.3. Results of traffic surveys**

A total of 28361 vehicles were recorded in the 18 surveys (54 hours). The busiest sites were Foss Island and Field Lane, followed closely by Gillygate (Figure 19). Field Lane the minor road/background site has a much higher vehicle count than first expected. These higher counts can to some extent be explained by the proximity of the site to Heslington Primary School, the University and the Science Park since many people will use this road to get to school/university/work in the morning. At other times of the day the road is much quieter.



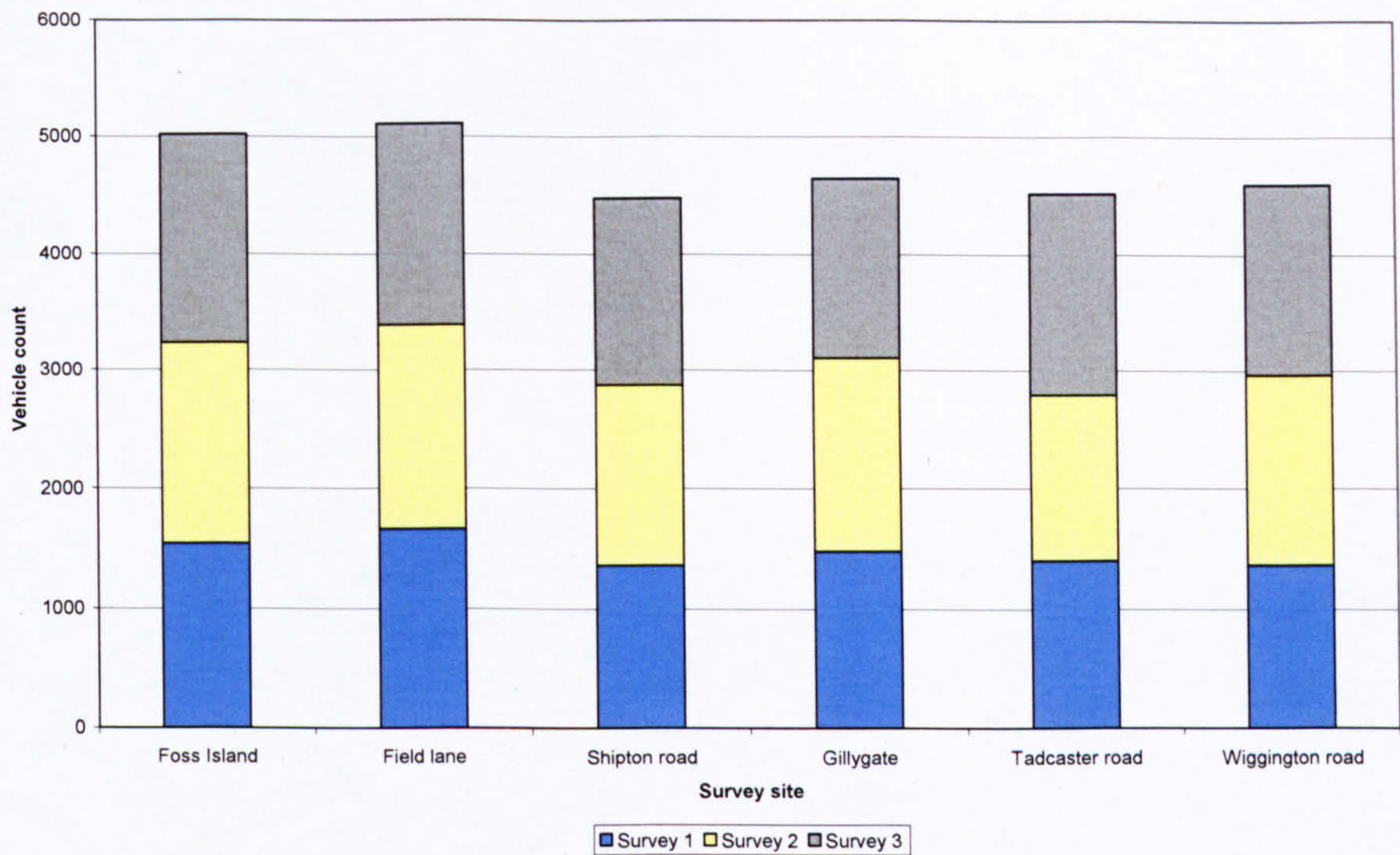


**Figure 19:** Breakdown of vehicle counts into the different survey periods by survey locations

In addition to the variation in vehicle count across the city, there is also a variation in counts over time. The first survey period (August/Early September) shows lower counts than survey 2 (October) and survey 3 (November). This difference is most likely a response to school holidays where all the school run traffic is removed from the system, plus the fact that more car journeys will be made in winter. For some sites the difference in traffic counts between survey 1 and survey 2 was as high as 14% (230 vehicles) and suggests that a substantial proportion of vehicles are removed from the road network of York as a result of school holidays. Since all sites are affected it is not only those roads that are in close proximity to schools where the effect of school holidays are felt.

Table 11 shows the breakdown of vehicle count into the 11-split categories. The most common vehicle type found at each site was unsurprisingly the car, ranging from 90% to 73% depending on site. Foss Islands Road has the highest proportion of HGVs (5.2% for all six classes); this road also shows a high proportion of LGVs with 19% of the vehicles surveyed falling into this category. Shipton Road experiences the least amount of HGV vehicles with only 0.2% of vehicles falling into one of the six HGV classes.



**Table 11:** Breakdown (%) of the vehicle count into the 11-category-LAEI-system. FI = Foss Island, FL = Field Lane, SR = Shipton Road, G = Gillygate, TR = Tadcaster Road, WR = Wiggington Road.

Vehicle type	FI	FL	SR	G	TR	WR	Total
Motorcycle	1.2	0.9	0.8	2.2	0.7	0.7	1.1
Car	73.9	90.3	82.6	73.1	77.5	83.3	80.2
Taxi	0.6	0.3	0.6	2.1	1.4	0.9	1.0
LGV	18.7	6.6	11.3	15.3	13.7	11.6	12.8
Bus or coach	0.3	0.5	2.5	4.2	2.7	0.3	1.7
Rigid HGV 2 axles	3.7	1.3	1.8	2.4	3.1	1.7	2.3
Rigid HGV 3 axles	0.8	0.1	0.2	0.5	0.4	0.4	0.4
Rigid HGV 4+ axles	0.3	0.0	0.1	0.1	0.1	0.1	0.1
Articulated HGV 3&4 axles	0.1	0.0	0.0	0.0	0.0	0.0	0.0
Articulated HGV 5 axles	0.1	0.0	0.0	0.0	0.1	0.1	0.1
Articulated HGV 6+ axles	0.2	0.0	0.0	0.0	0.1	0.8	0.2

The sites at Gillygate, Shipton Road and Tadcaster Road are part of the Park-and-Ride bus routes and thus have a greater number of vehicles into the bus/coach category e.g. Gillygate has the highest proportion of buses with 4.2% of all vehicles surveyed. The vehicle split at Gillygate also indicates the highest proportion of motorcycles and taxis (both representing around 2 % of the total vehicle count). The background/minor road nature of Field Lane is clearly seen, with around 90 % of all vehicles counted being cars, the smallest fraction of LGVs and only a relatively small proportion of HGVs and buses.

Since all buses/coaches and HGVs surveyed are diesel and all motorcycles/scooters are petrol, only the fuel types of taxis, cars and LGVs needed determining during the survey. The engine split for cars was 22 % diesel and 78 % petrol, with a negligible amount of cars running on LPG (0.03 %). The petrol/diesel split for taxis was found to be different with 39 % petrol and 61% diesel (no LPG taxis were surveyed). Finally, the majority of LGVs were diesel (96 %), with a small proportion of LPGs (0.1 %) and the remaining 4 % petrol. The breakdown of the vehicle fuel types are shown in Figure 20.



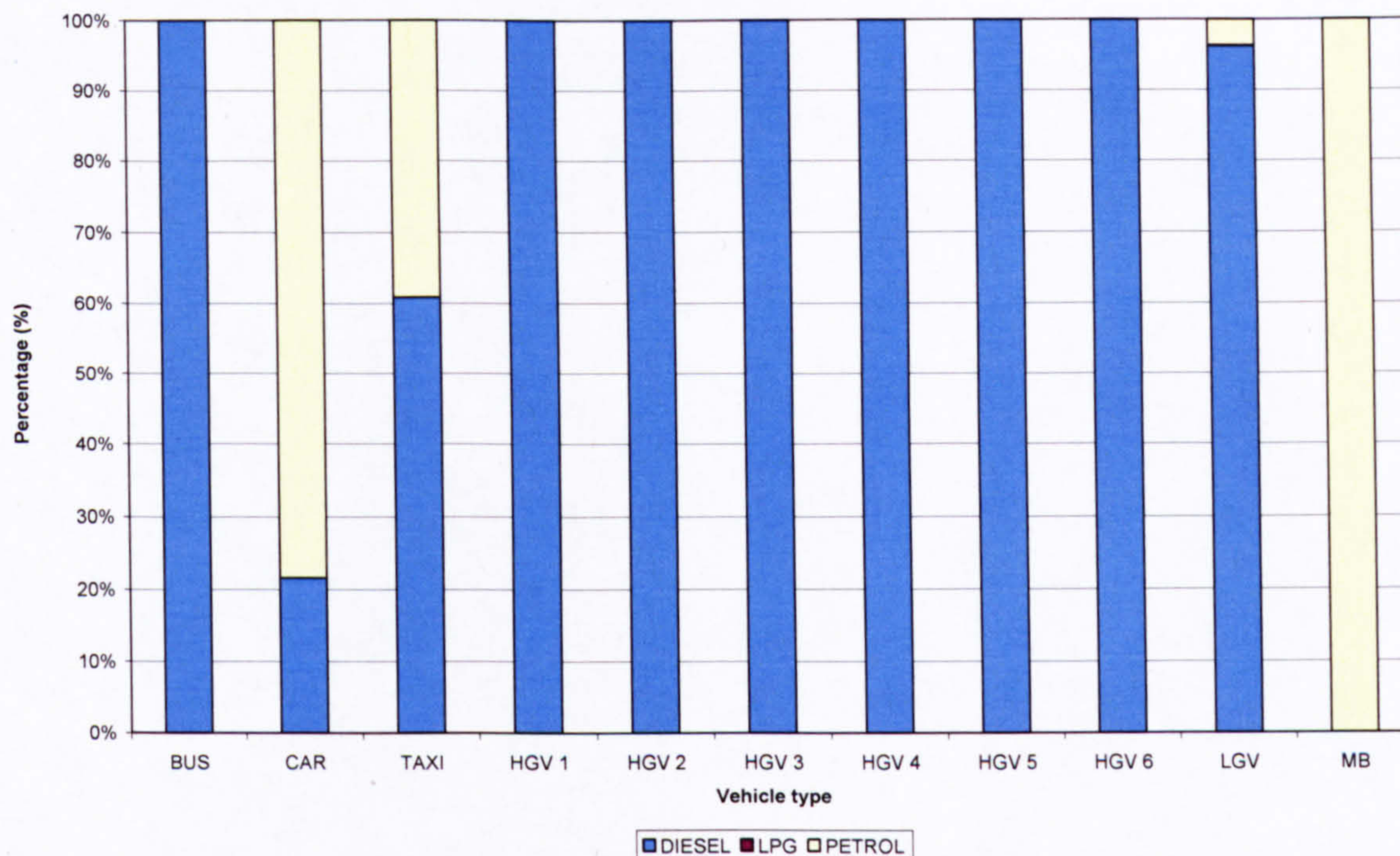


**Figure 20:** Breakdown of engine type (petrol/diesel) for each vehicle classification. For simplicity LPG and other vehicle types have been excluded since they only represent < 1% of the vehicles surveyed.

There is a set of mandatory vehicle emission standards, commonly referred to as EURO standards (see Table 12). Once the start date for these emission standards comes into force it is a legal requirement that all new vehicles adhere to the new standard. The York surveys found that around 3 % of the total vehicles included in the survey were pre-EURO standard. These vehicles are therefore not subject to any type of vehicle emissions control and are most likely to be the vehicles with highest emissions.

The majority of the vehicles surveyed are of EURO 3 standard, with 52 % falling into this bracket. EURO 2 and EURO 4 standard vehicles both contribute to a similar proportion of the total vehicle fleet (19.3 % and 19.4 % respectively).



**Table 12:** EURO standards and dates of introduction

Standard	Directive	Vehicle type	Date of introduction
EURO 1	91/444/EEC	Passenger cars	21-Dec-92
	93/59/EEC	Light commercial vehicles	01-Oct-94
	91/542/EEC	Heavy diesels	01-Oct-93
EURO 2	94/12/EC	Passenger cars	01-Jan-97
	96/69/EC	Light commercial vehicles	01-Oct-97
	91/542/EEC	Heavy diesels	01-Oct-96
EURO 3	98/69/EC	Passenger cars and light commercial vehicles	01-Jan-01
EURO 4	98/69/EC	-	01-Jan-06
EURO 5	-	-	01-Jan-08

#### 4.5.4. Implications for modelling

As already explained, a detailed understanding of traffic composition is required in the construction of a route type. For example, not only is it desirable to understand the overall proportions of traffic falling into the 11-category vehicle classification system, but additionally, within this category system, the breakdown of each of the specific vehicle types into the EURO standard classification system is required. Therefore, the AADT for each vehicle type is split into further sub-categories to represent the proportions of vehicles falling into the EURO standard classification system. Thus the sub-categories for each separate vehicle group (e.g. car, LGV etc.) add up to 100 %.

The systematic manual traffic surveys carried out in conjunction with the CYC were designed in such a way as to gain the maximum possible information regarding traffic composition. The data collected from the surveys were then used to re-calculate the traffic emissions contained within the York emissions inventory by creating a new route type (section 4.2.2.3). The new route type was based on the existing LAEI route type but the percentage breakdowns for each category were re-weighted according to the results collected in the traffic surveys.

The differences between the York specific route type and that of the pre-defined route type based on national average traffic statistics have been analysed. A noticeable difference between the two route types is the way in which HGV's are handled (Figure 21). According to the LAEI vehicle classification system (Table 7), HGV's are split into six separate categories. As explained earlier, each of these six categories are further sub-divided into EURO standards; thus each separate HGV category therefore sums to 100 % (i.e., all artic 2-axle HGVs all up to 100 %).



The first main difference between the national statistics data and York traffic survey data is that unlike the national-average route type, the York-specific route type does not assume the same percentage breakdown into EURO standards for the three rigid HGV classes and the three articulated classes. Instead the York-specific route type handles each category separately thus providing a more comprehensive traffic database (see Figure 21). Secondly, the traffic survey indicates that there are considerably more HGVs of EURO 4 standard using the York road network than what is suggested in the pre-defined route type. HGVs (both rigid and articulated) have the highest rate of emissions of all vehicle types. The emphasis placed on the newer EURO categories (EURO 3 and EURO 4) in the York-specific route type should lead to a reduction in overall emissions in comparison to the emissions calculated with the pre-defined route type. The traffic surveys have also highlighted a lower dominance of pre-1993, EURO 1 and EURO 2 standard HGV's. It is clear from Figure 21 that the change in HGV dominance will have a knock on impact in the calculation of emissions.

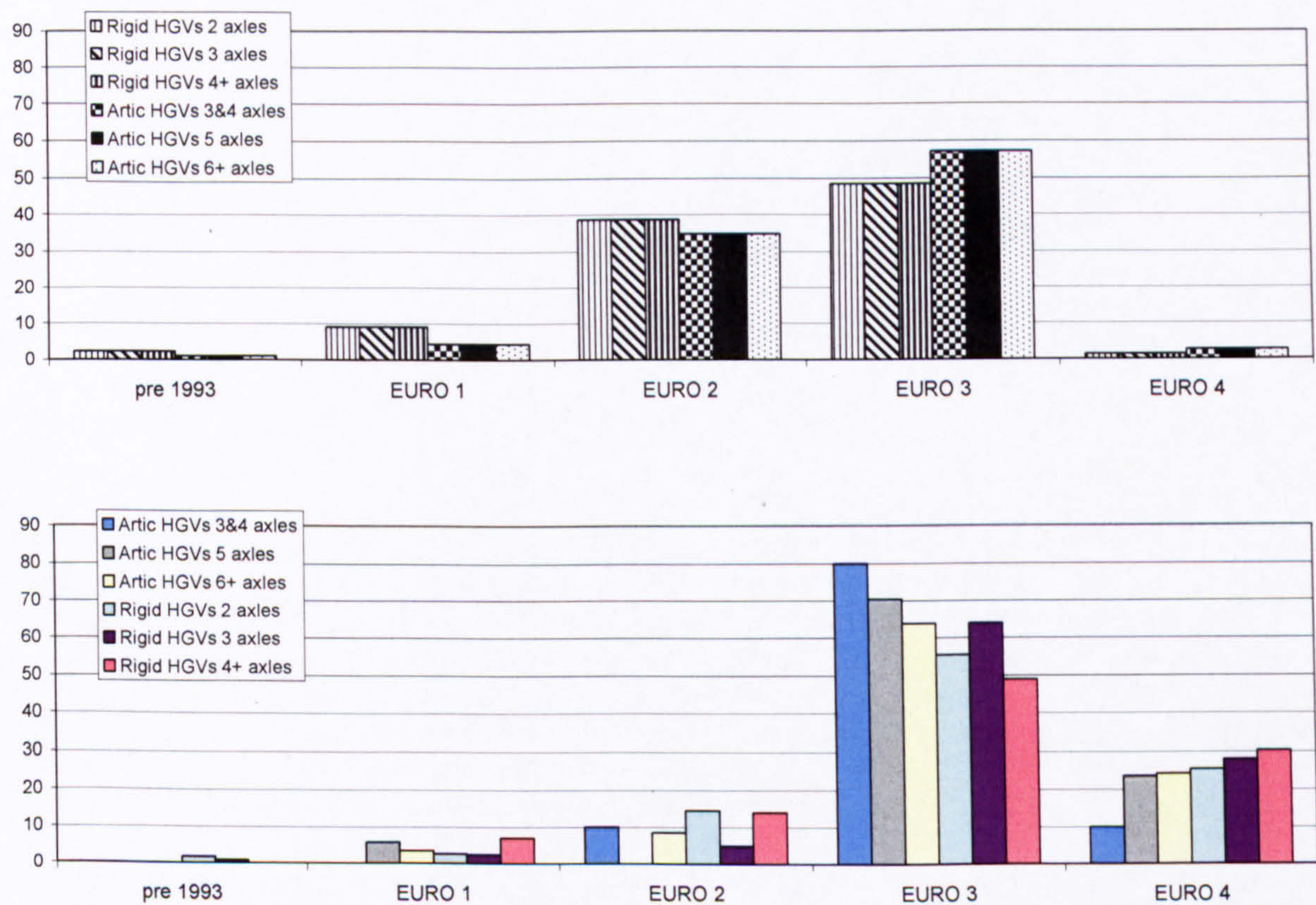


**Figure 21:** Percentage breakdown of rigid and articulated HGVs into the various categories contained with the emissions factors. All bars for each vehicle type add up to 100%. Top plot is the pre-defined DVLA route type (national average) and bottom is the York-specific route type (survey data).

A further important discrepancy between national average and York-specific vehicle composition is seen in the percentage of EURO 3 buses and coaches. The pre-defined route type indicates that 50 % of all buses/coaches are of EURO 3 standard, whereas the York traffic surveys have indicated the percentage of EURO 3 buses should be as high as 80 %. EURO 3 buses emit a



lower volume of emissions (tonnes yr<sup>-1</sup>) compared to the older emission standards (EURO 1 and 2) and so a greater proportion of this vehicle category in the York fleet will lead to a reduction in total emissions.

The City of York has an established and successful bus fleet; it has for some time had a fully operating Park and Ride service (with 5 different stations), plus more recently, FIRST travel have introduced a fleet of brand new buses on one of busiest routes in York (FTR service). It is therefore unsurprising that the buses in York are substantially newer than what is expected nationally.

In London, buses have for some time caught the attention of scientists as a result of primary NO<sub>2</sub> emissions. An initiative in London to reduce particulate (PM<sub>10</sub> and PM<sub>2.5</sub>) emissions resulted in particulate traps being introduced to the existing bus fleet (retro-fitting). These traps are designed to remove secondary particulates by the use of oxidation (NO<sub>2</sub> is converted from NO and subsequently used to oxidise the particulates). However, it is believed that these traps are actually increasing the emissions of primary NO<sub>2</sub> (Carslaw and Beevers, 2004a, 2004b; Carslaw, 2005).

Finally, the York route type shows that EURO 3 petrol cars are by far the most common type of car using the road network, with nearly 40 % of all cars surveyed in York falling into this category (see Figure 22); the percentage of EURO 3 petrol cars for the pre-defined route is only 17.

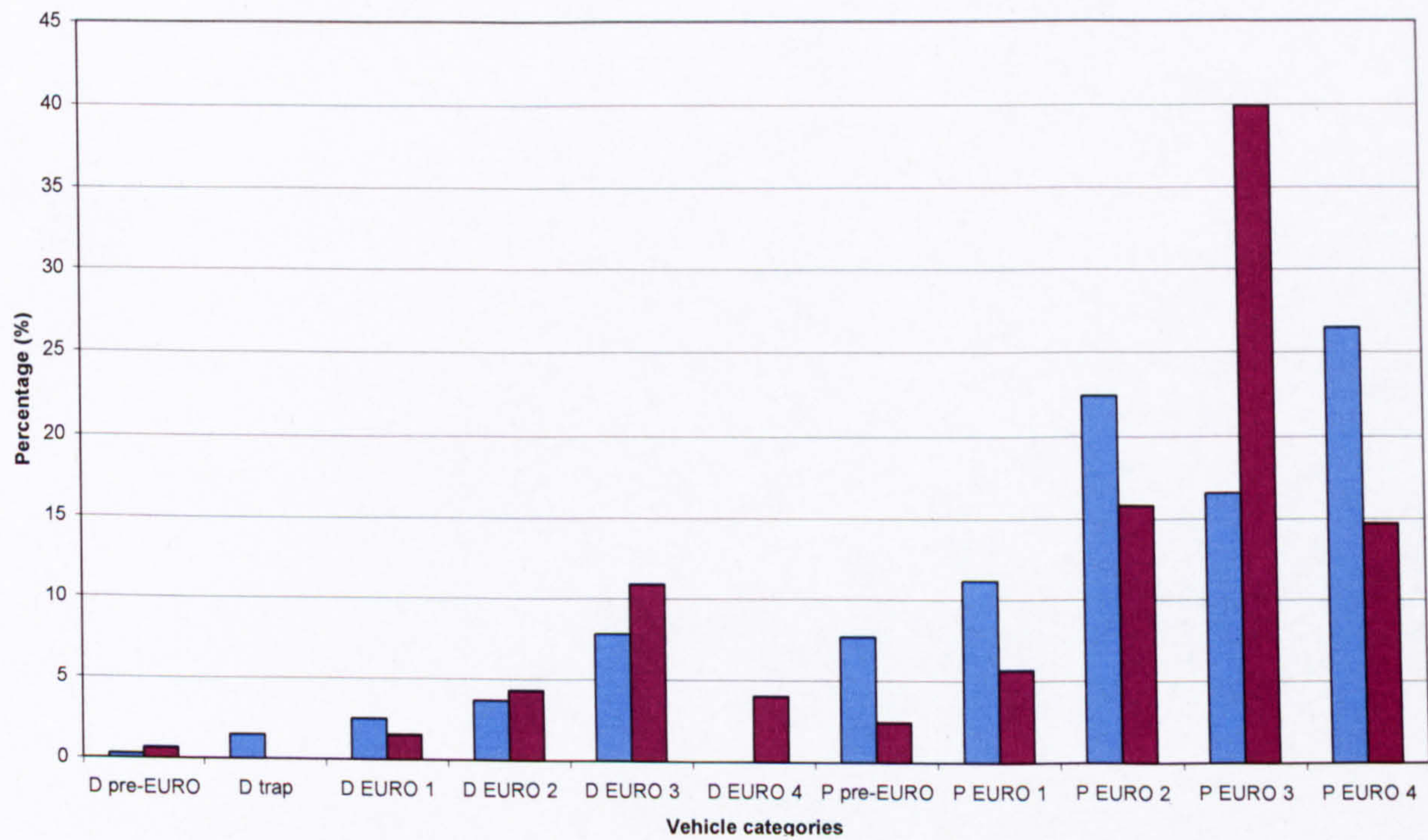


**Figure 22:** Percentage breakdown of cars into the various categories used by the model to calculate traffic emissions. LPG vehicles have been excluded from chart since the values are too small to distinguish on this scale. The purple bars illustrate the York traffic survey results, and the blue bars illustrate the national transport statistics. All bars for each of the two categories adds up to 100%.



In York the increased dominance of EURO 3 petrol cars subsequently means that there is a lower proportion of pre-EURO, EURO 1 and EURO 2 petrol cars; the emphasis has therefore been removed from the older emission standard vehicles (pre-EURO to EURO 2) to the newer, EURO 3 emission class. This change in petrol car standard will directly impact the emission totals for road traffic. Despite the fact that vehicle for vehicle, cars are not the top polluters, cars are the most common vehicle (~ 80 %) and so have an important role to play in the calculation of vehicle emissions. Additionally, there were also substantially more diesel EURO 3 and EURO 4 cars in York than compared to the national average. Again, this greater dominance of newer standard vehicles will impact directly on the emissions totals.

It should also be mentioned that unlike the pre-defined route type, LPG vehicles are included in the York-specific route type. However, only a handful of vehicles fall into the LPG categories (< 1 %) and are unlikely to affect the calculation of emissions for road traffic. In the future, the importance of LPG vehicles may increase and it will be interesting to see the effects that this class of vehicle will have on the road traffic emissions.

To illustrate the effect that a new, more locally relevant, route type can have on the model predictions, a base case model scenario has been created. This base case scenario has been created using default settings, and input recommendations from CERC (that is, the traffic emissions have been estimated using the national transport statistics data). The predictions of this base case can be used as a benchmark from which new model scenarios can be compared against. The base case scenario is described in full in the following paragraphs.

When carrying out modelling work the CYC usually import all emission sources contained within the emissions inventory (Figure 18) to ADMS-Urban so that ambient  $\text{NO}_x$  and  $\text{NO}_2$  concentrations can be modelled at various spatial locations across the city. However, these 'full scale' models (i.e. models that contain all emission sources) have long computational times. Therefore for the purpose of this sensitivity study, model outputs are limited to a few select areas of the City of York so that run times could be kept to a minimum. The analysis therefore focuses on five technical breach areas of the AQMA.

At each of the five technical breach areas the two or three adjacent roads to the monitoring station were selected, resulting in the final model scenarios containing just 18 road sources (see Figure 23) as opposed to the 921 roads (plus, other source types) shown previously. These five areas correspond to those areas of the city believed most unlikely to reach the air quality objectives. In each instance a permanent air quality monitoring station is in operation so that model results can be validated against real time measurements.





**Figure 23:** A schematic of the York road network. Blue lines are road sources not included in the model; red lines are those roads included in the model; black circles are the air quality monitoring sites.

To account for other emission sources in the area that would not otherwise be included in the model, local urban background concentrations were used as the background pollution input data (see Table 13). The local background data are split between Bootham ( $\text{NO}_x$ ,  $\text{NO}_2$  and  $\text{SO}_2$ ) and Dunnington ( $\text{O}_3$ ). Bootham is an urban background site situated in a playing field in the city centre away from any major sources. Dunnington is situated in a rural village 6 km to the east of the city centre. Measurements are made with commercial instrumentation by standard chemiluminescence ( $\text{NO}_x$ ,  $\text{NO}$  and  $\text{NO}_2$ ), UV absorption ( $\text{O}_3$ ) and fluorescence ( $\text{SO}_2$ ) techniques (AQEG, 2004).

**Table 13:** Background concentrations in ppb (annual means).  $\text{NO}_x$ ,  $\text{NO}_2$  and  $\text{SO}_2$  concentrations from Bootham,  $\text{O}_3$  from Dunnington. Data are for 2005

Pollutant	Mean	Max	Min
$\text{NO}_x$	12	181	1
$\text{NO}_2$	8	45	0
$\text{O}_3$	24	75	0
$\text{SO}_2$	2	32	0



The traffic emissions for the 18 road sources were calculated using a combination of emission factors and activity data (section 4.2.2.). The activity data were taken from the predictions of the traffic model SATURN, which has been used to predict AADT values for all major road sources included in the emissions inventory. The AADT predictions correspond to the 3-split category system (heavy, light and motorcycles). SATURN was also used to predict vehicle speeds for the major roads and these were incorporated into the emission calculations.

The meteorological data were obtained from the UK Meteorological Office weather station at Church Fenton, 12 km to the south west of the city (see Table 14).

**Table 14:** Meteorological data (annual mean values) recorded by the UK Meteorological Office at Church Fenton for 2005 (latitude 53.8, longitude-1.2)

Meteorological variable	Mean	Max	Min
Temperature (degrees)	10	29	-9
Wind speed (m/s)	4	22	0
Wind direction (degrees)	220	360	0
Precipitation (mm)	0	14	0
Cloud cover (oktas)	5	8	0
Humidity (%)	79	100	30

The year 2005 was chosen for the sensitivity tests, since this was the latest year in which a full year of meteorological data and background air pollution data were available at the time of writing.

Table 15 provides a brief summary of the additional input requirements for ADMS-Urban. In each case the base case model input settings have been provided with a brief justification. These input settings, along with those used to calculate the traffic emissions, have been used to predict the annual mean concentrations of NO<sub>x</sub> and NO<sub>2</sub> at the five-receptor sites illustrated in Figure 23 for the year 2005. This initial model scenario will be referred to as the base case throughout the remainder of this Chapter.



**Table 15:** Values of the various ADMS-Urban input requirements for the base case model scenario. A justification for the various input settings has been provided where there is a range of possible settings.

Input parameter	Value	Justification
Surface roughness	0.5 m	Default for suburbia – used following recommendation from CERC
Monin-Obukhov length	30 m	Default for cities and towns
Latitude	52	-
Chemistry scheme	Chemical reaction scheme (CRS)	CRS chosen since this is the more complicated chemistry scheme of the two available
Meteorological file	Church Fenton, 2005	This is the closest Met Office owned station for York.
Background file	NO <sub>x</sub> (NO, NO <sub>2</sub> ) and SO <sub>2</sub> concentrations from Bootham AQS; O <sub>3</sub> from Dunnington AQS.	Corresponds to the urban background pollutant concentrations for the City of York. Since only specific roads are being modelled, the urban background station will provide the ‘other’ emission sources for York and thus keeps model run times to a minimum.

The results of the base case model scenario are illustrated in Table 16. It can be seen that there is relatively little difference between the NO<sub>2</sub> predictions for the five receptor sites (~12 ppb). Unsurprisingly, the greatest NO<sub>x</sub> and NO<sub>2</sub> annual mean predictions are for those sites with the heaviest traffic flows (Lawrence Street and Fishergate). Table 16 also provides the total level of emissions (tonnes) used in ADMS-Urban. NO<sub>2</sub> emissions are not calculated explicitly, and instead are simply considered to be 10 % of NO<sub>x</sub>. Note that the emissions are expressed as a total for all road links included in the model scenario.

The observed NO<sub>x</sub> and NO<sub>2</sub> concentrations recorded at the five monitoring sites are also shown in Table 16. The predictions for the five receptor sites grossly underestimate the observations (both NO<sub>x</sub> and NO<sub>2</sub>), with predictions being around 25 % to 50 % lower than observations. It is possible that a certain degree of this underestimation is a consequence of the limited number of emission sources; a scenario using all sources should be more representative of York. However, since we are concerned only with the relative changes as a result of input changes, it is therefore thought adequate to use the reduced model in terms of the sensitivity tests. The results from a new model scenario where traffic emissions have been calculated with the York-specific data are shown in Table 17. The annual predictions shown in Table 17 can be directly compared against the base case predictions in Table 16 so as to gain an understanding of the impact the re-calculation in traffic emissions has had on ambient NO<sub>x</sub> and NO<sub>2</sub> predictions.



**Table 16:** Base case emissions (tonnes for the year 2005) and annual mean predictions (2005) of NO<sub>x</sub> and NO<sub>2</sub>. G = Gillygate, H = Holgate Road, N = Nunnery Lane, F = Fishergate, L = Lawrence Street.

Pollutant	Emissions (tonnes)	Annual means (ppb)					
		G	H	N	F	L	Mean
ADMS-Urban predictions							
NO <sub>2</sub>	1.2	11.8	11.9	11.9	12.7	12.8	12.2
NO <sub>x</sub>	12.0	22.3	22.1	23.1	28.7	25.9	24.4
Observations							
NO <sub>2</sub>	-	19	19	17	17	18	18
NO <sub>x</sub>	-	38	40	34	37	49	40
AADT estimates		13561	15187	9353	15927	17573	

**Table 17:** Estimated traffic emissions (tonnes for the year 2005) and annual mean predictions (2005) of NO<sub>x</sub> and NO<sub>2</sub> for the model scenario using the York specific transport data to calculate traffic emissions. G = Gillygate, H = Holgate Road, N = Nunnery Lane, F = Fishergate, L = Lawrence Street.

Pollutant	Emissions	Annual means (ppb)					
	(tonnes)	G	H	N	F	L	Mean
ADMS-Urban predictions							
NO <sub>2</sub>	0.91	11.5	11.6	11.6	12.2	12.4	11.9
NO <sub>x</sub>	9.1	21	20.8	21.8	26.2	23.8	22.7

It can be seen that the York relevant activity data (traffic surveys) has led to a substantial reduction in the estimation of traffic emissions, with the NO<sub>x</sub> and NO<sub>2</sub> emissions falling by around 24 %. As already highlighted, the reduction is a consequence of the greater importance of newer vehicles using the York road network in comparison to the proportions assigned in the national average route type. The results reflect the fact that newer vehicles emit substantially lower volumes of NO<sub>x</sub> and NO<sub>2</sub> compared to older vehicles. The reduction in traffic emissions is subsequently matched by a reduction in the annual mean predictions made with ADMS-Urban (2.5 % for NO<sub>2</sub> concentrations, and around 7 % for NO<sub>x</sub>). The difference in the magnitude of reduction in emissions and predicted concentrations is because traffic emissions are not the sole source of NO<sub>x</sub> and NO<sub>2</sub> emissions included in the model. The reduction in traffic emissions therefore only contributes to a relatively smaller reduction in the total volume of emissions included in the model scenarios.



It should be pointed out that despite the efforts deployed to fine tune the dispersion modelling process to York specific conditions, the difference between model predictions and observed NO<sub>x</sub> and NO<sub>2</sub> concentrations has widened. There is indeed still a great deal of room for improvement in the prediction of NO<sub>x</sub> and NO<sub>2</sub> concentrations in York.

Traffic speed is also an important aspect of emission calculation. The speed parameter setting in ADMS-Urban can vary from 5 km/hr to 130 km/hr (at intervals of 5 km/hr). To investigate the model sensitivity to this input variable, a number of new model scenarios have been created whereby the average speed of the 18 road links has been systematically varied. The predicted NO<sub>x</sub> and NO<sub>2</sub> concentrations at the five receptor sites are shown in Figure 24.

The predicted NO<sub>x</sub> and NO<sub>2</sub> concentrations at all five receptor sites behave in a similar manner (U shaped relationship between speed and predicted pollutant concentration). The greatest change in predicted NO<sub>2</sub> concentrations (and NO<sub>x</sub>, not shown) occurs when the average speeds are changed from their base case setting (~ 40 km/hr) and set to 5 km/hr, with the increases in NO<sub>2</sub> concentration ranging from 11 % to 17 % (24 % to 34 % for NO<sub>x</sub> concentrations) depending on site. Negative changes in predicted NO<sub>2</sub> concentrations are seen when average speeds are set to 50 - 70 km/hr but these reductions are marginal, ranging from 0.1 % to 0.5 % (0.1 to 1.3 % for NO<sub>x</sub>) depending on site. From a policy point of view, speeds in the region of 50 – 70 km/hr are most desirable since predicted NO<sub>x</sub> and NO<sub>2</sub> concentrations are at their lowest.

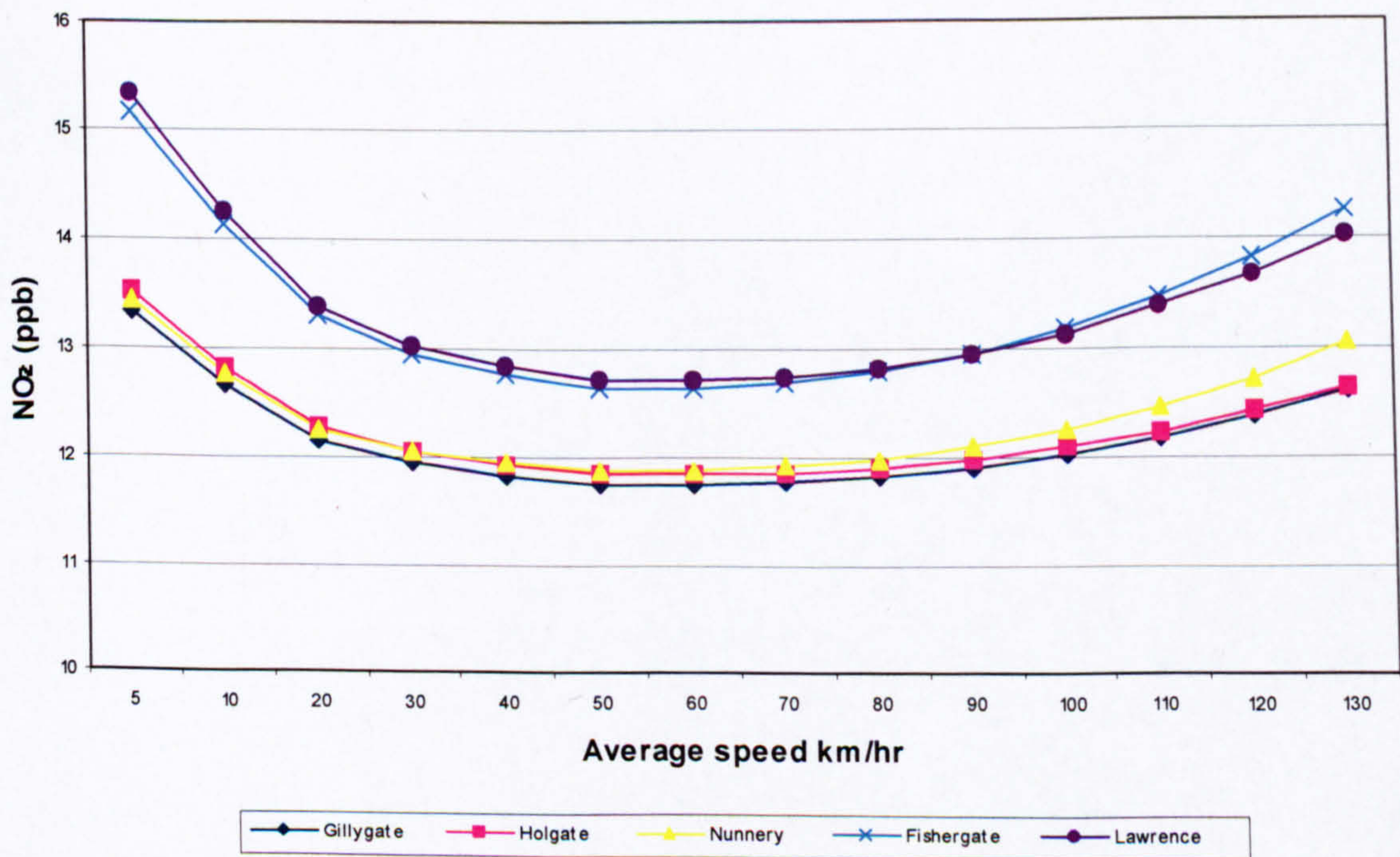


**Figure 24:** Annual mean NO<sub>2</sub> predictions for the five receptor sites as a result of varying the average speed of all vehicles. An average speed is assumed in the model for each road link.

To investigate the role of speed in the calculation of traffic emissions further, an additional speed survey has been undertaken in York. This speed survey is separate to that already outlined and



gives only a rough indication as to the types of speeds the vehicles using these roads are travelling; it is not meant to be a comprehensive picture of vehicle speed. However, since ADMS-Urban only requires one speed for each road-link it was felt that a simplistic survey such as this would be sufficient to provide a rough vehicle speed estimate.

The speed survey recorded over 5000 vehicles and was conducted at a location close to each of the roadside air quality monitors (Gillygate, Fishergate, Holgate Road, Lawrence Street and Nunnery Lane). The speeds were surveyed at each of the receptor points between the hours of 07:00 and 09:30 to get a picture of both non rush hour and rush hour traffic over five days. Vehicles travelling in both directions were included.

Speeds were recorded using a TSS LASER 500 speed gun. The gun emits a continuous stream of laser pulses. The time it takes for a pulse to reach the vehicle and be reflected back is recorded and the vehicle speed is then calculated from the difference between these pulse timings as the vehicle moves towards the speed gun. The LASER 500 can record speeds from 10 to 199 mph (16 - 320 km/hr) and is considered accurate to +/- 1 mph (1 km/hr).

Figure 25 highlights the average speed surveyed for each of the five road links alongside the speed estimates provided by the traffic model SATURN. It can be seen that the survey results are substantially lower than the SATURN predictions (for all sites). The difference is greatest at Holgate Road, where the estimated average speed from the SATURN model (~ 50 km/hr) is more than double the average speed recorded in the surveys (~ 16 km/hr).

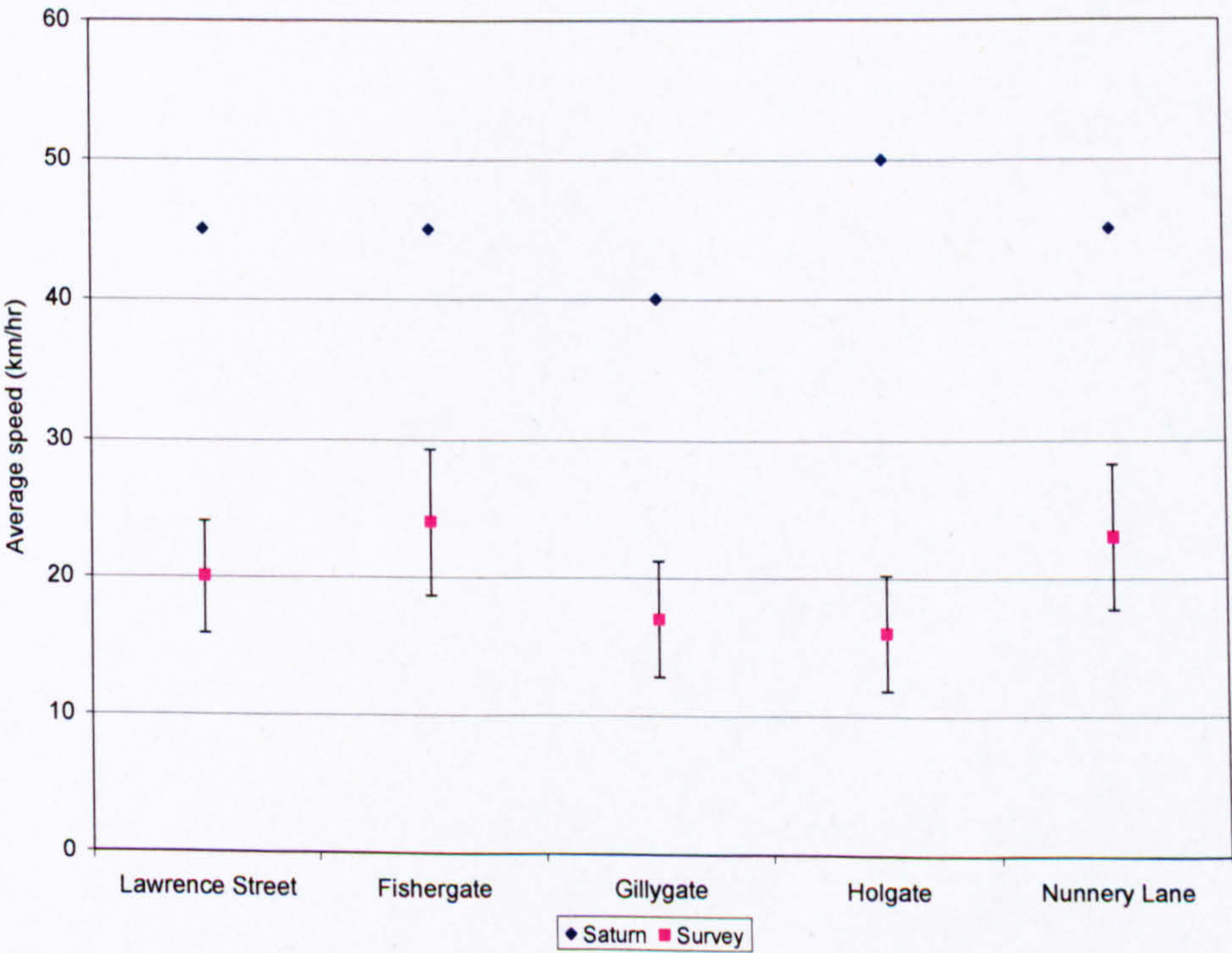


**Figure 25:** Average speeds recorded at the five specific sites. Error bars are standard deviations.

As was highlighted in Figure 25, the average speeds for the various road links included in the base case model scenario ranges from 40 km/hr to 50 km/hr (labelled as SATURN) and



substantially over estimate the average speeds recorded as part of the survey. Replacing the SATURN speeds with those from the traffic survey for the various road links included in the model scenario will result in an increase in the predictions made with ADMS-Urban (see Table 18).

Indeed, the increase in traffic speeds applied to the road sources has resulted in the annual mean NO<sub>x</sub> and NO<sub>2</sub> concentrations increasing by 10 % and 4 %, respectively compared to the base case scenario. Although, the annual mean predictions for the new speed scenario are still somewhat lower than the observed NO<sub>x</sub> and NO<sub>2</sub> concentrations (Table 16), this speed analysis has highlighted the importance of vehicle speed in the dispersion modelling process.

**Table 18:** Annual mean predictions (2005) of NO<sub>x</sub> and NO<sub>2</sub> for the model scenario using the new average speeds recorded from traffic surveys. G = Gillygate, H = Holgate, N = Nunnery Lane, F = Fishergate, L = Lawrence Street.

Pollutant	Annual means (ppb)					Mean
	G	H	N	F	L	
NO <sub>2</sub>	12.2	12.3	12.3	13.3	13.4	12.7
NO <sub>x</sub>	24.1	24.1	24.8	32.2	28.8	26.8

Indeed, like many other urban areas across the UK, congestion is a severe problem in York. The congestion charging zone initiated in London has gone some way to improving the traffic emissions associated with road traffic in London. Despite the fact that the zone’s primary aim was not specifically focused on air quality issues it has contributed to a reduction in air pollutant concentrations at a number of monitoring sites within the charging zone (Beevers and Carslaw, 2005). Indeed, should such a scheme be implemented in York, it seems likely that similar reductions in emissions would result.

A further model scenario has been created whereby both the traffic speed and traffic composition have been altered to resemble the conditions recorded in the traffic surveys. The traffic emissions and annual mean predictions for the new scenario are shown in Table 19. It can be seen from the table that alteration of the traffic speed and composition has resulted in a slight decrease in traffic emissions compared to the base case, with NO<sub>2</sub> emissions falling by ~ 17 % and NO<sub>x</sub> by ~ 10 %. The annual mean NO<sub>x</sub> and NO<sub>2</sub> concentrations predicted by ADMS-Urban have also fallen in comparison to the base case scenario. As has been already highlighted, a reduction in overall vehicle speed leads to an increase in the prediction of ambient NO<sub>x</sub> and NO<sub>2</sub> concentrations. However, the fact that substantially more vehicles using the road network of York are new (i.e., less than two years old) has lessened the increase in emission associated with vehicle speeds. The emission reductions associated with the cleaner vehicle fleet have therefore outweighed the increases associated with the change in vehicle speed.



**Table 19:** Emissions (tonnes per 2005) and annual mean predictions (2005) of NO<sub>x</sub> and NO<sub>2</sub> concentration for the new traffic emissions (York tailored) scenario. G = Gillygate, H = Holgate Road, N = Nunnery Lane, F = Fishergate, L = Lawrence Street.

Pollutant	Emissions (tonnes)	Annual means (ppb)					
		G	H	N	F	L	Mean
Base case							
NO <sub>2</sub>	1.2	11.8	11.9	11.9	12.7	12.8	12.2
NO <sub>x</sub>	12	22.3	22.1	23.1	28.7	25.9	24.4
New traffic scenario							
NO <sub>2</sub>	1.0	11.7	11.8	11.7	12.3	12.6	12.0
NO <sub>x</sub>	10.3	21.6	22.0	21.9	26.7	24.9	23.4

#### 4.5.5. Conclusion to traffic section

The results of the traffic surveys have ‘fine-tuned’ the York emissions inventory for the road sources with both the vehicle composition and average traffic speed were altered according to the survey results. Although the results from the surveys are not a complete assessment of the traffic fleet using the road network in York they do go some way to making the road traffic emissions more locally relevant to York. The main finding from this section of work is that the traffic emissions associated with York are slightly lower than those estimated for York using national traffic statistics, owing to the larger proportion of newer vehicles.

### 4.6. ADMS-Urban input sensitivity

A secondary aim of this Chapter is to investigate the sensitivity of ADMS-Urban to various input settings. The base case scenario outlined in the preceding Chapter has therefore been used to investigate the sensitivities of ADMS-Urban to other input parameters. Note, the traffic emissions used in the base case are calculated from basic settings (i.e., those used before the detailed traffic surveys) to allow for a comparison on a consistent basis.

#### 4.6.2. Sensitivities

Section 4.3 highlighted that ADMS-Urban is a new generation dispersion model that parameterises the boundary layer in terms of the Monin-Obukhov length. The ADMS-Urban model interface supplies a number of options regarding the Monin-Obukhov length setting; 100 m corresponding to large conurbations, 30 m for cities and towns, and finally 10 m for small towns. The Monin-Obukhov length for the base case scenario is set to 30 m.

Unstable atmospheres lead to greater rates of pollutant dilution as a result of convective mixing, thus causing lower ground level concentrations than if conditions are stable. The stability of the



atmosphere in urban areas is highly influenced by the urban heat island effect, which in turn is proportional to the size of the urban area. In theory a larger Monin-Obukov length (representative of unstable atmospheres) should result in lower ambient pollutant concentrations. To illustrate the sensitivity of ADMS-Urban to the Monin-Obukhov length, several scenarios have been created whereby all input parameters are held constant with the exception of the Monin-Obukhov length, which has been set to 100 m, 10 m and 0 m respectively.

Surface roughness is a measure of length (section 2.3.2.1). It is concerned with the interference the urban area (i.e. buildings etc) has on horizontal turbulence (wind flow). Large urban 'built up' areas will result in greater restriction to the horizontal movement of airflow and so rates of dispersion will be lower. Several new scenarios have been created whereby the surface roughness length has been varied (again, all other input variables are held constant at the settings used in the base case scenario); the new surface roughness lengths correspond to the options given in the ADMS-Urban user interface (1.0 m for cities/woodland; 0.5 m for open suburbia/parkland; 0.02 m for open grassland and 0.005 m for short grassland). Note, only the surface roughness length that are in someway representative of the conditions in York have been analysed.

A further input parameter to be tested in this section is the chemistry scheme. There are two chemistry schemes available for use in ADMS-Urban (section 5.3). The Derwent-Middleton scheme is based on observations from London (Derwent and Middleton, 1996). The hourly NO<sub>2</sub> concentrations (ppb) are calculated with the following equation from NO<sub>x</sub> concentrations in the range of 9.0-1141.5 ppb.

$$[\text{NO}_2] = 2.166 - (1.236 - 3.348A + 1.933A^2 - 0.326A^3) [\text{NO}_x] \quad \text{Equation 3}$$

where  $A = \log_{10}([\text{NO}_x])$

The other scheme, CRS, is based on a simplified set of eight reactions to represent the complex chemistry involving VOC, NO<sub>x</sub>, O<sub>3</sub> (Venkatram et al., 1994). The eight reactions are as follows:





Where ROC = Reactive organic compounds, RP = radical pool, SGN = stable gaseous nitrogen products and SNGN = stable non-gaseous nitrogen products.

The base case scenario uses the CRS since this contains more detailed chemistry than that of the NO<sub>x</sub>-NO<sub>2</sub> correlation. For the purpose of this sensitivity test a further scenario has been developed whereby the alternative chemistry setting (Derwent-Middleton) has been applied. Finally, a further three scenarios have been created to investigate primary NO<sub>2</sub> emissions since recent studies suggest primary NO<sub>2</sub> emissions are of greater importance than previously thought (AQEG, 2006). The primary NO<sub>2</sub> fraction has been adjusted from the model default 10 % of NO<sub>x</sub> emissions to 15 %, 18 % and 20 % (note, these fractions are within the likely primary NO<sub>2</sub> limits suggested in AQEG (2006)).

The predicted annual mean NO<sub>x</sub> and NO<sub>2</sub> concentrations for all the new sensitivity scenarios, along side the observations are shown in Table 20.

Table 20 shows that changing the minimum Monin-Obukhov length does have an affect on the predicted pollutant concentrations with the highest NO<sub>x</sub> and NO<sub>2</sub> predictions associated with lowest Monin-Obukhov lengths. This inverse relationship is expected. The predicted NO<sub>x</sub> concentrations increase by 5.9 % to 8.2 % (depending on site) as a result of reducing the Monin-Obukhov length from 30 m (base case) to 10 m.

It can be seen that by not specifying a Monin-Obukhov length, the predicted concentrations of NO<sub>2</sub> (NO<sub>x</sub>) increase by 3.6 % to 5.0 % (6.7 % to 9.7 %) depending on site. There is, in fact, little difference between not specifying a length and setting it at 10 m, this is true for both NO<sub>x</sub> and NO<sub>2</sub> predictions and suggests that the Monin-Obukhov length is not sensitive to small changes in its length, especially at the lower end of its range.

In general it can be seen that increasing the surface roughness length has less of an impact on NO<sub>x</sub> and NO<sub>2</sub> predictions than reducing it (Table 20). A lower surface roughness length assumes less obstruction in the ground level wind flow and so a greater level of dispersion; the annual mean predictions of NO<sub>x</sub> and NO<sub>2</sub> will therefore decrease as the surface roughness length is reduced. Despite most of these scenarios not being wholly representative of York it is interesting to see the effect of changing this variable on the annual mean NO<sub>2</sub> and NO<sub>x</sub> predictions made with ADMS-Urban.

Changing the chemistry setting resulted in an increase in the predicted NO<sub>2</sub> concentrations (ranging from 5 % to 22 % depending on site). It can be seen from Table 20, that those sites that experience the greatest changes in NO<sub>2</sub> concentration as a result of the alternative chemistry scheme, are the ones with the highest predictions of NO<sub>x</sub>. Since the Derwent-Middleton scheme is based on an empirical formula (3), which is itself derived from input NO<sub>x</sub> concentrations, it can be seen that for higher NO<sub>x</sub>, the resultant estimation of secondary NO<sub>2</sub> is higher. The predicted NO<sub>x</sub> concentrations remained constant. The use of the empirical relationship used to derive the NO<sub>2</sub> concentrations in the Derwent and Middleton scheme therefore could quite substantially influence the NO<sub>2</sub> predictions made with ADMS-Urban.



**Table 20:** Predicted annual mean (2005) NO<sub>2</sub> and NO<sub>x</sub> concentrations for the various sensitivity scenarios. G = Gillygate, H = Holgate Road, N = Nunnery Lane, F = Fishergate and L = Lawrence Street

	Parameter changed	Description	Predictions				
			G	H	N	F	L
NO <sub>2</sub>							
	Observations	-	19	19	17	17	18
	Base case	-	11.8	11.9	11.9	12.7	12.8
	York traffic emissions	York traffic surveys	11.7	11.8	11.7	12.3	12.6
3	Monin-Obukhov	100 m corresponding to large conurbations	11.8	11.8	11.9	12.7	12.7
4	Monin-Obukhov	10 m corresponding to small towns	12.2	12.3	12.4	13.2	13.3
5	Monin-Obukhov	0 m	12.3	12.3	12.5	13.3	13.5
6	Surface roughness	1.0 m corresponding to Cities/Woodland	11.8	11.9	12.0	12.8	12.8
7	Surface roughness	0.02 m corresponding to open grassland	11.3	11.4	11.4	12.0	12.2
8	Surface roughness	0.005 m corresponding to short grassland	11.2	11.3	11.3	11.9	12.0
9	Chemistry	Derwent and Middleton	12.6	12.5	13.3	15.5	14.4
10	Primary NO <sub>2</sub>	15%	11.9	12.1	11.9	12.8	12.9
11	Primary NO <sub>2</sub>	18%	12.0	12.2	12.1	13.1	13.2
12	Primary NO <sub>2</sub>	20%	12.1	12.3	12.2	13.3	13.3
NO <sub>x</sub>			G	H	N	F	L
	Observations	-	38	40	34	37	49
	Base case	-	22.3	22.1	23.1	28.7	25.9
	York traffic emissions	York traffic surveys	21.6	22.0	21.9	26.7	24.9
3	Monin-Obukhov	100 m corresponding to large conurbations	22.2	22.0	23.0	28.6	25.7
4	Monin-Obukhov	10 m corresponding to small towns	23.6	23.6	24.8	30.6	28.2
5	Monin-Obukhov	0 m	23.9	23.9	25.1	30.9	28.6
6	Surface roughness	1.0 m corresponding to Cities/Woodland	22.3	22.1	23.1	29.5	25.8
7	Surface roughness	0.02 m corresponding to open grassland	20.6	20.6	21.3	25.3	23.8
8	Surface roughness	0.005 m corresponding to short grassland	20.2	20.2	20.9	24.5	23.2
9	Chemistry	Derwent and Middleton	22.3	22.1	23.1	28.7	25.9
10	Primary NO <sub>2</sub>	15%	21.6	22.0	21.9	26.7	24.9
11	Primary NO <sub>2</sub>	18%	21.6	22.0	21.9	26.7	24.9
12	Primary NO <sub>2</sub>	20%	21.6	22.0	21.9	26.7	24.9



Finally, Table 20 illustrates the changes in NO<sub>x</sub> and NO<sub>2</sub> concentrations as a result of altering the primary NO<sub>2</sub> emissions. Unsurprisingly, in all three of the new scenarios, the NO<sub>x</sub> concentration remained invariant, whilst the NO<sub>2</sub> concentration increased. Consequently, the NO<sub>2</sub>: NO<sub>x</sub> ratio has increased. The annual mean NO<sub>2</sub> predictions made with these new primary NO<sub>2</sub> scenarios more closely resemble the observations (also seen in Table 20); however, there is still a large difference between predictions made with ADMS-Urban and observations.

#### 4.6.3. Meteorology sensitivity

Chapter 9 of the 2004 AQEG report (AQEG, 2004) highlighted the sensitivity of model outputs to meteorological data as an important area for further research:

*'Development of a better understanding of the effects of meteorology on NO<sub>2</sub> concentrations including: assessment of the significance of the choice in models of input meteorological data (station and year), via modelling sensitivity studies'*

For this reason, the sensitivity study has been extended to include the input meteorological data. Several years of meteorological data (2002 to 2006) from the Meteorological Office Church Fenton site have been used to create a further four scenarios. For each scenario all input parameters used in the base case scenario were held constant, with the exception of the meteorological file, which was varied on a yearly basis. The results for the annual mean NO<sub>2</sub> predictions are shown in Figure 26.

It can be seen that there is a degree of variability in the model predictions as a result of changing the input meteorological file and these differences are seen at all five receptor sites. In general, the greatest NO<sub>x</sub> and NO<sub>2</sub> predictions are seen when the 2003 and 2006 files are used, and the lowest for the files of 2004 and 2005.

Table 21 highlights the mean values of the meteorological parameters for the various years (2002 to 2006). It can be seen that the year with the lowest mean wind speed is 2003, with 4.1 ms<sup>-1</sup>; indeed, the year 2003 also has the lowest maximum wind speed of all the study years. The number of hours of meteorological data that are considered calm (i.e. wind speeds below 1 ms<sup>-1</sup>) has also been highlighted in Table 21. ADMS-Urban assumes a wind speed of 0.75 ms<sup>-1</sup> for all calm conditions. Calm conditions represent low levels of dispersion and so a greater proportion of calm hours should, in theory, result in higher annual mean predictions.



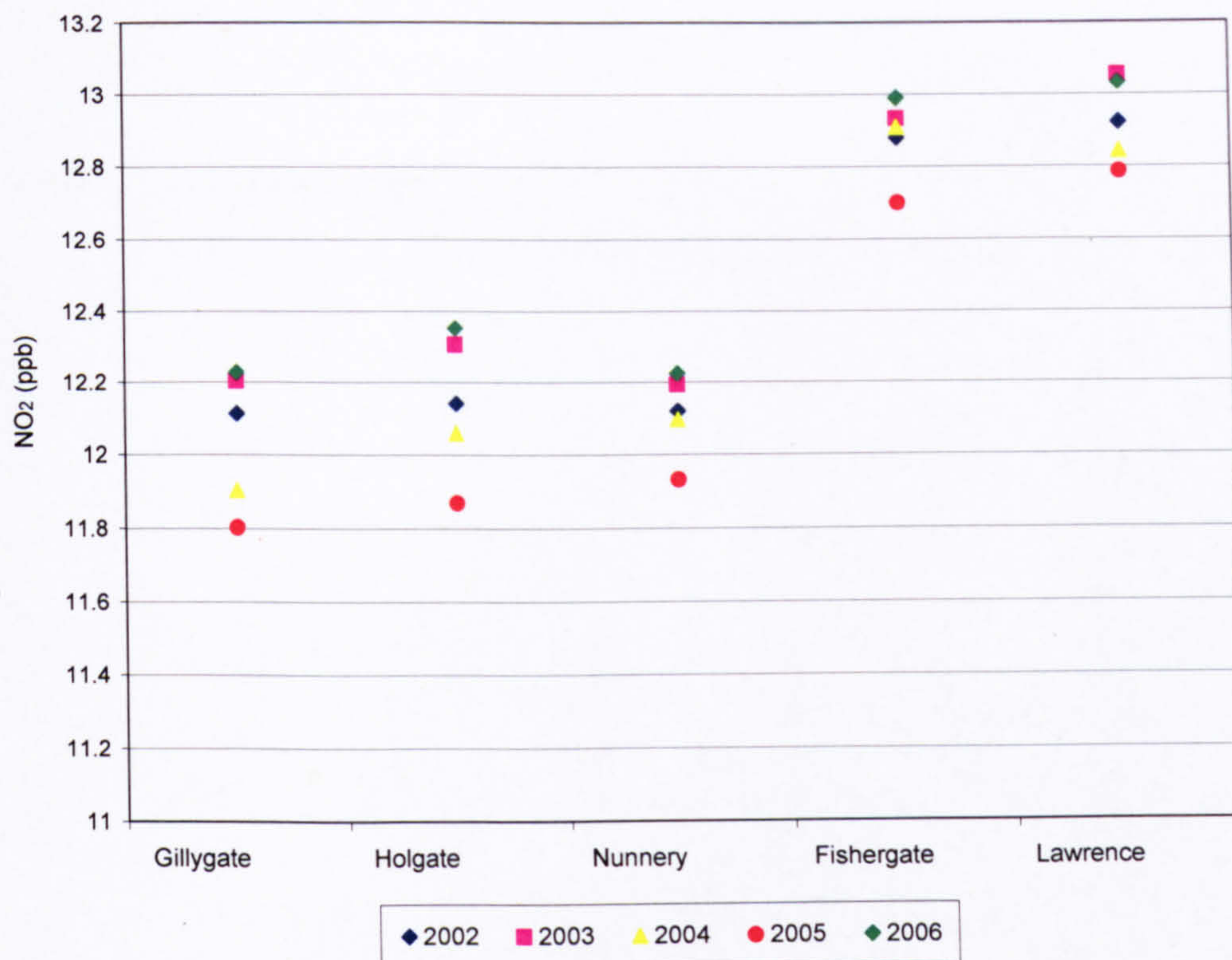


**Figure 26:** ADMS-Urban predicted annual mean NO<sub>2</sub> concentration for the years 2002 to 2006 for the five different study sites. Note, the 2005 year of data were used in the base case.

**Table 21:** Summary (annual mean and maximum) of meteorological data for the various years

		2002	2003	2004	2005	2006
Temp	Mean	10.2	10.1	10.4	10.3	10.6
	Max	29.2	30	28.2	29.4	30.5
Humidity	Mean	89	77	80	79	79
	Max	100	100	100	100	100
Wind speed	Mean	4.3	4.1	4.3	4.4	4.3
	Max	21.1	15.4	20.6	22.1	15.9
Wind direction	Mean	204	202	223	220	208
	Max	360	360	360	360	360
Precipitation	Mean	0.1	0.1	0.1	0.1	0.1
	Max	9.2	8.0	16.4	14.0	14.8
Cloud cover	Mean	5	4	5	5	5
	Max	8	8	8	8	8
Hours of calm	-	265	324	305	244	330
Hours of missing data	-	111	83	151	106	200

The years with the greatest number of calm hours were 2003 (324 hours) and 2006 (330 hours) and so correspond to the consistently high annual mean predictions seen at the five-receptor sites



for these years (Figure 26). The number of calm hours can also go some way to explain the lower annual means predicted with the 2004 and 2005 meteorological files since these two years have a relatively low number of calm hours at 305 and 244, respectively.

To further investigate the model uncertainty with regards to meteorology a bootstrap procedure has been created whereby the meteorological data used as inputs for ADMS-Urban has been artificially created from the pool of available data over the period 2002 to 2006. This type of analysis will allow the calculation of confidence intervals for the annual mean  $\text{NO}_2$  and  $\text{NO}_x$  predictions.

The procedure works by randomly sampling meteorological data from the five year dataset. There were two major considerations regarding the random sampling procedure. Firstly, since the various components of the meteorological data are correlated (i.e. the temperature at a particular point in time is related to humidity etc.) the random samples were made for all variables simultaneously. Additionally, because of the auto-correlation present in the meteorological data, it was decided to carry out block samples so that a degree of this data structure could remain intact. The size of block was set at 24 hours.

100 new meteorological files were created from random block samples of the pooled meteorological data (2002 to 2006). Each ADMS-Urban model scenario requires a full year of meteorological data (i.e., 365 days, or 8760 hours). Note, leap years have been ignored for sake of simplicity. Each newly created meteorological file consists of 8760 hours, and so 365 random blocks of data were sampled and stitched together to form a new data file. This process was repeated 100 times ( $n = 100$ ) and the 100 new meteorological files were then used as inputs to the base case scenario and resulted in 100 new predictions (annual means) of  $\text{NO}_2$  and  $\text{NO}_x$  concentrations for the five sites.

The predictions were then ranked in ascending order and the borders marking the middle 95% of data recorded. The results of the bootstrap procedure are illustrated in Figure 27 and Figure 28.



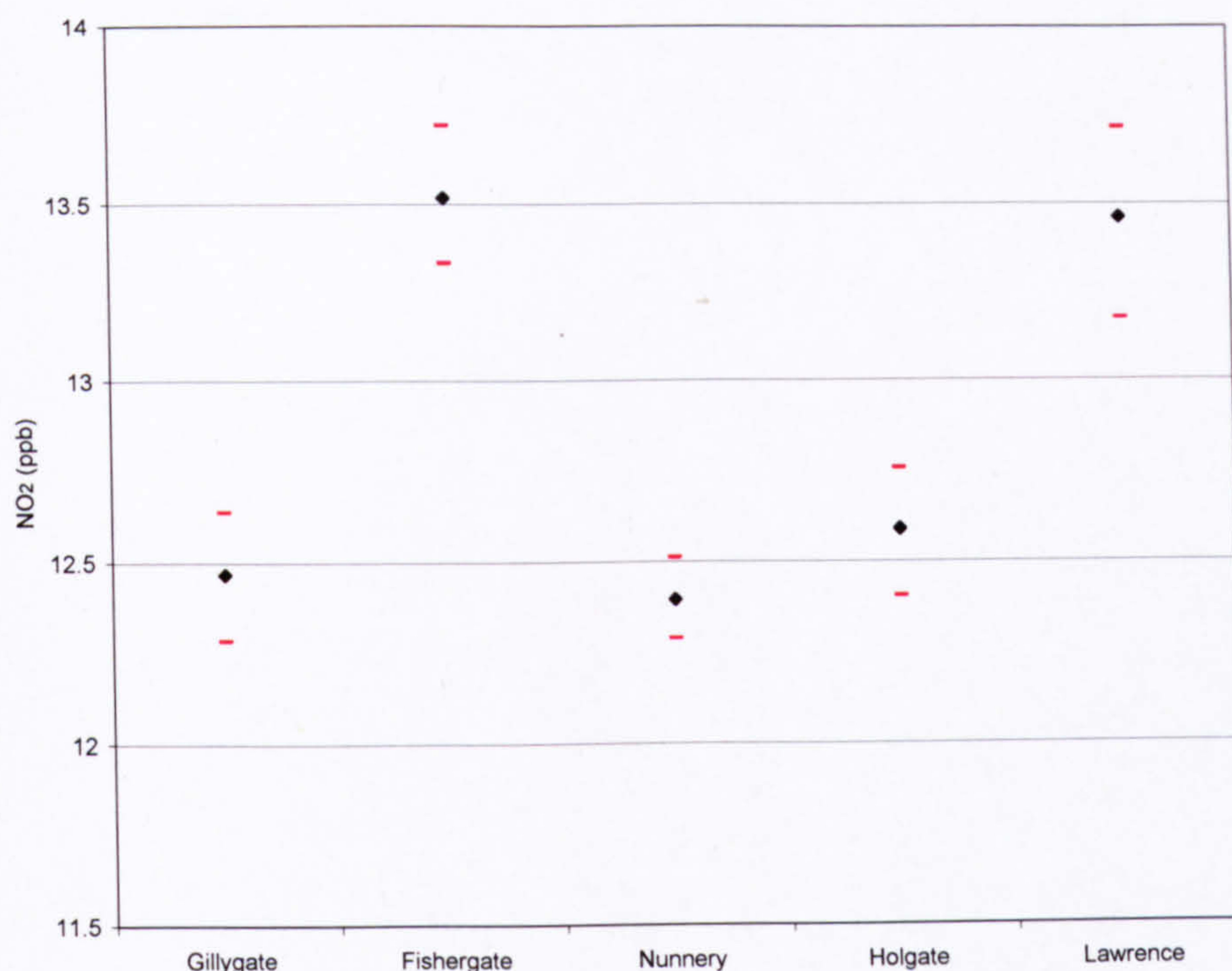


**Figure 27:** ADMS-Urban predicted annual mean NO<sub>2</sub> concentrations and 95% confidence intervals for the for the five different study sites.

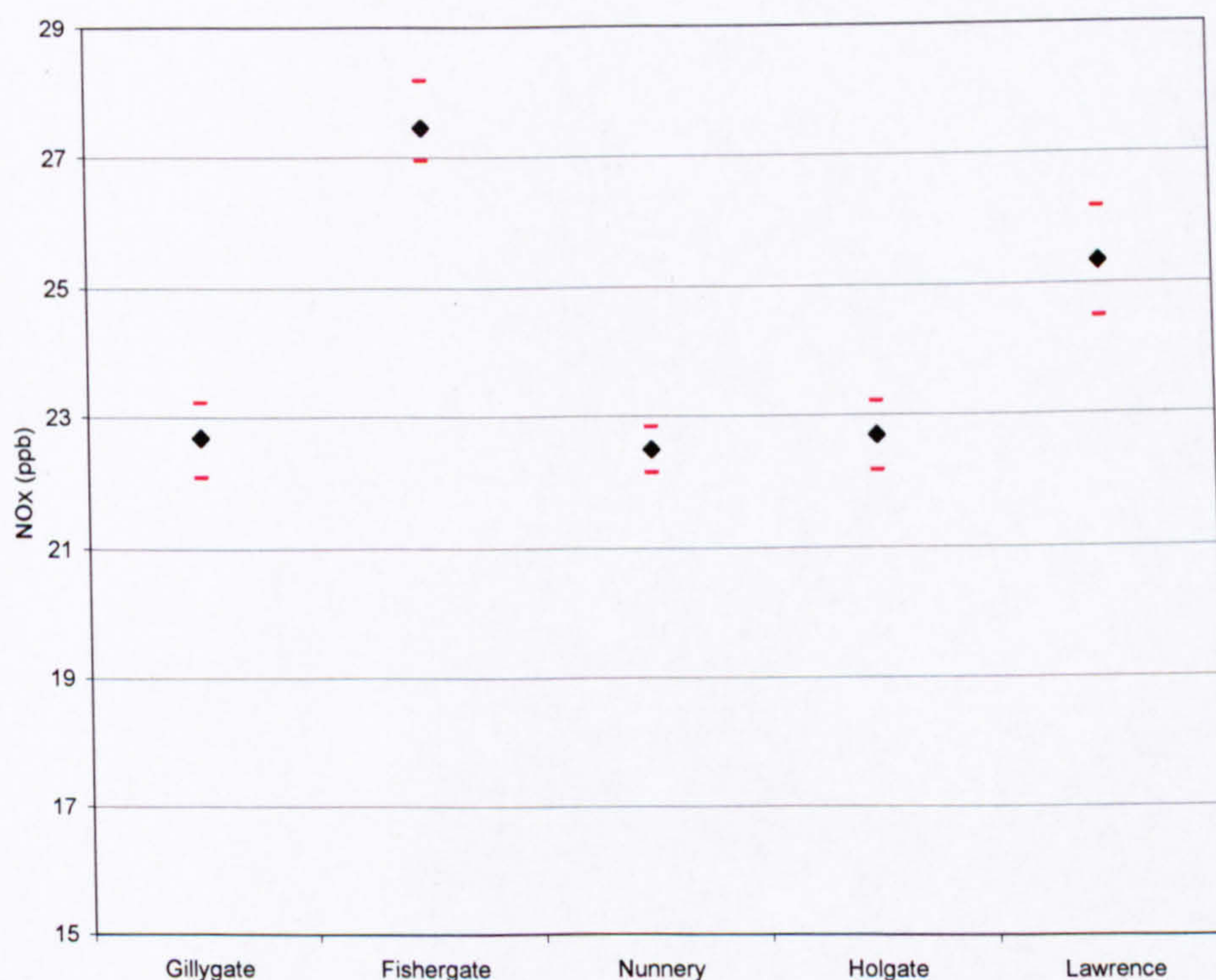


**Figure 28:** ADMS-Urban predicted annual mean NO<sub>x</sub> concentrations and 95% confidence intervals for the for the five different study sites.

The bootstrap procedure has highlighted the relative differences in model predictions as a result of the randomly sampled meteorological data. The two figures show that changing the



meteorological data within the existing limits does not lead to considerable differences in the model predictions. At all five sites the upper and lower confidence intervals are located close to the mean thus suggesting that there was little variability in the 100 model predictions.

The greatest uncertainties in the predicted mean concentrations of  $\text{NO}_2$  and  $\text{NO}_x$  occurs at Lawrence Street. This is most likely due to this street having the greatest emissions from road vehicles and so the greatest potential to change as a result of meteorological variability. The smallest uncertainties were seen at Nunnery Lane for both pollutants; this street is subject to the lowest volumes of traffic.

#### **4.6.4. Conclusion to ADMS-Urban sensitivity**

The sensitivity analysis has highlighted the changes in  $\text{NO}_x$  and  $\text{NO}_2$  concentrations as a result of varying the input parameters. In the majority of cases, the decision regarding what level to set input parameters is pretty straight forward, for example, in the case of the Monin-Obukhov length, a length of 30 m is desirable if an urban area is being considered. However, the choice of parameter setting may become difficult when there is no obvious answer; this is the case with the chemistry scheme. For example, it is unclear which scheme is more appropriate for a given area since both chemistry schemes predict  $\text{NO}_2$  concentrations, but give very different results.

Additionally, when modelling future year scenarios (i.e. years where meteorological data are not available), the advice from CERC is to use a 'representative year' of meteorological data. However, as we have shown in this section, meteorological data can have a substantial impact on the modelling results. It would be possible for the user to influence the results of a modelling scenario by using a favourable year of meteorological data. For example, in the case of York, the use of Church Fenton data from the year 2005 or 2002 would produce lower  $\text{NO}_x$  and  $\text{NO}_2$  concentrations than if the 2003 data-file were used. Discrepancies such as this would then be passed down into management decisions. It is therefore a potential source of uncertainty in the modelling results and should be appropriately addressed. An improvement would be to adopt the bootstrap system outlined in section 4.6.3. so as to reduce the bias associated with the choice of meteorological year. Another option would be to always run future scenarios using a variety of meteorological years.

### **4.8. Chapter summary**

This Chapter has highlighted the differences in model predictions as a result of tailoring the traffic emissions to York conditions. The traffic surveys carried out in York have illustrated the difference in vehicle composition using the York network as compared to the national average. A particularly interesting finding was the substantial differences in heavy vehicles, such as HGVs and buses, which were shown to be much newer than anticipated on a national level. Indeed, the model scenario created with York relevant traffic emissions showed a reduction in the annual mean  $\text{NO}_x$  and  $\text{NO}_2$  predictions when compared to the base case scenario (national average



traffic emissions). The traffic composition on a national level is unrepresentative of traffic emissions found on the York road network. The work carried out as part of this Chapter has been useful for the CYC who can now use the York specific data to calculate the traffic emissions for the urban area of York. Indeed, in the recent air quality modelling work carried out as part of the ongoing commitment by the air quality department at the CYC utilised the data collected in section 4.5.

This Chapter has also highlighted the sensitivities in ADMS-Urban predictions to the various input parameters. Despite many of the sensitivity scenarios tested in this analysis being unrealistic for the urban area of York it has highlighted the potential variability in the model predictions to changes in these parameters. This Chapter also illustrated the importance of primary NO<sub>2</sub> emissions in the prediction of ambient NO<sub>2</sub> concentration. The CYC will also incorporate a variety of primary NO<sub>2</sub> scenarios in future modelling work in an attempt to account for this variable. For the purpose of future modelling scenarios within this Chapter the default primary NO<sub>2</sub> fraction will be set to 18 % as this better resembles the NO<sub>2</sub>: NO<sub>x</sub> ratio seen in the measured data across York (this is explained in more detail in Chapter 7).

Finally, for completeness a further model scenario including all 921 road links in the York network has been created. This final model scenario contains all the emission sources outlined in section 4.2.3 (Figure 18). The results of this 'complete' model scenario are shown in Table 22.

**Table 22:** Observed and predicted annual mean (2005) NO<sub>2</sub> and NO<sub>x</sub> concentrations for the five technical breach sites in York. Predictions are for the model scenario that contains all emission sources in the urban area of York for the year 2005. The air quality background data for this new scenario has been collected from the monitoring site outside the urban area of York (Dunnington) so as to prevent double counting of emissions. All traffic emissions have been calculated using the survey data, and the primary NO<sub>2</sub> fraction has been set at 18 % of NO<sub>x</sub>. The meteorological data used for this scenario are for 2005.

	Predictions (ppb)					
	G	H	N	F	L	Mean
Observed						
NO <sub>2</sub>	19	19	17	17	18	18
NO <sub>x</sub>	38	40	34	37	49	40
Full model scenario						
NO <sub>2</sub>	15.2	14.9	16.4	17.8	15.9	16
NO <sub>x</sub>	25.4	25.1	28.9	35.0	27.8	28



It can be seen that the new model scenario predicts NO<sub>x</sub> and NO<sub>2</sub> concentrations in closer agreement to the observed annual mean concentrations (Table 22) than compared to the results presented in Table 17 and Table 19; this is especially true of the NO<sub>2</sub> concentrations which are now much more in line with the observations compared to the previous modelling scenarios described in Table 17 to Table 20. However, despite all these efforts, the results from the new model scenario shown in Table 22 still show quite substantial differences from the observed concentrations at the receptor sites. Nevertheless, the work carried out as part of this Chapter has therefore helped to establish a new base case model scenario (Table 22) for the City of York, which can be deployed by the CYC in its air quality management strategies.



## **5. NO<sub>x</sub> and NO<sub>2</sub> in York**

### **5.1. Chapter preview**

This Chapter summarises recent air quality (NO<sub>x</sub> and NO<sub>2</sub>) in York and the trends in concentrations since monitoring began in the city in 1999. Firstly, data from the automatic monitoring sites are compared against the annual and hourly objectives for NO<sub>2</sub> recommended in the NAQS. Next, the spatial characteristics of the concentrations of NO<sub>x</sub> and NO<sub>2</sub> in the City of York are explored. Finally, an insight into the temporal trends in NO<sub>x</sub> and NO<sub>2</sub> concentrations recorded in York over the period 1999 to 2006 is provided. The final section also examines NO<sub>x</sub> and NO<sub>2</sub> concentration data collected in urban areas other than York around the UK.

### **5.2. Air Quality Objectives**

#### **5.2.1. Introduction**

There are two air quality objectives concerned with the ambient concentrations of NO<sub>2</sub>; an hourly mean objective of 105 ppb not to be exceeded more than 18 times a year and an annual mean objective of 21 ppb (see section 2.2.2). It is a requirement of all local authorities to monitor and compare the air quality in their regions against these NO<sub>2</sub> objectives.

#### **5.2.2. Results: compliance with hourly and annual NO<sub>2</sub> objectives**

Table 23 shows a summary of the annual mean NO<sub>2</sub> concentrations at various sites around York in recent years. Since monitoring began there are a number of instances when the annual NO<sub>2</sub> objective has been breached in the city; the most recent of which occurred in 2005 at the urban centre site (City Centre). However, since the annual mean NO<sub>2</sub> concentration in 2006 at two sites (Gillygate and Lawrence Street) was only marginally below the objective value (both at 20 ppb) the quality of air in the City of York still remains an important concern.

The hourly NO<sub>2</sub> objective has not been breached until the hourly NO<sub>2</sub> concentration at a particular site exceeds 105 ppb for more than 18 hours in any one year. Table 24 shows the 18<sup>th</sup> highest hourly NO<sub>2</sub> concentration in York for the various monitoring sites for each of the study years (1999 to 2006) where data are available. At no point over the 8-year period have the NO<sub>2</sub> concentrations at the sites in York exceeded the hourly objective.



**Table 23:** Annual mean NO<sub>2</sub> concentration recorded at the various monitoring sites in the City of York. Those years with data capture less than 75% are highlighted in red and those years where the annual mean NO<sub>2</sub> concentration exceeds the objective are underlined.

Site	1999	2000	2001	2002	2003	2004	2005	2006
Bootham	12	12	13	13	18	10	10	11
Dunnington	10	10	8	8	10	8	9	10
Fishergate	18	18	16	19	<u>21</u>	18	17	17
City Centre	26	23	17	<u>23</u>	17	17	<u>23</u>	-
Gillygate	-	-	-	-	<u>26</u>	16	19	20
Lawrence street	-	-	-	-	<u>24</u>	21	18	20
Nunnery lane	-	-	-	-	19	17	17	18
Holgate Road	-	-	-	-	<u>27</u>	<u>22</u>	19	19

**Table 24:** The 18<sup>th</sup> highest hourly NO<sub>2</sub> concentration for each calendar year for the various monitoring sites in the urban area of York.

Site	1999	2000	2001	2002	2003	2004	2005	2006
Bootham	40	41	41	37	46	39	35	37
Dunnington	28	32	33	31	33	37	35	33
Fishergate	49	52	46	68	58	49	51	50
City Centre	57	53	56	52	52	67	81	-
Gillygate	-	-	-	-	62	54	87	53
Lawrence street	-	-	-	-	43	60	56	56
Nunnery lane	-	-	-	-	40	62	61	61
Holgate Road	-	-	-	-	60	89	71	71

When the air quality objectives were first released it was thought that only the larger cities of the UK would have an air quality problem (i.e., exceed the objectives), with the exception of monitors sited in close proximity to large industrial sources. However, since several relatively small urban areas, such as York, Cambridge, Canterbury and Tewkesbury, etc. and other more rural locations, such as the New Forest, discovered air quality issues it was thought necessary to investigate further.

The objective exceedences in NO<sub>2</sub> concentration experienced at York are indicative of the high volumes of traffic using the York road network. Indeed, at morning rush hour, queues of traffic are found on all major arterial routes and so a journey that would normally take 10



minutes, during this busy period can take up to 40 minutes. The sheer volume of traffic is therefore the most likely reason for the air quality problems in York. The congestion coupled with the narrow streets, some of which are street canyons, results in elevated concentrations.

## **5.3. Spatial trends**

### **5.3.1. Introduction**

Despite the City of York being a relatively small urban area (272 km<sup>2</sup>) there is substantial variation in the concentrations of NO<sub>2</sub> across the city (see Table 23 and Table 24). This section will analyse the measured NO<sub>x</sub> and NO<sub>2</sub> concentrations at the various monitoring stations across York to shed light on the spatial trends in the concentration of these pollutants.

The dynamic nature of York's air quality monitoring network has been highlighted in Table 5, Chapter 3. Over time stations have been brought online and other have been closed. The years with the highest number of operational sites are 2004 and 2005. The analysis of spatial trends will therefore solely concentrate on the NO<sub>x</sub> and NO<sub>2</sub> concentrations recorded for these two years.

### **5.3.2. Results and discussion: NO<sub>x</sub> and NO<sub>2</sub> concentration comparison**

Table 25 provides the mean concentrations of NO<sub>x</sub> and NO<sub>2</sub> recorded at the eight monitoring sites in operation between 1<sup>st</sup> January 2004 and 31<sup>st</sup> December 2005.

Concentrating first on the NO<sub>x</sub> concentrations at the various monitoring sites in York, it is possible to distinguish that the sites with the poorest air quality (i.e., the highest NO<sub>x</sub> concentrations) are those situated adjacent, or in close proximity, to roads. This is unsurprising since these sites in particular will be subject to higher levels of road traffic emissions (mainly in the form of NO). Indeed, to some extent the magnitude of the NO<sub>x</sub> concentration mirrors the traffic volume (or AADT), with, for example the highest average NO<sub>x</sub> concentrations (56 ppb) occurring at the site with the highest volume of local traffic (~17 600 vehicles per day) and the lowest NO<sub>x</sub> concentration (34 ppb) at the roadside site located near the road with the lowest traffic count (~ 9000 vehicles per day).

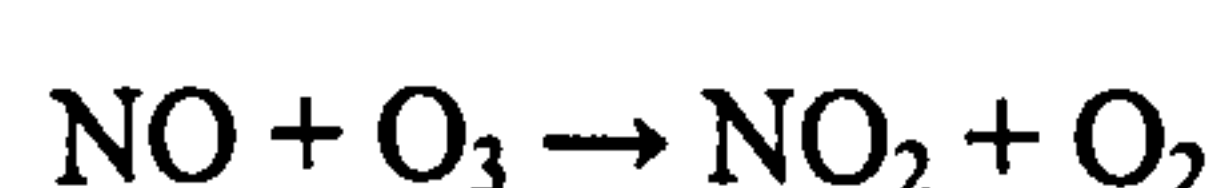
Gillygate, and to some degree, Holgate Road are suspected street canyons (where the height to width ratio of the street is greater than 1). The air quality monitors adjacent to these streets are therefore thought to be subject to poor rates of dispersion as a consequence of the street canyon characteristics. Poor dispersion rates prevent emissions escaping the canyon and so lead to elevated NO<sub>x</sub> and NO<sub>2</sub> concentrations at ground level.



**Table 25:** Mean concentrations of NO<sub>x</sub>, NO<sub>2</sub> and the NO<sub>2</sub>: NO<sub>x</sub> ratio recorded at the various monitoring sites in York for the period 1/1/2004 to 31/12/2005; percentage data captures for the air quality data, plus AADT estimate from the emission inventory for York

Site name	Type	NO <sub>x</sub> (ppb)	NO <sub>2</sub> (ppb)	NO <sub>2</sub> /NO <sub>x</sub>	Data capture (%)	AADT
Bootham	Urban bkg	16	10	0.6	94	-
Dunnington	Background	12	8	0.7	90	-
Fishergate	Roadside	38	17	0.4	94	15927
City centre	Urban centre	36	20	0.6	83	-
Gillygate	Roadside	38	17	0.4	90	13561
Lawrence St	Roadside	56	19	0.3	92	17573
Nunnery La	Roadside	34	17	0.5	95	9353
Holgate Rd	Roadside	41	20	0.5	86	15187

Despite being situated away from any major emission source, the urban centre site, City Centre, has the highest NO<sub>2</sub> concentration for the period in question. Urban centre sites often experience high NO<sub>2</sub> concentrations because the NO released from vehicles (and other combustion sources) will be able to mix and react with additional O<sub>3</sub> that has been brought down to ground level from aloft, and so, via reaction 39, form NO<sub>2</sub>.



39

The availability of O<sub>3</sub> can therefore determine the formation rate of secondary NO<sub>2</sub> and so despite the close proximity of roadside sites to emission sources, the NO<sub>2</sub> concentration present can often be lower than what is experienced at locations some distance away from emission sources, such as urban centre sites (AQEG, 2004). This dominance of NO<sub>2</sub> over NO at the urban centre site is illustrated by the high NO<sub>2</sub>: NO<sub>x</sub> ratio seen at the City Centre site. Indeed, as already mentioned, the annual mean NO<sub>2</sub> concentration at the City Centre site has twice exceeded the annual NO<sub>2</sub> objective in the last 5 years. In large urban areas it is the roadside sites that usually experience the greatest NO<sub>2</sub> concentrations and not the Urban Centre sites as shown in Table 25. This difference between York and other urban areas will be revisited in the following sections of this Chapter.

The urban background site represents the general level of air quality in an urban area without the direct influence of any particular emission source. The background site is located 6 km east of the urban area of York (see Chapter 3, section 3.4) and represents the quality of air in a relatively clean atmosphere. The high NO<sub>2</sub>: NO<sub>x</sub> ratios are therefore expected at these two sites since neither is subject to large quantities of fresh NO<sub>x</sub> emissions.



### 5.3.3. Results and discussion: diurnal profiles

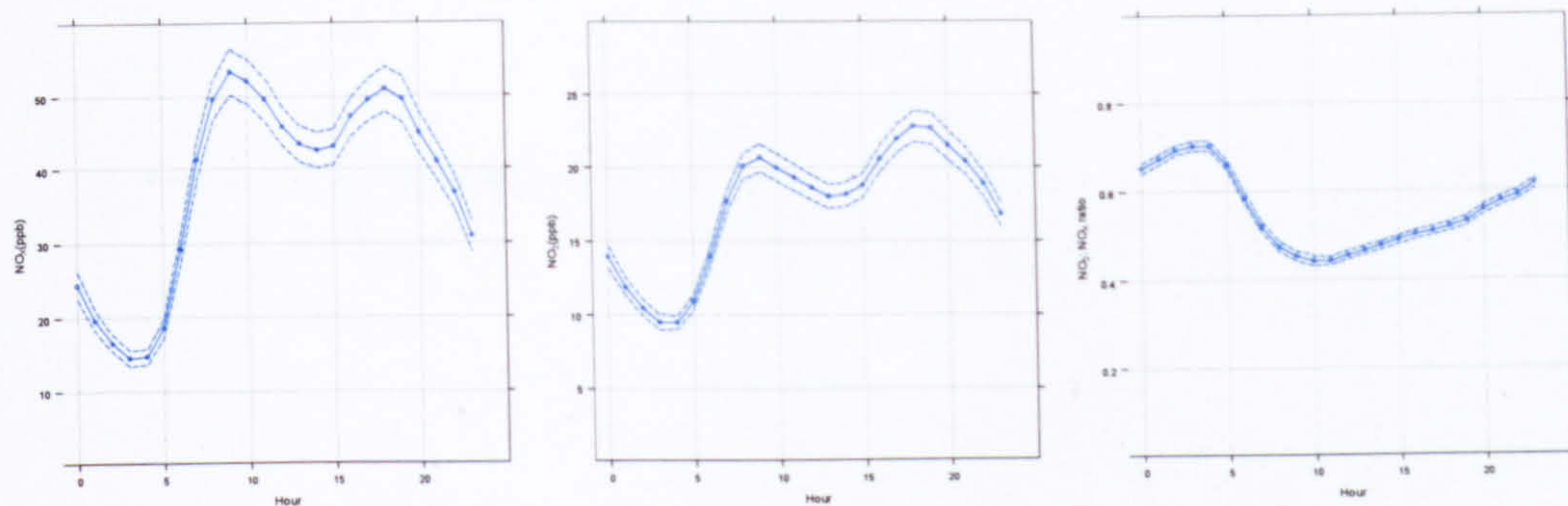
Ambient  $\text{NO}_x$  and  $\text{NO}_2$  concentrations vary throughout the day. Figure 29 illustrates the diurnal profiles of  $\text{NO}_x$ ,  $\text{NO}_2$  and the  $\text{NO}_2$ :  $\text{NO}_x$  ratio at the sites of Gillygate (a), City Centre (b), Bootham (c) and Dunnington (d). Gillygate has been chosen to represent the diurnal profiles of all roadside sites in York since they are all similar and also because Gillygate is the only site where hourly traffic counts are available (Figure 30).

During the morning rush hour period the ambient  $\text{NO}_x$  at roadside sites becomes dominated by fresh  $\text{NO}_x$  emissions (Figure 29a(i)), namely in the form of NO, thus the  $\text{NO}_2$ :  $\text{NO}_x$  ratio falls substantially, see Figure 29a(iii). During the remainder of the day the  $\text{NO}_2$ :  $\text{NO}_x$  ratio steadily increases, reflecting the fact that NO is continuously destroyed and  $\text{NO}_2$  continually produced via reaction 39. The  $\text{NO}_2$ :  $\text{NO}_x$  ratio is generally highest during the night (00:00 – 05:00) reflecting the low NO emissions and the absence of  $\text{NO}_2$  photolysis. The diurnal variation in traffic counts (Figure 30) closely resembles the diurnal variations in  $\text{NO}_x$  and  $\text{NO}_2$  concentration seen at the roadside site of Gillygate (and indeed, the concentration profiles for the four remaining roadside sites not shown) and so provides evidence of the strong influence of traffic emissions at these roadside sites. The urban centre site (City Centre) displays a similar diurnal  $\text{NO}_2$ :  $\text{NO}_x$  profile to the roadside sites (Figure 29b(iii)) and thus also suggests a strong road source influence.

There are clear differences in the diurnal profiles of Bootham (Figure 29c) and Gillygate (Figure 29a). Firstly, the Bootham  $\text{NO}_2$ :  $\text{NO}_x$  ratio is at all times of the day greater than at Gillygate, reflecting the fact that the majority of  $\text{NO}_x$  at Bootham is in the form of  $\text{NO}_2$ . Additionally, the fall in the ratio during the morning rush hour is less pronounced at Bootham than Gillygate, and its subsequent recovery during the remainder of the day occurs at a quicker rate than the upturn in concentration observed at the roadside site (Figure 29a(iii) and Figure 29c(iii)). The diurnal  $\text{NO}_2$ :  $\text{NO}_x$  profile for Dunnington (Figure 29d(iii)) is similar to that of Bootham but the fall in ratio during the early morning period is less pronounced. Again, the highest hourly  $\text{NO}_2$  concentrations at the urban background (Bootham) and background (Dunnington) sites are seen during the afternoon rush hour period.

As highlighted in the previous paragraphs, the hours of the day that the  $\text{NO}_2$  hourly mean objective is most likely to be breached (with concomitant risks of high public exposure) are during the afternoon 'rush hour' period (between 15:00 and 20:00). This afternoon phenomenon is most likely a combination of three factors: firstly, the steady build up of  $\text{NO}_2$  throughout the daytime period through reaction 39; secondly, the steady build up of ambient  $\text{O}_3$  concentrations formed through photochemical reactions (reactions 10 – 18); and finally the injection of fresh  $\text{NO}_x$  emissions (mainly NO) during the afternoon rush hour period that can react with the relatively high  $\text{O}_3$  to form more  $\text{NO}_2$ .

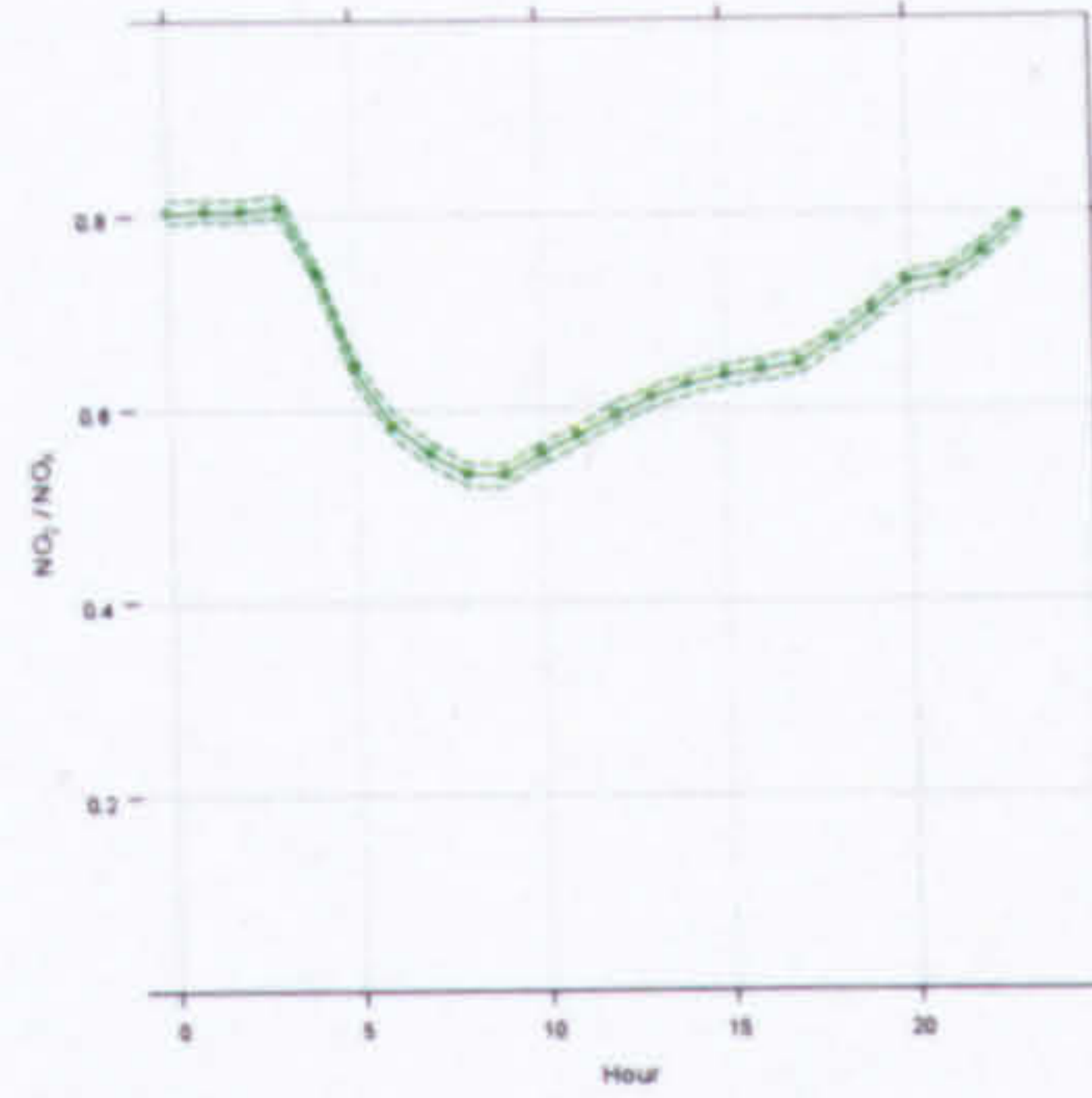
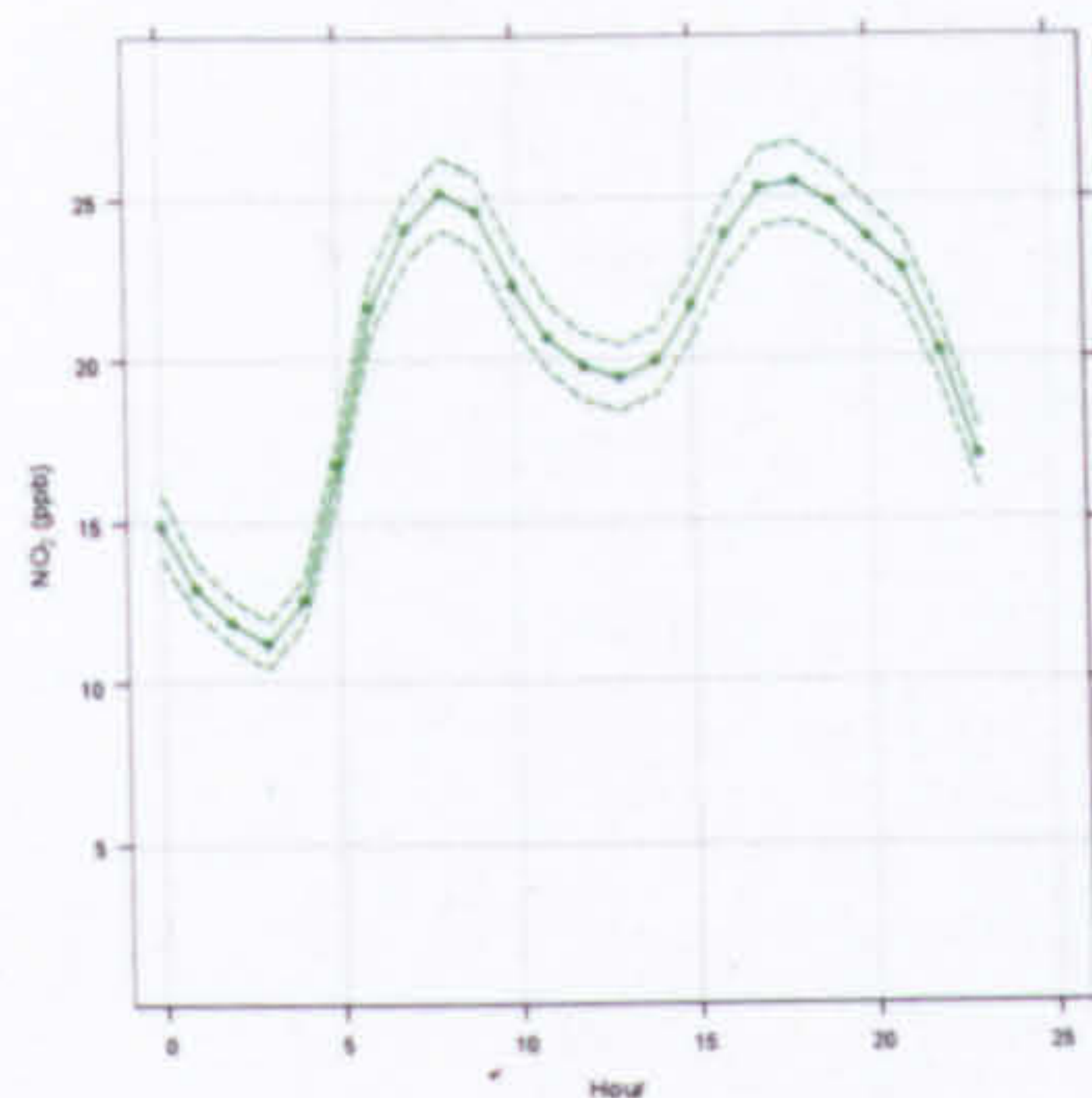
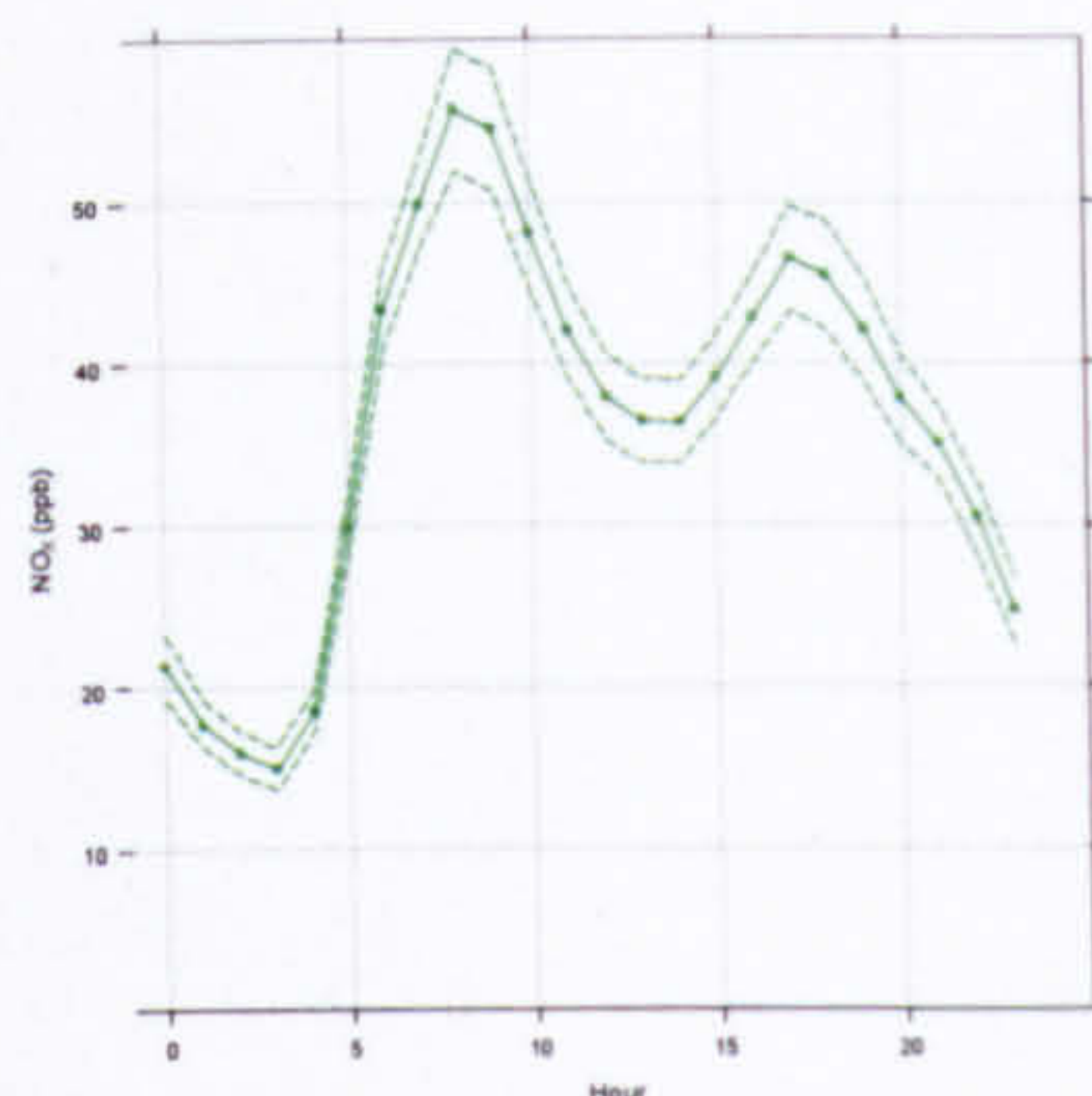




a) i)

ii)

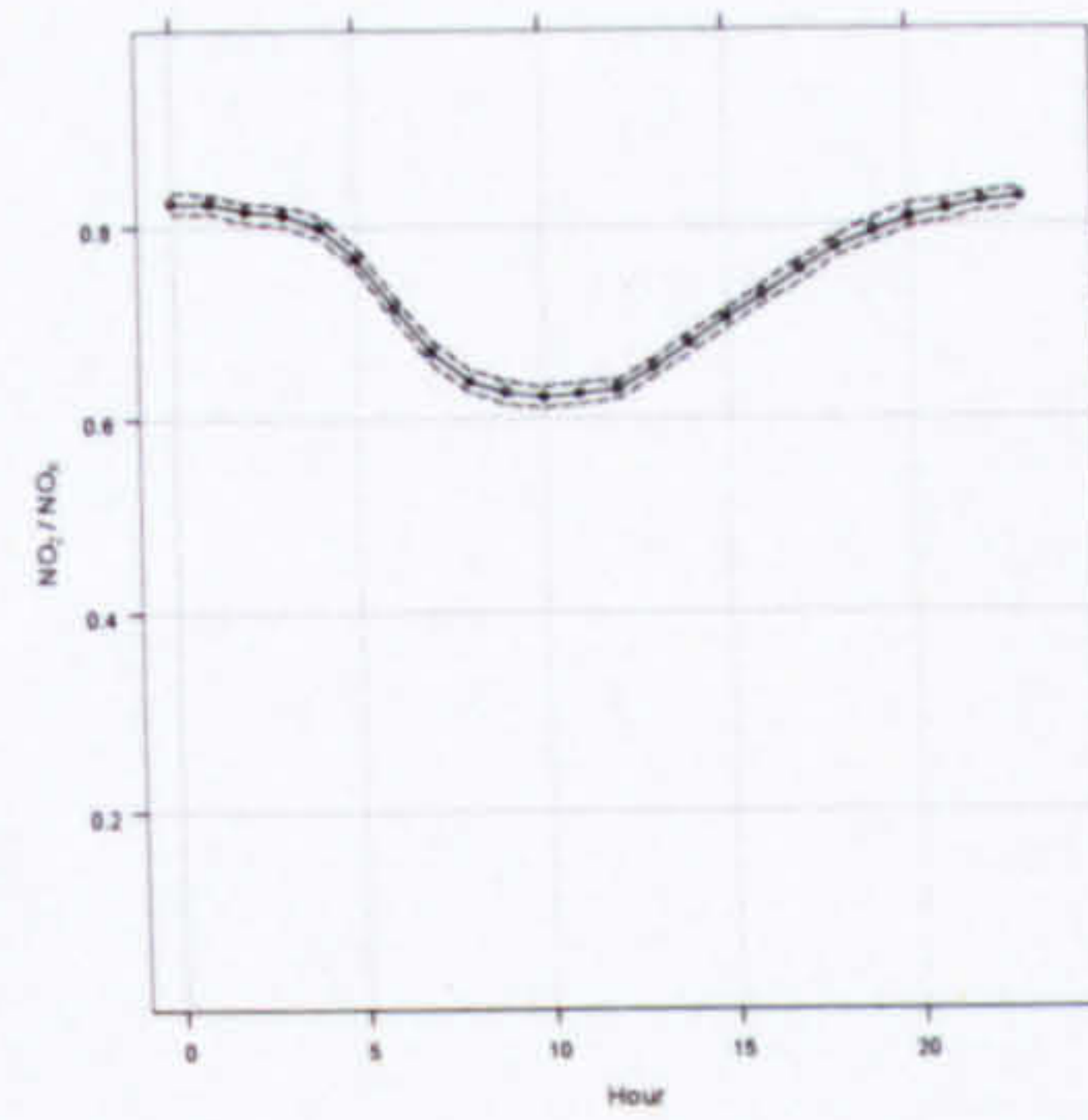
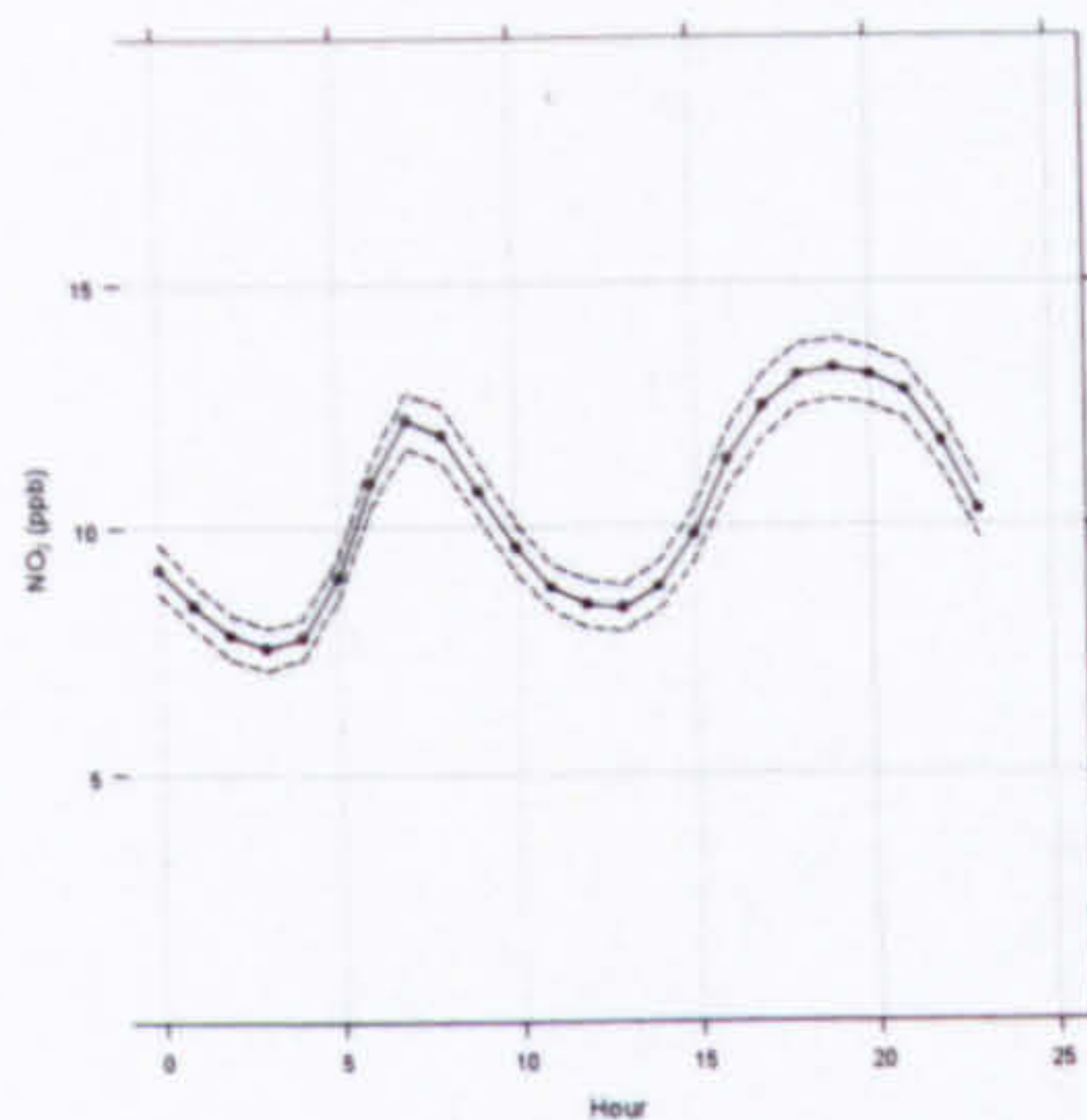
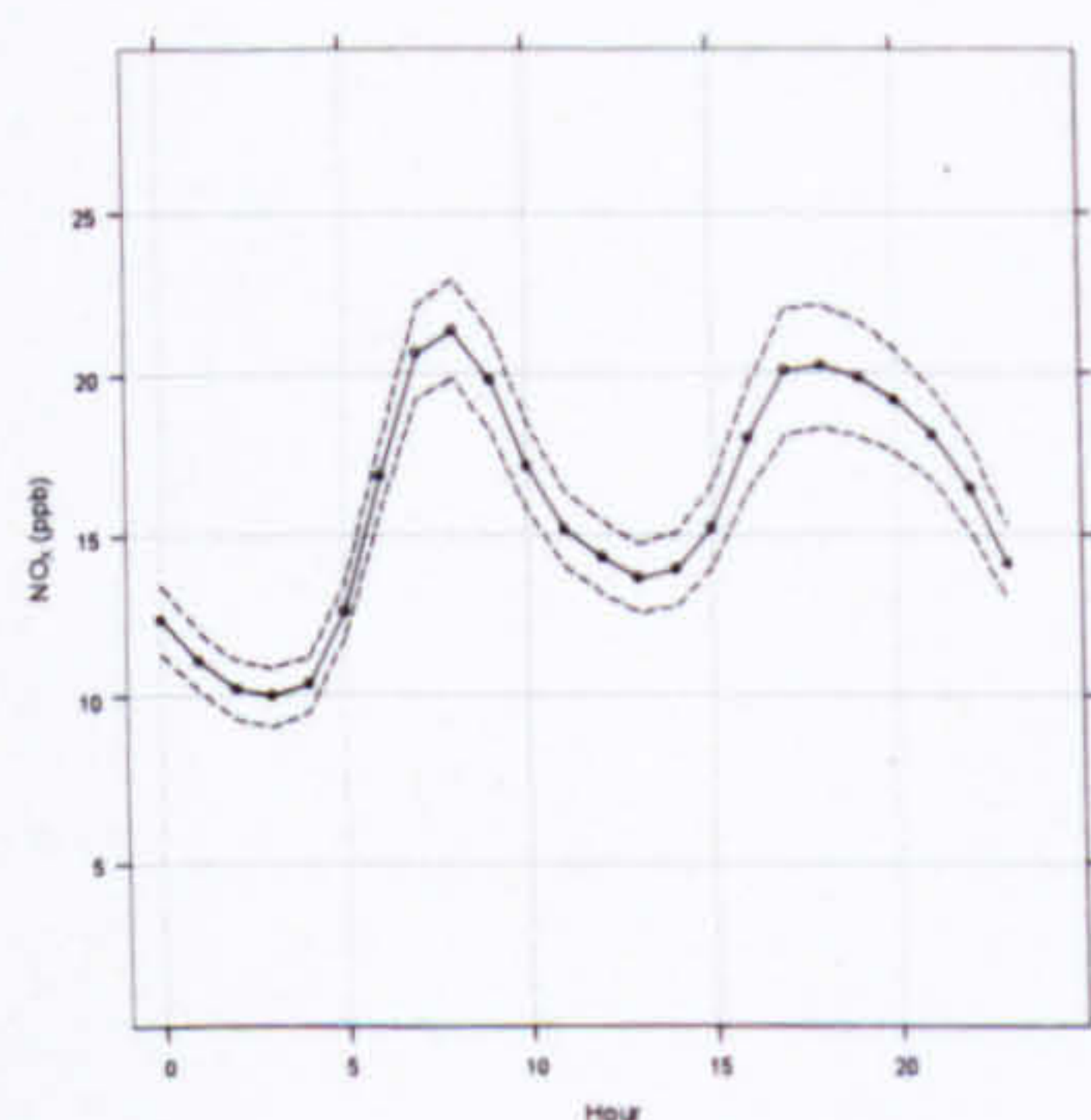
iii)



b) i)

ii)

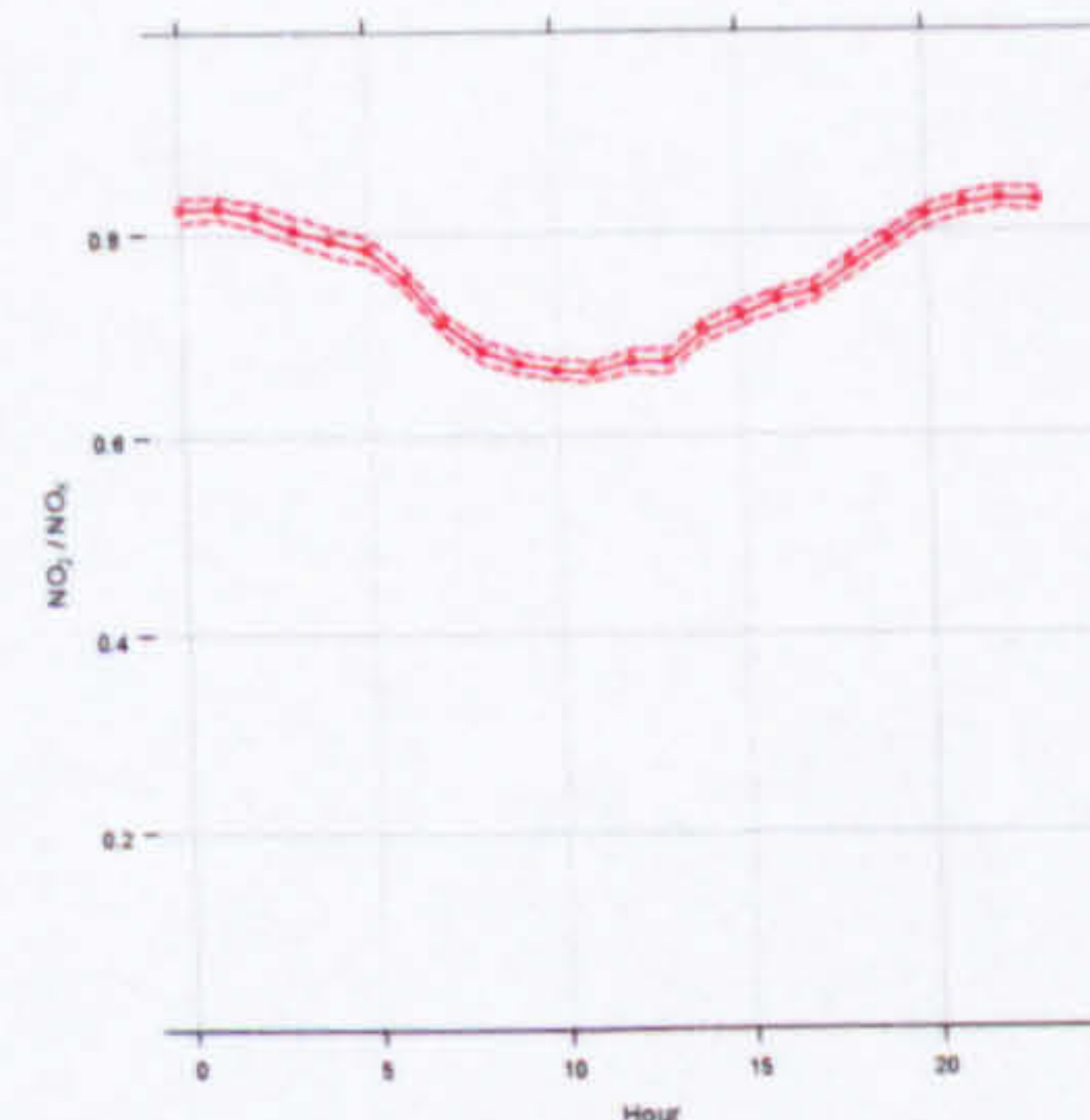
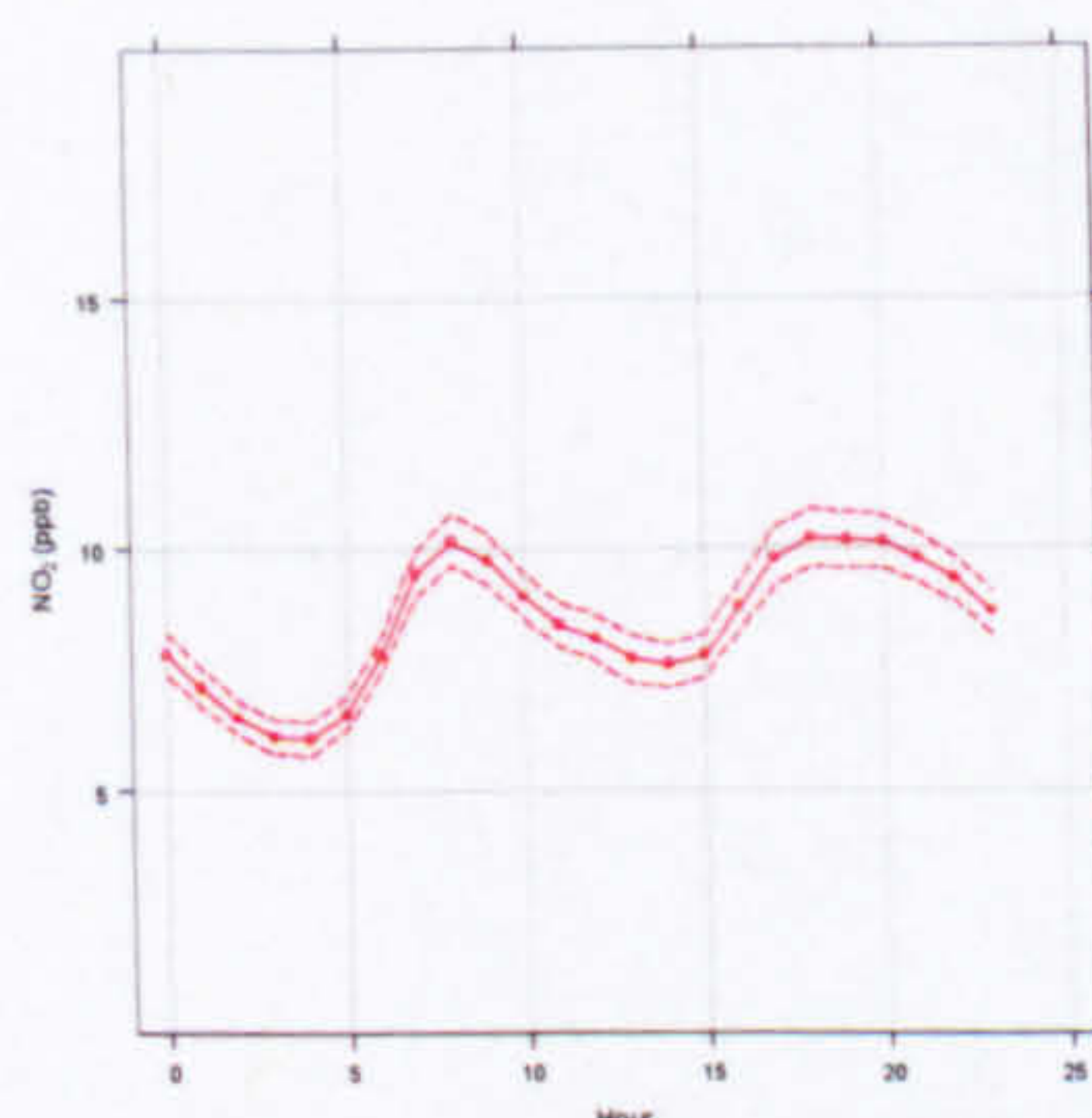
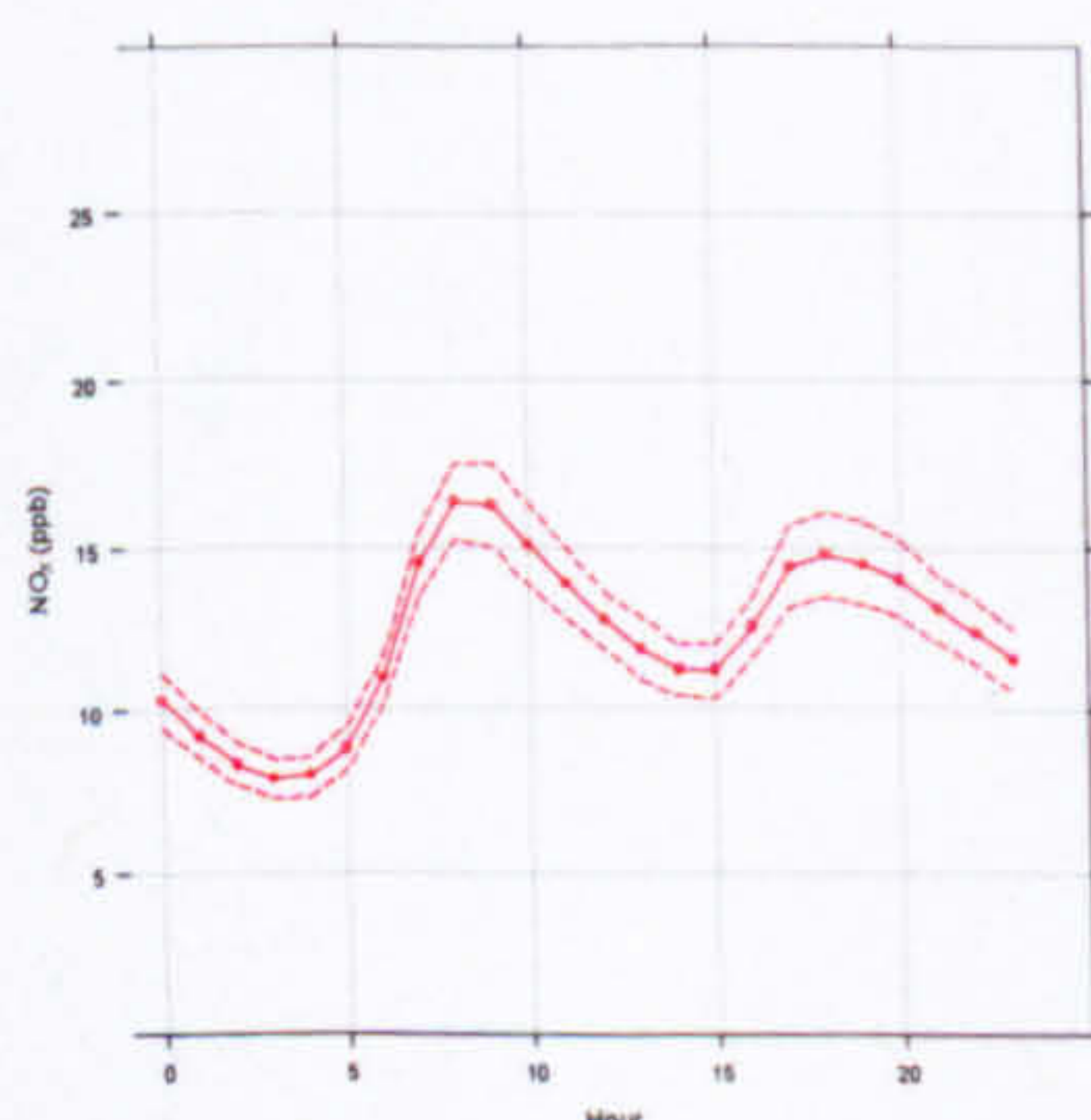
iii)



c) i)

ii)

iii)



d) i)

ii)

iii)

**Figure 29:** Mean hourly ratios of  $\text{NO}_x$  (i),  $\text{NO}_2$  (ii) and the  $\text{NO}_2:\text{NO}_x$  ratio (iii) for each hour of the day for the sites of Gillygate (a), City Centre (b), Bootham (c) and Dunnington (d). The 95% confidence intervals are shown by the dashed lines. Note: the diurnal plots use different scales to retain detail.



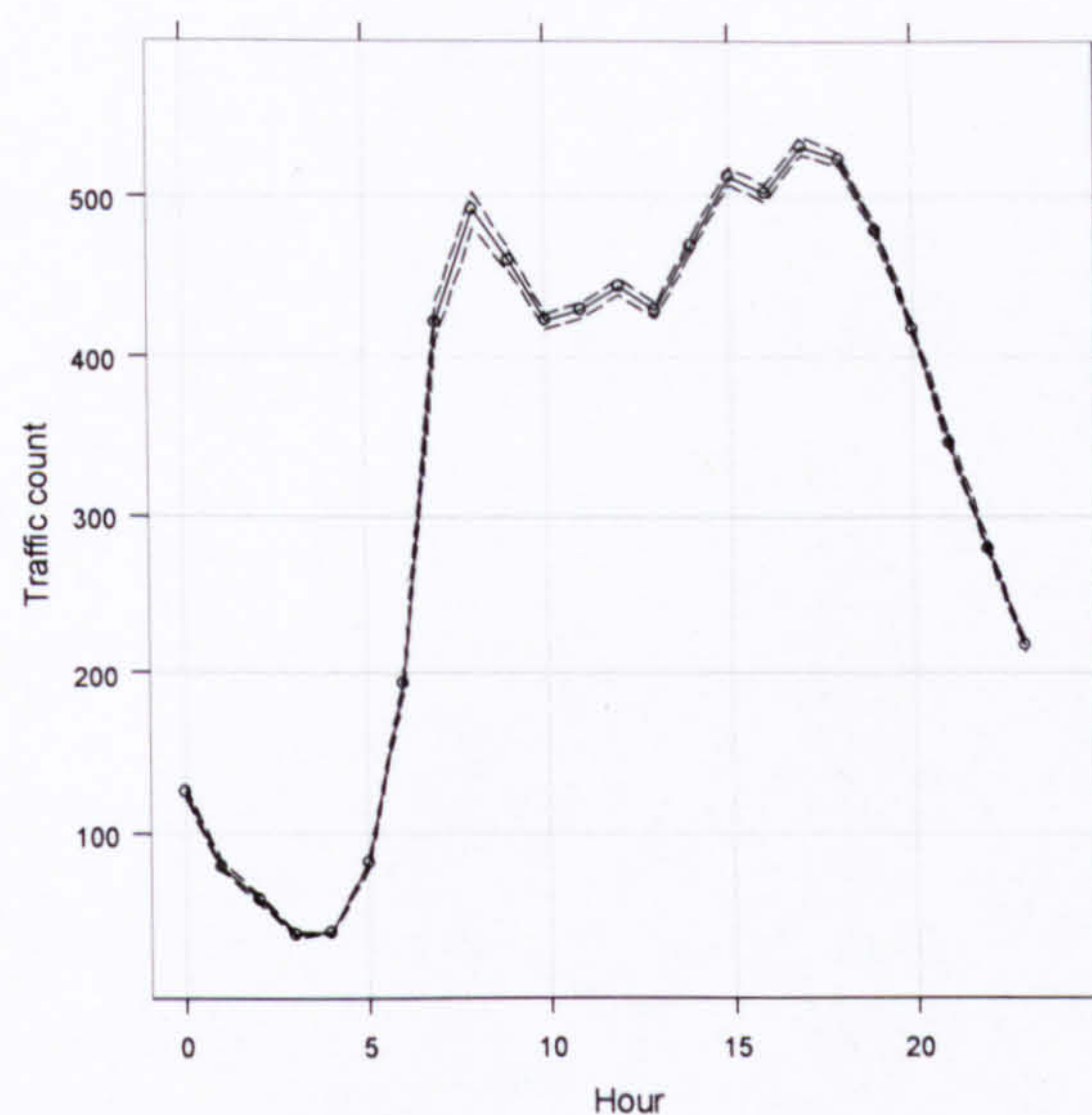


**Figure 30:** Mean hourly traffic counts from the automatic traffic counter for the inbound lane of traffic at Gillygate.

The diurnal profile of  $\text{NO}_2$  concentrations seen at the roadside sites in York (represented in Figure 29a(ii)) is somewhat different to the profile of  $\text{NO}_2$  concentrations for roadside sites in larger urban areas. As an example, the ambient  $\text{NO}_2$  concentrations for the same period are shown in Figure 31a(ii) for the roadside site of Marylebone Road in London. It can be seen in Figure 31a(ii) that high hourly  $\text{NO}_2$  concentrations are typically seen at both the morning and afternoon rush-hour periods as opposed to the dominance of the early afternoon period over the morning period seen in the York diurnal profiles (Figure 29a(ii)). This difference in the timings of peak  $\text{NO}_2$  is interesting and could be a consequence of differing  $\text{O}_3$  concentrations in the two urban areas. The daily build up of  $\text{O}_3$  concentration does not usually influence the urban  $\text{NO}_2$  concentrations too greatly in large urban areas since it is readily destroyed at the cities outskirts as an air parcel travels over the urban area; it is therefore only the suburbs adjacent to large urban areas where ambient  $\text{O}_3$  concentrations could potentially influence the formation of  $\text{NO}_2$ . Indeed, the diurnal profiles of the London suburban sites of Hillingdon or Haringey (Figure 31b(ii) and Figure 31c(ii)) show a greater peak in  $\text{NO}_2$  concentration during the afternoon compared to morning. Since York is a much smaller city than that of London, it is possible that, unlike London, the ambient  $\text{O}_3$  concentrations can directly influence the roadside  $\text{NO}_x$  and  $\text{NO}_2$  concentrations in York. The air quality ( $\text{NO}_x$  and  $\text{NO}_2$  concentration) at roadside sites in York (and possibly other similar sized cities) can therefore be more accurately likened to suburban sites of large cities such as London rather than their roadside counterparts.



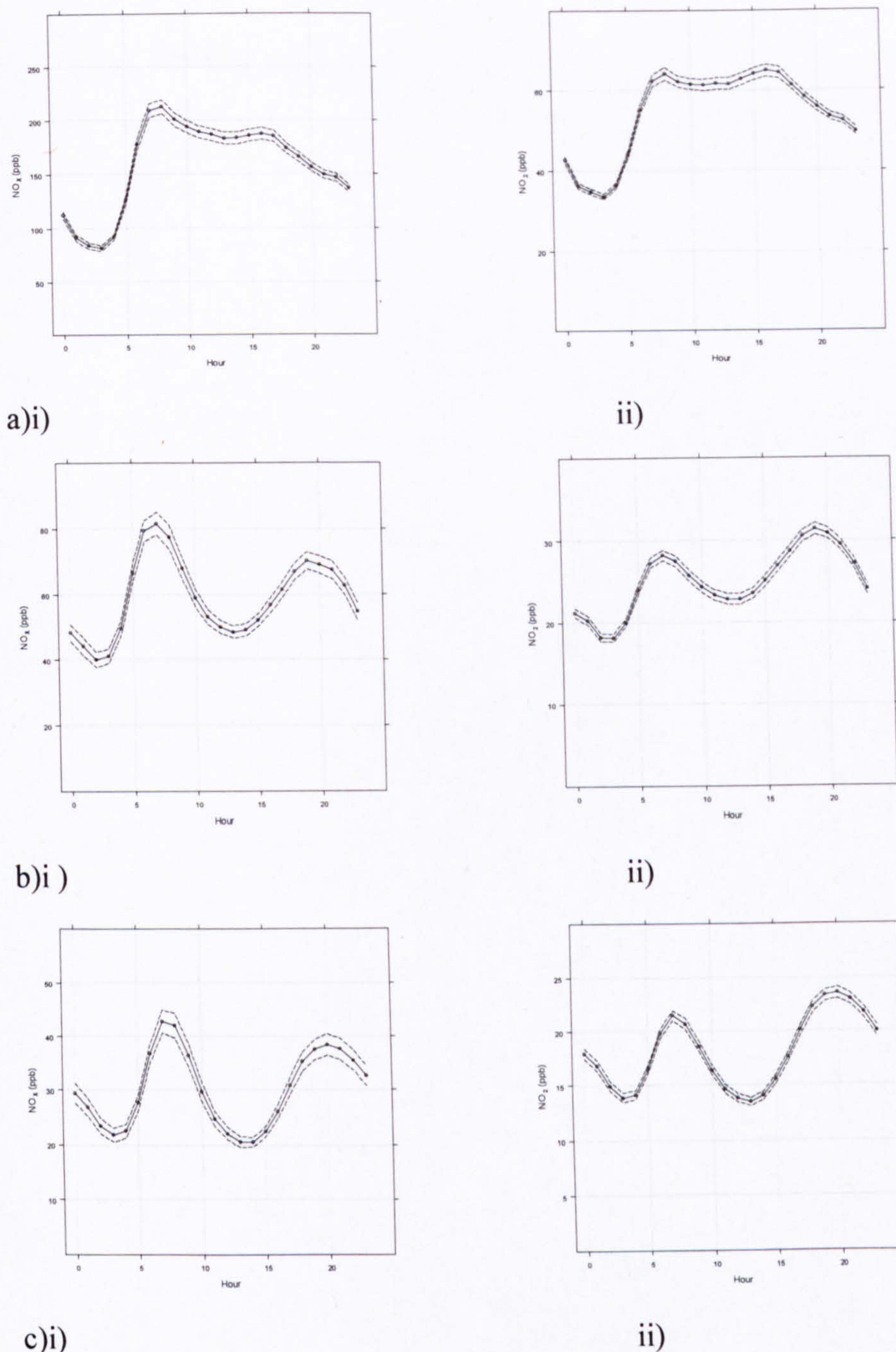


**Figure 31:** Diurnal profile of  $\text{NO}_x$  and  $\text{NO}_2$  concentration for the roadside monitoring site at Marlybone Road, London (a); the suburban site at Hillingdon, London (b) and Haringey, London (c).

#### 5.3.4. Results and discussion: Urban and roadside $\text{NO}_x$ and $\text{NO}_2$ increment

Figure 32 illustrates the differences in  $\text{NO}_x$  and  $\text{NO}_2$  concentrations between Dunnington, Bootham and the City Centre site. It is apparent that the general urban background  $\text{NO}_x$  and  $\text{NO}_2$  concentrations recorded at Bootham (15.8 and 10.3 ppb, respectively) are only slightly higher than those concentrations recorded outside the city at Dunnington (12.2 ppb for  $\text{NO}_x$ , and 8.4 ppb for  $\text{NO}_2$ ). However, there is a substantial difference in  $\text{NO}_x$  and  $\text{NO}_2$  concentrations between the urban background (Bootham) and urban centre sites (City Centre); with a 10 ppb difference in  $\text{NO}_2$  concentrations, and a 20 ppb difference in those for  $\text{NO}_x$ . The evidence suggests that



ambient concentrations of  $\text{NO}_x$  and  $\text{NO}_2$  in the centre of York are almost double those seen at locations outside the urban area.

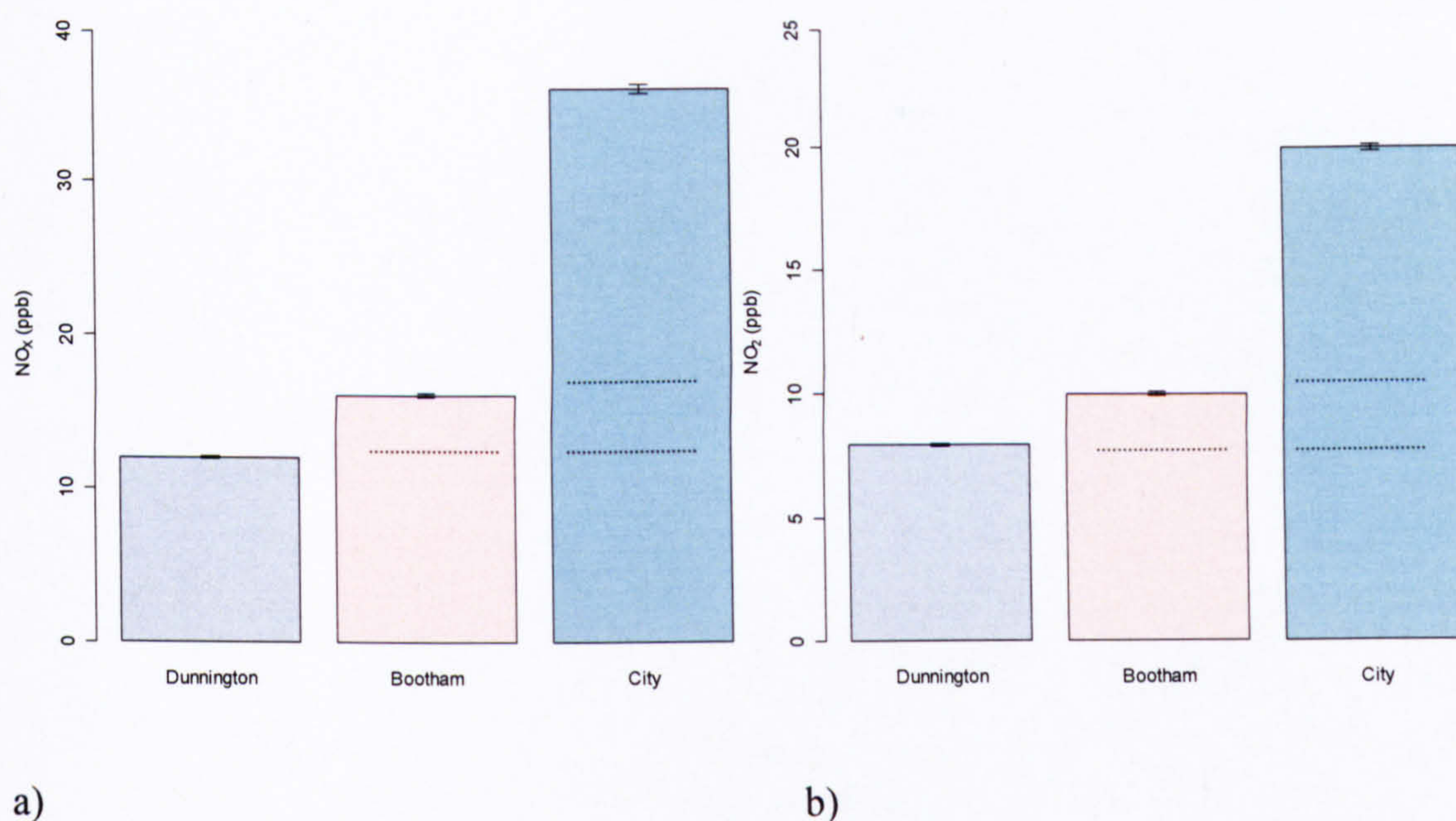


**Figure 32:** Mean  $\text{NO}_x$  (a) and  $\text{NO}_2$  (b) concentrations for the two-year period (2004 to 2005) for the sites of Dunnington, Bootham and City Centre, York. The standard errors are shown.

It is apparent from the previous section that the  $\text{NO}_x$  and  $\text{NO}_2$  concentrations at the majority of monitoring sites in York are dominated by the impact of road traffic emissions. It is possible to crudely calculate the roadside increment of  $\text{NO}_x$  and  $\text{NO}_2$  concentration (i.e. the amount of  $\text{NO}_x$  and  $\text{NO}_2$  which is directly associated with road traffic) by subtracting the urban background concentrations from those of the roadside sites (AQEG, 2004). Figure 33 illustrates the mean  $\text{NO}_x$  and  $\text{NO}_2$  concentrations for the roadside sites and urban background site for the two-year period.

It can be inferred from Figure 33a that the site with the greatest  $\text{NO}_x$  roadside increment is Lawrence Street with over 70 % of the mean  $\text{NO}_x$  recorded at this site a consequence of local traffic; this is no surprise since this site is subject to the highest traffic volumes of the roadside sites in York (see Table 25). Over 60 % of the mean  $\text{NO}_x$  concentrations at Holgate Road are considered to be of road traffic origin (AADT ~ 15 000). Figure 33b shows that the mean  $\text{NO}_2$  roadside increment ranges from 41 % to 50 % of the total; the Holgate Road site is influenced most by the local road traffic. There is a large difference in the  $\text{NO}_x$  and  $\text{NO}_2$  concentrations between urban background and urban roadside locations.



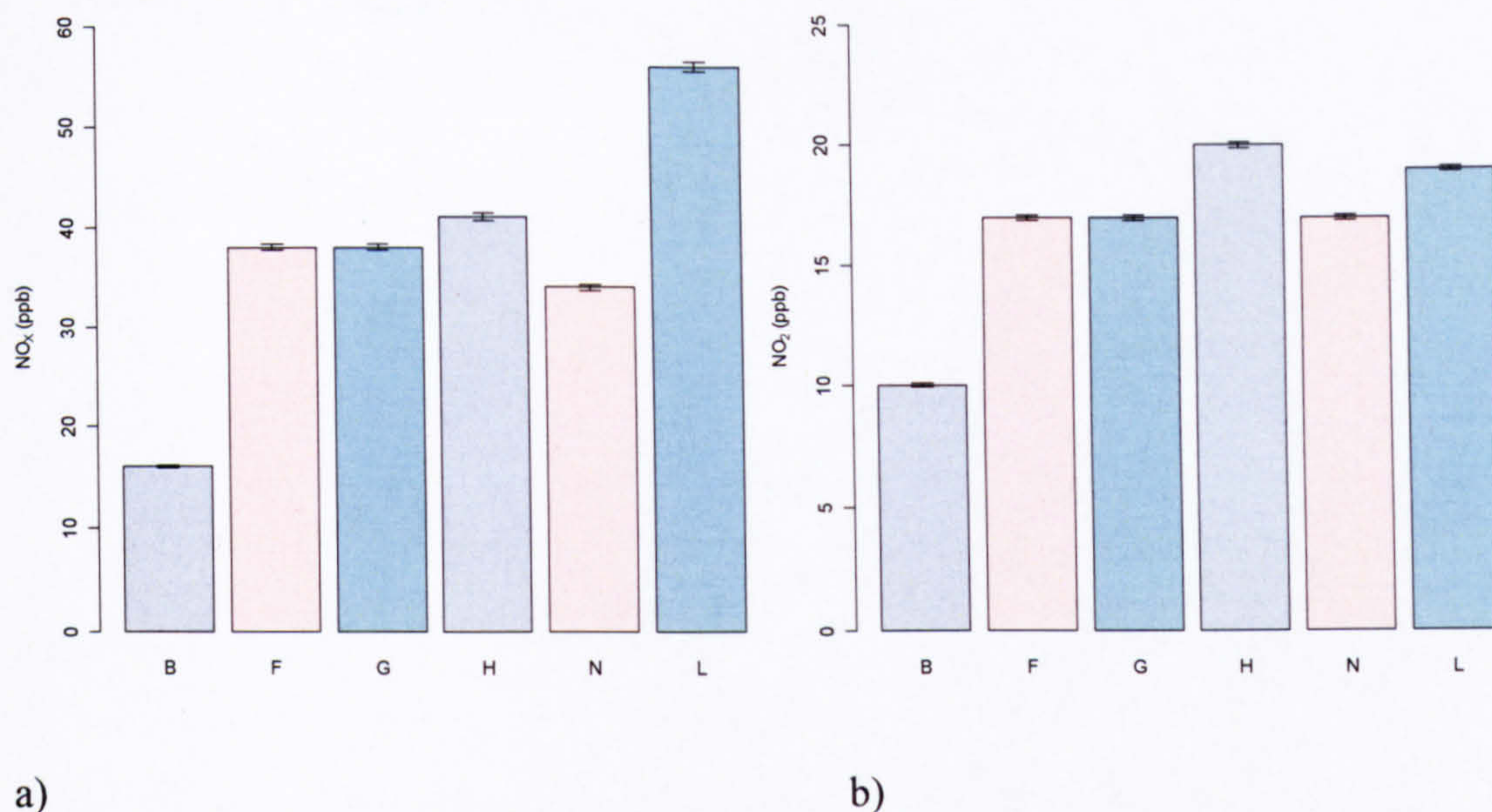


**Figure 33:** Mean NO<sub>x</sub> (a) and NO<sub>2</sub> (b) concentrations for the urban background site of Bootham and the various roadside sites. B = Bootham, F = Fishergate, G = Gillygate, H= Holgate Road, N = Nunnery Lane and L = Lawrence Street. Standard error bars are shown.

### 5.3.5. Spatial trends summary

This section has highlighted the differences in NO<sub>x</sub> and NO<sub>2</sub> concentrations across the relatively small urban area of York. Interestingly, some of the highest NO<sub>2</sub> concentrations during this two-year period were seen at the urban centre site. This is important in terms of public exposure since despite much of the urban centre of York being pedestrianised for most of the day, it is still possible to experience high concentrations of NO<sub>2</sub> as a direct result of the busy roads in the adjacent urban areas. Indeed, this section has shown that the NO<sub>2</sub> concentrations can actually be greater at non roadside urban sites than the roadside locations themselves since the NO<sub>x</sub> emissions (mainly NO) have been mixed with air parcels that contain higher O<sub>3</sub> levels (more O<sub>3</sub> rich) and thus NO<sub>2</sub> formation has been boosted (O<sub>3</sub> entrainment). This section has speculated that this NO<sub>2</sub> formation may be strongly enhanced by ambient O<sub>3</sub> concentrations, something that is believed unlikely in the centres of larger urban areas (such as London).

It should also be pointed out that although it is not possible to monitor the air quality in York at every particular street or location, the sites chosen by the CYC provide a good indication of the air quality at the types of locations that are commonly encountered across the city. These locations were selected to represent those environments where people live and work and therefore are the most relevant when considering potential health impacts.



## 5.4. Temporal trends

### 5.4.1. Introduction

The general decrease in  $\text{NO}_x$  concentrations observed across the UK over the past 15 years has been attributed to the improvements in vehicle emission technologies (that is, the introduction of the increasingly more stringent EURO standards, see section 1.6.2). Indeed, the 2004 AQEG document, '*Nitrogen Dioxide in the UK*', reported an average overall decrease in  $\text{NO}_x$  concentrations of 5.1 % per year at a range of urban sites across the UK (background, centre and roadside) for the period 1993 to 2000 (AQEG, 2004). This universal fall in annual  $\text{NO}_x$  concentrations has also been accompanied by an overall decrease (3.1 % per year) in ambient  $\text{NO}_2$  concentrations, with the less steep decline in  $\text{NO}_2$  concentrations resulting from the partitioning behaviour between  $\text{NO}_x$  and  $\text{NO}_2$  (for example, when NO makes up the largest fraction of  $\text{NO}_x$  (i.e. urban roadsides) a reduction in  $\text{NO}_x$  will have a relatively smaller impact on the  $\text{NO}_2$  concentration).

More recently, despite a continued decrease in  $\text{NO}_x$  concentrations, the rate of reduction in  $\text{NO}_2$  has slowed, stopped, or in some cases reversed (AQEG, 2006). These opposing trends in the respective concentrations of  $\text{NO}_x$  and  $\text{NO}_2$  became the principal focus of a further AQEG report, '*Trends in primary  $\text{NO}_2$* ', and a number of subsequent journal articles (Carslaw and Beevers, 2004 a, 2004b; Carslaw, 2005). The shift in the  $\text{NO}_2$  trend was first noticed in London, at a range of roadside, kerbside and urban background sites in the capital. However, AQEG have also reported the occurrence of this phenomenon at a range of site types in cities outside London e.g. Bath, Bury, Oxford and Wrexham (AQEG, 2006).

It is of interest to investigate the trends in  $\text{NO}_x$  and  $\text{NO}_2$  concentrations in York so that the CYC can make relevant and scientifically sound policy decisions regarding urban air quality. Such information will be valuable to the CYC in assisting with their ongoing commitments to improving the quality of air in the city, and especially within and around the AQMA. It is also of interest to investigate the trends in  $\text{NO}_x$  and  $\text{NO}_2$  concentrations in York to see how they compare with the observed trends in London and other cities across the UK. This section will focus solely on the four long-term monitoring sites in York (Fishergate, Bootham, Dunnington and City Centre).

### 5.4.2. Results: trend detection in York

Descriptive statistics of the observed  $\text{NO}_x$  and  $\text{NO}_2$  concentrations for the period 1999 to 2006 are shown in Table 26. Similarly to the results shown in section 5.2 of this Chapter, the mean  $\text{NO}_x$  and  $\text{NO}_2$  concentrations vary considerably from site to site reflecting the differences in emissions. The highest mean  $\text{NO}_x$  concentration for the study period is seen at the roadside site of Fishergate and the lowest concentration at the background site of Dunnington. Similarly to the results shown in the previous section, the highest mean  $\text{NO}_2$  concentration for the period



occurred at the City Centre site (~20 ppb). The NO<sub>2</sub> concentration at Fishergate (roadside site) was marginally lower than that at the City Centre at ~18 ppb. The maximum hourly NO<sub>2</sub> concentration recorded over the study years (1999 to 2006) also occurred at the City Centre site (102 ppb).

A general insight into the changes in pollutant concentration over time (general direction of change) can be achieved by re-computing the descriptive statistics for a more recent period (that is, 2005 – 2006), and comparing the results with those for the whole study period (1999 – 2006); this approach was adopted by Aleksic et al. (2005) and is also shown in Table 26.

In the majority of cases, the descriptive statistics show a reduction in NO<sub>x</sub> concentration for the more recent period (2005 to 2006) when compared to the full study period (1999 to 2006), suggesting that NO<sub>x</sub> concentrations have fallen over the 8 years of study. An interesting finding is the reduction in the spread of data (indicated by the IQR); this is especially true of the NO<sub>x</sub> concentrations at Fishergate where the IQR was 10 ppb lower in the latter study period compared to the full period. The situation is similar for the NO<sub>2</sub> concentrations, which exhibit a reduction in all descriptive statistic concentrations at the site of Bootham and Fishergate. However, some descriptive statistic concentrations at Dunnington exhibit no change; additionally the 75<sup>th</sup> percentile and IQR at the City Centre are greater for the more recent period (2005-2006) compared to the full 8-year average (1999 - 2006) and so suggests a difference in behaviour in the NO<sub>2</sub> concentration from those of NO<sub>x</sub>.

The results displayed in Table 26 therefore indicate that over the period 1999 to 2006 both the NO<sub>x</sub> and NO<sub>2</sub> concentrations recorded at the long-term monitoring site in York have fallen. To provide firmer conclusions regarding the change in pollutant concentrations over the study years, the NO<sub>x</sub> and NO<sub>2</sub> concentrations require a more thorough investigation.

Figure 34 displays the annual mean NO<sub>x</sub> and NO<sub>2</sub> concentrations for each of the long-term monitoring sites in York to clearly illustrate the changes in pollutant concentrations over the study years.



**Table 26:** Descriptive statistics for NO<sub>x</sub> (a) and NO<sub>2</sub> (b) concentrations (ppb) for the periods 1999 to 2006 and 2005 to 2006 for sites with long-term concentration records. The maximum value illustrates the maximum hourly pollutant concentration recorded in the study period (i.e., 1999 – 2006).

<b>a)</b>	<b>Bootham</b>	<b>City Centre<sup>1</sup></b>	<b>Dunnington</b>	<b>Fishergate</b>
<b>Period 1999 – 2006</b>				
25 <sup>th</sup> percentile	8	15	6	17
Mean	18.7	36.5	13.7	43.9
Median	13	27	10	33
75 <sup>th</sup> percentile	22	48	16	57
IQR	14	33	10	40
Maximum	543	492	248	462
<b>Period 2005 – 2006</b>				
25 <sup>th</sup> percentile	7	13	5	16
Mean	16.7	25.4	12.6	36.4
Median	11	36	9	28
75 <sup>th</sup> percentile	19	47	15	46
IQR	12	34	10	30
Maximum	306	492	181	455

<b>b)</b>	<b>Bootham</b>	<b>City Centre<sup>1</sup></b>	<b>Dunnington</b>	<b>Fishergate</b>
<b>Period 1999 – 2006</b>				
25 <sup>th</sup> percentile	6	11	4	10
Mean	12.3	19.9	9.0	17.8
Median	10	18	7	16
75 <sup>th</sup> percentile	17	27	12	24
IQR	11	16	8	14
Maximum	61	102	49	90
<b>Period 2005 – 2006</b>				
25 <sup>th</sup> percentile	5	10	4	10
Mean	10.4	17.4	8.9	16.5
Median	9	20	7	15
75 <sup>th</sup> percentile	14	28	12	22
IQR	9	18	8	12
Maximum	53	102	45	69

<sup>1</sup> Note that for the City Centre site the two-year period is for 2004 – 2005 (as opposed to 2005 – 2006) since the site was closed down at the end of 2005.



Linear regression has been applied to establish trends in the pollutant concentration; where the response variable ( $Y_i$ ) is the pollutant concentration and the sole explanatory variable ( $X_{li}$ ) is time (years). The parameter  $\beta_1$  is basically a description of the amount of change in the mean values of  $\text{NO}_x$  (or  $\text{NO}_2$ ) concentration as a result of a single unit increase in time (year); the slope coefficient ( $\beta_1$ ) represents the rate of change in pollutant concentration over time.

The precision of the regression coefficient estimate ( $\beta_1$ ) can be determined by calculating 95 % confidence intervals. Confidence intervals can be loosely interpreted as the range of possible values for the true, but unknown,  $\beta_1$  coefficient. If the range of values for  $\beta_1$  includes zero then it is not possible to convincingly reject the null hypothesis (that is, there is no trend in the pollutant concentration over time). Wider confidence intervals illustrate a lower reliability in the estimated slope coefficient since the 'true' coefficient could lie anywhere between the upper and lower 95 % confidence bands. Confidence intervals are calculated from the standard errors associated with the linear regression procedure.

Linear regression has also been deployed in the studies by Aleksic et al. (2005) and Jo et al. (2000) to investigate trends in urban air quality. Aleksic et al. (2005) investigated the temporal changes in benzene concentrations across the state of New York. Jo et al. (2000) used linear regression to investigate the trends in  $\text{CO}$ ,  $\text{NO}_2$ ,  $\text{NO}_x$  and  $\text{O}_3$  concentrations at two major cities in South Korea.

A linear regression based on each of the descriptive variables included in Table 26 has been performed for the annual  $\text{NO}_x$  and  $\text{NO}_2$  concentrations for the four different long-term monitoring sites in York. The rate of change in  $\text{ppb yr}^{-1}$  and  $\% \text{ yr}^{-1}$  is shown in Table 27. The rate of change ( $\% \text{ yr}^{-1}$ ) has been calculated with respect to the first year of measurement (see equation 4).



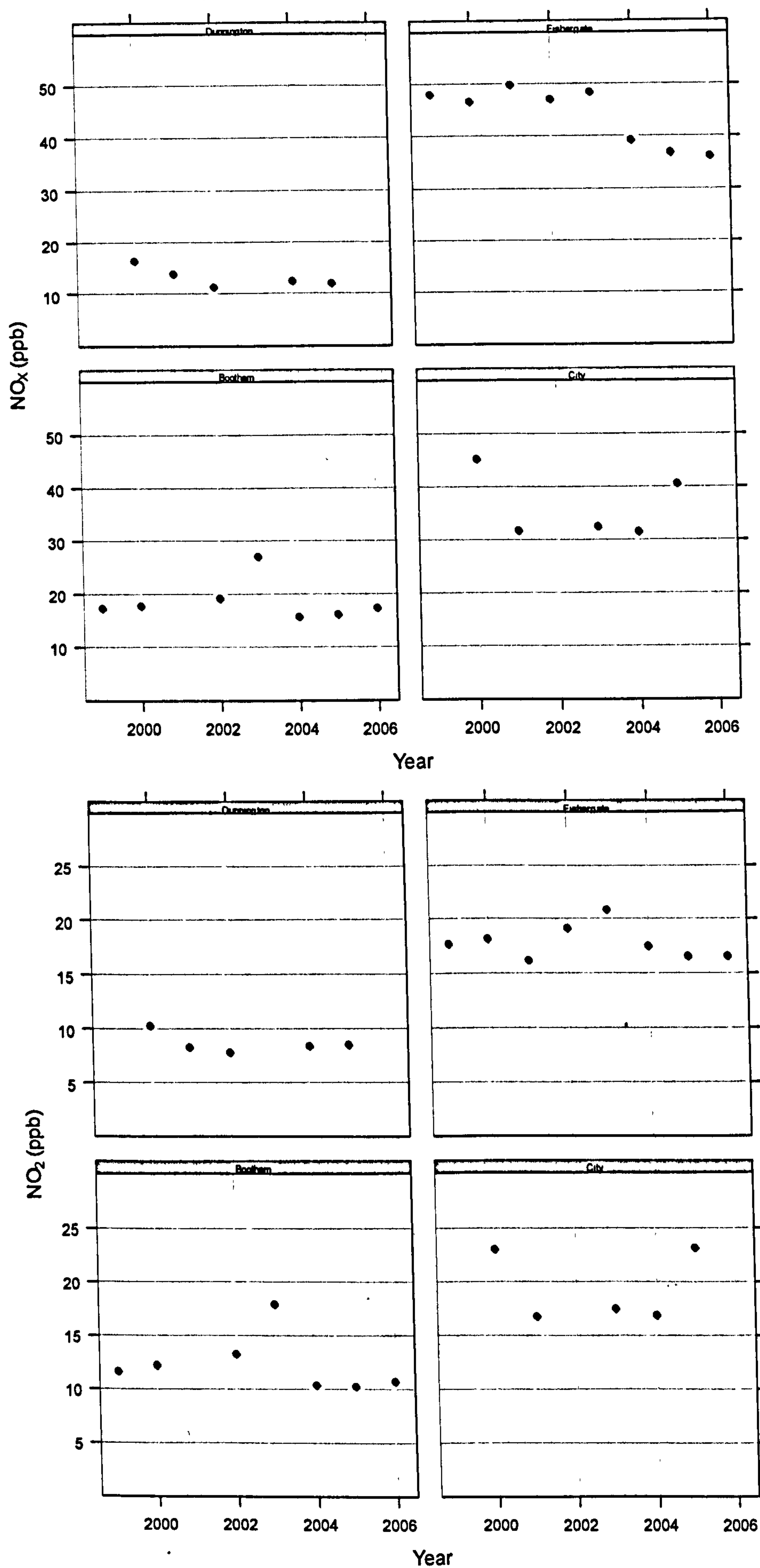


**Figure 34:** Annual mean NO<sub>x</sub> (a) and NO<sub>2</sub> (b) concentration for the Dunnington, Bootham, City Centre and Fishergate sites (from left to right). Only those years with data capture above 80% have been included in the plots.



**Table 27:** Estimated annual change in NO<sub>x</sub> and NO<sub>2</sub> concentrations for the period 1999 to 2006 for different descriptive statistics. \* illustrates those sites where the trend is statistically significant at the  $p < 0.01$  level or better. The ppb yr<sup>-1</sup> values are taken directly from the linear regression calculation ( $\beta_1$ , or slope coefficient). The percentage annual changes are calculated with respect to the first year of measurement (i.e., 1999).

		Mean		Median		Maximum		First		Third		IQR	
		Ppb yr <sup>-1</sup>	% yr <sup>-1</sup>	ppb yr <sup>-1</sup>	% yr <sup>-1</sup>	ppb yr <sup>-1</sup>	% yr <sup>-1</sup>	ppb yr <sup>-1</sup>	% yr <sup>-1</sup>	Ppb yr <sup>-1</sup>	% yr <sup>-1</sup>	ppb yr <sup>-1</sup>	% yr <sup>-1</sup>
Bootham	NO <sub>x</sub>	-0.11	-0.63	-0.33	-2.54	16.32	9.12	-0.24	-3.06	-0.34	-1.62	-0.10	-0.74
	NO <sub>2</sub>	-0.22	-1.91	-0.25	-2.50	0.79	1.69	-0.12	-2.39	-0.30	-1.90	-0.18	-1.68
Dunnington	NO <sub>x</sub>	-0.61	-3.74	-0.66	-5.05	-11.46	-5.82	-0.54	-6.03	-0.74	-3.91	-0.20	-2.00
	NO <sub>2</sub>	-0.18	-1.78	-0.14	-1.59	1.06	2.52	-0.17	-2.86	-0.17	-1.32	0.00	0.00
City Centre	NO <sub>x</sub>	-0.80	-1.78	-1.31	-3.46	49.92*	20.13*	-1.16	-4.84	-1.24	-2.11	-0.08	-0.23
	NO <sub>2</sub>	-0.02	-0.08	-0.43	-1.87	5.02	6.44	-0.41	-2.71	0.06	0.19	0.47	3.10
Fishergate	NO <sub>x</sub>	-1.94*	-4.05*	-1.17*	-3.24*	4.64	1.28	-0.12	-0.66	-2.89*	-4.52*	-2.77*	-6.03*
	NO <sub>2</sub>	-0.14	-0.77	-0.14	-0.89	-0.10	-0.14	0.11	1.07	-0.32	-1.29	-0.42	-2.91



$$\text{Annual rate of change} = ((C_1 - Z) / C_1) * 100$$

Equation 4

where  $C_1$  is the concentration in year 1 (i.e., 1999)

$Z$  is the total estimated reduction in pollutant concentration (ppb) over the study period (i.e.,  $\beta_1 * \text{no. of study years}$ ; where  $\beta_1$  is the slope coefficient (calculated by linear regression))

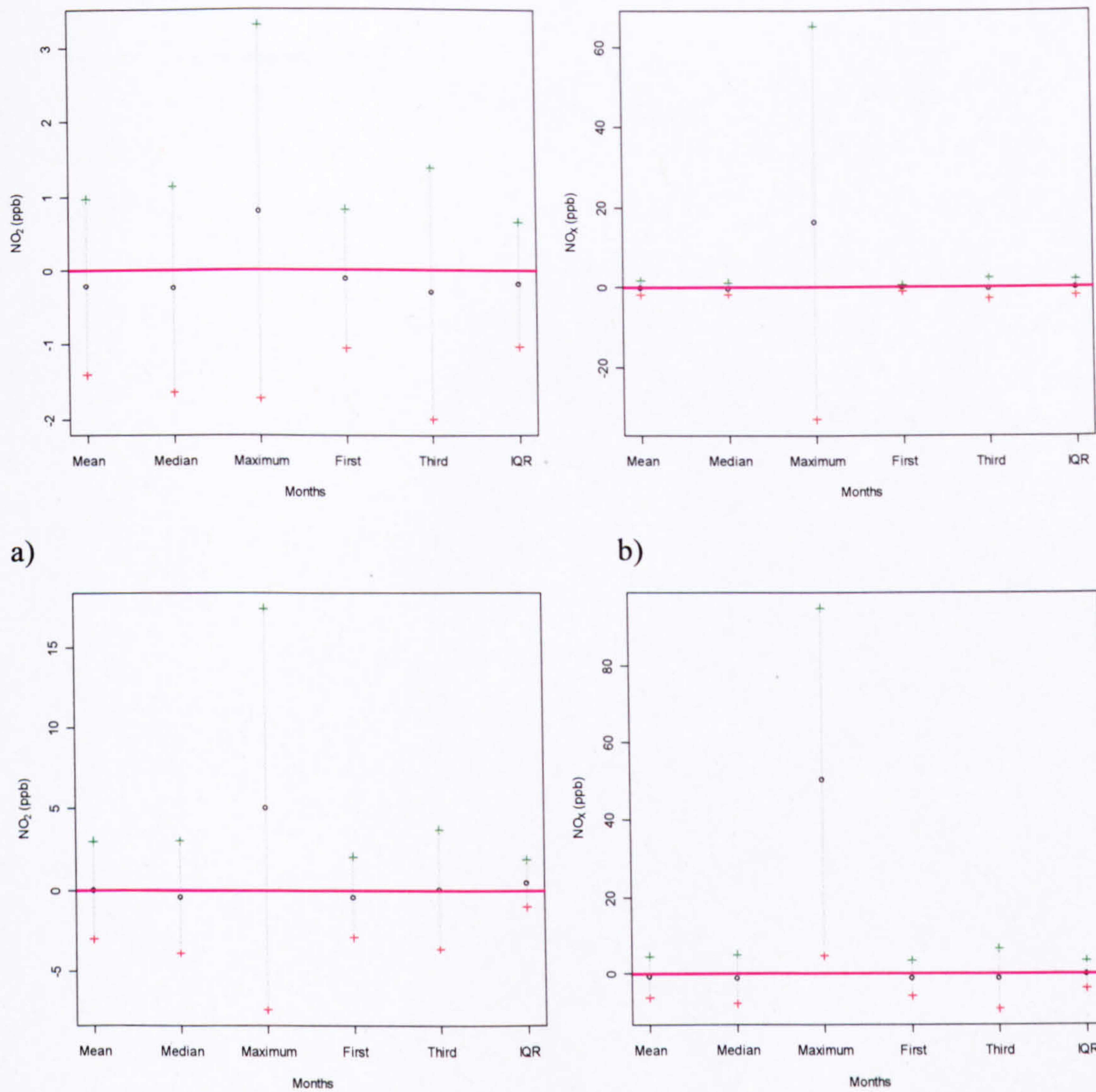
The linear regression results have also been displayed graphically (Figure 35), alongside the 95% confidence intervals. As stated previously, those coefficients where the confidence intervals cross the zero trend line cannot be considered as statistically significant. Generally speaking, wider confidence intervals suggest the slope estimate is less robust.

All four sites exhibit a negative slope coefficient for the annual mean  $\text{NO}_x$  concentration (Table 27 and Figure 35). However, only the slope coefficient for Fishergate ( $\text{NO}_x$ ) is statistically significant ( $p < 0.01$ ) with the linear regression at the three remaining sites indicating only a slight gradient in the line of best fit ( $\beta_1$  ranging from 0.1 to 0.8  $\text{ppb yr}^{-1}$ ). It is therefore only possible to reject the null hypothesis (that is, the slope coefficient is equal to zero) at Fishergate, where the evidence suggests that over the study years the mean ambient  $\text{NO}_x$  concentrations have decreased by around 1.9 ppb per year ( $\sim 4\%$  with respect to 1999 concentrations).

The linear regression analysis also reveals that the median  $\text{NO}_x$  concentrations at Fishergate, along with the 75<sup>th</sup> quartile (labelled 'third' in Figure 36) have significantly declined over the study years. Furthermore, the slope coefficient for the  $\text{NO}_x$  IQR at Fishergate has decreased significantly ( $-6\% \text{ yr}^{-1}$ ) suggesting that the overall spread in  $\text{NO}_x$  concentrations at Fishergate has declined. These results therefore provide strong evidence to suggest a decline in  $\text{NO}_x$  concentration over the study period at this roadside location. Despite the results of the linear regression analysis suggesting a decline in the mean, median, 25<sup>th</sup> quartile, 75<sup>th</sup> quartile and IQR in  $\text{NO}_x$  concentrations at the three remaining sites, these results are not statistically significant. It can therefore be concluded that the  $\text{NO}_x$  concentrations at Fishergate behave differently (i.e., seen a greater rate of decline) compared to the  $\text{NO}_x$  concentrations at the remaining sites.

Analysis of the regression diagnostics for  $\text{NO}_x$  concentrations indicates that both the assumptions regarding constancy of variance and the normality of errors were sufficient to carry out linear regression. However, the diagnostics for the sites of Bootham and Fishergate showed the regression to be heavily influenced by the 2003 annual mean. Subsequently, linear models with this value removed led to a greater rate of reduction in annual mean  $\text{NO}_x$  concentration for both sites, with the new slopes being -0.8 ppb and -2.0 ppb ( $p < 0.01$ ) for Bootham and Fishergate, respectively





d)

**Figure 35:** Slope coefficient with 95 % confidence intervals for long-term monitoring sites of a) Bootham NO<sub>2</sub>, b) Bootham NO<sub>x</sub>, c) City centre NO<sub>2</sub>, d) City Centre NO<sub>x</sub>, The upper confidence band is illustrated by a green cross, the lower band by a red cross. In each plot the zero trend line (null hypothesis) is shown by the horizontal pink line.



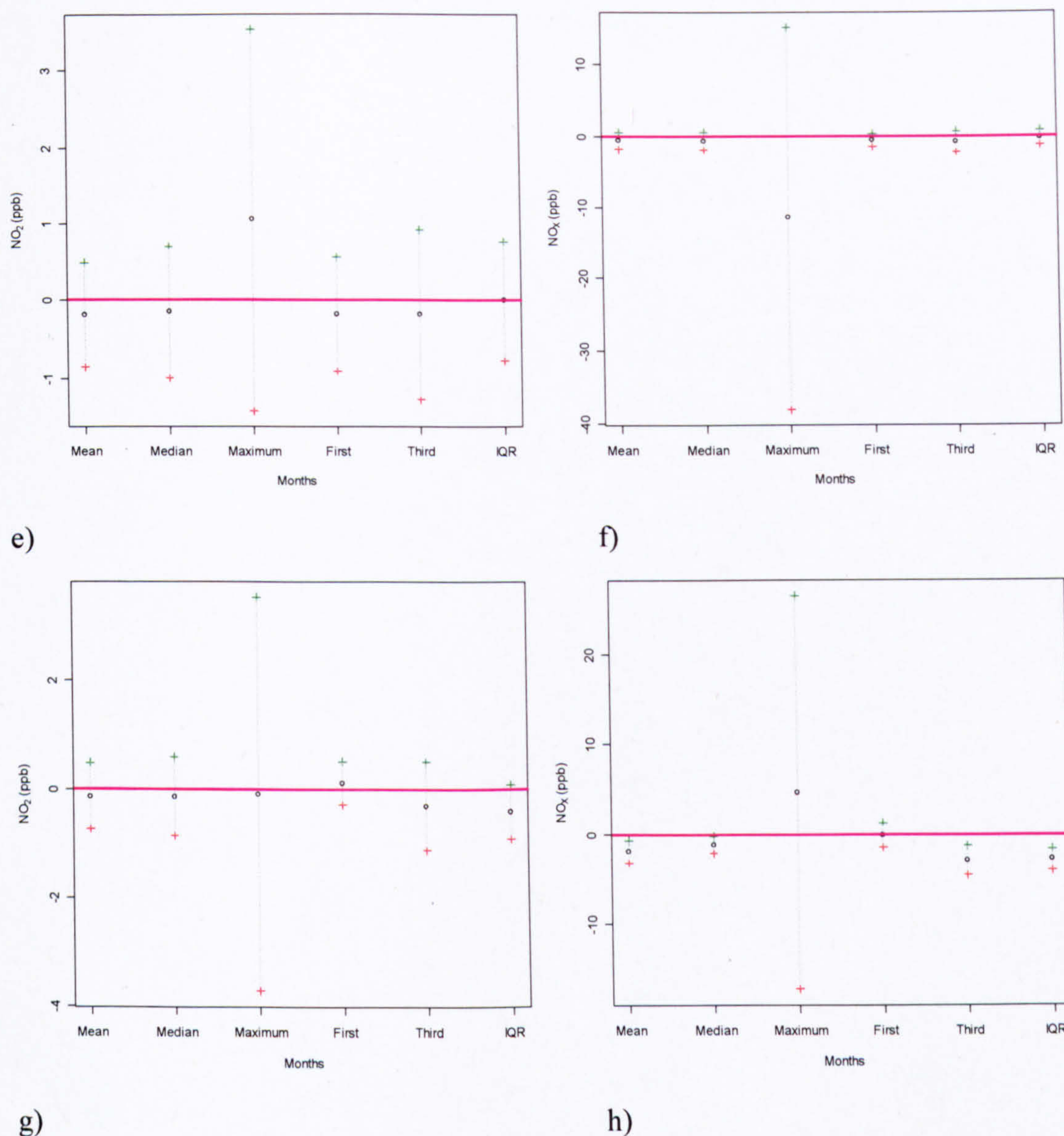


**Figure 35 continued** Slope coefficient with 95 % confidence intervals for the long-term monitoring sites of e) Dunnington NO<sub>2</sub>, f) Dunnington NO<sub>x</sub>, g) Fishergate NO<sub>2</sub>, h) Fishergate NO<sub>x</sub>. The upper confidence band is illustrated by a green cross, the lower band by a red cross. In each plot the zero trend line (null hypothesis) is shown by the horizontal pink line.

Interestingly, the trend analysis revealed an increase in maximum NO<sub>x</sub> concentrations for the sites of Bootham, City Centre and Fishergate thus indicating an increase in the maximum ambient NO<sub>x</sub> concentrations recorded at these sites; however, only the positive trend at the City Centre site is statistically significant ( $p < 0.01$ ). This positive slope in maximum NO<sub>x</sub> concentrations contradicts the negative slope coefficients for the mean, median, IQR, 25<sup>th</sup> and 75<sup>th</sup> quartile concentrations seen at these sites. It provides evidence therefore, that although in general NO<sub>x</sub> concentrations are declining, there is a general increase in peak NO<sub>x</sub> concentrations. Figure 36 illustrates the annual maximum NO<sub>x</sub> concentrations at the site of City Centre; the positive change in NO<sub>x</sub> concentration can clearly be seen. This statistically



significant increase in maximum NO<sub>x</sub> concentrations suggests that ‘pollution episodes’ at this site (City Centre) are becoming more frequent.

Similarly, to the NO<sub>x</sub> concentrations already discussed, the linear regression for the annual mean and median NO<sub>2</sub> concentrations exhibited a negative trend for all sites. In all cases the slope coefficients are not significant and suggest that although ambient NO<sub>2</sub> concentrations in York have decreased, they have not changed **significantly** over the past 8 years. Again, removal of the 2003 annual mean improved the fit of the regression diagnostics for Bootham and Fishergate but it did not change the statistical significance of the slopes. This finding provides firmer evidence of the findings in Table 26, which suggested a difference in behaviour in the observed NO<sub>x</sub> and NO<sub>2</sub> concentrations at the various monitoring sites over the study period.

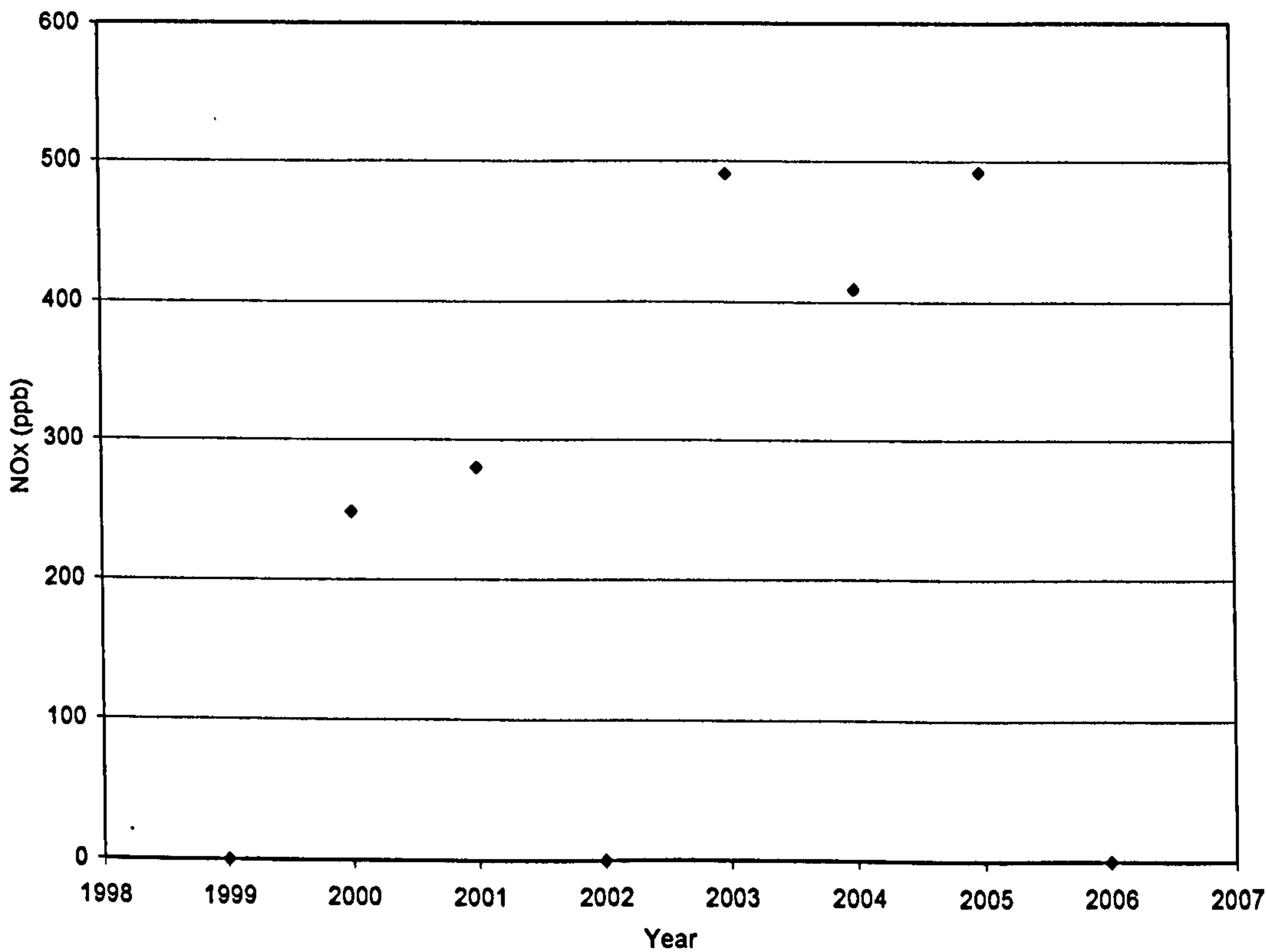


**Figure 36:** Annual maximum NO<sub>x</sub> concentration at City Centre monitoring site for the period 1999 to 2006.

Moreover, similarly to the NO<sub>x</sub> concentrations shown above, the linear regression using annual maximum NO<sub>2</sub> concentrations exhibited positive slope coefficients for the sites of Bootham and the City Centre suggesting that maximum NO<sub>2</sub> concentrations measured at these sites have increased over the study years (although it should be noted that none of the trends in maximum NO<sub>2</sub> concentrations were statistically significant). Subsequent linear regression using the 18<sup>th</sup> highest hourly NO<sub>2</sub> concentration for each particular year revealed positive slopes at three out of the four long-term sites, but again none were statistically significant at any level.



There are a number of similarities between the air quality data collected in York and those data reported in the AQEG report (i.e., London, Bath, Bury, Oxford, Manchester, Bath etc.). Firstly, the quite large differences in the annual rate of change in pollutant concentration for the different site types is similar to that reported by AQEG (i.e., the greater rate of reduction in NO<sub>x</sub> concentrations at Fishergate (roadside site) compared to Bootham (urban background site) or City Centre (urban centre site). Indeed, the 2006 AQEG report found a much steeper decline in the ambient NO<sub>x</sub> concentrations of roadside sites compared to background locations. This difference most likely reflects the fact that the ambient NO<sub>x</sub> concentrations at a roadside site (e.g. Fishergate) will be more heavily influenced by a decrease in vehicular NO<sub>x</sub> emissions, compared to an urban background or an urban centre site (e.g. Bootham and the City Centre site, respectively).

Secondly, the general difference in behaviour of NO<sub>x</sub> and NO<sub>2</sub> concentrations over the period is also similar to the results reported by AQEG (i.e., the greater rates of reduction in NO<sub>x</sub> concentrations in comparison to NO<sub>2</sub>). The relatively small reduction in the ambient NO<sub>2</sub> concentrations compared to NO<sub>x</sub> found in York, indicated by the lack of statistical significance, agrees with AQEG’s findings for London and numerous other cities in the UK.

This difference in general behaviour of NO<sub>x</sub> and NO<sub>2</sub> concentrations has been illustrated and highlighted by AQEG and numerous scientific studies by examining the NO<sub>2</sub>: NO<sub>x</sub> ratio. Figure 37 therefore illustrates the annual mean NO<sub>2</sub>: NO<sub>x</sub> ratio for the four long-term monitoring sites, and the linear regression slope coefficients are shown in Table 28.

**Table 28:** Estimated slope coefficient for the change in NO<sub>2</sub>: NO<sub>x</sub> ratio over the period 1999-2006. \* illustrates those sites where the trend is statistically significant at the  $p < 0.1$  level

Site	Slope Coefficient	Std error.	p value
Dunnington	0.02	0.009	0.15
Bootham	-0.01	0.003	0.02 *
City Centre	0.01	0.003	0.04 *
Fishergate	0.02	0.004	0.01 *



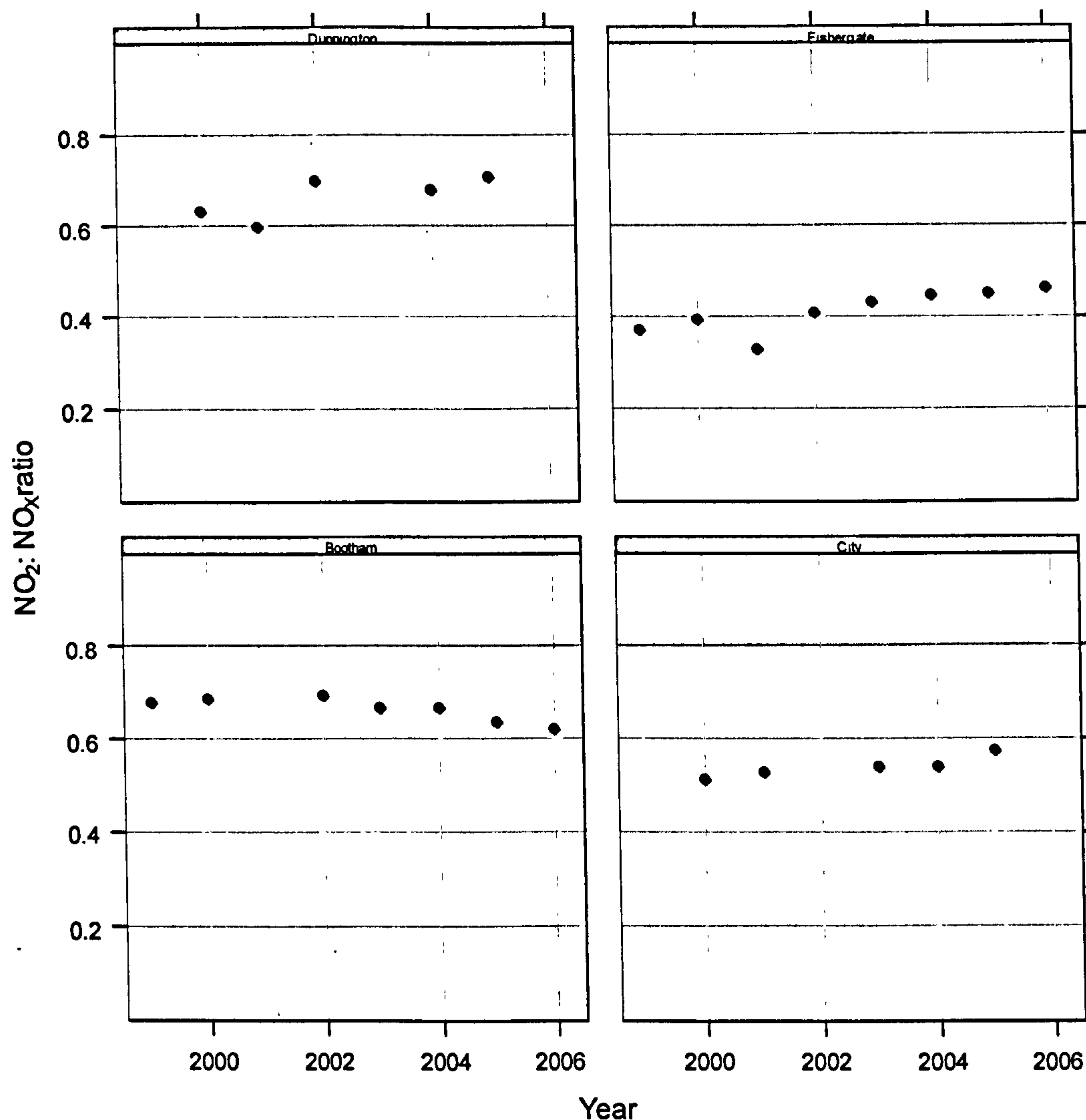


**Figure 37:** Annual mean NO<sub>2</sub>: NO<sub>x</sub> ratio for the sites Dunnington, Bootham, City Centre and Fishergate (from left to right). Only those years with data captures above 80% have been included in the plots.

It can be seen in Figure 37, and Table 28, that a positive trend in the NO<sub>2</sub>: NO<sub>x</sub> ratio has occurred for the pollutant concentrations at Dunnington, City Centre and Fishergate. This positive trend in NO<sub>2</sub>: NO<sub>x</sub> ratio is consistent with the findings reported in AQEG 2006 and journal articles (Carslaw and Beevers, 2004a, 2004b).

It is widely accepted that the recent change in the NO<sub>2</sub>: NO<sub>x</sub> ratio seen at many sites across London is as a result of increasing primary NO<sub>2</sub> emissions (AQEG, 2006; Carslaw and Beevers, 2004a, 2004b). Two distinct sources/types of primary NO<sub>2</sub> emissions have been identified. Firstly, NO<sub>2</sub> emissions from an increase in the number of diesel vehicles (namely EURO-III) entering the market, and secondly, the use of catalytically regenerative particle traps on buses (Carslaw, 2005).

Diesel vehicles are known to emit higher quantities of NO<sub>2</sub> compared to petrol vehicles. Jenkin (2004b) estimated the percentage of NO<sub>x</sub> emitted as NO<sub>2</sub> released from diesel vehicles is as high as 11.8 (±1.2) % compared to the 5 % assumed for petrol. Furthermore, the Carslaw



(2005) study nominates the increase in diesel vehicles as a likely cause as to the increasing NO<sub>2</sub>: NO<sub>x</sub> ratio and suggests that over the period from 2001 to 2004 increases in diesel vehicles are responsible for around 8 % of the increase in NO<sub>2</sub>: NO<sub>x</sub> ratio. It is therefore a possibility that an increase in the amount of diesel vehicles in York could be responsible for the increase in NO<sub>2</sub>: NO<sub>x</sub> ratio seen at the various monitoring sites. The fact that the greatest change in NO<sub>2</sub>: NO<sub>x</sub> ratio over the period (greatest annual increase) has been observed at a roadside site in York further supports this theory.

Transport for London have retro-fitted the majority of London buses with particle regenerative traps. These traps are designed to reduce the amount of particulates emitted from the buses by forming NO<sub>2</sub>, which is then used to oxidise trapped particles in the engine. A number of studies have investigated the increase in NO<sub>2</sub> emissions from buses fitted with these devices and several studies have suggested that their introduction has led to some of the increase in NO<sub>2</sub> concentrations seen across London (Carslaw, 2005; AQEG, 2006). However, since the buses in York have not been fitted with particle re-generation traps it is possible to firmly exclude the bus fleet as a possible explanation for the increase in the NO<sub>2</sub>: NO<sub>x</sub>.

The increase in background O<sub>3</sub> concentration has also been identified as a potential cause of the change in NO<sub>2</sub>: NO<sub>x</sub> ratio observed at many locations across the UK (AQEG, 2004). However there is some debate as to whether the overall increase in background O<sub>3</sub> concentration would significantly influence the ambient NO<sub>2</sub> found in the city centres of large urban areas (AQEG, 2006). The inner city O<sub>3</sub> concentration will be lower than background locations since the O<sub>3</sub> present in a typical air mass entering a large city, such as London, will be quickly destroyed by NO (reaction 39); the capacity of the air mass to oxidise NO to NO<sub>2</sub> is therefore seriously diminished as it progresses through an urban area. The NO<sub>2</sub> concentration is subsequently only thought to be affected by increasing O<sub>3</sub> concentrations in the suburbs, with the air quality within inner cities remaining largely unaffected. However, as this study has already hinted, it is possible that O<sub>3</sub> is playing a larger role in the NO<sub>x</sub> to NO<sub>2</sub> relationship at some sites in York than what is usually observed in larger urban areas. The size of York in comparison to London, for example, could potentially allow a sufficient proportion of O<sub>3</sub> in an ambient air parcel to reach the centre of York and so influence the formation of NO<sub>2</sub>.

O<sub>3</sub> has been measured at the background site of Dunnington since 1999. Figure 38 illustrates the annual mean O<sub>3</sub> concentrations for this period. It can be inferred that a general increase in O<sub>3</sub> has occurred over the 8-year period (slope coefficient of 0.9 ppb yr<sup>-1</sup>); however this trend was not significant. Analysis of the regression diagnostics highlighted the annual mean in 2002 to be highly influential and its subsequent removal resulted in the slope increasing to 1.2 ppb yr<sup>-1</sup> ( $p < 0.01$ ).



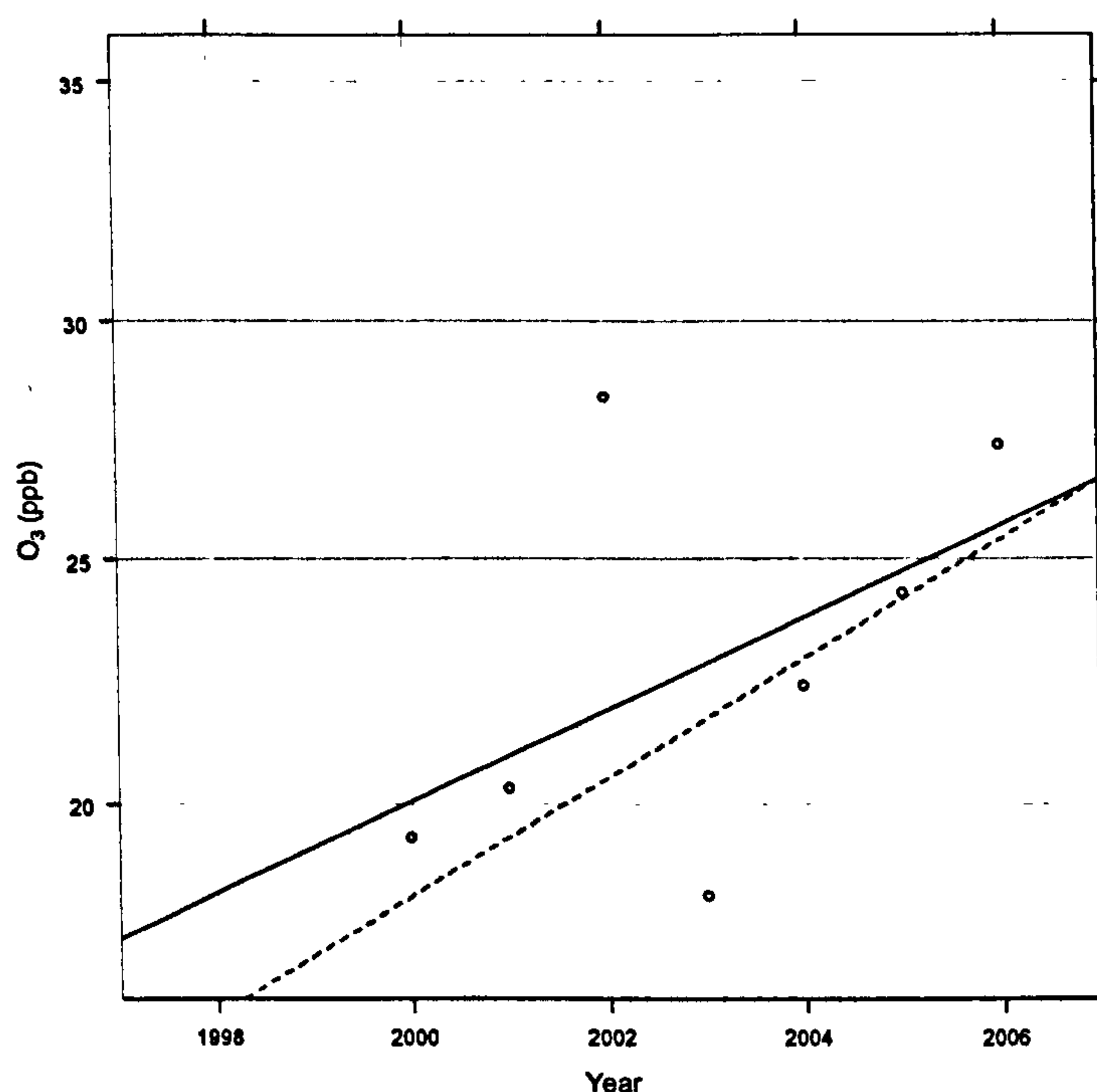


**Figure 38:** Annual mean O<sub>3</sub> concentrations observed at Dunnington background site. The solid red line illustrates the linear regression using all available data. The dashed red line illustrates the linear regression line without the 2002 annual mean.

The increase in NO<sub>2</sub>: NO<sub>x</sub> ratio experienced at a number of sites across York (Figure 37) could therefore be a response to the increase in ambient O<sub>3</sub> concentrations (Figure 38). However, it is difficult to establish any real conclusions about the influence of O<sub>3</sub> on the NO<sub>2</sub>: NO<sub>x</sub> ratio in York since O<sub>3</sub> is not measured simultaneously at any of York's urban sites (Bootham, City centre and Fishergate).

The change in the NO<sub>2</sub>: NO<sub>x</sub> ratio at the urban background site of Bootham is the opposite to that of the other monitoring sites, with the reduction in NO<sub>2</sub> concentrations at this site being greater, both in absolute and relative terms, than the reduction in NO<sub>x</sub>. Subsequently the NO<sub>2</sub>: NO<sub>x</sub> ratio has decreased over the 8-year period (Table 28). This trend is not observed at any other site in York and goes against the general findings reported in the AQEG (2006) document.

The main difference at the Bootham monitoring site compared to the other long-term urban monitoring sites (Fishergate and City Centre) is its proximity to vegetation. The Bootham monitoring site is located away from main roads in the York Hospital gardens. Large trees and grassland flank the surrounding area, whereas the vegetation cover in and around the areas adjacent to the City Centre and Fishergate monitoring sites is minimal. It is therefore possible that the surrounding vegetation is having some affect on the localised chemistry of NO<sub>x</sub>, NO<sub>2</sub> and O<sub>3</sub> concentrations at Bootham. The decreasing NO<sub>2</sub>: NO<sub>x</sub> ratio at Bootham could therefore be a consequence of complex chemical processes stemming from the greater rates of biogenic VOC emissions (e.g. terpenes, pinenes etc.) in the area.



### 5.4.3. Results: trend detection in other UK cities

The CYC is not the only Local Authority to collect continuous  $\text{NO}_x$  and  $\text{NO}_2$  concentration measurements. Indeed, a vast quantity of pollutant concentration data is freely available from the UK Air Quality Achieve website (<http://www.airquality.co.uk/archive/index.php>).

Trends (annual changes) in the  $\text{NO}_x$  and  $\text{NO}_2$  concentrations for UK cities other than York have been calculated using the same procedure as outlined in the previous Chapter and are presented in Table 29.

Only locations where  $\text{NO}_x$  and  $\text{NO}_2$  data have been collected continuously over the period 1999 to 2006 were considered for comparison with the data collected in York. A total of 38 sites are included in the study; 9 are classified as urban background, 8 as roadside and 14 are defined as urban centres. Additionally a further 4 sites classified as urban industrial, plus 1 rural and 2 suburban sites were also used in the analysis. Table 29 also provides a rough estimation of the city's size by providing the latest population census data.

In each case a linear trend line has been fitted and the annual change in the pollutant concentrations has been calculated (ppb and %) to give an overall understanding of the relative changes in  $\text{NO}_x$  and  $\text{NO}_2$  concentrations across the UK over the period 1999 to 2006. Additionally, the slope coefficients and 95% confidence intervals are shown in Figure 39.

There is substantial variation between the slope coefficients calculated for the various sites included in this study (see Figure 39), with the annual percentage change in  $\text{NO}_x$  concentrations ranging from 1.3 % to -5.8 % and those for  $\text{NO}_2$  ranging from 3 % to -4.8% (with respect to 1999 concentrations).

For 35 of the 38 monitoring sites the linear regression analysis revealed a negative change in the annual mean  $\text{NO}_x$  concentration. 10 of the 35 sites with negative trends in  $\text{NO}_x$  concentration (29 %) were statistically significant at the  $p < 0.1$  level or greater. The 10 significant negative trends were split fairly evenly across the different site types, with 30 % of the significant negative trends occurring at both urban centre and roadside sites, followed closely by urban background (20 %) and urban industrial (20 %). The  $\text{NO}_x$  trends at the sites of Aberdeen, Bristol Old Market and Walsall Willingham were positive (0.01, 0.6 and 0.1 ppb year<sup>-1</sup>, respectively) but were not statistically significant.



**Table 29:** Estimated trend in annual mean NO<sub>x</sub> and NO<sub>2</sub> concentration for a range of monitoring sites across the UK for the years 1999 to 2006. Statistical significance: \* p < 0.1 or greater. BA = background, UB = urban background, RO = roadside, UC = urban centre, SU = suburban, UI = urban industrial and RU = rural. Data from the UK air quality archive (<http://www.airquality.co.uk/archive/index.php>); population estimates taken from the 2001 census (online). The percentage reductions are calculated with respect to 1999 pollutant concentrations.

Site	Type	Population 1	NO <sub>x</sub> trend		NO <sub>2</sub> trend	
			ppb yr <sup>-1</sup>	% yr <sup>-1</sup>	ppb yr <sup>-1</sup>	% yr <sup>-1</sup>
York: Fishergate	RO	166008	-1.94*	-4.05*	-0.14	-0.77
York: Bootham	UB	166008	-0.11	-0.63	-0.22	-1.91
York: Dunnington	BA	166008	-0.61	-3.74	-0.18	-1.78
York: City Centre	UC	166008	-0.80	-1.78	-0.02	-0.08
1 Lady Bower	RU	NA	-0.16	-2.46	-0.20	-3.44
2 Billingham	UI	36720	-1.15*	-3.75*	-0.48*	-2.83*
3 Leamington Spa	UB	45114	-0.53	-2.26	-0.39	-2.49
4 Exeter	RO	98125	-0.28	-0.49	0.13	0.65
5 Oxford	UC	110103	-0.38	-0.39	0.89*	3.02*
6 Norwich Roadside	RO	120895	-0.28	-0.91	-0.08	-0.47
7 Norwich Centre	UC	120895	-0.79*	-3.71*	-0.45*	-3.15*
8 Thurrock	UB	127815	-1.03*	-2.70*	-0.16	-0.82
9 Middlesbrough	UI	140849	-0.36	-1.77	-0.08	-0.65
10 Redcar	SU	145123	-0.11	-0.70	0.03	0.26
11 Bath	RO	158692	-2.77	-2.32	0.64	2.00
12 Bury	RO	177235	-6.29*	-4.46*	-0.11	-0.29
13 Aberdeen	UB	212125	0.01	0.03	0.09	0.67
14 Barnsley Gawber	UB	221298	-1.06*	-4.65*	-0.68*	-4.82*
15 Salford Eccles	UI	222380	-1.53	-3.49	-0.41	-1.86
16 Brighton	RO	228933	-1.16*	-2.47*	0.33	1.75
17 Wolverhampton	UC	243548	-0.37	-1.29	-0.21	-1.34
18 Stoke on Trent	UC	244643	-0.53	-1.44	-0.08	-0.42
19 Rotherham	UC	252167	-0.38	-1.03	0.20*	1.17*
20 Bolton	UB	258435	-0.23	-0.76	0.03	0.15
21 Walsall Alumwell	UB	259125	-1.30	-2.57	0.14	0.68
22 Walsall Willenhall	SU	259125	0.10	0.41	0.22	1.47
23 Newcastle	UC	259668	-1.07	-3.57	-0.16	-1.00
24 Nottingham	RO	263522	-1.51*	-3.46*	-0.70*	-3.02*
25 Leicester	UC	270493	-0.80	-2.19	-0.48	-2.20
26 Sandell West Bromich	UB	290076	-1.31	-4.29	-0.56	-3.11
27 Bristol Old Market	RO	376146	-3.93	-3.39	0.67	2.33
28 Bristol centre	UC	376146	0.56	1.31	-0.30	-1.53

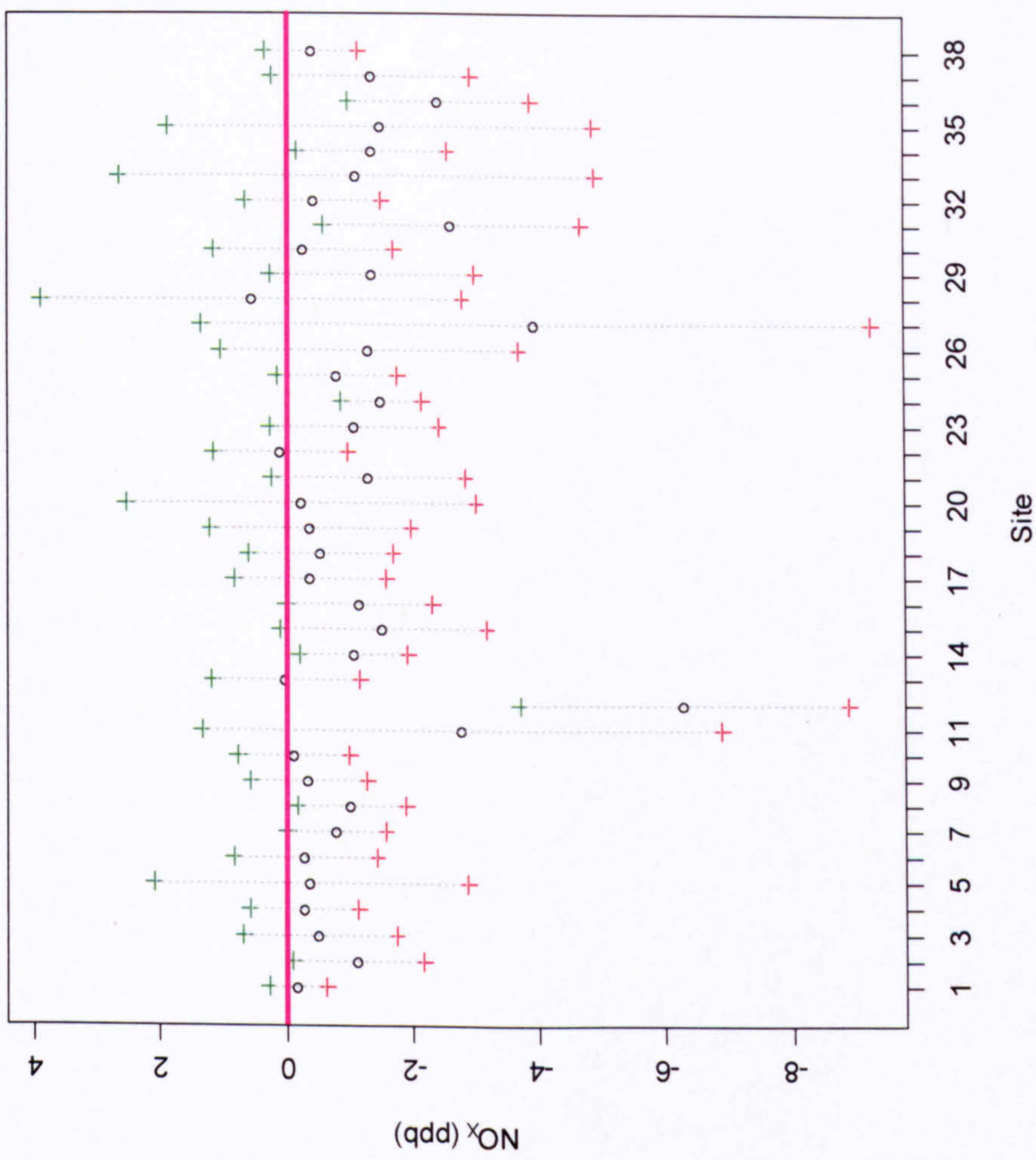
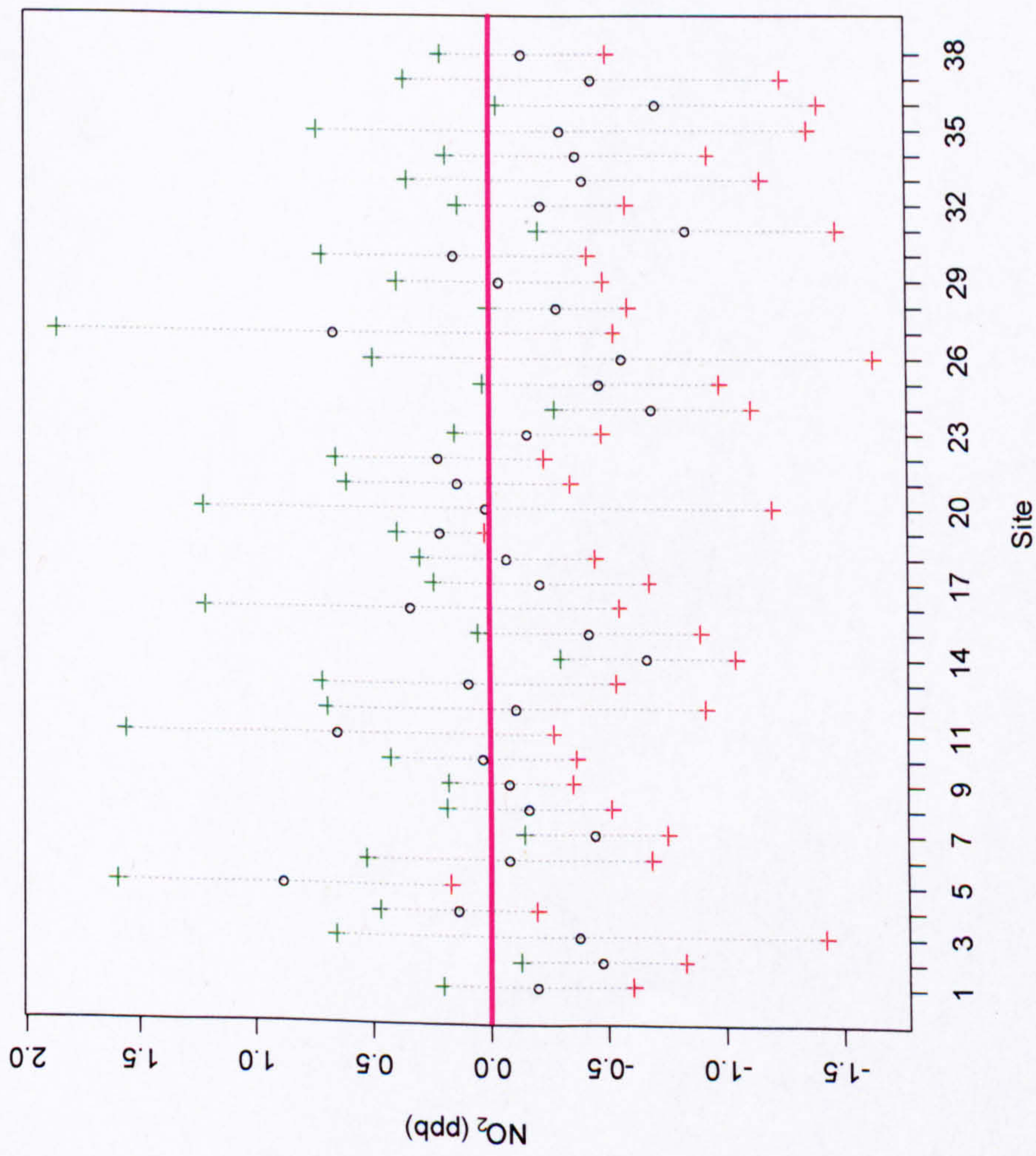


29	Manchester Background	UB	401207	-1.36	-3.47	-0.04	-0.17
30	Manchester centre	UC	401207	-0.27	-0.59	0.15	0.67
31	Bradford	UC	457132	-2.62*	-5.81*	-0.84*	-4.10*
32	Glasgow background	UB	471371	-0.42	-0.82	-0.23	-0.84
33	Glasgow kerbside	RO	471371	-1.12	-0.85	-0.41	-1.12
34	Glasgow centre	UC	471371	-1.35*	-3.43*	-0.36	-1.79
35	Sheffield Centre	UC	500900	-1.49	-3.46	-0.31	-1.63
36	Sheffield Tinsley	UI	500900	-2.44*	-4.29*	-0.72*	-2.96*
37	Leeds	UC	680424	-1.35	-2.91	-0.44	-1.95
38	Birmingham	UC	969846	-0.40	-1.20	-0.14	-0.72

In an attempt to determine whether the size of population (a proxy for urban area size) had any bearing on the rate of annual change in pollutant concentration, linear regression with the slope estimate ( $\beta_1$ , ppb yr<sup>-1</sup>) as the dependant variable and the population order (lowest too highest) as the independent variable was carried out. Should the population size affect the magnitude of trend, the resultant slope coefficient will be statistically different from zero.

The analysis revealed a slight negative trend (-0.02), Figure 40, and so crudely suggests that there is a greater annual reduction in NO<sub>x</sub> concentrations as population increases; however this trend was not statistically significant and so does not provide firm evidence to reject the null hypothesis of zero relationship.





a)

b)

**Figure 39:**  $\text{NO}_2$  (a) and  $\text{NO}_x$  (b) slope coefficients and 95 % confidence intervals for the other cities chosen for inclusion within this study. Trends have been calculated for the period 1999 to 2006. The sites are in increasing population order, as shown in Table 29 but excluding York sites (Lady Bower to Birmingham).



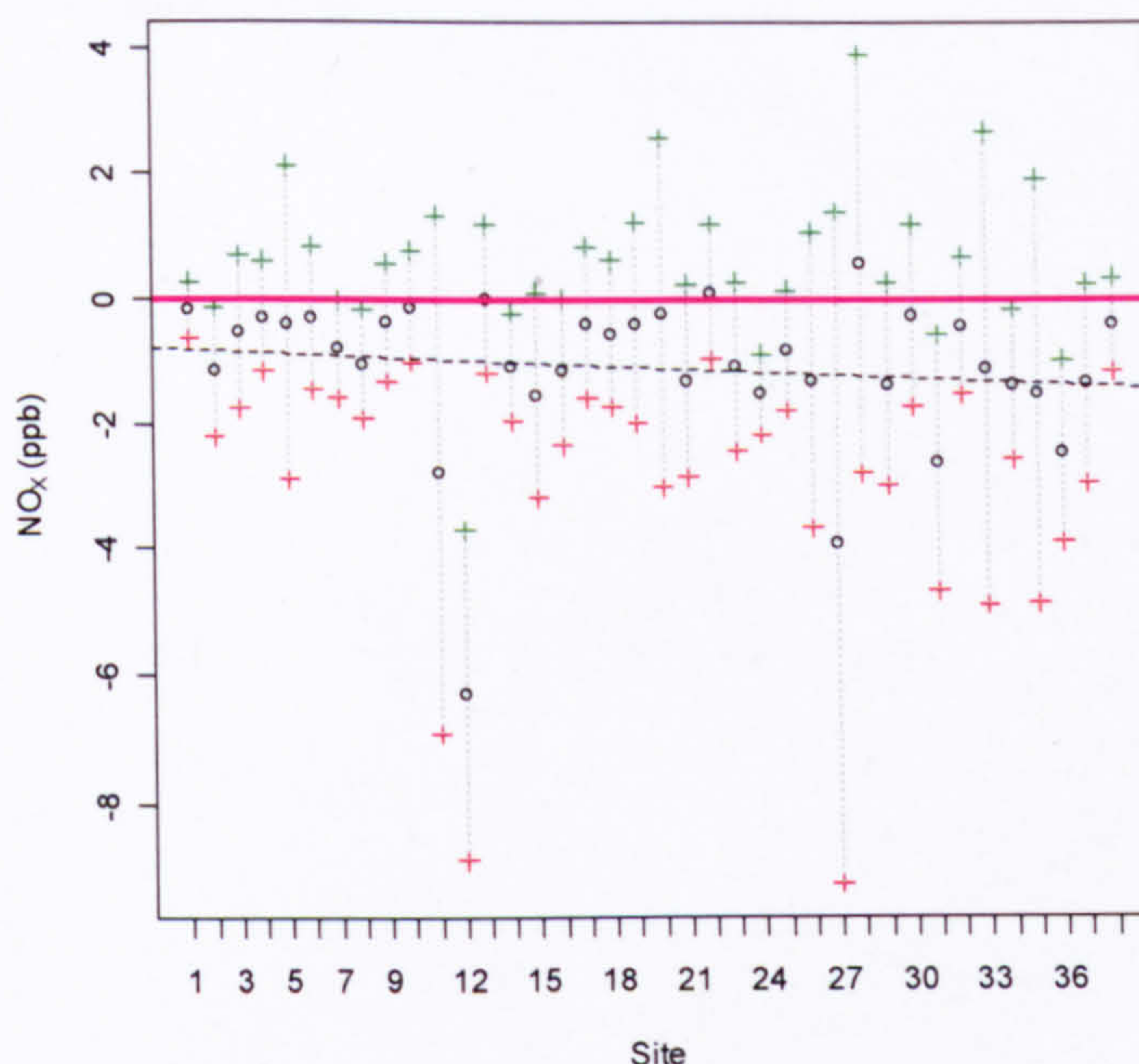


**Figure 40:** Estimated annual change in  $\text{NO}_x$  for the period 1999 to 2006 for the cities included in Table 29. The upper band of the 95 % confidence interval is illustrated by a green cross and the lower band by a red cross. The site order corresponds to Table 29. Linear regression shown by dashed black line ( $Y = \text{slope coefficient}$ ,  $x = \text{population order}$ )

The  $\text{NO}_2$  trend at 26 of 38 sites was negative, ranging from  $-0.8 \text{ ppb yr}^{-1}$  at Bradford to  $-0.04 \text{ ppb yr}^{-1}$  at the Manchester background site. Of these 26 sites seven (27%) are statistically significant at the  $p < 0.01$  level (Billingham, Norwich Centre, Barnsley Gawber, Nottingham, Bristol Centre, Bradford and Sheffield Tinsley). Similarly to the annual changes in  $\text{NO}_x$  concentration, the majority of statistically significant negative trends in  $\text{NO}_2$  were quite evenly spread between site types, with 3 out of the 7 occurring at urban centre sites, two at urban industrial sites (Billingham and Sheffield Tinsley), one at a roadside site and finally one at an urban background location (see Table 29).

The remaining 12 sites displayed a positive annual trend in  $\text{NO}_2$  concentration over the study period; the slope coefficients at two of these 12 sites were statistically significant (Oxford and Rotherham), both classified as urban centre sites. The range of positive slope coefficients varied from the marginally positive at  $0.03 \text{ ppb yr}^{-1}$  at Bolton and Redcar to  $0.9 \text{ ppb yr}^{-1}$  at Oxford.

The same analysis as shown previously for  $\text{NO}_x$  concentrations, where linear regression was used to determine whether population size has any relation as to the rate of change in pollutant concentrations, has been undertaken. Again, the linear regression analysis suggested a slightly negative trend ( $-0.009$ ,  $p < 0.01$ ) thus suggesting that the  $\text{NO}_2$  concentrations at the monitoring sites situated in larger urban populations are decreasing at a faster rate than those with smaller populations (see Figure 41). This trend is statistically significant at the  $p < 0.01$  level and so suggests that there is indeed some truth



in the hypothesis that the size of urban area influences the trend in NO<sub>2</sub> concentration over the period 1999 to 2006. It may be the case that for larger urban areas, such as Birmingham or Leeds, there is more scope for an improvement in pollutant concentration. However, since 6 of the 10 largest urban areas included in this study are urban centre sites, this significant negative trend may be a consequence of the behaviour of NO<sub>2</sub> concentrations at similar site classifications occurring in a similar manner; this is something that will be explored further in following paragraphs.

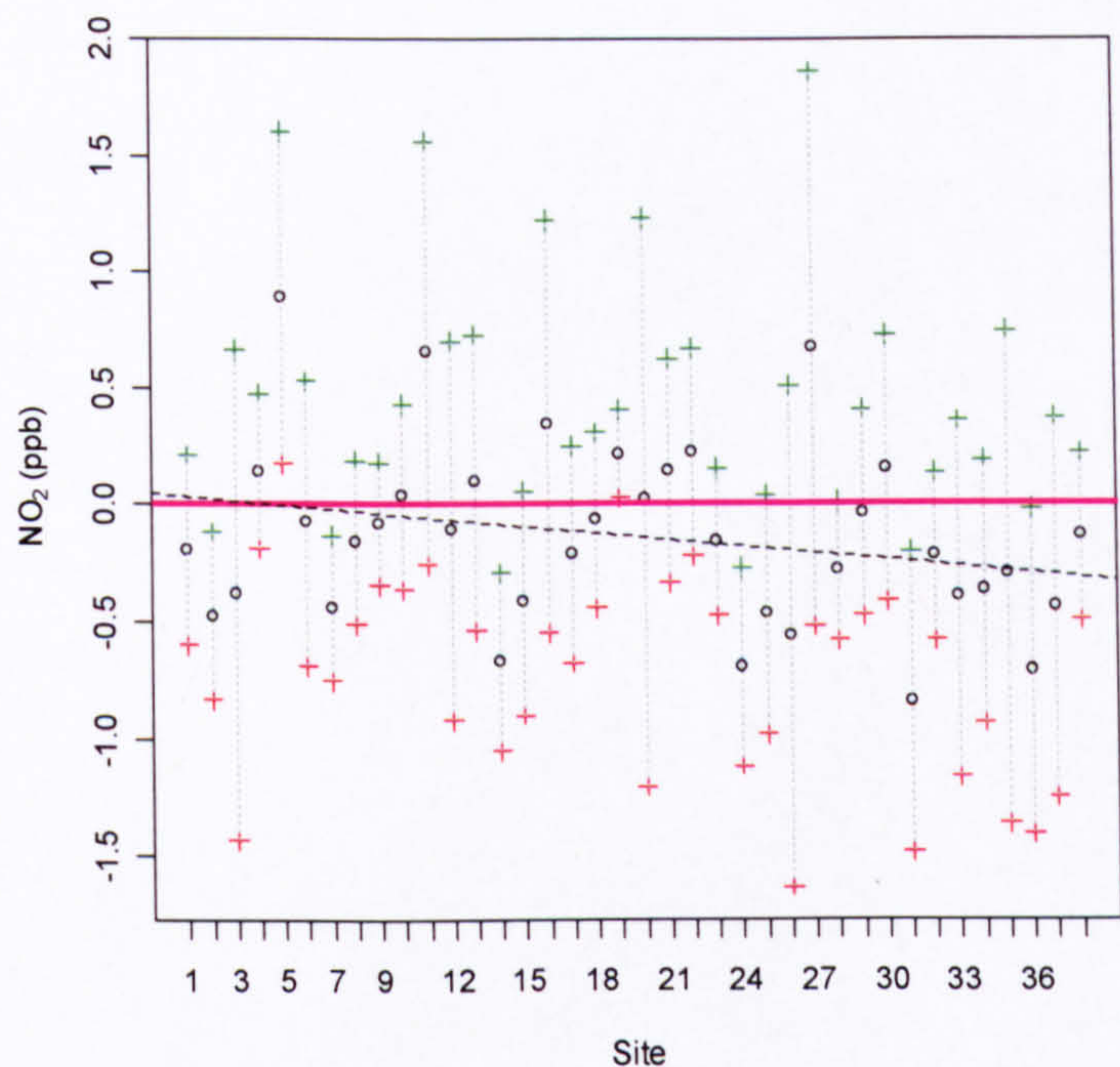


**Figure 41:** Estimated annual change in NO<sub>x</sub> for the period 1999 to 2006 for the cities included in Table 29. The upper band of the 95 % confidence interval is illustrated by a green cross and the lower band by a red cross. The site order corresponds to Table 29. Linear regression shown by dashed black line ( $Y = \text{slope coefficient}$ ,  $x = \text{population order}$ )

Rather crudely, the difference in the slopes for NO<sub>x</sub> and NO<sub>2</sub> concentrations shown in Figure 40 and Figure 41 suggest a difference in the behaviour of NO<sub>x</sub> and NO<sub>2</sub> concentrations. The reasons behind differences such as this are fundamental to our understanding of urban air quality.

Similarly to the findings for York (presented in section 5.4.2) the absolute and relative reductions in NO<sub>x</sub> concentration for the other cities exceed those of NO<sub>2</sub> at the majority of sites (Table 29) leading to an increase in the NO<sub>2</sub>: NO<sub>x</sub> ratio. This statement is supported further by the fact that the number of statistically significant negative regression slopes (at the  $p < 0.01$  level) is greater for NO<sub>x</sub> compared to NO<sub>2</sub>. The results in Table 29 therefore agree with the general opinion of the 2006 AQEG report, which states an increase in the NO<sub>2</sub>: NO<sub>x</sub> ratio (AQEG, 2006).



On a similar note, three sites mentioned explicitly in the 2006 AQEG document (Bath, Bury and Oxford) have been included in this analysis. It can be inferred that the increase in NO<sub>2</sub>: NO<sub>x</sub> ratio for these three cities, presented in Table 29, is consistent with the slope coefficients presented in the AQEG report. Indeed, for the sites of Bath and Oxford a positive change in NO<sub>2</sub> concentration over the study years has been reported (+2.0 % yr<sup>-1</sup> and +3.0 % yr<sup>-1</sup>, respectively); whereas in the case of Bury the significant reduction in NO<sub>x</sub> concentration (-4.5 % yr<sup>-1</sup> at the p< 0.01 level) was not mirrored in the NO<sub>2</sub> reduction (-0.3 % yr<sup>-1</sup>) over the period in question.

Interestingly, it is also apparent from Table 29 that the absolute decrease in NO<sub>x</sub> at the urban industrial sites included in this study is also substantial, possibly representing reductions in industrial emissions as a result of improvements in abatement technology over the 8-year period.

It should however be pointed out that not all trends in NO<sub>x</sub> and NO<sub>2</sub> concentration agree with the findings of AQEG. In fact, for some of the cities included in Table 29, the changes in NO<sub>x</sub> and NO<sub>2</sub> concentrations contradict the generally accepted view that the NO<sub>2</sub>: NO<sub>x</sub> ratio is increasing. This opposing NO<sub>2</sub>: NO<sub>x</sub> trend has already been highlighted at the urban background site of Bootham in section 5.4.2, and is also evident at several monitoring sites included in Table 29. For example, the NO<sub>x</sub> concentration at Lady Bower reservoir decreased by -0.16 ppb yr<sup>-1</sup> (-2.5 % yr<sup>-1</sup>), whereas the reduction in NO<sub>2</sub> was slightly greater at -0.2 ppb yr<sup>-1</sup> (-34 % yr<sup>-1</sup>). Additionally, the NO<sub>x</sub> at the Bristol Centre site marginally increased (0.6 ppb yr<sup>-1</sup>), whereas the NO<sub>2</sub> concentration fell annually (-0.3 ppb yr<sup>-1</sup>). There are also several sites where despite the absolute decreases in NO<sub>x</sub> exceeding those of NO<sub>2</sub>, the relative changes show the reverse to be true; for example: Glasgow background, Wolverhampton, Barnsley Gawber and Leamington Spa. Of the sites included in this study, the ones where the NO<sub>2</sub>: NO<sub>x</sub> ratio has reduced over the study years mainly occur at urban background sites. This is most likely due to the partitioning between NO<sub>x</sub> and NO<sub>2</sub> at these site types.

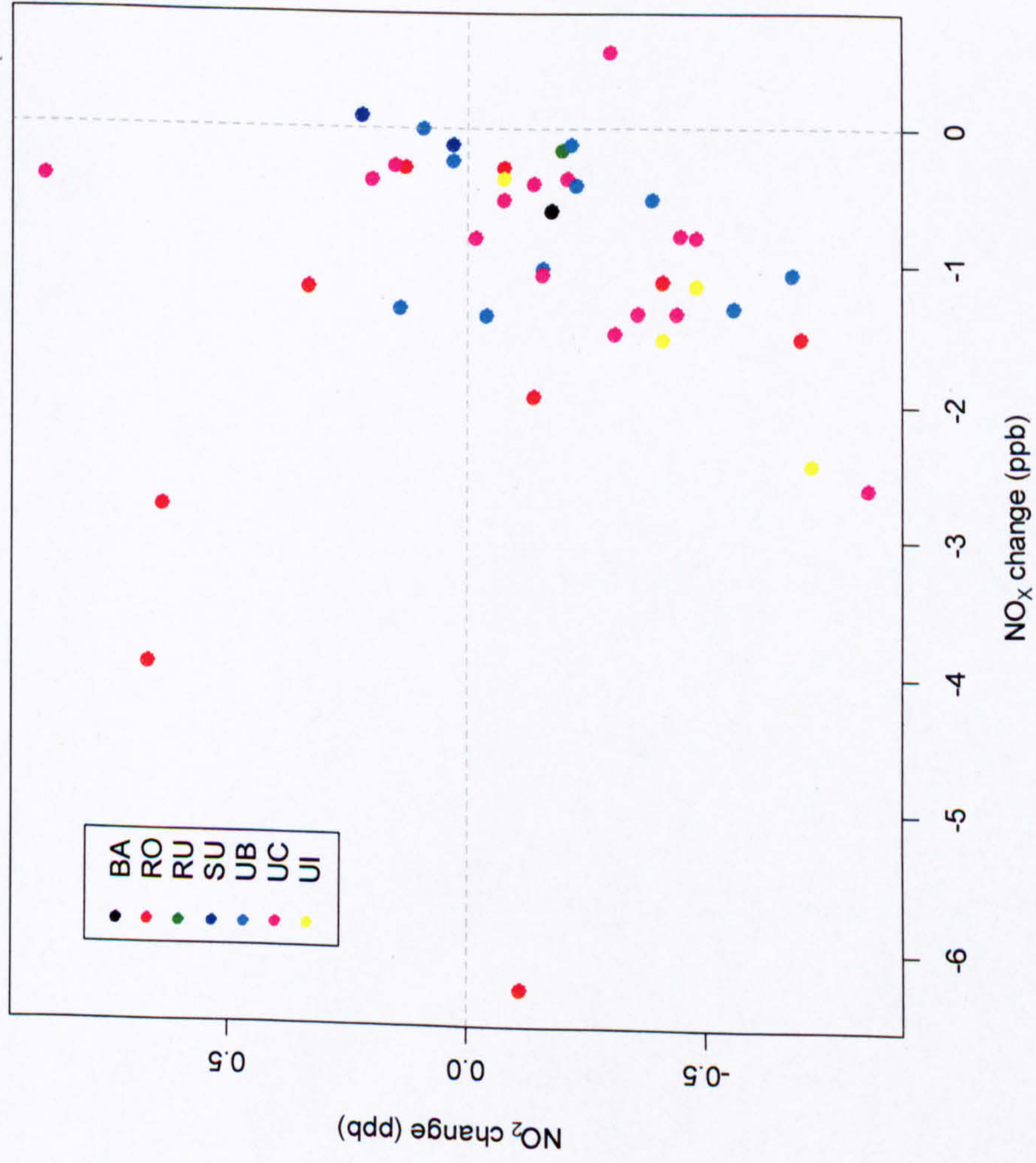
The discussion in the preceding paragraphs has highlighted similarities in NO<sub>x</sub> and NO<sub>2</sub> concentration behaviour within monitoring site classifications i.e., a general agreement in NO<sub>x</sub> concentrations trends for urban centre sites, for example. To further examine the possibility that the changes in NO<sub>2</sub>: NO<sub>x</sub> ratio may be related to the types of monitoring site, the annual change in NO<sub>x</sub> concentration has been plotted against the annual change in NO<sub>2</sub> for each site, see Figure 42 (for both absolute (ppb) and relative changes (%)). Should the data of the same site type classification clump (or group) together in distinct regions, it is likely that the NO<sub>x</sub> and NO<sub>2</sub> concentrations are behaving similarly for sites of the same classification.

It can be seen from Figure 42a that there is a great deal of scatter in the absolute trend coefficients for the roadside sites, suggesting that there is no universal trend

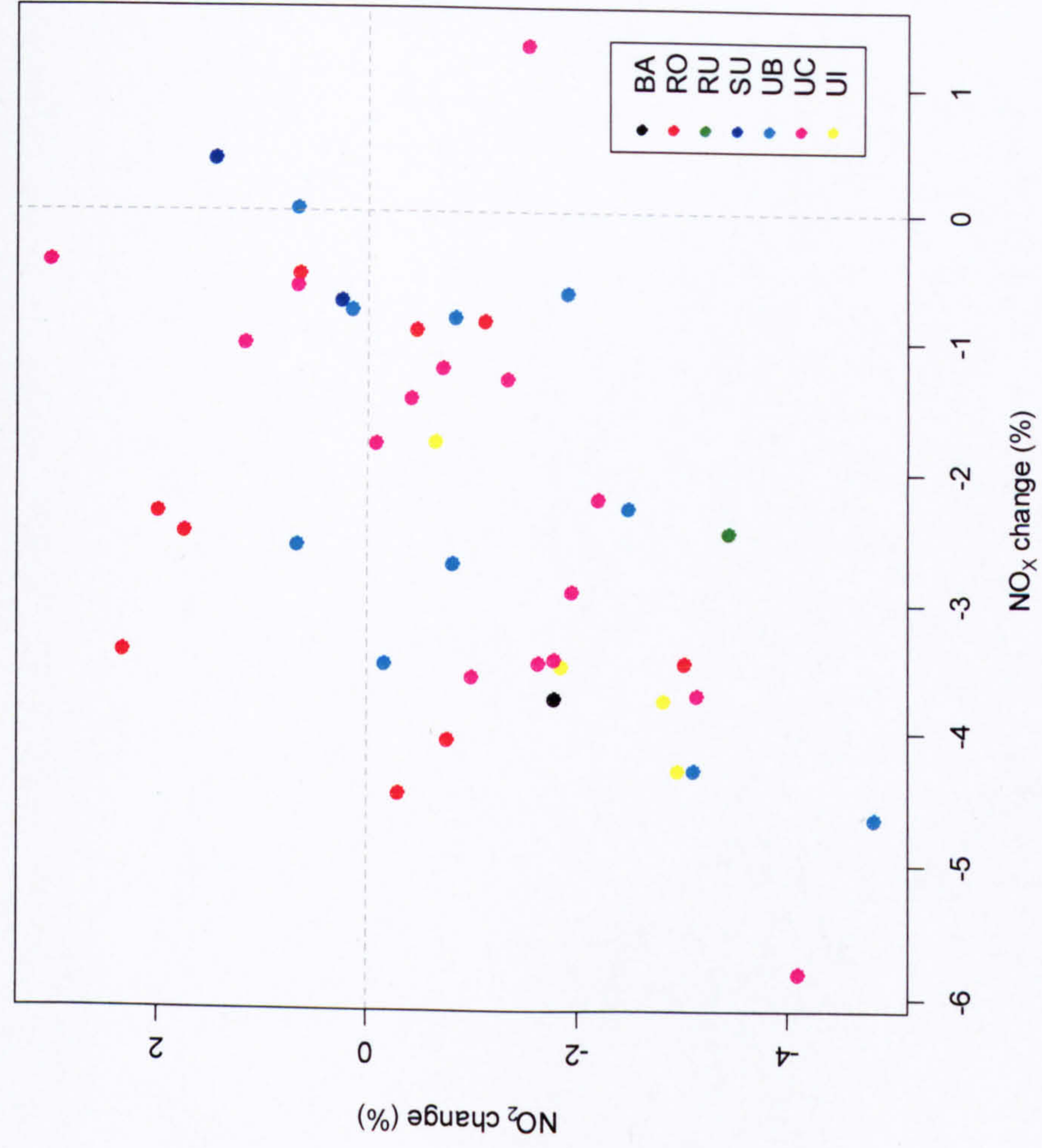


(common behaviour) in  $\text{NO}_x$  and  $\text{NO}_2$  concentration at this site type across the UK. The situation is similar for urban background and urban centre sites which, despite showing relatively less scatter in Figure 42a, again do not display a common trend in  $\text{NO}_x$  and  $\text{NO}_2$  concentration. Figure 42b illustrates the percentage changes in  $\text{NO}_x$  and  $\text{NO}_2$  concentration as opposed to absolute changes shown in Figure 42a. However, it can be seen that the relative changes in  $\text{NO}_x$  and  $\text{NO}_2$  concentration do not reveal any definite patterns in the coefficients either. Indeed, both plots shown in Figure 42 illustrate that the changes in  $\text{NO}_x$  and  $\text{NO}_2$  concentrations over the study years 1999 to 2006 experienced at the various site types do not follow any consistent pattern and suggest that the factors controlling the changes in the pollutant concentrations over time are complex.





a)



b)

**Figure 42:** Scatterplot of the estimated  $\text{NO}_x$  and  $\text{NO}_2$  linear regression slope coefficient (a) and annual percentage change (b) for the various sites (includes York sites). BA = background, RO = roadside, RU = rural, SU = suburban, UB = urban background, UC = urban centre and UI = urban industrial



#### 5.4.4. Results and discussion: long-term monthly trends.

Where data are available the monthly means of  $\text{NO}_x$  and  $\text{NO}_2$  concentrations have been calculated. Figure 43 illustrates those monthly mean  $\text{NO}_2$  concentrations recorded at the four long-term sites in York, and Figure 44 illustrates the monthly mean  $\text{NO}_x$  concentrations. Figure 45 shows the monthly mean  $\text{O}_3$  concentrations recorded at the site of Dunnington for the same period.

Generally, the highest  $\text{NO}_x$  and  $\text{NO}_2$  concentrations are seen during the winter months, with a general improvement in air quality through spring and summer. The high wintertime  $\text{NO}_x$  and  $\text{NO}_2$  concentrations are a result of higher emissions during these months (i.e. increased use of domestic heating and a greater number of journeys being made by car). Additionally, meteorological conditions associated with winter (that is, cold, stagnant atmospheres which are prone to inversions) also promote the accumulation of  $\text{NO}_x$  emissions close to the surface and so ground level concentrations can increase substantially at this time of year. This pattern is seen in both  $\text{NO}_2$  and  $\text{NO}_x$  concentrations at all sites across the city.

The seasonal trend in  $\text{O}_3$  concentrations is roughly the reverse of the  $\text{NO}_x$  and  $\text{NO}_2$  trend, with the greatest monthly  $\text{O}_3$  concentrations occurring in the warmer spring and summer months (Figure 45). This trend in ambient  $\text{O}_3$  concentration measured at Dunnington follows the general trend in  $\text{O}_3$  concentrations seen across the Northern Hemisphere. The review paper by Monks (2000) details the possible causes of this spring/summer maxima. Its driving mechanisms are still not entirely understood, however, it is believed that both photochemical production and stratosphere-troposphere exchange are significant contributors to the formation of tropospheric  $\text{O}_3$  (see Monks, 2000 for a fuller description).

Figure 43a showed that the 2003 Bootham  $\text{NO}_2$  concentrations for February to May are unusually high compared the monthly mean concentrations in other years. The peak  $\text{NO}_2$  and  $\text{NO}_x$  concentrations were not observed to this extent at other sites in operation at the time. Unfortunately the  $\text{NO}_x$  and  $\text{NO}_2$  concentrations for the background site of Dunnington are not available for this period. 2003 has been noted as an exceptional year for pollution as a result of the intense summer temperatures and winds predominantly originating from the east (AQEG, 2006). The  $\text{O}_3$  concentrations recorded for York during this period are low and so are consistent with the peak in  $\text{NO}_2$  concentrations. However, it is strange that the high  $\text{NO}_2$  concentrations did not persist for the summer months like that of other cities. It is therefore not clear what caused these high monthly  $\text{NO}_x$  and  $\text{NO}_2$  concentrations at Bootham during the spring of 2003. These high  $\text{NO}_x$  and  $\text{NO}_2$  concentrations were also seen in the 2003 annual mean (section 5.4.2).



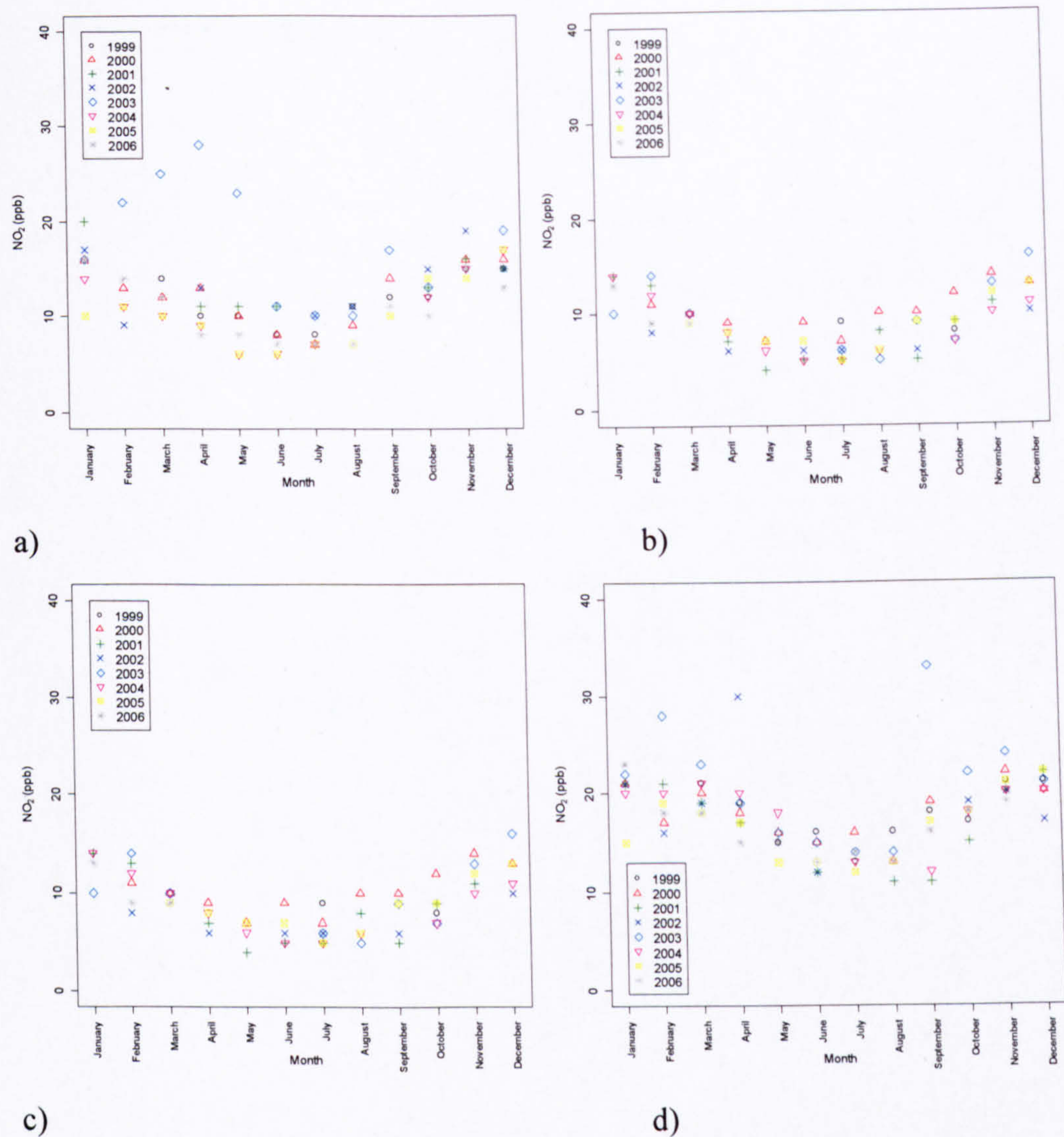


**Figure 43:** Monthly mean NO<sub>2</sub> concentrations for Bootham (a), Dunnington (b), City Centre (c) and Fishergate (d) for the period 1999 to 2006.



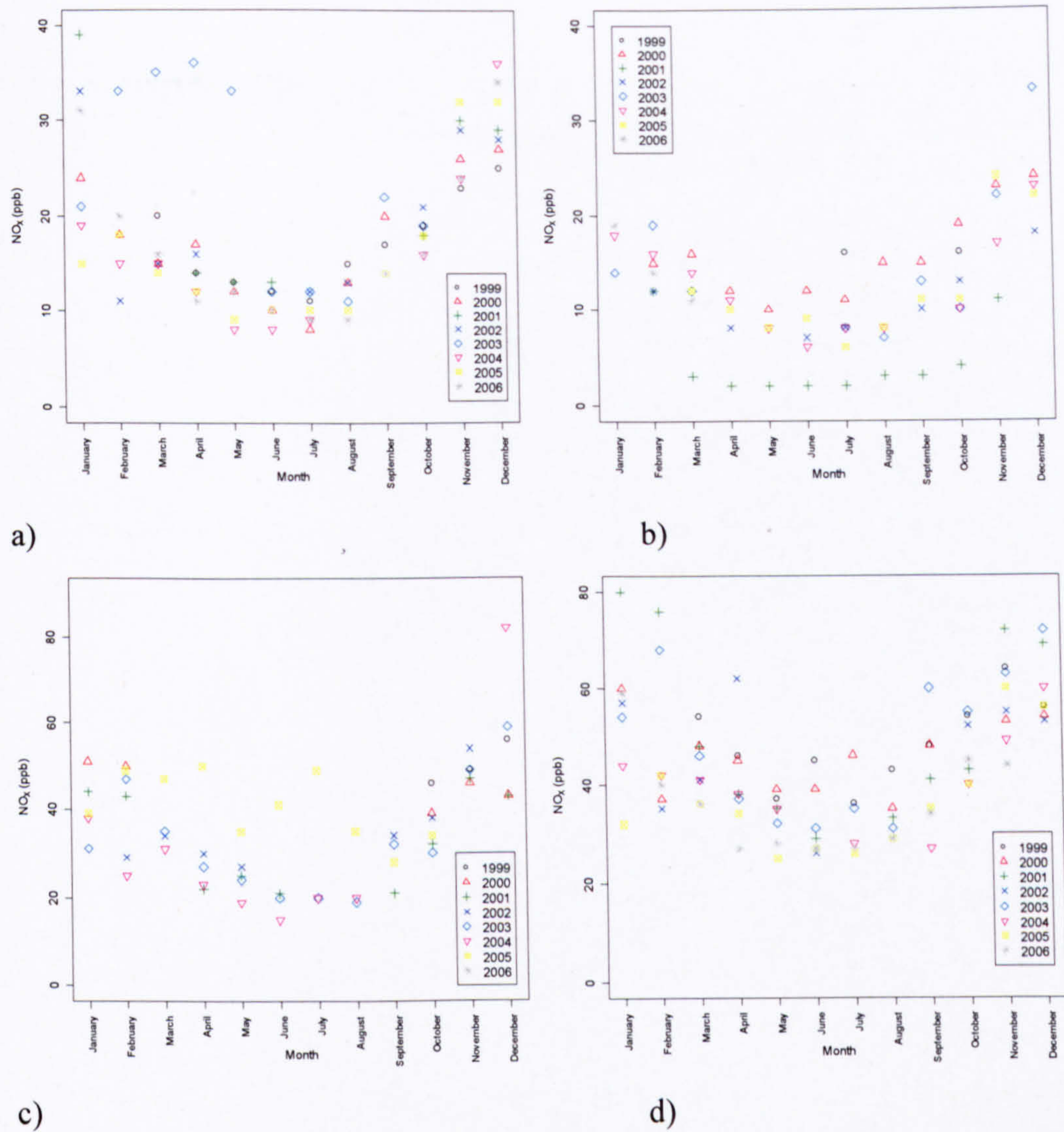


**Figure 44:** Monthly mean NO<sub>x</sub> concentrations for Bootham (a), Dunnington (b), City Centre (c) and Fishergate (d) for the period 1999 to 2006.

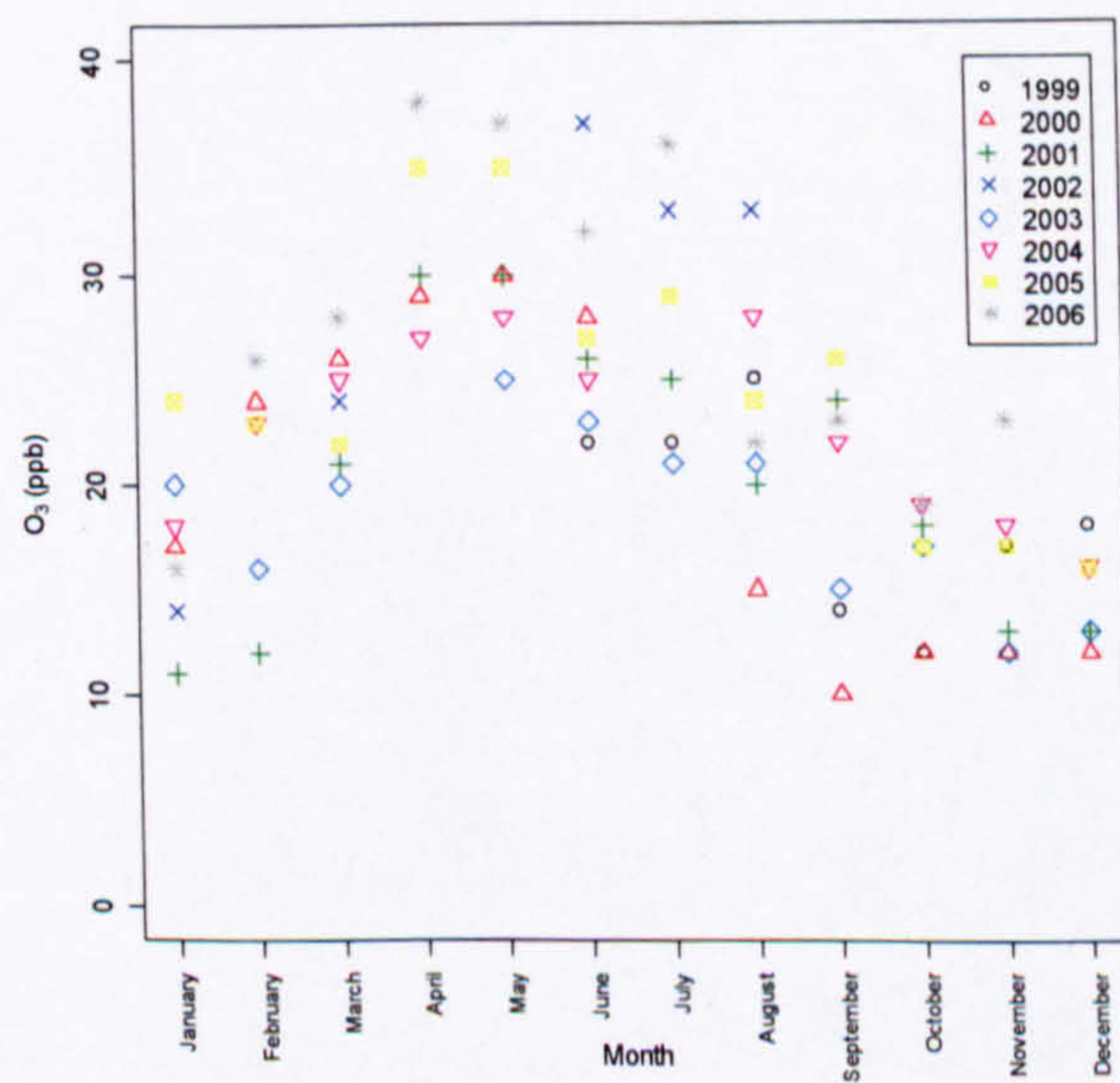


**Figure 45:** Monthly mean O<sub>3</sub> concentrations for Dunnington for the period 1999 to 2006.



Similar to the changes in annual mean  $\text{NO}_x$  and  $\text{NO}_2$  concentration reported in sections 5.4.2 and 5.4.3, it is possible to investigate the change over time in pollutant concentration for the different months of the year (i.e., the change in the mean  $\text{NO}_x$  concentration for January over the years 1999 to 2000). Figure 46 and Figure 47 illustrate the resultant slope coefficient calculated by the use of linear regression using the monthly mean pollutant concentration as the dependent variable and year as the independent variable.

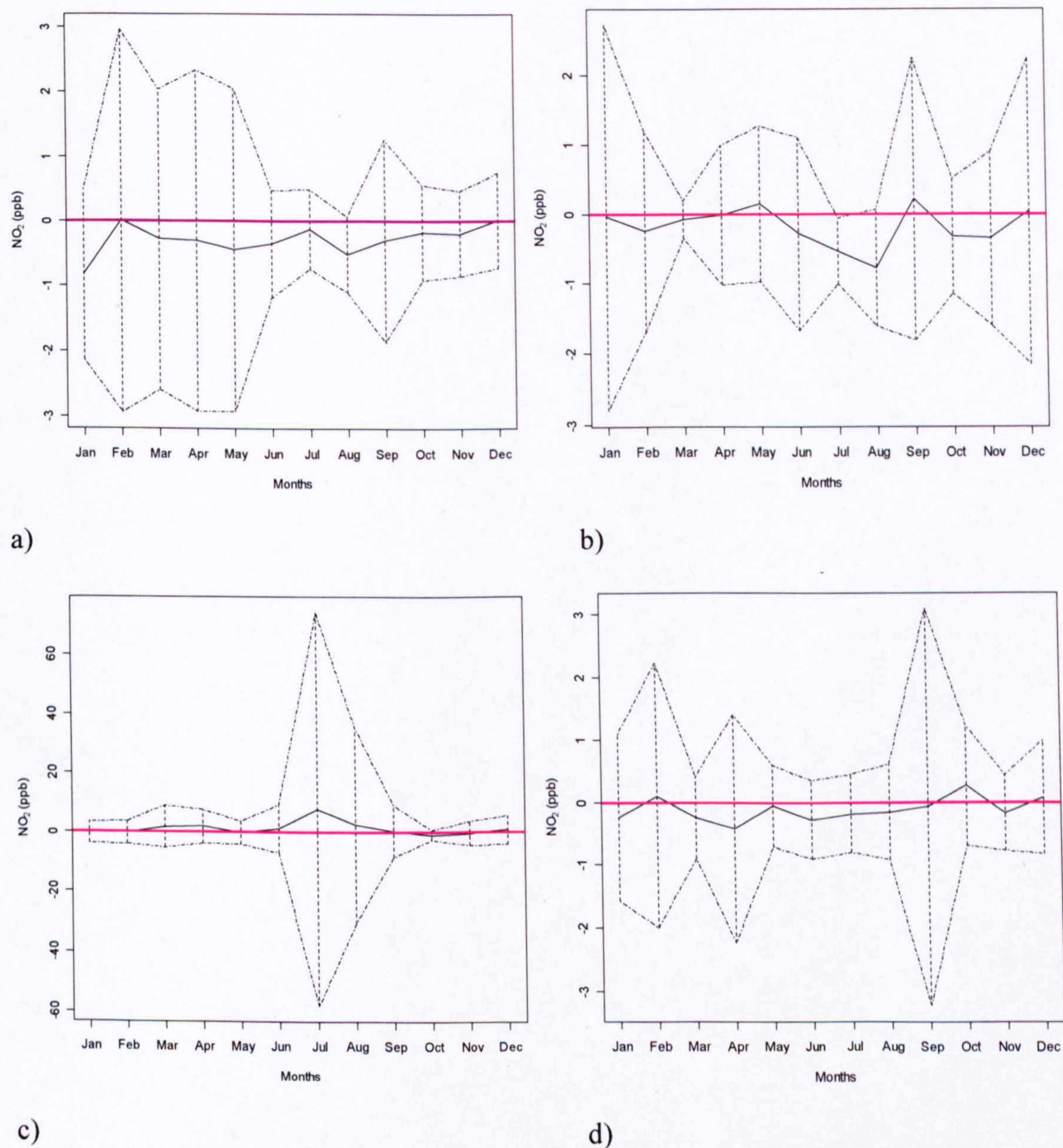


**Figure 46:** The calculated slope coefficients for the change in monthly mean  $\text{NO}_2$  concentrations for the period 1999 to 2006. Plot a) is for Bootham, b) Dunnington, c) City Centre and d) for Fishergate. The solid black line represents the slope coefficient calculated from linear regression, The dashed lines represent the 95% confidence intervals for each monthly slope coefficient. The solid pink line illustrates the null hypothesis of no change in monthly mean  $\text{NO}_2$  concentration over the study years (i.e., zero trend).



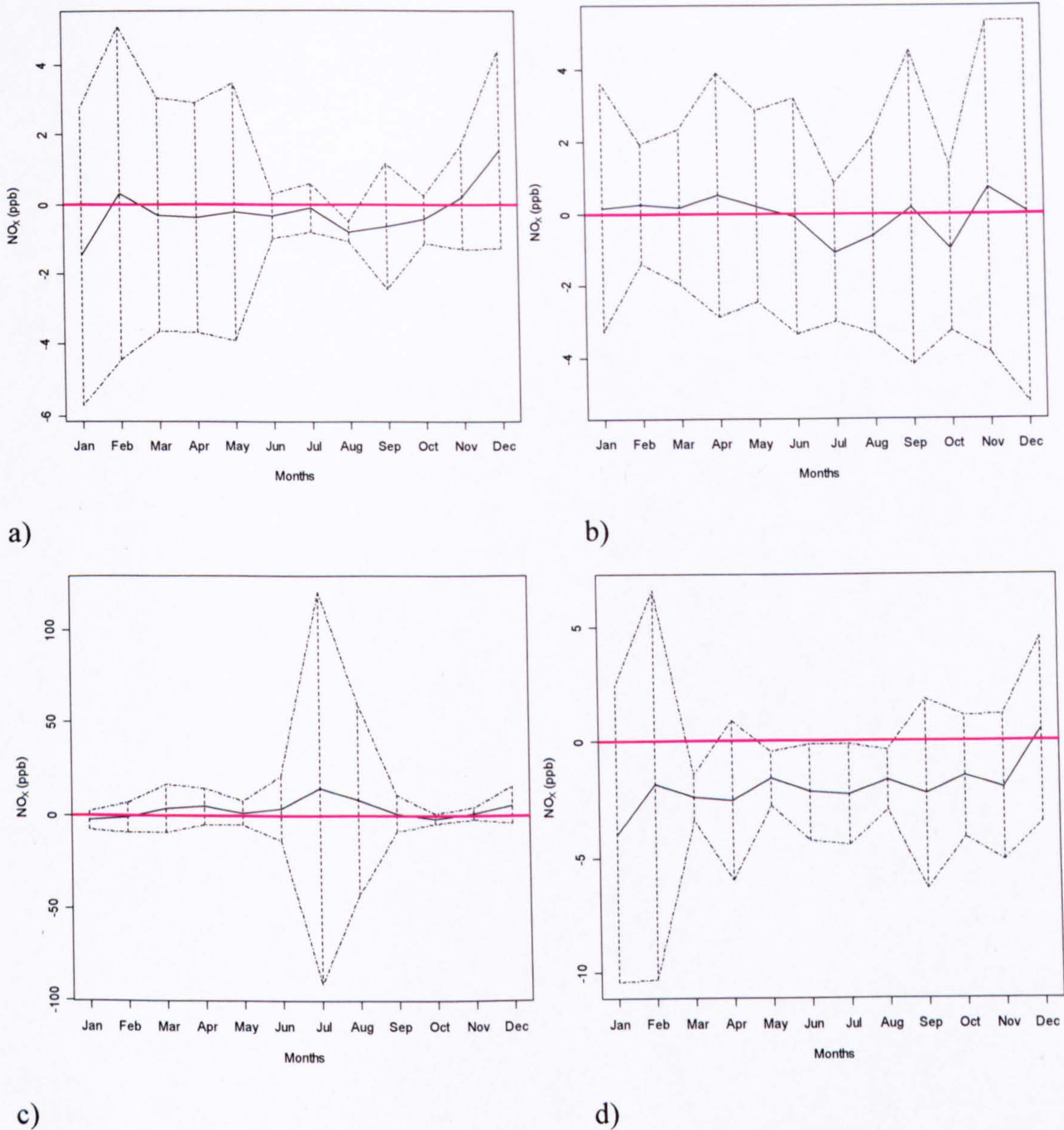


**Figure 47:** The calculated slope coefficients for the change in monthly mean  $\text{NO}_x$  concentrations for the period 1999 to 2006. Plot a) is for Bootham, b) Dunnington, c) City Centre and d) for Fishergate. The solid line represents the slope coefficient calculated from linear regression, The dashed lines represent the 95% confidence intervals for each monthly slope coefficient. The solid pink line illustrates the null hypothesis of no change in monthly mean  $\text{NO}_x$  concentration over the study years (i.e., zero trend).

Figure 47 illustrates great variability in the monthly mean  $\text{NO}_2$  coefficient estimates. On the whole, the majority of slope coefficients ( $\beta_1$ ) for the site of Bootham, Dunnington and Fishergate were negative; however only a single significant reduction in  $\text{NO}_2$  concentration was revealed for the month of July at Dunnington ( $-0.5 \text{ ppb yr}^{-1}$ ). The monthly regression for the City Centre site showed great fluctuation in the estimated slope coefficient, with the majority of months showing a positive trend in  $\text{NO}_2$  concentration (although none were statistically significant).



The story is somewhat different for NO<sub>x</sub> concentrations (Figure 47). The regression analysis for the sites of Dunnington and City Centre revealed great fluctuation between negative and positive slopes for the various months of the year. At Dunnington, the majority of monthly NO<sub>x</sub> trends were positive; however the 95% confidence intervals were large for all 12 months and so indicate poor precision in the estimation of the slope coefficient at this site. Similarly, the monthly NO<sub>x</sub> trends at the City Centre site were also highly variable (switching from positive to negative throughout the year) and again the confidence intervals are extremely large (this is especially true for the summer months). It is therefore not possible to infer with any great confidence the seasonal changes in NO<sub>x</sub> concentration at Dunnington and City Centre.

The change in monthly mean NO<sub>x</sub> concentration for the period 1999 to 2006 is statistically significant for the months of March, May, June, July and August at the site of Fishergate, with all of these months exhibiting a negative trend in monthly mean NO<sub>x</sub> concentrations. The greatest reduction in monthly mean NO<sub>x</sub> concentration at Fishergate (-2.4 ppb yr<sup>-1</sup>) is seen in March, however, the change in NO<sub>x</sub> for the months of June and July are fairly similar at -2.2 ppb yr<sup>-1</sup> and -2.3 ppb yr<sup>-1</sup>, respectively. The significant downward trend in **annual mean** NO<sub>x</sub> concentrations seen at Fishergate in section 5.4.2 therefore appears to be a consequence of a significant reduction in NO<sub>x</sub> concentrations during the spring and early summer months of March, May, June and July.

The monthly trends in NO<sub>x</sub> at Bootham were also mainly negative and interestingly, the negative trend in the NO<sub>x</sub> concentrations at this site during the month of August was statistically significant (-0.8 ppb yr<sup>-1</sup>).

The greater rates of reduction in NO<sub>x</sub> concentration over NO<sub>2</sub> at Fishergate imply an increase in the NO<sub>2</sub>: NO<sub>x</sub> ratio. Indeed, the results presented in Figure 46 and Figure 47 are consistent with the increase in NO<sub>2</sub>: NO<sub>x</sub> ratio (annual means) seen in section 5.4.2. Subsequently, it can be inferred from Figure 46 and Figure 47 that the increases in NO<sub>2</sub>: NO<sub>x</sub> ratios observed at Fishergate (and to a lesser extent at Dunnington and City Centre) appear to concentrate during the spring/summer months of the year.

An increase in the NO<sub>2</sub>: NO<sub>x</sub> ratio during the spring/summer months of the year hints that the increase in ratio could be related to ambient O<sub>3</sub> since this time of year corresponds to the highest O<sub>3</sub> concentrations (Figure 45). To investigate this theory further the monthly mean O<sub>3</sub> concentrations from the background station of Dunnington have been analysed in a similar manner to the monthly NO<sub>x</sub> and NO<sub>2</sub> concentrations. The background station of Dunnington provides an indication as to the likely ambient O<sub>3</sub> concentration entering the City of York.



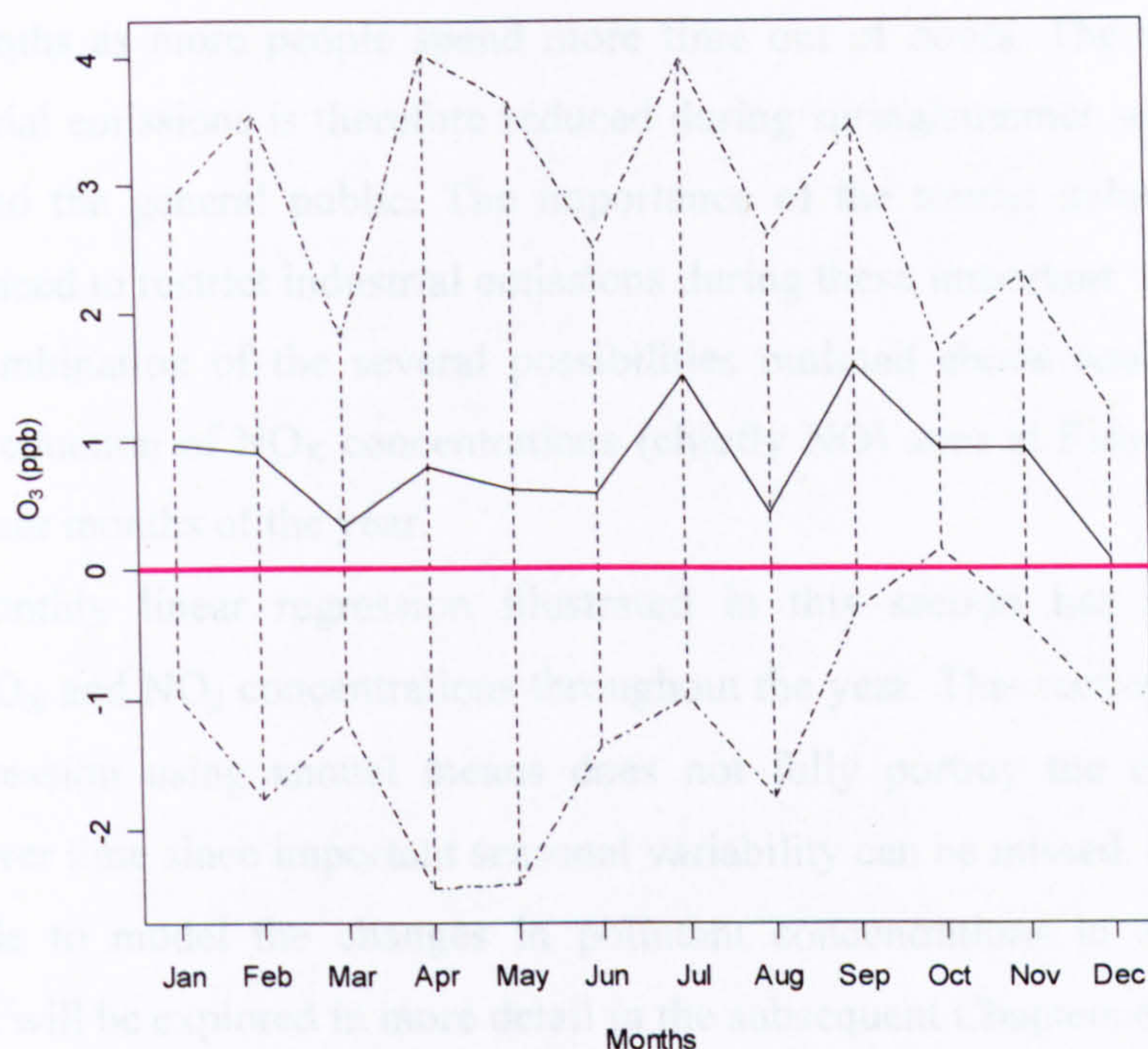


**Figure 48:** Estimated O<sub>3</sub> slope coefficients for each month of the year for Dunnington (1999 to 2006). 95% confidence intervals for the estimated slope coefficients are also shown (dashed lines). The Pink line shows the null hypothesis (zero trend line).

It can be seen from Figure 48 that the monthly O<sub>3</sub> trends are all positive (greater than the pink horizontal line) highlighting the fact that ambient O<sub>3</sub> concentrations have significantly increased in this month. However only the slope estimate for October is statistically significant at the  $p < 0.01$  level.

It is likely that the increase in ambient O<sub>3</sub> concentration across York (seen by the positive slope coefficients) will have contributed to the formation of NO<sub>2</sub> and so could be a possible reason for the increased NO<sub>2</sub>: NO<sub>x</sub> seen at Fishergate for some months of the year. It should however be noted that the months where the significant reductions in NO<sub>x</sub> are found (March, May, June and July) do not correspond with significant increases in ambient O<sub>3</sub>; however, as already highlighted these two pollutants are not monitored simultaneously and so increase in the ambient O<sub>3</sub> cannot be fully dismissed.

The significant decreases in NO<sub>x</sub> concentration (thought to be mainly caused by reduced NO concentrations) at the roadside site of Fishergate and the urban background station of Bootham during the summer months of the year could also be a consequence of differences in traffic volume throughout the year. For example, the influx of day visitors during the summer could potentially alter the fleet of vehicles using the York road network compared to other months of the year. Additionally, the relatively warmer temperatures during the spring/summer months compared to the rest of the year could also contribute to greater convective turbulence in the city and so lead to greater rates of dispersion. Furthermore, the emission rates for many industries are not constant throughout the year, with restrictions in place on emissions during



the summer months as more people spend more time out of doors. The smell and unsightly nature of industrial emissions is therefore reduced during spring/summer so that the effects are less noticeable to the general public. The importance of the tourist industry in York would further fuel the need to restrict industrial emissions during these important 'tourist' months. It is likely that a combination of the several possibilities outlined above could contribute to the greater rate of reduction of NO<sub>x</sub> concentrations (chiefly NO) seen at Fishergate and Bootham during the summer months of the year.

The monthly linear regression illustrated in this section has highlighted a large variability in NO<sub>x</sub> and NO<sub>2</sub> concentrations throughout the year. This section therefore indicates that linear regression using annual means does not fully portray the changes in pollutant concentration over time since important seasonal variability can be missed. It might therefore be more reasonable to model the changes in pollutant concentrations in a non-linear fashion (something that will be explored in more detail in the subsequent Chapters of this thesis).

#### **5.4.5. Temporal trends summary**

The temporal trends section has highlighted that the trends in annual mean NO<sub>x</sub> and NO<sub>2</sub> concentrations found in the centre of York have similar characteristics to those seen in London and other cities in the UK. However, the lack of statistical significance has made it difficult to firmly establish conclusions regarding the general behaviour of NO<sub>x</sub> and NO<sub>2</sub> concentrations in York.

This section also investigated the ambient O<sub>3</sub> concentrations measured at the background site of Dunnington. It was apparent that the annual O<sub>3</sub> at Dunnington has increased substantially over the 8-year period (correspondingly to other rural O<sub>3</sub> monitoring sites across the UK) and this Chapter has suggested that this increases in background O<sub>3</sub> could be a main contributor (along with an increase in primary NO<sub>2</sub> emissions from diesel vehicles) to the increase in NO<sub>2</sub>: NO<sub>x</sub> ratio observed at the long-term monitoring sites across the City of York.

This section has also shown the trends in monthly NO<sub>x</sub> and NO<sub>2</sub> concentrations at the four long-term sites in York. In all cases the reductions in NO<sub>x</sub> concentrations were greater than those seen in the ambient NO<sub>2</sub> concentrations; however the majority of these reductions were not significant. The statistically significant reductions in monthly NO<sub>x</sub> concentration (seen at Fishergate and Bootham) solely occurred during spring and summer, therefore suggesting that the overall improvement in air quality at these sites was limited to this time of year. Section 5.4.4 offered some possible explanations as to the likely causes of the differing rates of reduction in NO<sub>x</sub> concentration throughout the year; however this requires further investigation before firmer conclusions can be made.



## 5.5. Chapter summary

Section 5.2 highlighted the years in which the ambient  $\text{NO}_2$  concentration exceeded the annual objective. Despite the last exceedence occurring in 2005 (City Centre site) the annual mean  $\text{NO}_2$  concentrations at a number of roadside sites in 2006 showed near exceedence values indicating that the air quality problems in York have not yet been solved. The analysis of hourly data showed that at no point over the eight years of continuous monitoring have the concentrations exceeded the objective level. However, subsequent linear regression suggested that maximum hourly concentrations at a number of sites across the urban area of York have increased over the study years.

The spatial differences in  $\text{NO}_x$  and  $\text{NO}_2$  concentrations across the City of York have also been highlighted. Despite York's relatively small urban area the concentrations of  $\text{NO}_x$  and  $\text{NO}_2$  can vary quite substantially (i.e. section 5.3 highlighted a difference of 10 ppb in  $\text{NO}_2$  concentrations between the urban background and urban centre sites). Such differences in air quality across urban areas are expected (due to spatial differences in emissions); however, it is surprising that at the urban centre site the concentrations substantially exceed those of the urban background site located several hundred metres away (see Figure 8, Chapter 2). Additionally, the high annual mean  $\text{NO}_2$  concentrations at the urban centre site (City Centre), situated away from roads, highlight that it is not solely the air quality in the direct vicinity of road traffic that is influenced by vehicular emissions.

This Chapter has also highlighted the various long-term trends in  $\text{NO}_x$  and  $\text{NO}_2$  concentrations over time. At all four long-term monitoring sites in York (Dunnington, Bootham, City Centre and Fishergate) the annual mean and median concentrations of  $\text{NO}_x$  and  $\text{NO}_2$  have fallen.

Additionally, this Chapter has also explored the long-term trend in  $\text{O}_3$  concentration at Dunnington. In many urban areas  $\text{NO}_2$  formation is limited by the availability of  $\text{O}_3$  (oxidant). In larger cities like London, the influence of inner city  $\text{O}_3$  concentrations was thought too minimal to influence the changes in the  $\text{NO}_2$ :  $\text{NO}_x$  ratio observed across the capital (AQEG, 2006). However, this Chapter has presented evidence to suggest that the  $\text{NO}_2$  concentrations in the urban area of York behave differently to those found in the centre of larger urban areas (e.g. Marylebone Road, London), and more like the  $\text{NO}_2$  concentrations seen at suburban sites. Therefore it is likely that the increase in background  $\text{O}_3$ , highlighted in section 5.4.2, will influence ambient  $\text{NO}_2$  concentrations in the city centre of York to some degree and could help explain the general increase in  $\text{NO}_2$ :  $\text{NO}_x$  ratio experienced at a number of the long-term monitoring sites.

Finally, the linear regression using monthly mean concentrations (section 5.4.4) highlighted that the greatest reductions in  $\text{NO}_x$  over the past 8 years occurred during the spring and summer months (that is, March, May, June and July for the roadside site of Fishergate; August for the urban background site of Bootham). This summertime reduction is interesting in



terms of air quality management because of the successful tourist industry in York. During the warmer months of the year the City of York experiences a massive influx of visitors, many of whom travel by car. The summer reductions in  $\text{NO}_x$  could therefore reflect the increasing success of the Park and Ride schemes, introduced in the late 1990s, alongside the other air quality management strategies (variable messaging boards and control of traffic light timings) which over time may have led to an improvement in  $\text{NO}_x$  during these busy periods. Additionally, it is also likely that seasonal differences in industrial emissions around the City of York could assist in the greater rates of reduction in  $\text{NO}_x$  concentration during these summer months compared to other months of the year.

The linear regression for monthly  $\text{O}_3$  concentrations revealed a significant increase in the monthly mean  $\text{O}_3$  concentration measured at the background site of Dunnington for all months of the year (however, only the annual increase in  $\text{O}_3$  for the month of October was statistically significant). It is therefore a possibility that the year round increase in local background  $\text{O}_3$  concentration could have contributed to the significant decreases in  $\text{NO}_x$  (as a result of destroying  $\text{NO}$ ) seen at the sites of Bootham and Fishergate. However, to make any definite conclusions about the cause of  $\text{NO}_x$  reduction (and the subsequent increase in  $\text{NO}_2$ :  $\text{NO}_x$  ratio), simultaneous measurements of  $\text{O}_3$ ,  $\text{NO}_x$  and  $\text{NO}_2$  are needed.

Finally, this Chapter has highlighted the strong seasonality inherent in the pollutant data. It is likely that much further information can be gained using non-linear statistical techniques as will be explored in subsequent Chapters.



## **6. Long-term generalised additive modelling analysis**

### **6.1. Chapter preview**

This Chapter will provide a more detailed analysis of the long-term trends in  $\text{NO}_x$  and  $\text{NO}_2$  concentrations already investigated in the previous Chapter. The statistical technique of generalised additive modelling will be deployed to investigate the non-linear structure in the pollutant data. The dispersion model, ADMS-Urban, will also be used to analyse and predict long-term trends in  $\text{NO}_x$  and  $\text{NO}_2$  concentrations over the period 1999 to 2006. The two different modelling techniques will be compared.

### **6.2. Introduction and literature review**

#### **6.2.1. Trend analysis**

The effective management of any target species, be it air pollution or wildlife populations, requires the careful consideration and analysis of long term monitoring data (Fewster et al., 2000; Siriwardia et al., 1998). Trends in monitoring data need to be analysed and the reasons behind the trends investigated if adequate recommendations for management are to be made. It is for this reason that it was considered desirable to investigate the  $\text{NO}_x$  and  $\text{NO}_2$  concentrations at a variety of monitoring sites in York.

Linear regression is commonly used in scientific studies to analyse trends where the response variable is regressed against a time based explanatory variable (Fiester and Balzer, 1991; Shreffler and Barnes, 1996; Fiore et al., 1998; Jo et al., 2000; Aleksic et al., 2005). The subsequent slope coefficient corresponds to the mean rate of change in response per unit of time. However, the model fit ( $R^2$ ) of linear models will be decidedly poor, and any non-linear structure in the data lost, where non-linear relationships occur. This poor model fit therefore represents a major disadvantage of linear regression when applied to 'real' datasets.

Many studies have avoided the issue of nonlinearity by applying modelling techniques other than linear regression when analysing trends in a particular species. The majority of these papers in an air quality setting have focused on  $\text{O}_3$  concentration trends. Thompson et al. (2001), review a selection of statistical methods for the normalisation of  $\text{O}_3$  concentrations with respect to meteorological variables. The various techniques analysed are broken down into the categories of regression, extreme value, and space-time. The actual statistical techniques covered by Thompson et al. (2001) include classification and regression tree analysis (CART), cluster analysis and non-linear regression. In a series of papers, Gardner and Dorling (1999; 2000a; 2000b) applied MLPN (multilayer perception neural networks) to investigate  $\text{O}_3$  concentrations at a variety of locations across the UK. The studies found that the unconstrained technique of neural networks is successful in representing the complex, non-linear, associations between hourly  $\text{O}_3$  and its predictor variables. In addition, Davis et al. (1998) applied cluster



analysis to again investigate O<sub>3</sub> concentration trends, but this time for Texas, USA. This study separated data into seven cluster groups that had significantly different O<sub>3</sub> concentrations. For each cluster group the relationship between meteorology and O<sub>3</sub> was individually modelled. The methodologies adopted by these papers provide a more 'sensitive' estimate of O<sub>3</sub> concentration trends than that of linear statistical analysis. Finally, Huang and Smith (1999) applied CART to the investigation of ground-level O<sub>3</sub> measurements in Chicago, USA. The CART methodology separated data into different meteorological clusters and the subsequent trend in O<sub>3</sub> concentration for each cluster was then investigated.

Recently, the use of the unconstrained regression based modelling technique, generalised additive modelling, has been deployed in a variety of studies spanning a range of scientific settings: Fewster et al., 2000; Suarez-Soanne et al., 2002; Reiss, 2006; Zheng et al., 2007; Carslaw et al., 2007; Heikkinen et al., 2007. Generalised additive models (GAMs) are a less restrictive form of statistical modelling that instead of assuming (a priori) a linear relationship between response and explanatory variable(s), represent this relationship by a flexible smooth curve (Hastie and Tibshirani, 1990). The curve can take any functional form and so can more accurately characterize the trend in the target species.

There are many examples of GAMs being applied to a variety of long term datasets in an attempt to reveal patterns and changes in the response variable over time. For example, Fewster et al. (2000) and Suarez-Soanne et al. (2002) use the flexibility inherent in GAMs to respectively model the long-term changes in UK farmland and Spanish steppe, bird populations. The paper by Reiss (2006) illustrates the successful application of generalised additive modelling when analysing trends in daily concentrations of benzene and 1,3-butadiene. Finally, the Zheng et al. (2007) study, concerned with daily O<sub>3</sub> concentrations in the eastern United States, uses GAMs to assess the changes in pollutant data in a long-term dataset. In each example the time variable was represented by a smooth term so as to allow the non-linearity in the response-time relationship to be accurately modelled. The smooth function also reduces the variability in the response data thus revealing the underlying trend.

### **6.2.2. Confounding factors**

A major bugbear of trend analysis is the issue of confounding factors. Confounding factors can 'mask or falsely emphasize' trends (patterns) in the target species (Carslaw et al., 2007) and for this reason, trend detection is usually carried out using normalised, as opposed to raw, data. In many circumstances the relationships between the confounding factors and the target species are non-linear. It is therefore also desirable to use a flexible, unconstrained, technique when controlling for confounding factors.

Epidemiological studies are a good example of how confounding factors can interfere with trends. These studies attempt to establish a causal relationship between an air pollutant and certain health effects (cause-specific mortality or morbidity). Epidemiological studies must



therefore normalise the health data (response variable), with respect to confounding factors, such as temperature, season etc., which would otherwise cloud the dose-response relationship. For this reason, generalised additive modelling has been successfully deployed in epidemiological studies for well over a decade (Baccini et al., 2007). The literature on this topic is extensive and covers both a variety of pollutants ( $PM_{10}$ ,  $PM_{2.5}$ ,  $PM_{10-2.5}$ ,  $NO_2$ ,  $SO_2$ ,  $O_3$ ) and health effects (total mortality, cardiovascular mortality, respiratory mortality, hospital admissions etc.); some recent examples include: O'Neil et al. (2004); Samoli et al. (2006); Schlink et al. (2006); Larrieu et al. (2007); Kan et al. (2007); Qian et al. (2007); Segala et al. (2008).

In epidemiological studies the most common confounding factors include meteorological variables (such as temperature and humidity), long-term trend and seasonal effects. Some papers include unique additional terms e.g. the study by Larrieu et al. (2007), which investigates the effects of daily number of hospitalisations (cardiovascular diseases, cardiac diseases and ischemic heart diseases) as a result of  $PM_{10}$ ,  $NO_2$  and  $O_3$  concentrations and includes an indicator term for influenza epidemics and holidays. Additionally, the study by Qian et al. (2007), which investigates the association of daily cause-specific mortality with particulates in China, includes indicators for days with extremely hot or cold temperatures and also extremely humid days as confounding factors.

### 6.2.3. Exploratory analysis

GAMs are also used to understand the relationships between a response variable and its main drivers or explanatory variables (Davis and Speckman 1999; Holland et al. 2000; Fewster et al., 2000; Aldrin and Haff 2005; Reiss 2006; Carslaw et al., 2007; Carslaw and Carslaw, 2007; Zheng et al. 2007). For example, Fewster et al. (2000) used GAMs to formally identify and quantify the importance of a variety of explanatory variables in explaining the variability in bird population abundance. The paper calculated the individual contribution of each explanatory variable in terms of explaining the variability in mean bird numbers and subsequently ranked the various explanatory variables in order of importance.

Aldrin and Haff (2005) used GAMs to quantify the importance of meteorology and traffic related parameters on the air quality ( $PM_{10}$ ,  $PM_{2.5}$ ,  $NO_x$  and  $NO_2$ ) in Oslo, Norway. The conclusions drawn from this work suggested that the number of vehicles in the area, along with the wind direction and wind speed were the most important predictor variables for the air pollutant concentrations.

Additionally, GAMs have also been utilised by Holland et al. (2000) to investigate the dependence of sulphur dioxide ( $SO_2$ ) on seasonal cycles and meteorology in the U.S. The models developed explained 42% to 79% of the variability in  $SO_2$  concentration depending on the site.



Davis and Speckman (1999) predicted one day in advance, the daily and 8hr average  $O_3$  concentration at Houston, Texas using a relatively complex GAM. Previous modelling attempts using other techniques (linear and non-linear regression models) had met with difficulties due to the complex meteorological processes involved. The GAM developed in this study included wind components, cloud cover, maximum  $O_3$  concentration from the previous day, maximum daily temperature and morning mixing height as explanatory variables.

Finally, Carslaw et al. (2007) used a GAM approach to investigate the influence of traffic emissions on air quality ( $NO_x$ ,  $NO_2$ , CO, benzene and 1,3-butadiene) at Marylebone Road, London. The results showed that complex wind flow patterns in addition to traffic emissions were important in explaining pollutant concentrations.

### **6.3. Aims**

A principal aim of this Chapter is to analyse the trends in air quality data ( $NO_x$  and  $NO_2$ ) for the various monitoring sites in York over time. In an effort to explain the greatest amount of variability in  $NO_x$  and  $NO_2$  concentrations models including various important explanatory terms will be created. These covariate models take into consideration the confounding influences of meteorology and season when predicting  $NO_x$  and  $NO_2$  concentrations. The use of normalised data (as opposed to raw data) should more accurately reflect the trend in pollutant emissions. The analysis will follow the same procedure as that highlighted in the Reiss (2006) and Zheng et al. (2007) studies where the confounding factors are modelled by smooth terms.

Additionally, this Chapter will also use a dispersion model to predict  $NO_x$  and  $NO_2$  concentrations for the same period. By applying a GAM to the  $NO_x$  and  $NO_2$  predictions made with ADMS-Urban it will be possible to identify the key driving factors of the dispersion model.

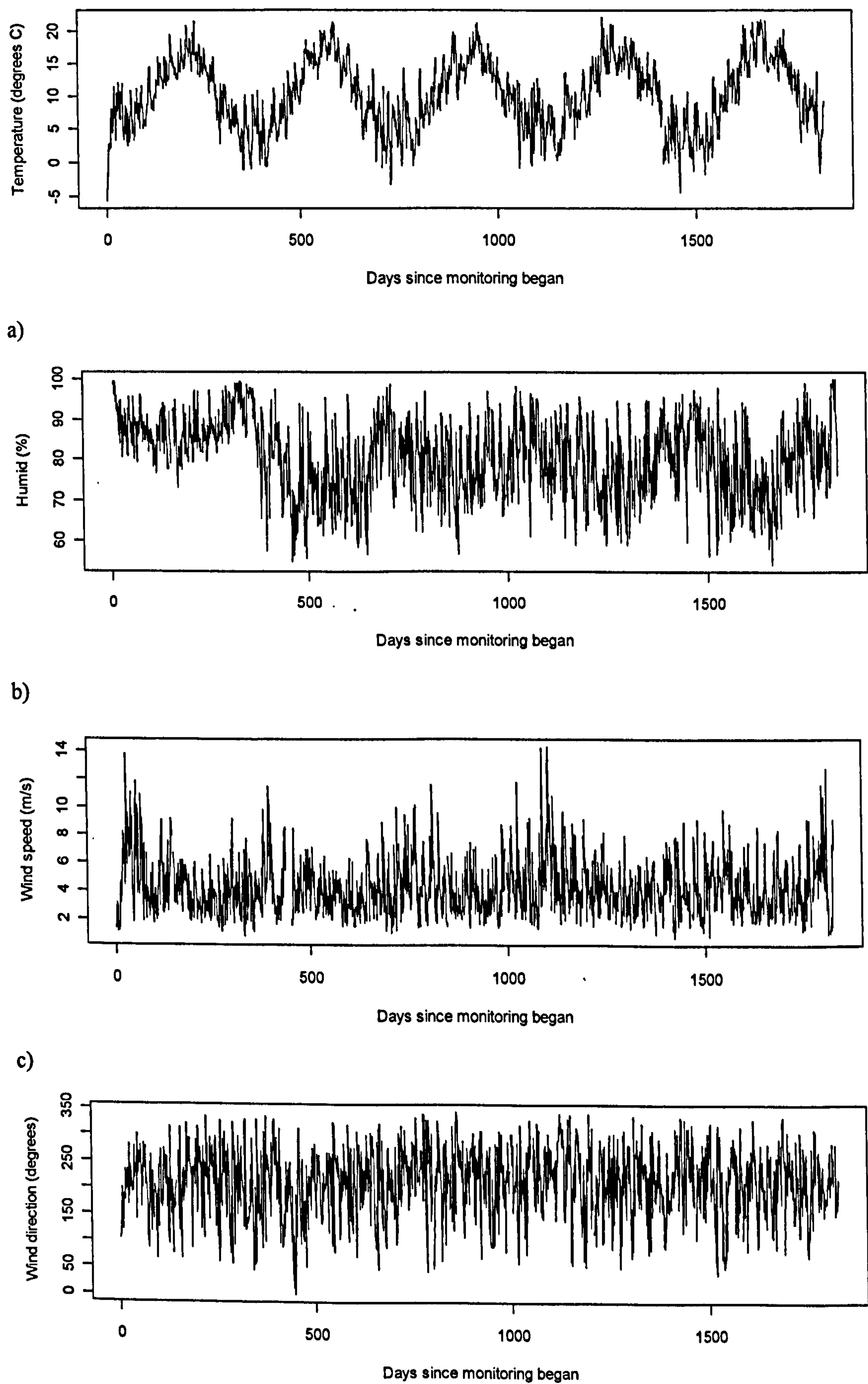
## **6.4. Data**

### **6.4.1. Meteorological data**

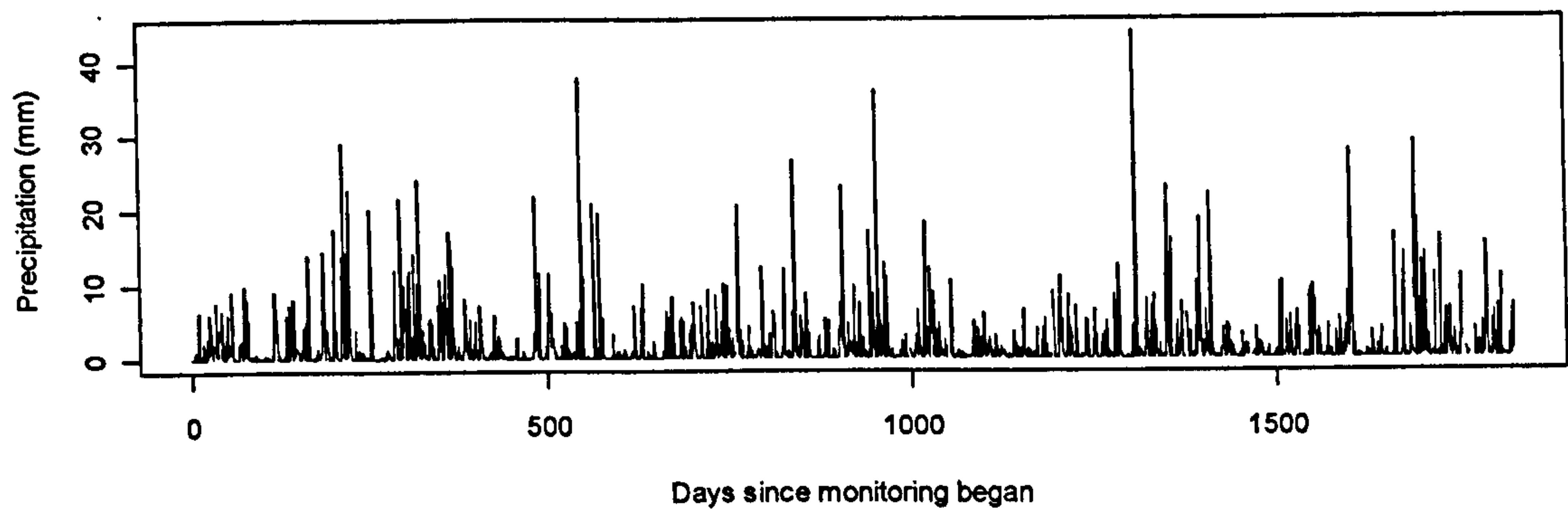
Continuous meteorological data from the UK Meteorological Office operated site at Church Fenton for the 1<sup>st</sup> January 2002 to 31<sup>st</sup> December 2006 are included in the analysis. Twenty four hour means have been calculated from hourly raw data; only those days where data capture exceeds 18 hours a day have been included in the final dataset. The meteorological variables available at Church Fenton include: wind speed (m/s), wind direction (degrees from north), temperature ( $^{\circ}C$ ), humidity (%), precipitation (mm) and cloud cover (Oktas). Figure 49 illustrates the time-series plots of the various meteorological variables for Church Fenton. The meteorological data are very noisy. Temperature is the only variable that has any noticeable



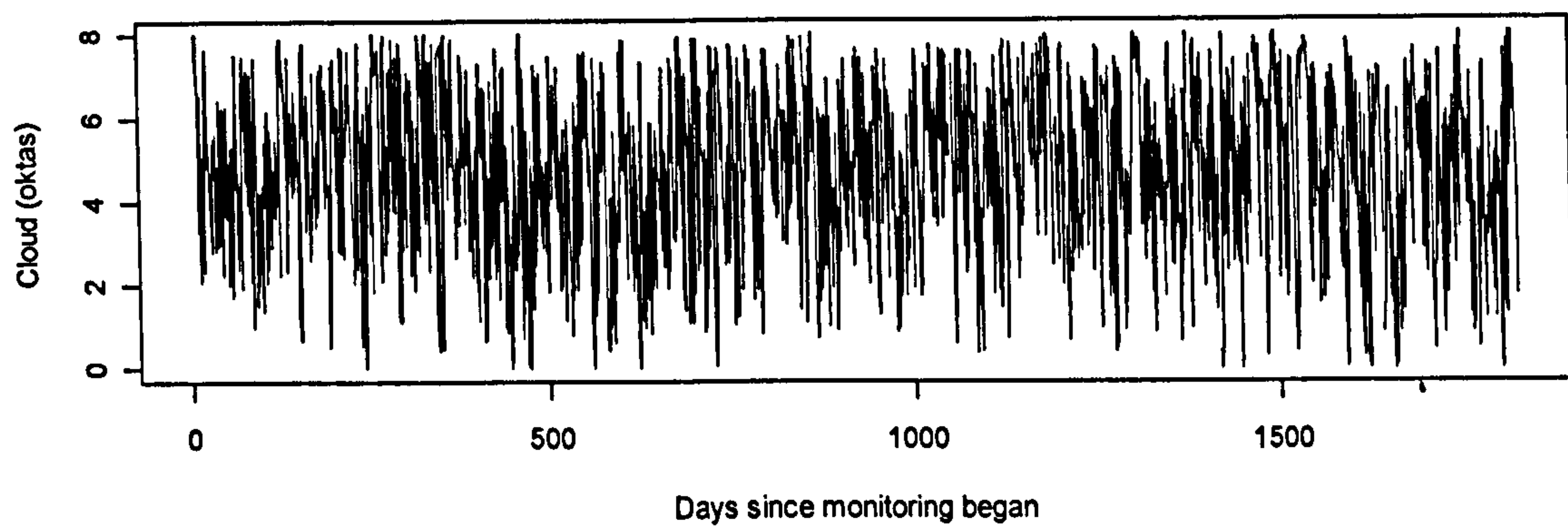
regular structure to it, with lower temperatures in winter, and higher temperatures in summer (Figure 49).







e)



f)

**Figure 49:** Time series plots of the various meteorological variables recorded at the Meteorological Office station at Church Fenton. d) wind direction (degrees); e) precipitation (mm); cloud cover (oktas)

#### 6.4.2. Air quality data

As already highlighted in Chapter 3 the air quality monitoring network in York has changed substantially over time. The datasets available for analysis cover a variety of years depending on the site in question. This variety has led to difficulties in applying universal statistical analysis to the seven monitoring sites. Additionally, the availability of meteorological data for York has also further restricted the length of datasets.

For the purpose of this Chapter, 24-hr  $\text{NO}_x$  and  $\text{NO}_2$  data for three sites (Bootham, City Centre and Fishergate) from 1<sup>st</sup> January 2002 to 1<sup>st</sup> April 2006 will be considered. This is the longest possible continuous period that coincides with the availability of meteorological data and also background pollutant data collected at the site of Dunnington. Twenty four hour  $\text{NO}_x$  and  $\text{NO}_2$  data from a further four sites (Gillygate, Holgate Road, Nunnery Lane and Lawrence Street) will also be considered for the period 1<sup>st</sup> January 2004 to 1<sup>st</sup> April 2006, the longest continuous period for these sites. Again, the 24-hr  $\text{NO}_x$  and  $\text{NO}_2$  concentrations have been calculated from 1-h means and only days with 18 hours of data or more have been included in the final dataset. Missing data have been omitted from the dataset i.e., set to NA.



Time series for the four long-term measurement sites are shown in Figure 50 and Figure 51. These concentration data show evidence of seasonality at each of the monitoring sites under study. The highest concentrations generally occur during the winter months and correspond to those months of the year with the greatest level of emissions. The summer months generally display the lowest concentrations throughout the annual cycle.



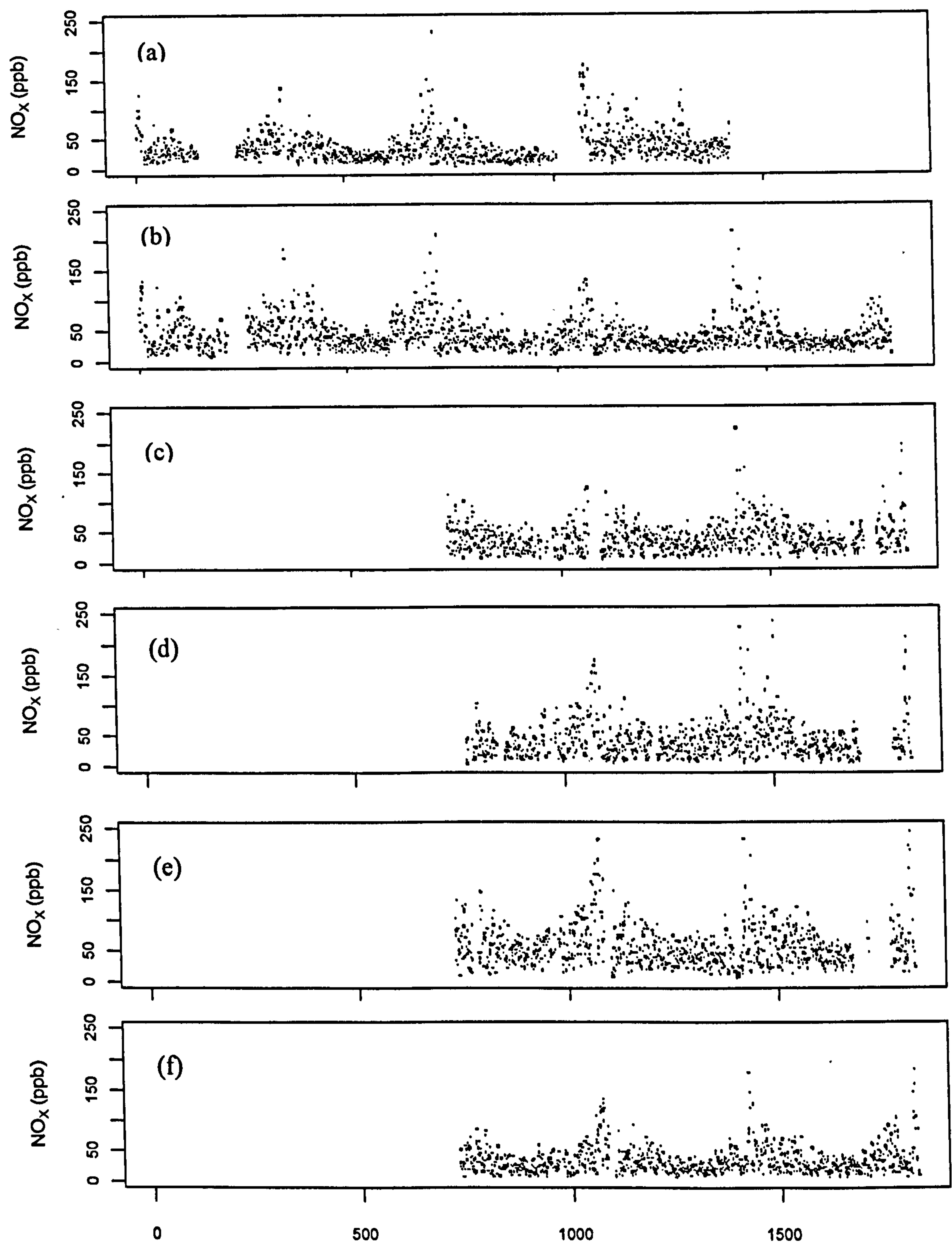


**Figure 50:** Time series of 24-h mean  $\text{NO}_x$  concentrations at the monitoring sites in York (a) Bootham, (b) City Centre, (c) Fishergate, (d) Gillygate, (e) Holgate, (f) Lawrence.



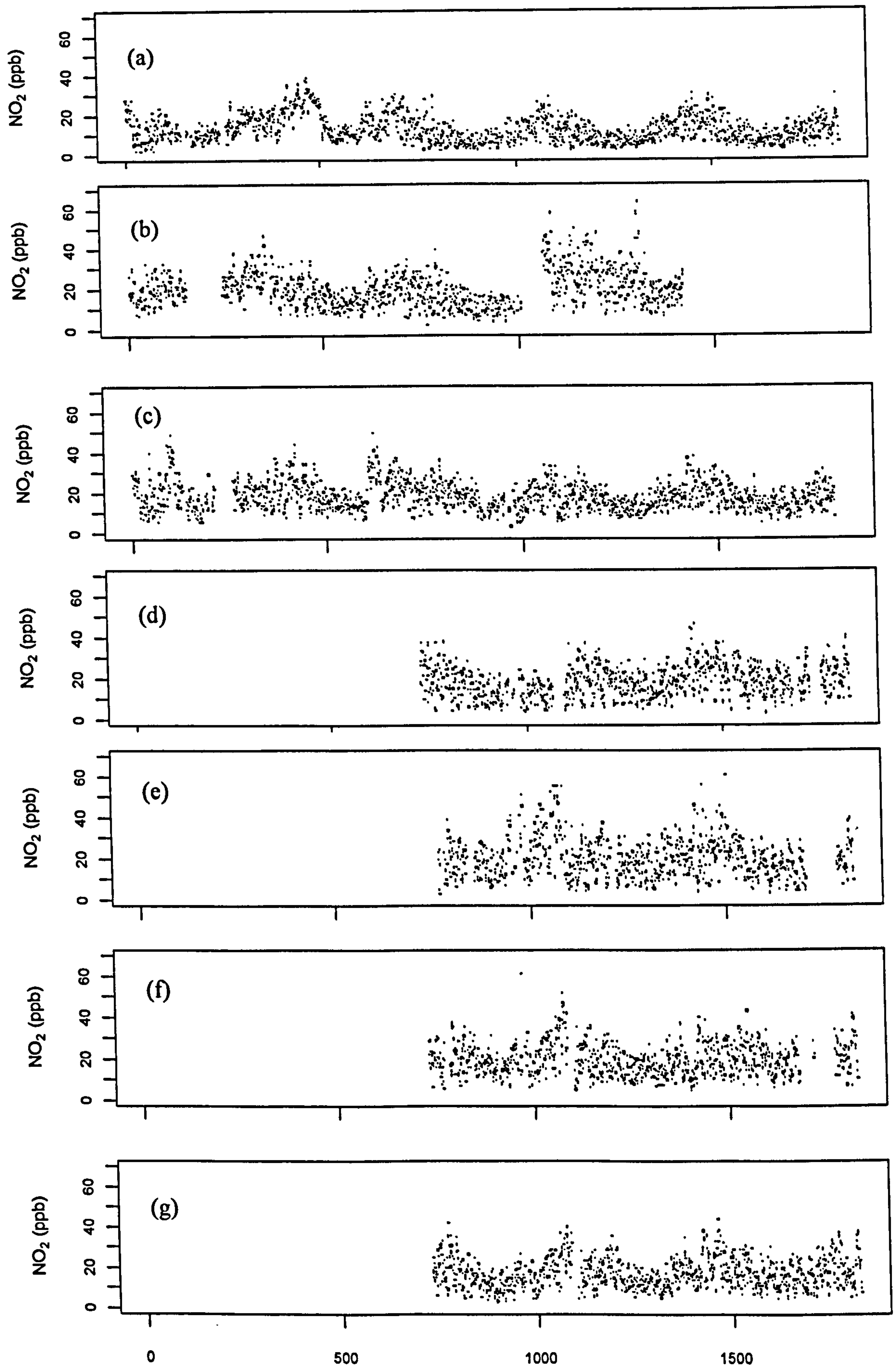


**Figure 51:** Time series of 24-h mean NO<sub>2</sub> concentrations at the monitoring sites in York (a) Bootham, (b) City Centre, (c) Fishergate, (d) Gillygate, (e) Holgate, (f) Lawrence, (g) Nunnery.



## 6.5. Statistical model methodology

### 6.5.1. Linear regression

As highlighted in the previous Chapter (section 5.4.2), linear regression attempts to explain the variability in response data by fixing a straight line relationship between XY data points. There are a number of assumptions that should be upheld when applying linear regression. Firstly, and quite obviously, linear regression assumes that the relationship between the two variables under examination (Y and X) can be represented by a linear function. Secondly, linear regression assumes that the residuals created by the linear model are normally distributed and that their variance is constant. Additionally, the residuals are also assumed to be independent of one another. This effectively means that the  $i^{\text{th}}$  residual is not related to the  $j^{\text{th}}$  residual, nor the  $k^{\text{th}}$  or  $l^{\text{th}}$  etc. and so, therefore, knowing the value of a certain residual does not provide any information regarding any other residual in the same series. This aspect of independence is often difficult when analysing a time series, since, for example, the concentration at a particular point in time is often related to the concentration of the preceding period, and also to the that of the subsequent period. An important aspect of model development is therefore the examination of a model's residuals. Temporal autocorrelation is especially important when predicting future concentrations however since the primary aim of this study is to analyse and understand historic datasets it is of less importance and so has not been considered.

Regression models with multiple explanatory terms are known as general linear models. It basically describes the mean value of Y using more than one explanatory variable. Therefore, instead of the single  $X_1$  variable, there are a number of explanatory variables ( $X_1, \dots, X_n$ ); multiple linear regression is often represented by the following equation:

$$Y_i = \beta_0 + \beta_1 X_{1i} + \beta_2 X_{2i} + \dots + \beta_n X_{ni} + \epsilon_i \quad \text{Equation 5}$$

### 6.5.2. Generalised linear modelling

In many 'real life' situations the assumptions of linear regression do not apply. Generalised linear models (GLMs) offer an alternative form of statistical modelling and are ideal for use with non-normal data. GLMs use a link function to bridge the gap between the structural part of the model (i.e., the part that describes the mean value of Y using the value of  $\beta_0, \dots, \beta_n$ ), and the residual part of the model, also known as the model errors (i.e., the part that describes the variability in the mean Y values that cannot be explained by the explanatory variable(s)). The use of this link function therefore allows for a greater range of models and includes response variables that follow any exponential distribution (i.e., normal, poisson, binomial, gamma etc.). Instead of least squares, the values of  $\beta$  are estimated through a technique called maximum likelihood (ML) estimation.



The link function can be represented by the following:

$$g(E\{Y_i\}) = \beta_0 + \beta_1 X_{i1} + \beta_2 X_{i2} + \dots + \beta_n X_{in} \quad \text{Equation 6}$$

Where,  $g()$  is the link function which transforms the predicted  $Y$  to a different scale, the right hand side of the equation is the structural part of the model.

Linear regression is an important example of a GLM in which the response variable follows normal distribution and has constant variance. The link function for a linear model is known as the identity function.

### 6.5.3. Generalised additive models

Generalised additive models (GAMs) are an extension of GLMs in which the linear predictors ( $\beta_{0...n}$ ) are replaced by non-parametric smooth terms ( $s_{0...n}$ ) (Wood, 2002), see equation 6. These smooth terms are not assumed to take any pre-defined form and instead are dependent on the data present. GAMs are extremely flexible and so can often much better represent the complex relationship between response and explanatory terms in a 'real world' situation than GLMs or linear regression models. The use of these 'smooths' often increases the prediction capability of the statistical model. GAMs are also useful for data analysis when there is no a priori understanding of the relationship.

$$g(E\{Y_i\}) = \beta_0 + s_1 X_{i1} + s_2 X_{i2} + \dots + s_n X_{in} \quad \text{Equation 7}$$

where  $g()$  is the link function,  $s()$  is the smooth function unique to each  $X$  variable.

GAMs are considered a non-parametric statistical tool, however it is possible to fit both parametric (linear) and non-parametric (smooth) terms to a GAM and so in some cases, these model types may be thought of as semi-parametric.

The smooth function used in GAMs can be likened to any scatterplot smoother e.g. running mean, running median, kernel estimate. However, splines, such as cubic splines, are used commonly with the application of GAMs. These types of 'smooths' are basically a collection of polynomials, with a separate polynomial fitted for each neighbourhood.

The smooth function represents a relationship between the individual explanatory variable in question and the response variable. For example, the relationship between  $\text{NO}_x$  concentration and temperature is shown in Figure 52. The smooth curve is constructed using partial residuals (i.e., the residuals after removing the effects of all other predictors); it effectively isolates the variability in the response variable that is solely a consequence of the explanatory variable under examination.



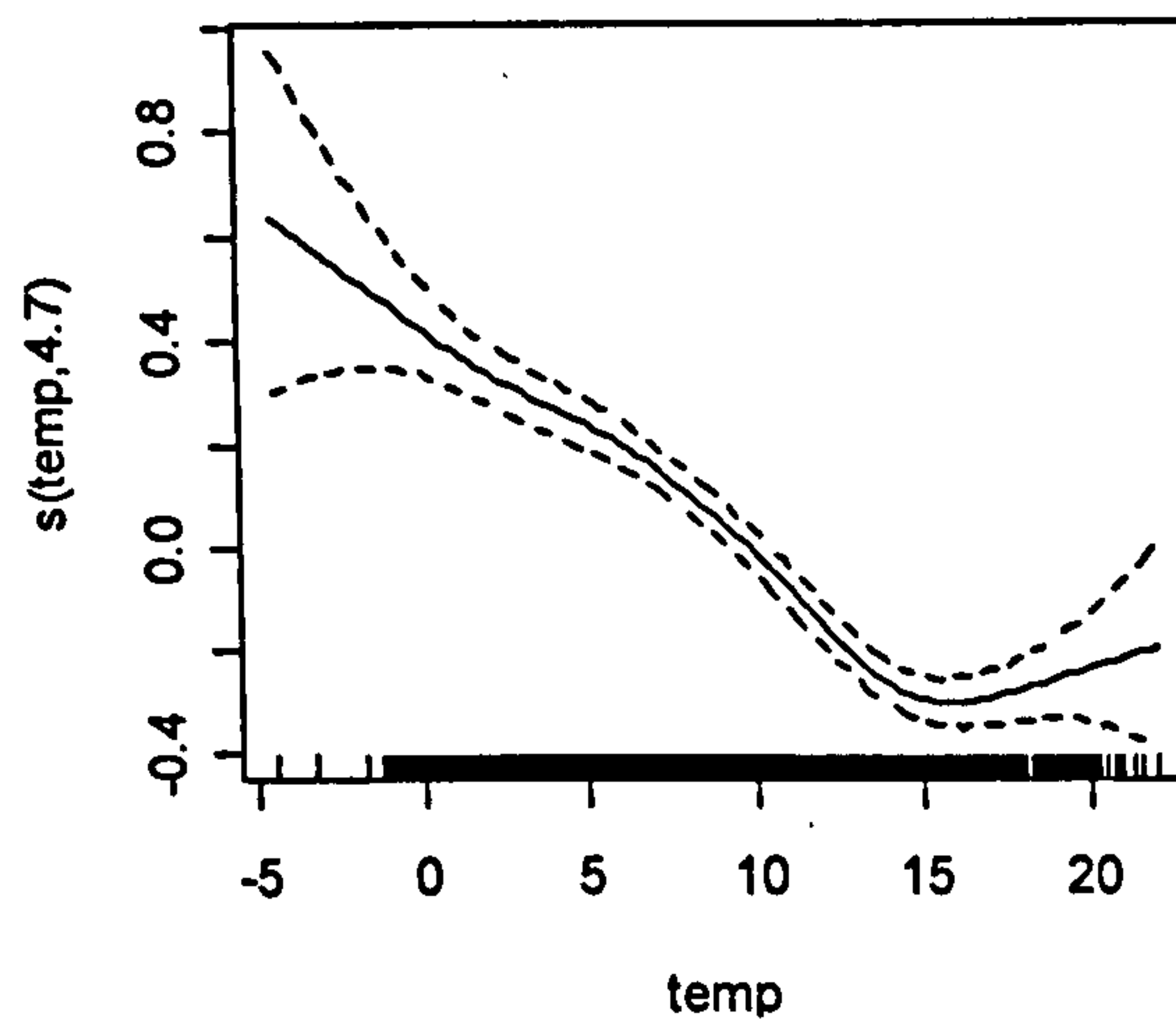


**Figure 52:** Fitted smooth curve for  $\text{NO}_x$  and temperature at the background site of Dunnington. The solid line is the smooth function of temperature and  $\text{NO}_x$  concentration. The dashed line illustrates the 95% confidence intervals for the smooth curve.

The plot also contains a rug plot (vertical black lines at the base of the plot). The rug plot illustrates the presence of data. It can be seen that at the ends of the smooth, where the data capture is low, the confidence intervals are wider.

The smooth function essentially reduces the variability in the data. The underlying pattern that exists between two variables (temperature and  $\text{NO}_x$  concentration in the example above) remains, but the finer scale fluctuation is ignored. GAMs are suitable for trend analysis since the short-term fluctuation inherent in time series data can be ‘filtered out’ and the longer-term data structure revealed.

The problem of using a technique such as generalised additive modelling is that the results can be difficult to interpret. Linear models are easily understood, as they illustrate the rate of change in  $Y$  as a result of a unit increase in  $X$ . GAMs however calculate a smooth term which can be of any structural form and so it is difficult to convey this into an easily understood rate of change. Additionally, inference of GAMs becomes increasingly difficult if more than one variable is used in the smooth estimation e.g.  $s(X_1, X_2, X_3)$ .

#### 6.5.3.1. Model development - smooths and associated degrees of freedom

The level of degrees of freedom used in the smooth term determines the level of detail captured by the curve and so is therefore an important consideration in the GAM modelling framework (Wood, 2006). The level of detail is referred to as wigglyness in Wood (2002). The smooth curve’s wigglyness is positively associated with the degrees of freedom.

To illustrate this concept, Figure 53 shows three smooth relationships between the explanatory variable (days since monitoring began) and the  $\text{NO}_x$  concentrations at Bootham. Figure 53a illustrates the curve when a high degree of freedom is chosen ( $\sim 40$ ). It can be seen from the plot that the smooth curves shows fluctuations in Bootham  $\text{NO}_x$  concentration on a



fine temporal scale. Figure 53b, however, shows the same relationship but the degrees of freedom selected are much lower ( $\sim 10$ ). This plot skims over much of the fine detail (short-term fluctuation) in the trend curve illustrated in Figure 53a. The third plot (Figure 53c) shows the smooth curve where degrees of freedom have been set to  $\sim 4$ . In this plot only the general changes in  $\text{NO}_x$  concentration over time are shown.

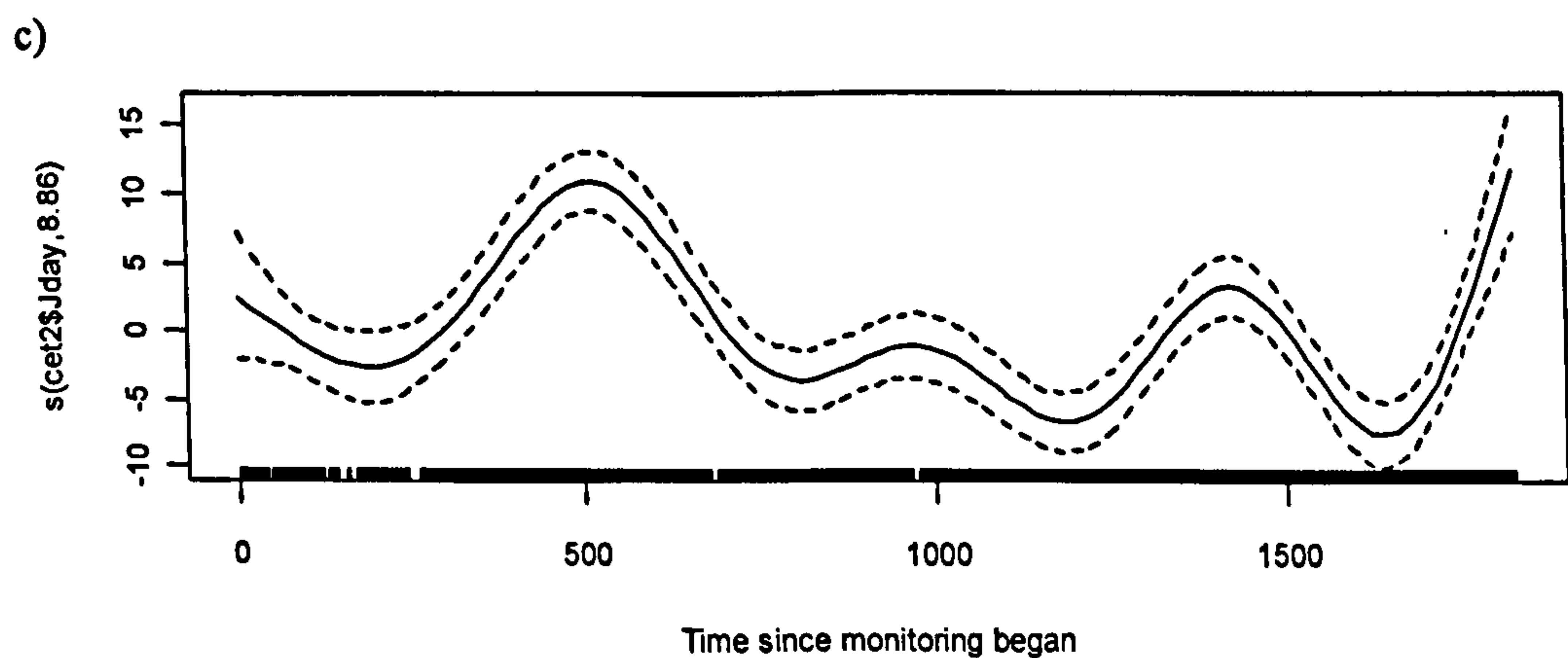
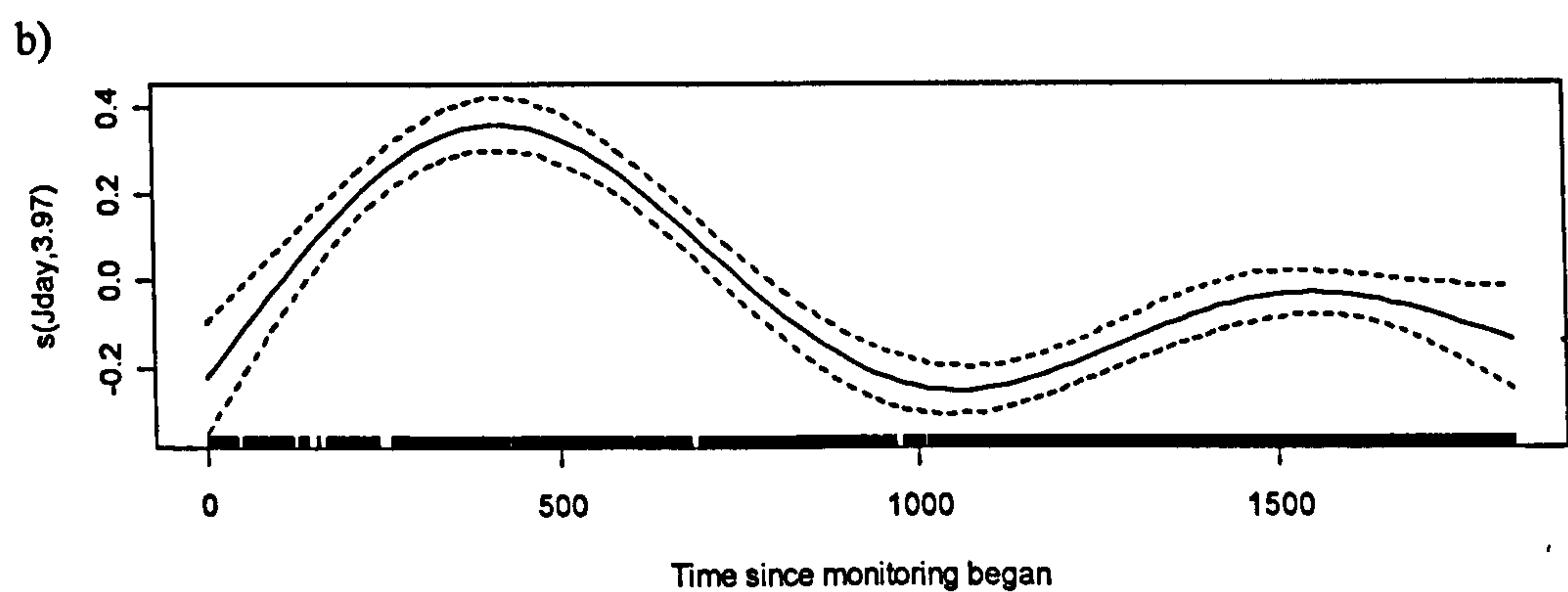
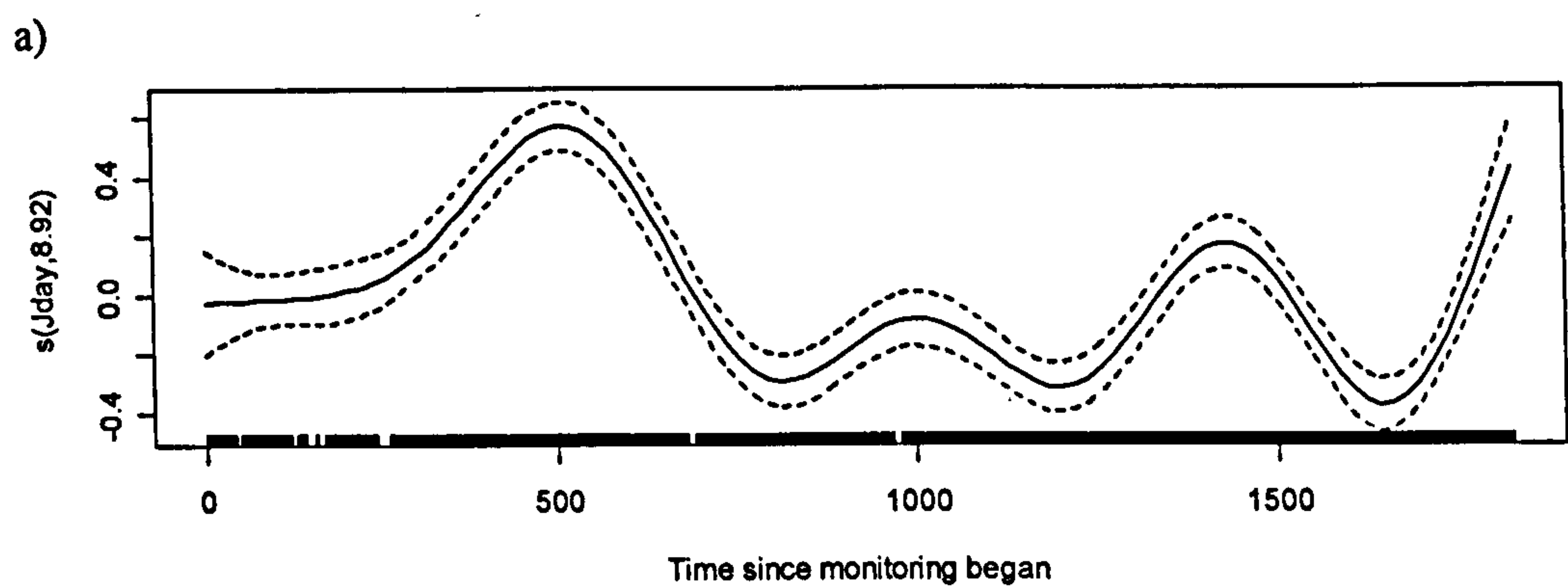
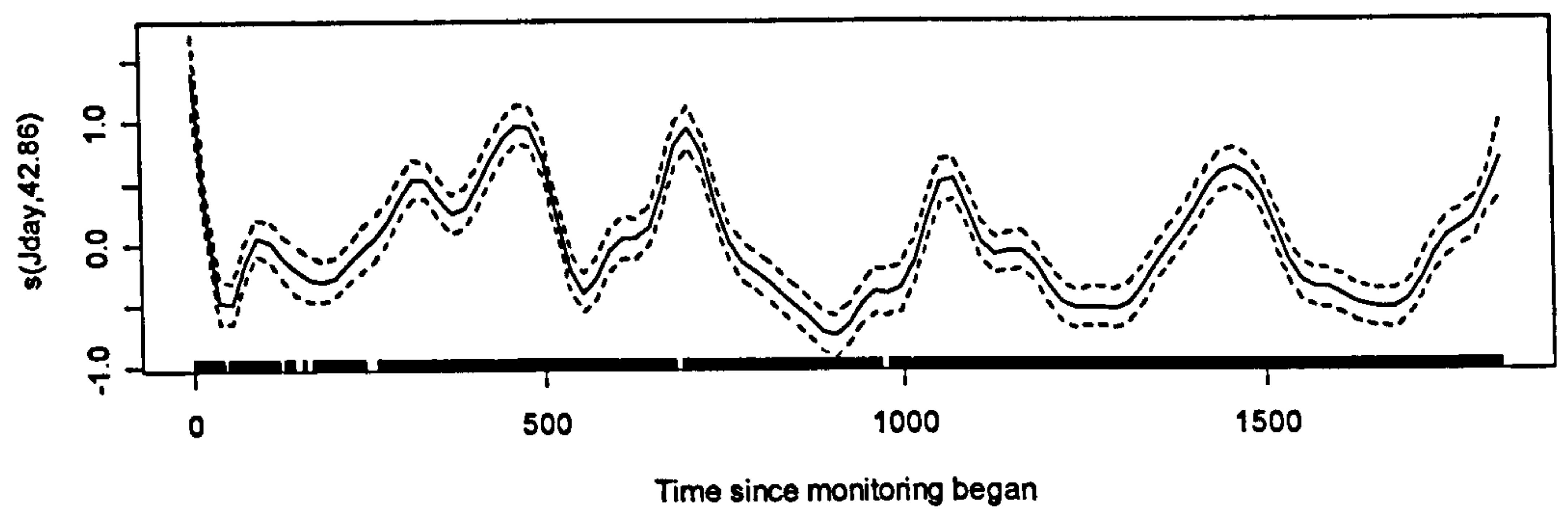
Fewster et al. (2000) state that the number of degrees of freedom used in the creation of smooth curves should depend on the objectives of the study. For example, if the aim of the investigation were to illustrate inter-annual fluctuations then a highly wiggly curve, representing the trend in pollutant concentration on a fine resolution, would be desirable (Figure 53a). However, if the study is more concerned with the general trend then lower degrees of freedom should be selected (Figure 53b). The degrees of freedom are also related to the length of the dataset, since a long study period would demand a higher number of degrees of freedom compared to a shorter dataset to maintain the same level of detail (Fewster et al., 2000).

The penalised regression splines, developed by Wood and Augustin (2002) contained within the 'mgcv' package in the R statistical software, calculate the optimum degrees of freedom while controlling for excessive 'wigglyness'. These splines therefore offer a relatively simple model construction process (the modeller does not need to select a level of degrees of freedom) as well being computationally cheap. Penalised regression splines have already been applied in a number of studies in the scientific literature; examples include Samoli et al. (2006), Carslaw et al. (2007), Carslaw and Carslaw (2007), Larrieu et al. (2007), Qian et al., (2007) and Segala et al. (2008). Figure 53d illustrates the smooth curve for  $\text{NO}_x$  and time using the automatic procedure.

It is important to note that these automatic selection schemes have been criticised since the automated process will select the same level of flexibility in the smooth curve irrespective of the overall study aims. However, since there is no correct answer to the choice in the number of degrees of freedom, it is often felt that the simplicity offered by the automatic selection procedure is desirable and reduces the subjectivity inherent in the methodology.

In an attempt to reduce the number of assumptions associated with the GAM modelling technique, this study will use the penalised regression splines to define the degrees of freedom used in the smooth curves for all the explanatory variables, save the trend term. The degrees of freedom for the trend terms will be manually chosen to reflect the long-term changes in  $\text{NO}_x$  and  $\text{NO}_2$  concentration at the various monitoring sites; it will be held constant so that the trend curves for different sites and pollutants can be compared on a consistent basis.





d)

**Figure 53:** Smooth plots of NO<sub>x</sub> concentration as a function of time (days since monitoring began), for the NO<sub>x</sub> concentrations at Bootham urban background monitoring site. Each smooth has been created under varying values of degrees of freedom (shown in parentheses on Y axis).



### 6.5.3.2. Model development – selection of explanatory terms

Similar to multiple linear regression, correlation between explanatory variables is not desirable. The correlation between the explanatory variables can be checked using Pearsons Product Momentum Correlation (Pearsons). Correlation reflects the degree to which two variables are related and ranges from +1 to -1 (with +1 representing a perfect positive linear relationship and -1 representing a perfect negative correlation). A correlation of 0 represents no correlation.

Where correlation is discovered, only one of the two correlated terms should be included in the final model (the term that led to the greatest increase in explained deviance). For the purpose of this Chapter, a strict correlation criterion of 0.5 was used so as to prevent the possibility of co-linearity occurring in the model selection procedure.

To find the optimal explanatory models for  $\text{NO}_x$  and  $\text{NO}_2$  (i.e., those that explain the greatest amount of variability in their concentrations), this study adopts a forward stepwise approach, whereby the choice of explanatory variables is made according to statistical significance and the generalised cross validation (GCV) score. Only explanatory variables with a significant association with the response variable ( $\text{NO}_x$  or  $\text{NO}_2$  concentration) will be accepted in the final model.

Table 30 provides a step-by-step example of the model selection procedure. It should be noted that similarly to Carslaw et al. (2007) the complex wind speed and wind direction interaction in the canyon has been modelled as an interactive term, (u,v), where u is [wind speed].sin(wind direction) and v is [wind speed].cos(wind direction).

Each potential explanatory variable is added in turn as a single smooth term and the explained deviances for each uni-variate model ranked in descending order (stage 1). Table 30 shows that the term for Bkg  $\text{NO}_x$  explained the largest amount of variability in the Fishergate  $\text{NO}_x$  concentration (55.4%).

Each of the remaining explanatory variables is then tried alongside the initial term selected in stage 1 (Bkg  $\text{NO}_x$ ) until the combination of two explanatory variables that explains the highest percentage deviance is discovered (Bkg  $\text{NO}_x$  and u,v in Table 30). Following this procedure explanatory terms are added to the model until the addition of another term led to an increase in the GCV score.



**Table 30:** Stepwise selection procedure for the development of the Fishergate NO<sub>x</sub> GAM. The percentage deviance explained and GCV score for each combination of potential explanatory variables considered in the model construction process is shown. Jday is the number of days since monitoring began, Bkg is the background NO<sub>x</sub> concentration, u,v is the interactive wind speed – wind direction term, Temp is the temperature, precip is precipitation and cloud is the cloud cover.

Stage	1 <sup>st</sup> term	2 <sup>nd</sup> term	3 <sup>rd</sup> term	4 <sup>th</sup> term	5 <sup>th</sup> term	6 <sup>th</sup> term	% Deviance explained	GCV	Rank within each stage
1	Bkg NOX						55.4	0.1216	1
	Jday						5.83	0.2454	5
	U,V						34.5	0.1730	2
	Temp						18.4	0.2099	4
	Humidity						21.9	0.1982	3
	Precip						1.21	0.2559	7
	Cloud						1.65	0.2504	6
2	Bkg NOX	U,V					64.6	0.0983	1
	Bkg NOX	Jday					59.9	0.1110	2
	Bkg NOX	Temp					56	0.1195	4
	Bkg NOX	Humidity					58.6	0.1106	3
	Bkg NOX	Precip					55.9	0.1214	5
	Bkg NOX	Cloud					56	0.1195	4
3	U,V	Jday					39.6	0.1614	3
	U,V	Temp					53.6	0.1225	1
	U,V	Humidity					47.2	0.1377	2
	U,V	Precip					34.6	0.1736	5
	U,V	Cloud					34.8	0.1710	4
4	Bkg NOX	U,V	Jday				69.2	0.0871	1
	Bkg NOX	U,V	Temp				67.8	0.0902	2
	Bkg NOX	U,V	Humidity				67.7	0.0886	3
	Bkg NOX	U,V	Precip				64.8	0.0985	5
	Bkg NOX	U,V	Cloud				65.5	0.0964	4
5	Bkg NOX	U,V	Jday	Temp			72.4	0.0786	1
	Bkg NOX	U,V	Jday	Humidity			70.9	0.0811	2
	Bkg NOX	U,V	Jday	Precip			69.4	0.0871	4
	Bkg NOX	U,V	Jday	Cloud			70.3	0.0844	3

Additionally, stage 3 of the selection procedure outlined in Table 30 illustrates how the model selection procedure can be checked. In this stage, the most important explanatory term selected in stage 1 (in this instance, Bkg NO<sub>x</sub>) is replaced by the variable which was ranked second (i.e., u,v) and the remaining explanatory terms are tried along side this term. In theory, the removal of the highest ranked term from the model should result in an increase in the GCV score and a decrease in deviance explained. Indeed, it can be seen from stage 3 (Table 30) that removal of the background NO<sub>x</sub> term resulted in a substantial reduction in the deviance explained and also higher GCV scores than that seen for the models tested in stage 2. It is desirable to check the model selection procedure in this manner after the completion of each stage.

Despite these rules, the procedure is still somewhat subjective. For instance, the addition of some explanatory terms might actually reduce the GCV score but not lead to a substantial increase in the explained deviance; indeed in some instances the explained deviance may remain unchanged. It is therefore the decision of the modeller to determine whether the new variable



should be included or not. Where such decisions arise, the simpler of the two models (i.e., the one that contains the fewest parameters) would always be preferred as this makes interpretation easier.

## **6.6. Results**

### **6.6.1. Model estimation**

NO<sub>x</sub> and NO<sub>2</sub> GAMs have been developed to describe the maximum variability in the 24-hr mean NO<sub>x</sub> and NO<sub>2</sub> concentrations for the various sites under study. A total of 14 models have been created, two (NO<sub>x</sub> and NO<sub>2</sub>) for each of the seven monitoring sites. In each case the Y variable (NO<sub>x</sub> or NO<sub>2</sub> concentration) has been transformed logarithmically so as to conform to the assumptions of normal distribution. Similarly to the existing air quality studies by Reiss (2006), Zheng et al. (2007) and Carslaw et al. (2007) well known confounding factors (meteorology and season) have been considered in the model development process.

Using the forward selection stepwise procedure outlined previously, the most important drivers of NO<sub>x</sub> and NO<sub>2</sub> concentration were selected and included in the model as smooth functions. The list of potential explanatory variables included: Jday (day since monitoring began), year, day of year, month, temperature, humidity, cloud cover, precipitation, the interactive wind tem 'u, v', background NO<sub>x</sub>, background NO<sub>2</sub>, background O<sub>3</sub>, background SO<sub>2</sub>. In many instances the co-linearity between the various explanatory terms meant that some variables could not be included in the presence of others (see Table 31). Background NO<sub>2</sub> and background O<sub>3</sub> for example were found to be correlated (0.68) and in all seven cases, background NO<sub>2</sub> explained a greater proportion of the variability in NO<sub>2</sub> concentrations than background O<sub>3</sub>; consequently the latter term was dropped from the model selection procedure. Similarly, the close correlation between background NO<sub>x</sub> and background NO<sub>2</sub> (0.9) prevented the use of both these terms in the various NO<sub>2</sub> GAMs; instead the background NO<sub>2</sub> concentrations were generally more important than those of background NO<sub>x</sub>. Other examples of correlation were treated in a similar manner.

Where applicable (where a significant relationship existed), an explanatory variable for time has been included in the fitted models. A time variable will allow the trend in NO<sub>x</sub> and NO<sub>2</sub> concentration to be examined. In all cases the explanatory variable 'year' was favoured over 'Jday' to represent the trend in NO<sub>x</sub> and NO<sub>2</sub> concentration since it was felt that year better represented the long-term trend. Using year, as opposed to Jday, also allows the use of the explanatory term month (which should represent a degree of seasonality present in the pollutant concentrations); month could not be included if Jday was used since Jday and month are positively correlated (Table 31).



Table 31: Pearson’s correlation for the various covariates considered for inclusion in the GAMs. Correlated terms are highlighted in red

	Jday	Year	Day of Year	Day of Month	Day of week	Month	Temp	U	V	Precip	Cloud cover	Humidity	Bkg NO <sub>x</sub>	Bkg NO <sub>2</sub>	Bkg O <sub>3</sub>
Jday	1.0														
Year	0.9	1.0													
Day of Year	0.7	0.3	1.0												
Day of Month	0.0	0.0	0.0	1.0											
Day of week	0.0	0.0	0.0	0.0	1.0										
Month	0.7	0.3	1.0	-0.1	0.0	1.0									
Temperature	0.4	0.2	0.5	0.0	0.0	0.5	1.0								
U	0.1	0.1	0.1	0.1	0.0	0.1	0.1	1.0							
V	-0.1	-0.1	-0.1	0.0	0.1	-0.1	-0.2	-0.1	1.0						
Precipitation	0.1	0.0	0.1	0.0	0.1	0.1	0.0	0.1	0.0	1.0					
Cloud cover	0.0	0.0	-0.1	0.0	0.0	-0.1	0.0	0.2	0.0	0.3	1.0				
Humidity	0.1	0.1	0.1	0.0	0.1	0.1	-0.2	0.4	-0.1	0.4	0.5	1.0			
Bkg NO <sub>x</sub>	0.0	-0.1	0.1	-0.1	-0.1	0.1	-0.4	0.1	-0.1	-0.1	-0.2	0.2	1.0		
Bkg NO <sub>2</sub>	-0.1	0.0	0.0	-0.1	-0.2	0.0	-0.3	0.1	-0.2	-0.1	-0.1	0.2	0.9	1.0	
Bkg O <sub>3</sub>	-0.1	0.0	-0.2	0.1	0.1	-0.2	0.2	-0.1	0.2	0.1	-0.1	-0.5	-0.7	-0.7	1.0



The fitted models for the various monitoring locations are shown in Table 32 and Table 33 for NO<sub>x</sub> and NO<sub>2</sub> respectively. In each of the final fitted models all terms were found to be statistically significant at the  $p < 0.01$  level or better.

**Table 32:** Terms included in the NO<sub>x</sub> GAMs for the seven monitoring sites. The order of variables represents the various stages of the model selection procedure. Where, ‘year’ is the year monitoring data were recorded, ‘u,v’ represents the interactive wind speed-wind direction component, ‘Bkg NO<sub>x</sub>/NO<sub>2</sub>’ is the background NO<sub>x</sub>/NO<sub>2</sub> concentrations recorded at Dunnington, ‘temp’ is temperature and ‘month’ is the month of the year.

Site	1 <sup>st</sup> term	2 <sup>nd</sup> term	3 <sup>rd</sup> term	4 <sup>th</sup> term
Bootham	s(Bkg NO <sub>x</sub> )	s(u,v)	s(year)	s(month)
City Centre	s(Bkg NO <sub>x</sub> )	s(u,v)	s(year)	s(month)
Fishergate	s(Bkg NO <sub>x</sub> )	s(u,v)	s(year)	s(month)
Gillygate	s(u,v)	s(Bkg NO <sub>x</sub> )	s(year)	s(temp)
Holgate	s(u,v)	s(Bkg NO <sub>x</sub> )	s(year)	s(month)
Lawrence St	s(Bkg NO <sub>x</sub> )	s(u,v)	s(year)	s(temp)
Nunnery Lane	s(Bkg NO <sub>x</sub> )	s(u,v)	s(month)	s(year)

**Table 33:** Terms included in the NO<sub>2</sub> GAMs for the seven monitoring sites. The order of variables represents the various stages of the model selection procedure. Where, ‘year’ is the year monitoring data were recorded, ‘u,v’ represents the interactive wind speed-wind direction component, ‘Bkg NO<sub>x</sub>/NO<sub>2</sub>’ is the background NO<sub>x</sub>/NO<sub>2</sub> concentrations recorded at Dunnington, ‘temp’ is temperature and ‘month’ is the month of the year.

Site	1 <sup>st</sup> term	2 <sup>nd</sup> term	3 <sup>rd</sup> term	4 <sup>th</sup> term
Bootham	s(Bkg NO <sub>2</sub> )	s(u,v)	s(year)	s(month)
City Centre	s(Bkg NO <sub>2</sub> )	s(u,v)	s(year)	s(month)
Fishergate	s(Bkg NO <sub>2</sub> )	s(u,v)	s(year)	s(month)
Gillygate	s(u-v)	s(Bkg NO <sub>2</sub> )	s(temp)	
Holgate	s(u-v)	s(Bkg NO <sub>2</sub> )	s(year)	s(month)
Lawrence St	s(Bkg NO <sub>2</sub> )	s(u-v)	s(year)	s(temp)
Nunnery Lane	s(Bkg NO <sub>2</sub> )	s(u-v)	s(month)	s(year)

It can be seen that there is much similarity in the choice of explanatory variables included in the various fitted models, with all models containing the variables for wind and background pollutant. Interestingly, in the majority of cases the explanatory variable month was found to



explain a higher percentage deviance in the response variable than temperature. The exception to this observation was for the NO<sub>x</sub> and NO<sub>2</sub> concentrations at Gillygate and Lawrence Street, where 'temperature' was more important than 'month'.

Table 34 illustrates the individual contributions of the various explanatory variables included in the fitted models. The individual contribution has been calculated by taking the difference in explained percentage deviance between the fully fitted model and a model with the term of interest removed. The total percentage deviance explained is also shown in Table 34. Note, that the individual contributions do not add up to make the total since the contribution of the various explanatory terms shown in Table 34 are calculated from the models which already contain other variables; the individual contribution is therefore just to provide the relative importance of each term in respect to the other variables included in the final fitted models.

Despite the general similarity in choice of explanatory variables, the relative importance of each individual term varies from site to site (see Table 34). The background pollution term was the most important variable in explaining the variation in NO<sub>x</sub> and NO<sub>2</sub> concentration at Bootham; explaining around 19 % and 25 % for the respective NO<sub>2</sub> and NO<sub>x</sub> concentrations. The importance of these terms at this site is unsurprising, since Bootham is an urban background site and is not subject to any specific local emission source. The background pollutant term explained a large percentage of the response term variability at the majority of sites.

The wind term (speed-direction) was an important explanatory/confounding factor in all the GAMs. Indeed, for a number of roadside sites this term actually explained the greatest relative percentage deviance in the response variable. Other air quality studies have also found the wind speed – wind direction interactive term important in explaining the concentration of airborne pollutants (e.g. Aldrin and Haff, 2005; Carslaw and Carslaw, 2007; Carslaw et al., 2007). It should be noted that the contributions of wind speed and wind direction before transformation offered less in terms of percentage explained deviance than the combination of u and v terms.



**Table 34:** The contributions to percentage deviance explained for the various explanatory variables calculated by removing the term of interest from the fully fitted model and comparing the difference in explained deviance. B = Bootham C = City Centre, F = Fishergate, G = Gillygate, N = Nunnery Lane, H = Holgate Road and L = Lawrence Street.

Explanatory variable	B	C	F	G	H	L	N
<b>NO<sub>2</sub></b>							
Bkgd NO <sub>2</sub>	19.1	8.5	9.7	10.4	5	11.9	8.5
U,V	6.2	8.9	13	30.9	36.1	18.7	18.9
Temperature				4.2		3.3	
Month	5.7	4.1	8.7		3.4		8
Year	7.4	15.8	3.7	1.7	2.5	3.6	1
TOTAL	83.6	60.1	71.1	75.2	75.9	63.4	66.7
<b>NO<sub>x</sub></b>							
Bkgd NO <sub>x</sub>	25	13.7	12.3	10.2	7.2	8.6	8.4
U,V	2.8	13.7	9.2	39.7	35	23.7	21.3
Temperature				4		2.4	
Month	2.6	2.2	3.3		2.4		4.5
Year	5.5	10.3	3		1	6.9	1.4
TOTAL	88.1	71.7	71.4	77.5	76.4	59	67.6

Interestingly, the relative importance of the wind speed-direction interaction term was much greater at the sites of Gillygate and Holgate Road compared to the remaining roadside locations. For example, the individual contribution of this term in explaining the total variation in NO<sub>2</sub> concentrations is around 13 %, 19 % and 19 % at the sites of Fishergate, Lawrence Street and Nunnery Lane respectively, whereas at Gillygate and Holgate Road this percentage increases to around 31 % and 36 % respectively. The monitoring stations at the latter two sites are located inside street canyons and so the importance of the 'u,v' term could be a reflection of the complex wind patterns and recirculation processes which occur within the street. The relatively low percentage explained deviance attributed to the interactive wind term for the remaining roadside locations (Fishergate, Nunnery Lane and Lawrence Street) could therefore be a reflection of the reduced influence that wind flow has at these non-street-canyon locations.

The response curves for each of the explanatory variables included in the various models have been created and analysed, and those for the Fishergate NO<sub>2</sub> model are illustrated in Figure 54. The Fishergate NO<sub>2</sub> model was chosen to illustrate the smooth plots since this site



contains all explanatory variables shown in Table 34, and also is generally representative of the types of relationships seen in the other models for the various sites.

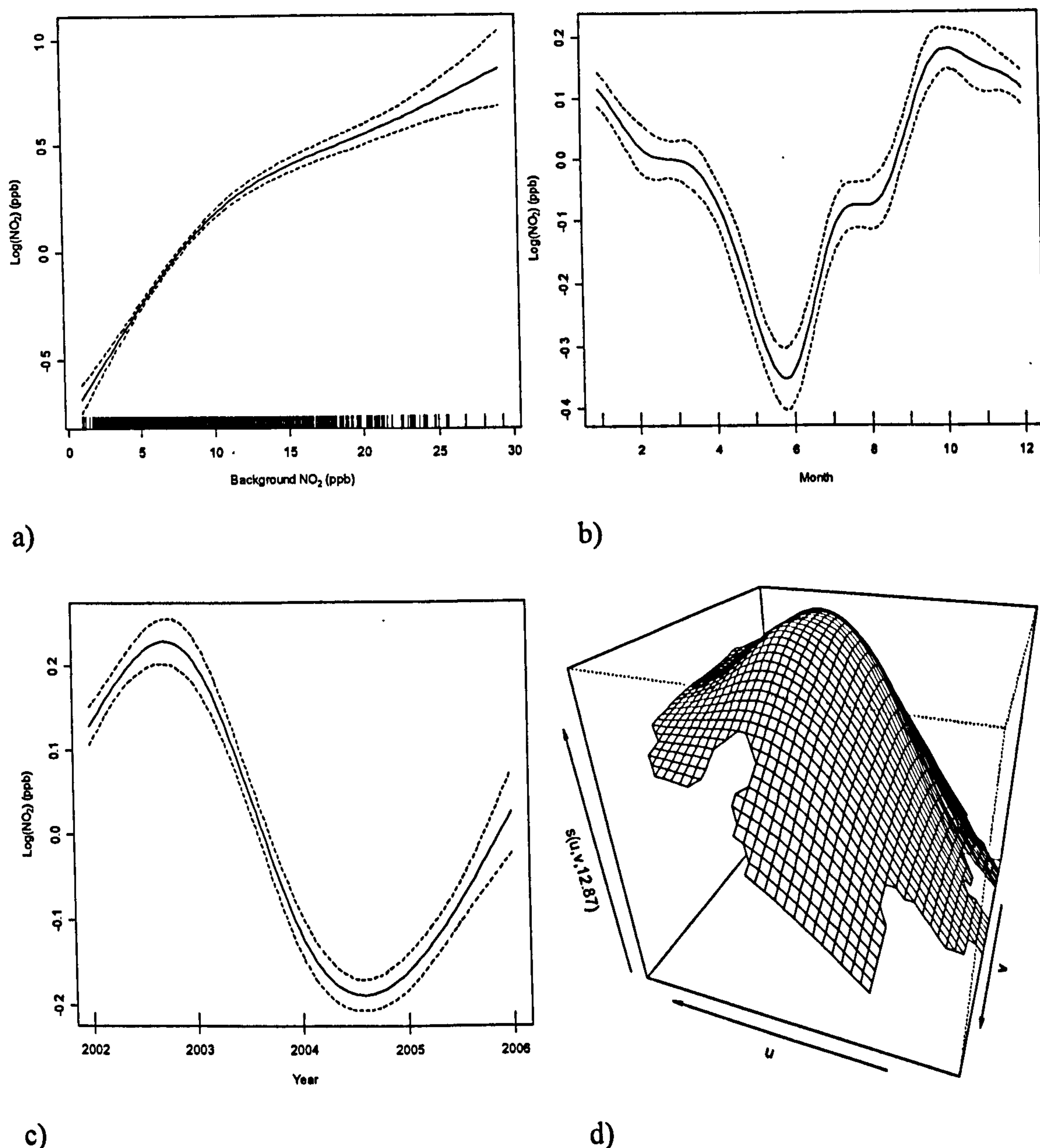


**Figure 54:** Fitted components of the Fishergate NO<sub>2</sub> model: (a) smooth function of background pollutant concentration,  $s(\text{BkgNO}_2)$  (b) smooth function of month,  $s(\text{month})$ , (c) smooth function of trend,  $s(\text{year})$ , (d) bivariate smooth function of wind components,  $s(u,v)$ .

In each case the smooth plots can be described in ‘real’ terms. Figure 54a illustrates the Fishergate NO<sub>2</sub> response curve to background NO<sub>2</sub> concentration. It can be seen that the NO<sub>2</sub> concentration increases almost proportionately to background pollutant concentration. This pattern is expected since localised emissions will enhance the existing ambient concentrations (background) present across the city.

The month term, although not strictly a ‘measurable’ covariate (in the sense that this variable does not change in response to external factors) is still important in explaining the regular ‘noise’ inherent in the pollution data (Figure 54b). The plot shows that the lowest NO<sub>2</sub>



concentrations occur during the summer months of the year, and the highest during the winter. This annual variation reflects the changes in emissions and so is not unexpected.

As can be seen from Table 34, the models developed with  $\text{NO}_x$  and  $\text{NO}_2$  concentrations recorded at the sites of Gillygate and Lawrence Street favour temperature over month as an explanatory variable. As was clearly seen in Figure 49, temperature varies regularly over an annual period. Therefore temperature simply illustrates a degree of seasonality present in the  $\text{NO}_x$  and  $\text{NO}_2$  concentrations at this site, with the low temperatures in winter being associated with elevated  $\text{NO}_x$  and  $\text{NO}_2$  concentrations, and the opposite occurring in summer. As explained earlier the correlation between temperature and month prevents both terms being included in the final models.

The trend term (Figure 54c) illustrates the general change in  $\text{NO}_x$  concentration at Fishergate over the study years. It can be seen that an overall decline in  $\text{NO}_x$  concentrations has occurred at this site; however, there appears to be an upturn in  $\text{NO}_x$  concentrations during the latter period (2005 to 2006). The trend term will be discussed in greater detail in the following sections of this Chapter.

The  $\text{NO}_2$  response curve for the interactive wind speed-direction term is shown in Figure 54d. The centre of the plot (0,0) represents the monitoring site. The combination of street geometries and wind interaction with the pollutant concentration determines the shape of the plot. Figure 54d shows that the highest concentrations are seen at the centre of the plot (peak in the 3D surface). It is, however, quite difficult to interpret the 3D surface and so an alternative plot (polar plot) which uses these same data, has been produced and is shown in Figure 55. Again, the centre of the plot is where the monitoring equipment is sited. The colouring of Figure 55 illustrates the magnitude of  $\text{NO}_2$  concentration.

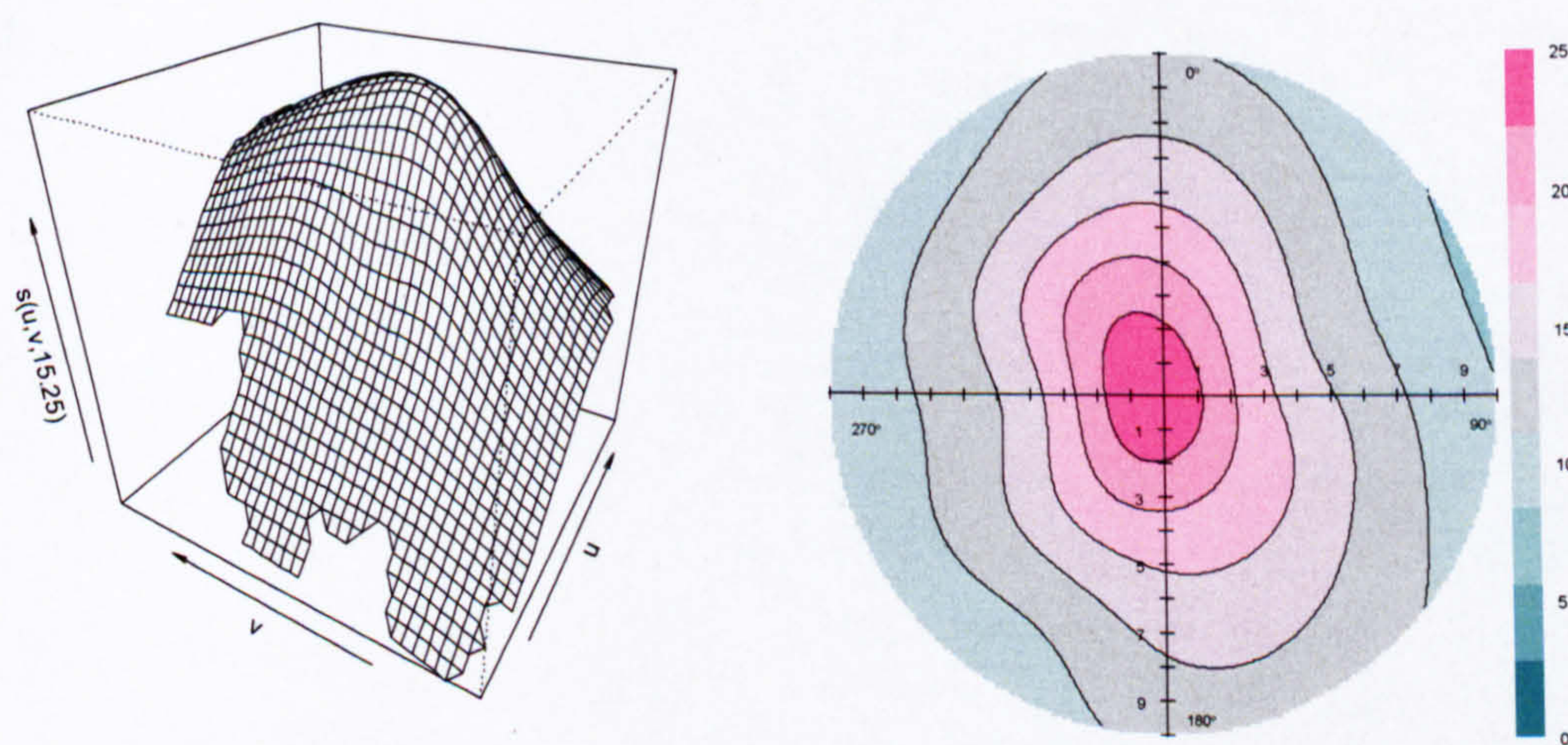


**Figure 55:** Perspective plot (a) and polar plot (b) of the interactive wind speed – wind direction smooth curve for the Fishergate  $\text{NO}_2$  concentrations.



Figure 55 shows that the highest concentrations (purple/pink) are located directly adjacent to the monitor (around the centre of the plot). Since these high concentrations occur at low wind speeds, the monitoring site is influenced strongly by ground level emission sources (see Chapter 2, section 2.3.2.3). There is also a slight 'bulge' in the pollutant concentrations from the north (0 degrees) and south (180 degrees). By referring back to the map of Fishergate (reproduced as Figure 56 for ease of comparison), it can be seen that these 'bulges' coincide with two busy roads. For those periods when the wind is flowing parallel to Fishergate (i.e., from the north or south) the associated  $\text{NO}_2$  concentrations are higher than for alternative wind directions. The interactive wind smooth curve for Fishergate  $\text{NO}_2$  concentrations therefore strongly suggests that the majority of  $\text{NO}_2$  in the area is the result of emissions from adjacent roads.

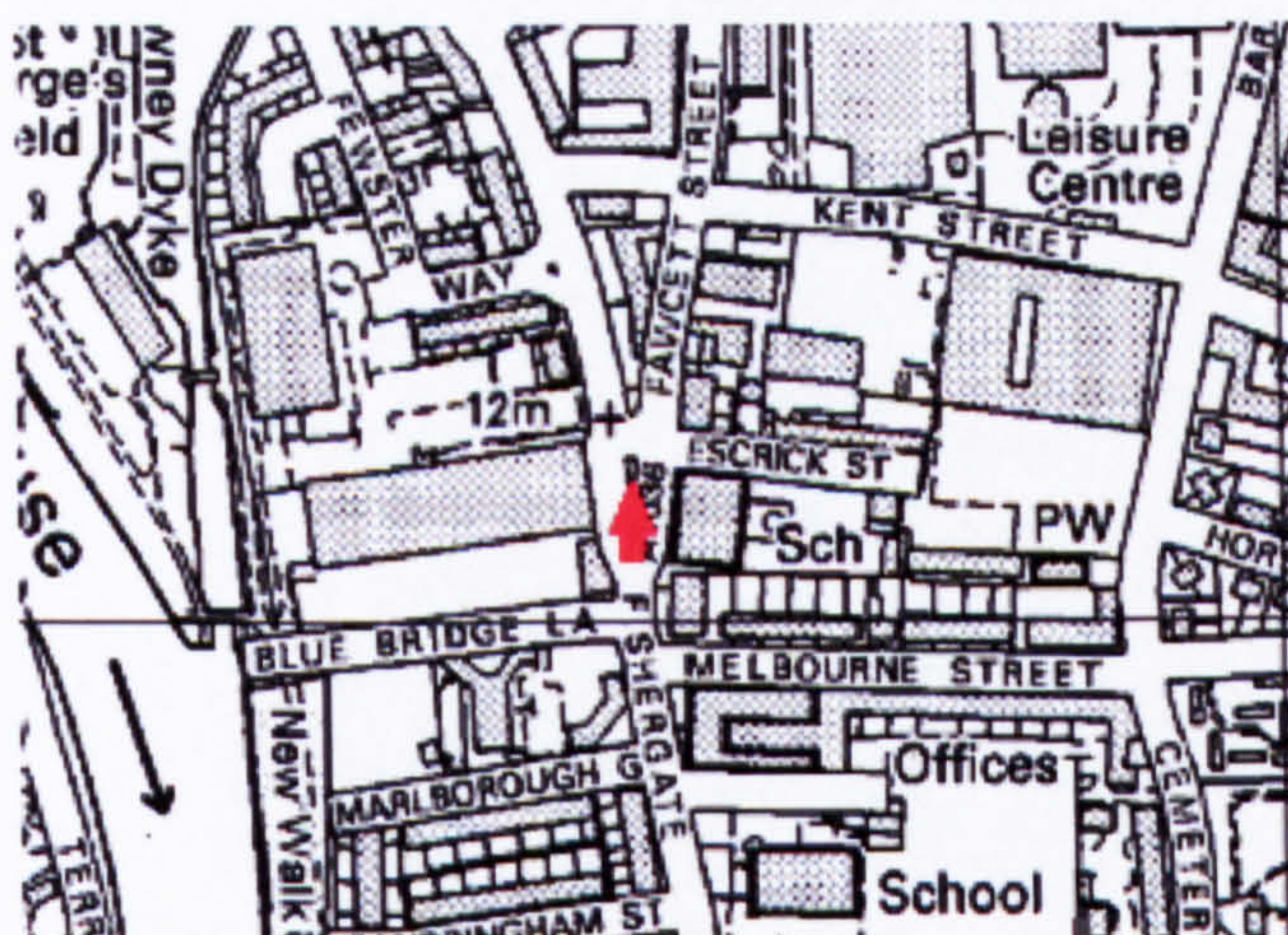


**Figure 56:** Map of Fishergate monitoring site. Black circle illustrates the location of the monitoring equipment.

The smooth plots for wind flow display the greatest variation (difference) between sites. This difference is expected since each site is subject to unique wind flows determined by the local environment and so each wind-term smooth plot therefore illustrates the unique wind interaction with pollutant concentration present at each site. These plots can offer an insight into the localised emission sources.

Figure 57 illustrates the smooth curves for the 'u,v' term for the seven monitoring sites. Since there is little difference in the structure of plots for  $\text{NO}_x$  and  $\text{NO}_2$  at each site, only the  $\text{NO}_2$  curves are shown. As mentioned before the centre of the plot (0,0) represents the monitoring site.

In each case the influence of road traffic emissions from localised roads are shown by higher pollutant concentrations. For example, Figure 57d (Gillygate) shows a higher band of  $\text{NO}_2$  concentrations to the east (30 to 180 degrees) of the monitor for all wind speeds. This patch of higher  $\text{NO}_2$  concentration corresponds to the direction of Gillygate itself (see Figure 13).



Additionally, the site of Holgate Road (Figure 57e) also shows high NO<sub>2</sub> concentrations to the NE (~80 degrees), which again, corresponds to the location of the street of Holgate, specifically its junction with The Mount (see Figure 14).

The site of Bootham is interesting because it is an urban background site and it not strongly affected by local pollution sources. There is a large hospital building to the NE of the monitor; which corresponds to low NO<sub>2</sub> concentrations. However, a small car park to the SE of the monitor could explain the high concentrations when the wind blows from this direction. Since the car park is situated close to the monitor it is likely that this source will correspond to the high concentrations at low wind speeds. Additionally, it is likely that the high concentrations at this site from this direction at higher wind speeds could be a consequence of the street of Bootham, which is, situated in this direction some +100 metres.



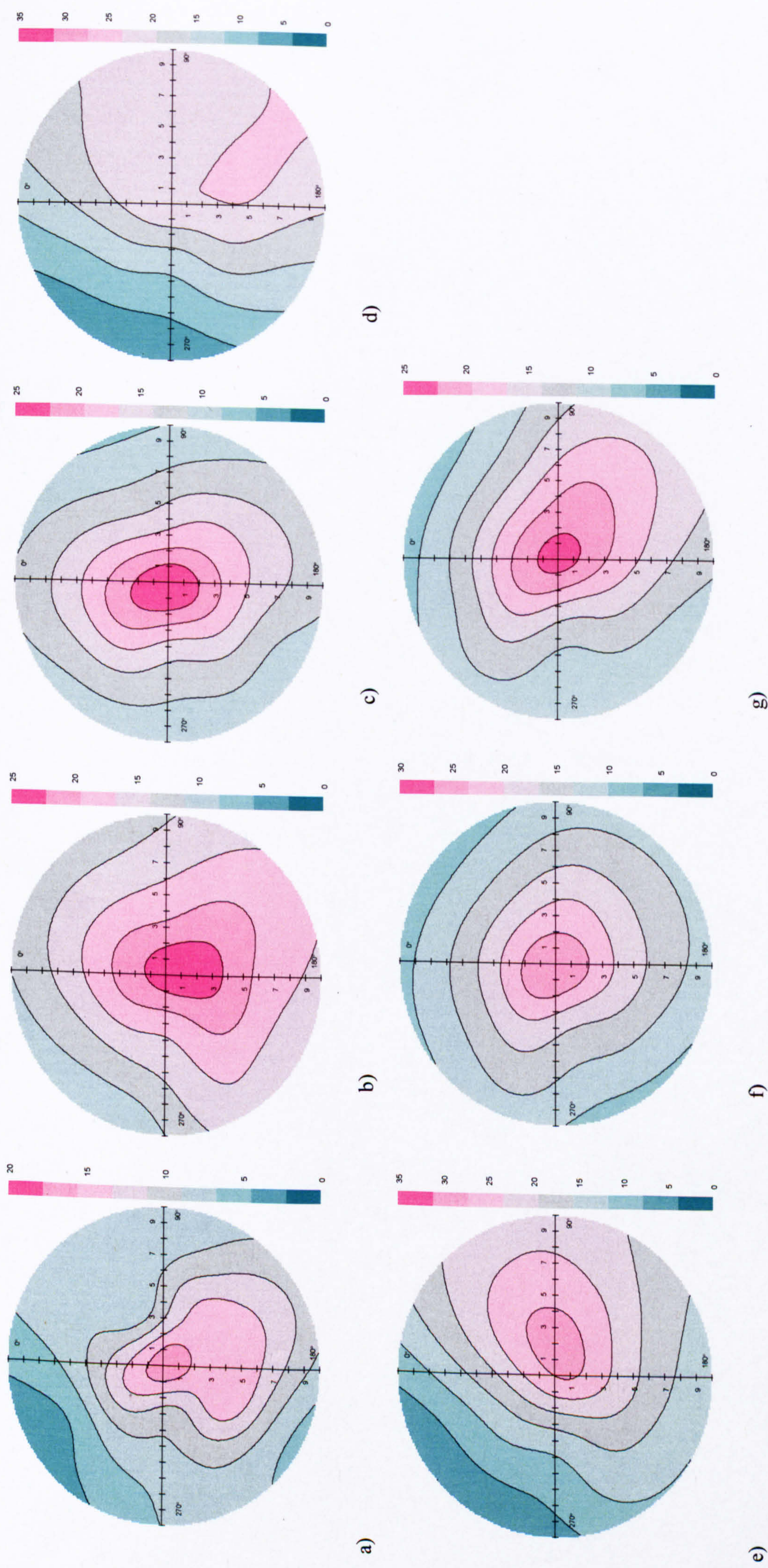


**Figure 57:** 'u,v' response curves for observed  $\text{NO}_2$  concentrations for each of the monitoring sites in York. The plot illustrates a smooth surface with both wind speed and wind direction are taken into account. a) Bootham, b) City Centre, c) Fishergate, d) Gillygate, e) Holgate Road, f) Lawrence Street and g) Nunnery Lane..



### 6.6.2. Trend estimation

To fully understand the behaviour in  $\text{NO}_x$  and  $\text{NO}_2$  concentration it is desirable to inspect and analyse the changes in concentration data over time (i.e., the trend in pollutant concentration data). It may then be possible to identify reasons for the temporal changes in pollutant data.

As can be seen from the previous section all models for the three long term sites contain a variable for time (s(year)). Figure 54c has already illustrated the trend curve for the  $\text{NO}_2$  concentrations at Fishergate; this plot was created using the `plot.gam` function inherent in the 'mgcv' package. However, it is possible to illustrate the smooth curves for various explanatory variables independent of the mgcv package. This independence allows for greater flexibility in the presentation of results, and, as will be explained later, allows for the independent estimation of confidence intervals.

Figure 58 and Figure 59 therefore illustrate the changes in  $\text{NO}_x$  and  $\text{NO}_2$  concentrations in response to the time variable. These plots are created by holding constant, at their median value, the input data of the various explanatory terms, with the exception of the explanatory term in question (i.e., trend term). The GAM (already established on the full dataset) is then used to predict the pollutant concentration in question using this 'patched' dataset. By subsequently plotting the predicted response values against the corresponding explanatory variable, the relationship between the target variable and explanatory term is established.

A number of studies have mentioned the inadequacies of the confidence intervals created within the GAM framework. For this reason, separate confidence intervals have been created for the trend curve. 95 % confidence intervals (precision of the estimated smooth curve) have been calculated using a jack-knife technique.  $N$  random samples of 70 % of the input data are made and a GAM is fitted to each sub-sample (where  $n = 499$ ). These data are sorted in ascending order and the 95 % confidence intervals extracted. The mean smooth curve, and its 95 % confidence intervals, provides a more robust estimate of the response of  $\text{NO}_x$  and  $\text{NO}_2$  concentration to variation of the term in question over the study period. Similarity to the Fewster et al. (2000) study a jackknife procedure was selected over a bootstrap.

Only the smooth curves for the sites of Bootham, City Centre and Fishergate have been analysed since the data availability at the sites of Gillygate, Holgate Road, Lawrence Street and Nunnery Lane is too short (2.5 years) to determine any meaningful trend in 24-hr mean  $\text{NO}_x/\text{NO}_2$  concentration.

The curves in Figure 58 and Figure 59 illustrate the respective changes in  $\text{NO}_2$  and  $\text{NO}_x$  concentrations over the study years whilst accounting for the other explanatory variables included in the final fitted models (i.e., confounding factors). The trends in  $\text{NO}_x$  and  $\text{NO}_2$  concentrations shown in Figure 58 and Figure 59 therefore more closely resemble the trend in emissions at each site than raw  $\text{NO}_x$  and  $\text{NO}_2$  measurements. It also seems likely that the trends illustrated in these figures could be a consequence of underlying meteorological factors that



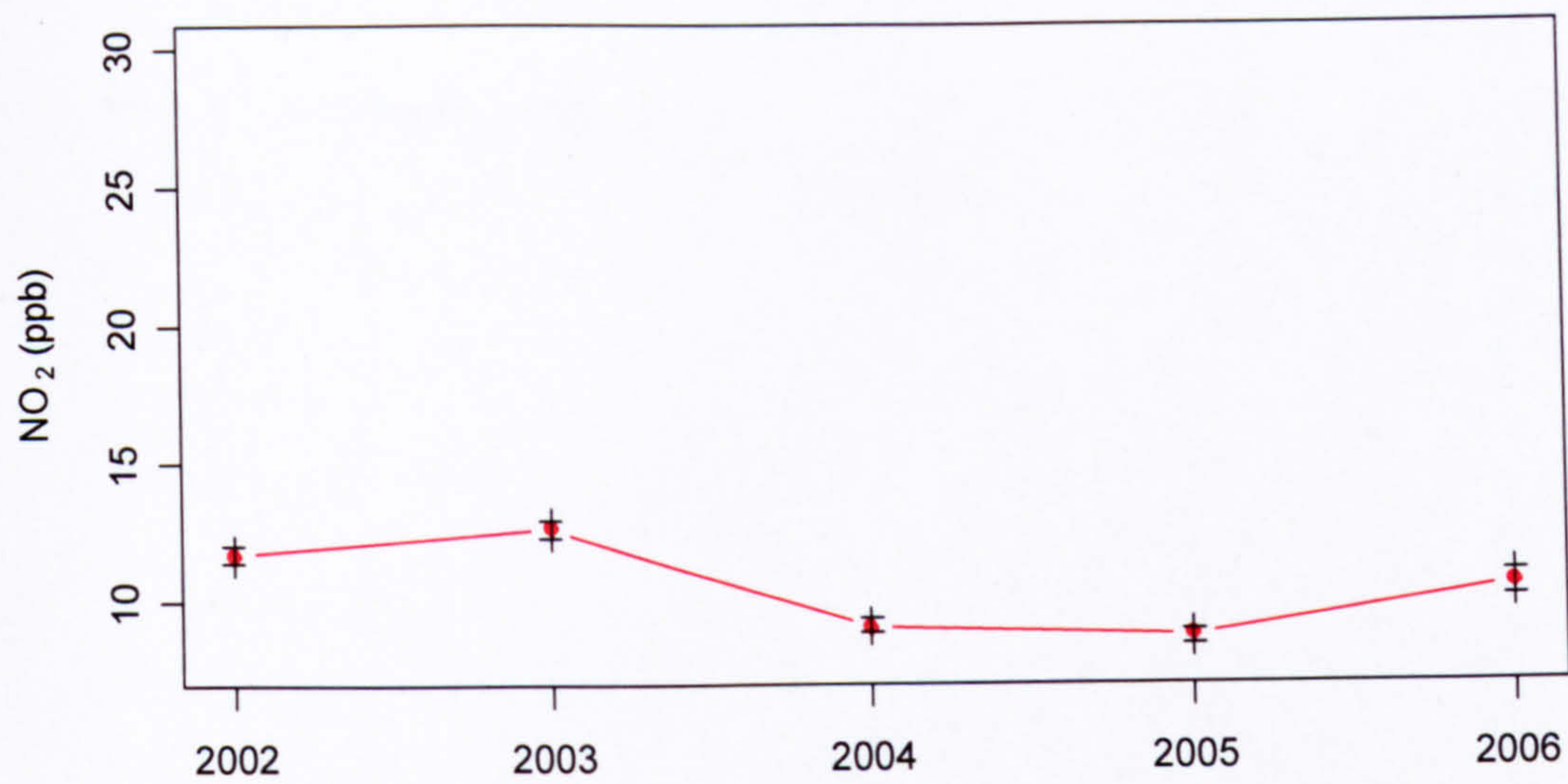
have not already been included in the model; indeed, this seems likely given that the highest values are for the year 2003, which was particularly bad in terms of air pollution problems.

It can be seen that all sites experience some year-to-year variability in  $\text{NO}_x$  and  $\text{NO}_2$  concentrations; this is especially true of the data recorded at the City Centre site. Figure 59a and c shows that the  $\text{NO}_2$  concentrations at the urban background site of Bootham and the roadside site of Fishergate appear to increase towards the end of the study period. This increase in concentration was also seen in the  $\text{NO}_x$  concentrations for both these sites.

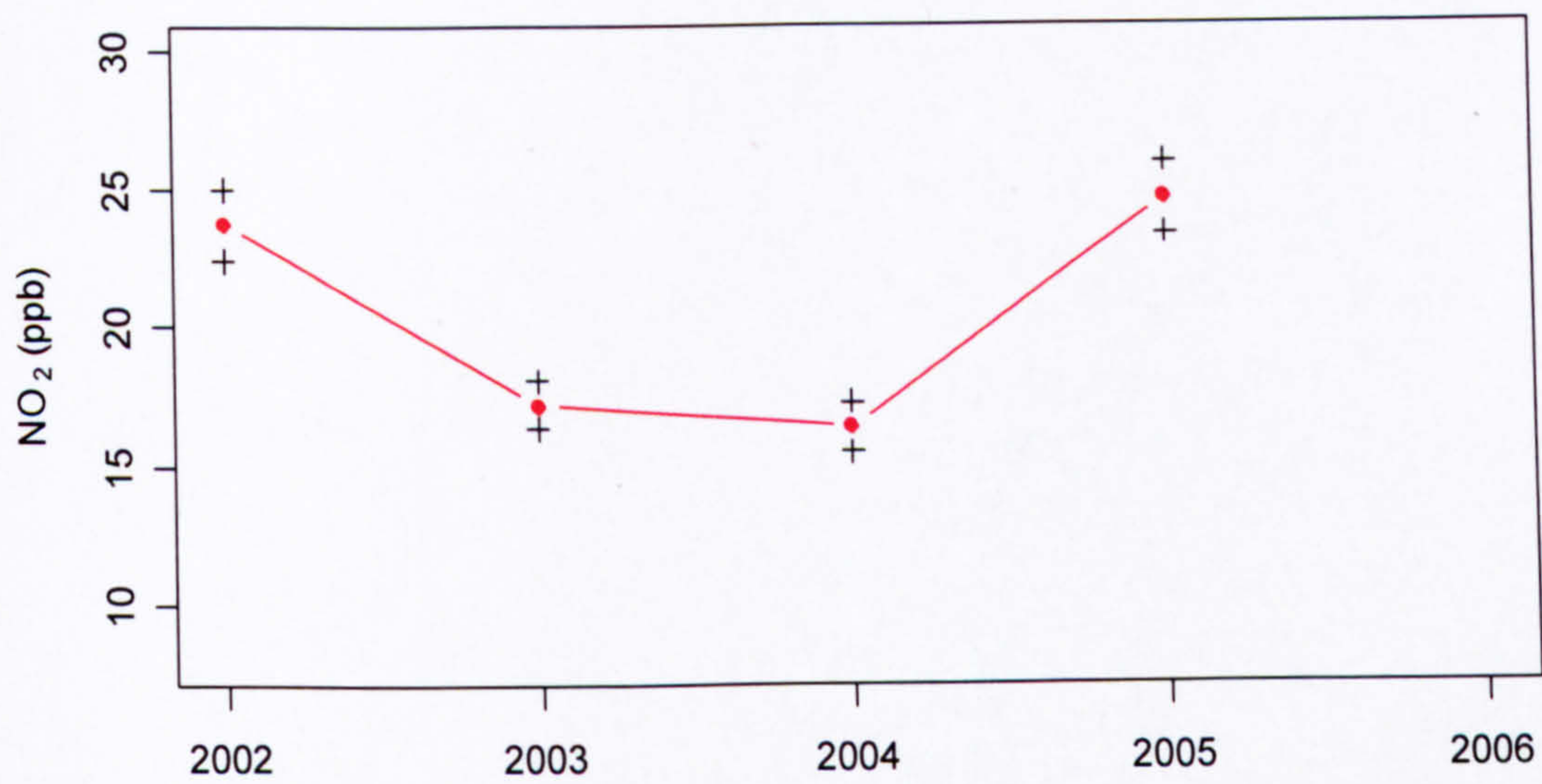
The 95 % confidence intervals highlight the certainty with which the response curve has been created. It can be seen that the confidence intervals for the City Centre site (both  $\text{NO}_x$  and  $\text{NO}_2$ ) are generally wider than for Bootham and Fishergate and so indicate that the estimation of trend at this site is less precise than that of the remaining two sites.

Overall, the trends in both  $\text{NO}_x$  and  $\text{NO}_2$  concentration do not indicate any visible signs of improvement in air quality in York. In fact, towards the latter end of the study period, the ambient  $\text{NO}_x$  and  $\text{NO}_2$  concentrations at a number of sites are increasing, with this increase being most likely attributable to a change in localised  $\text{NO}_x$  and  $\text{NO}_2$  emissions.

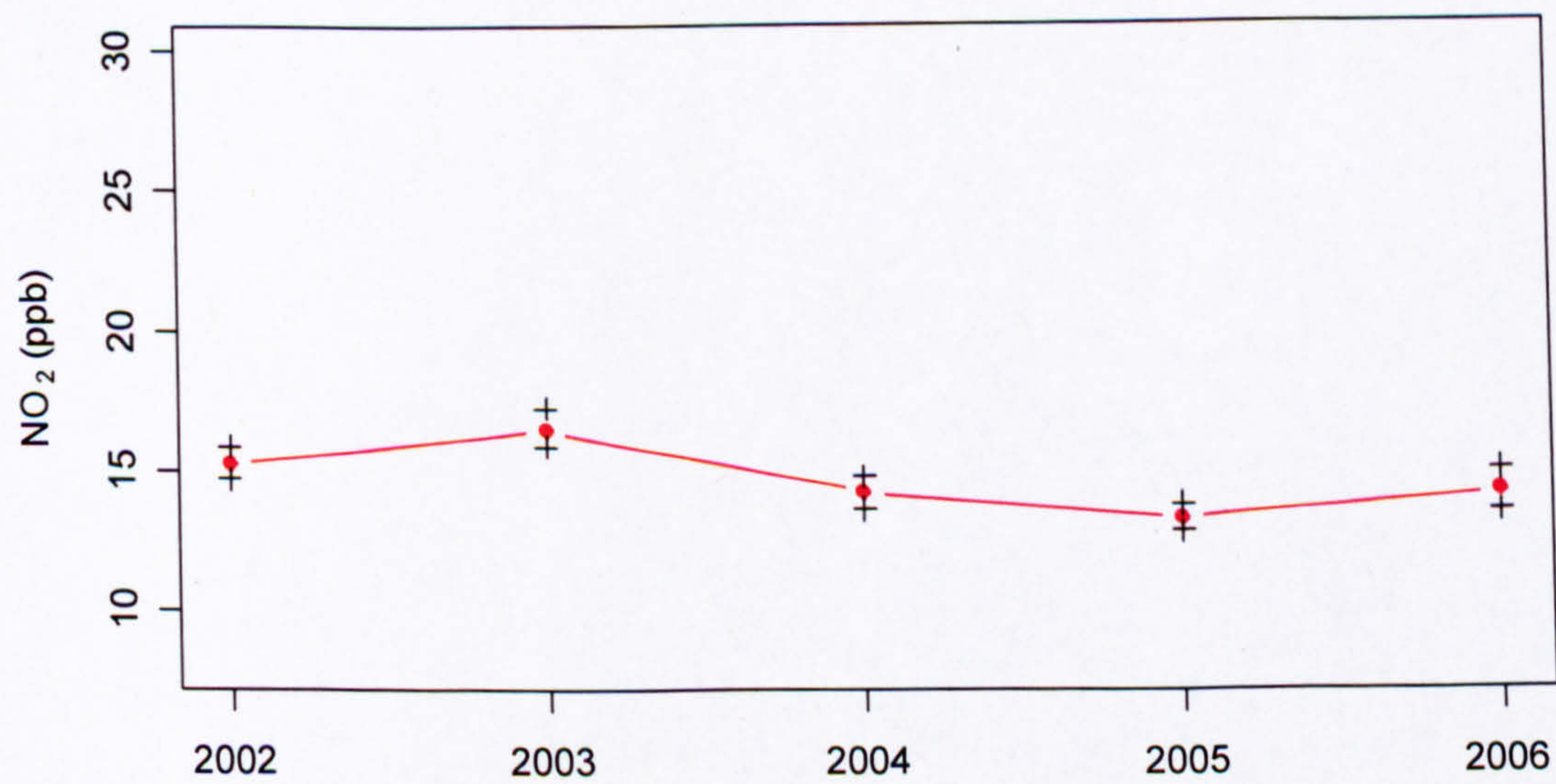




a)



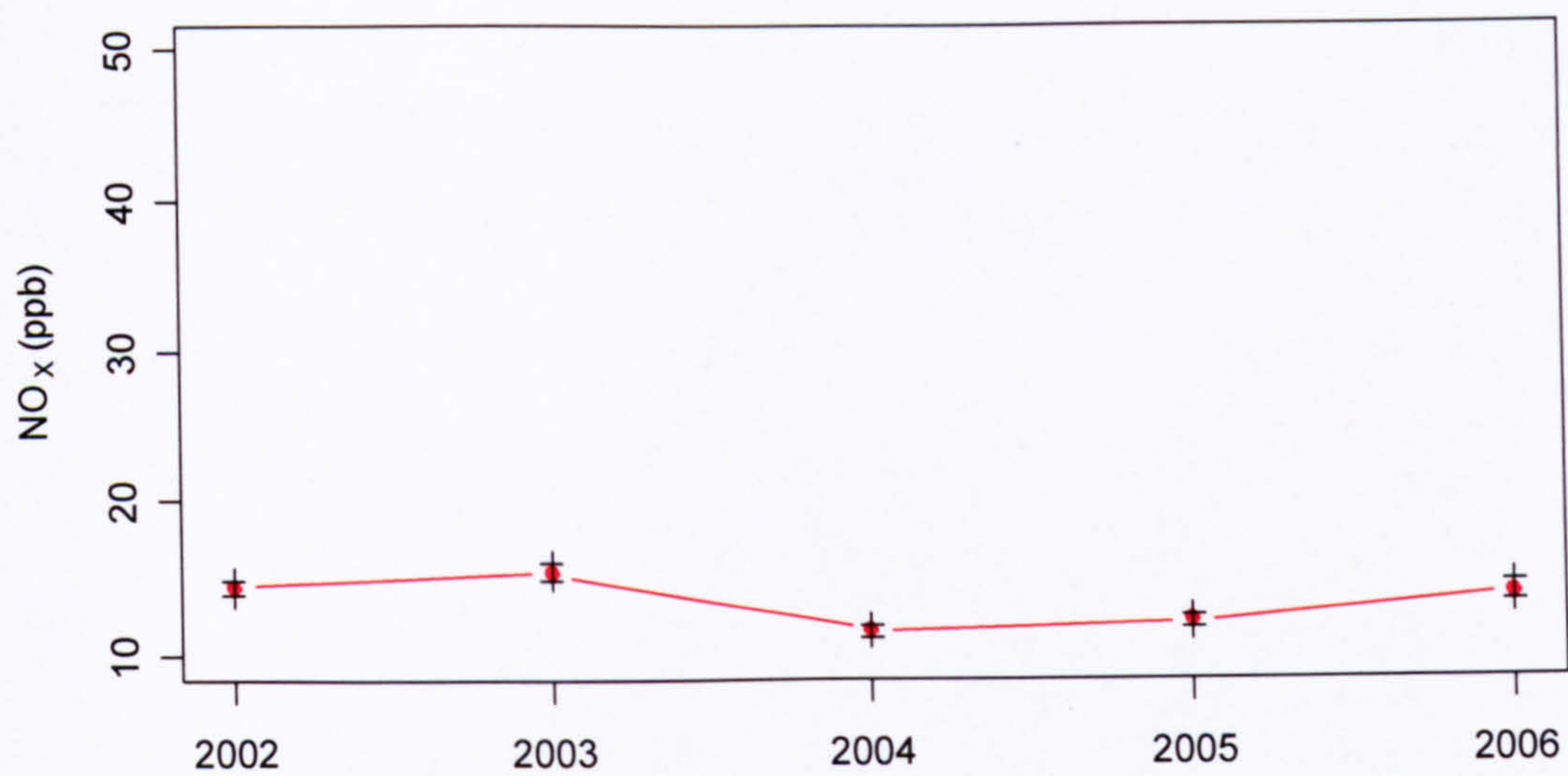
b)



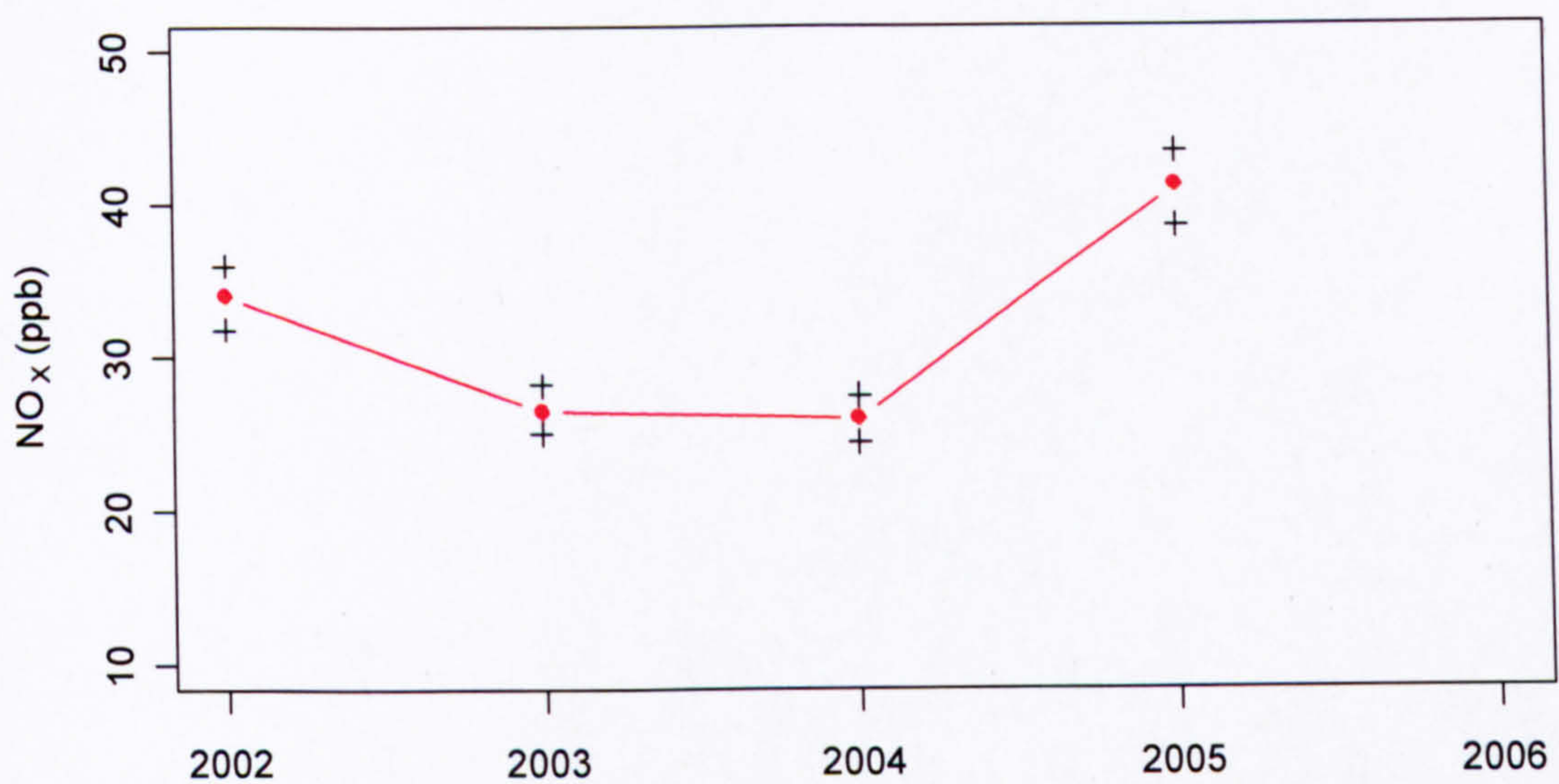
c)

**Figure 58:** Fitted  $s(\text{year})$  smooth curves for NO<sub>2</sub> concentrations for the three long-term monitoring sites to the time variable (year). From top to bottom: a) Bootham, b) City Centre, c) Fishergate. 95% confidence intervals shown by black crosses .

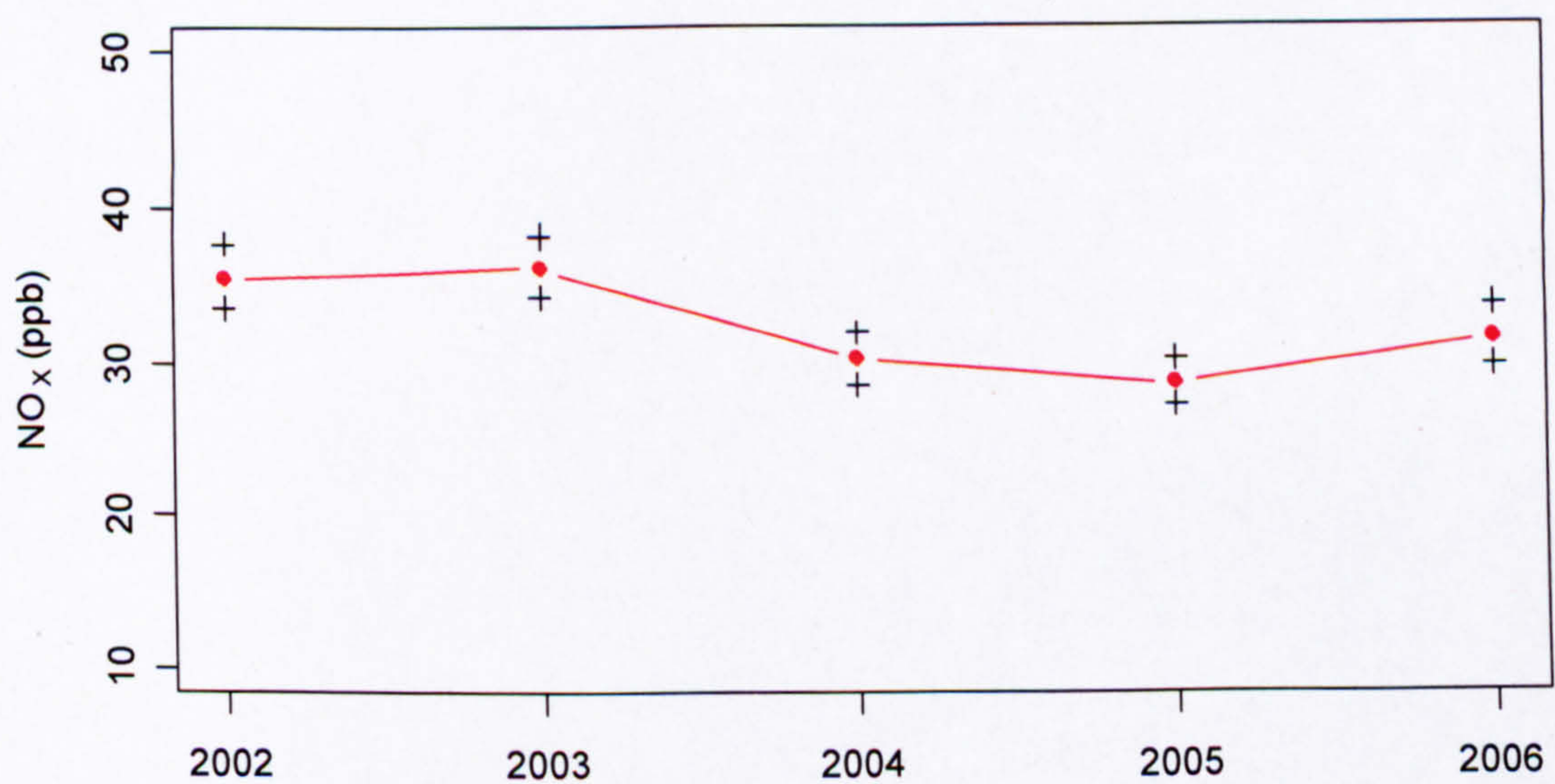




a)



b)



c)

**Figure 59:** Fitted  $s(\text{year})$  smooth curves for NO<sub>x</sub> concentrations for the three long-term monitoring sites to the time variable (year). From top to bottom: a) Bootham, b) City Centre, c) Fishergate. 95% confidence intervals shown by black crosses.



#### 6.6.4. Regression diagnostics

For completeness, the regression diagnostics for each model were analysed to check that the assumptions of regression were being followed. Figure 60 illustrates the diagnostic plots for the Fishergate NO<sub>x</sub> model (this model is representative of the results for the other sites and so to prevent repetition only the diagnostics for this model will be shown).

It can be seen that the log transformation of the NO<sub>x</sub> concentrations produced normally distributed residuals shown by the straight diagonal line in the Q-Q plots (Figure 60a) and the residuals being normally distributed in the histogram (Figure 60c). The residuals vs. fitted plot (Figure 60b) should show an even scatter of points above and below the zero line. A trend in the residuals in this plot would indicate that the variance of the response is related to its mean and would therefore be in violation of the assumption of constant variance. The residual vs. fitted plot shown in Figure 60b however is acceptable. Finally, Figure 60d clearly displays the desired positive linear relationship between the fitted and response values.

As mentioned previously autocorrelation has not been considered within this study since the primary aim is to analyse historic data and not to predict future concentrations.



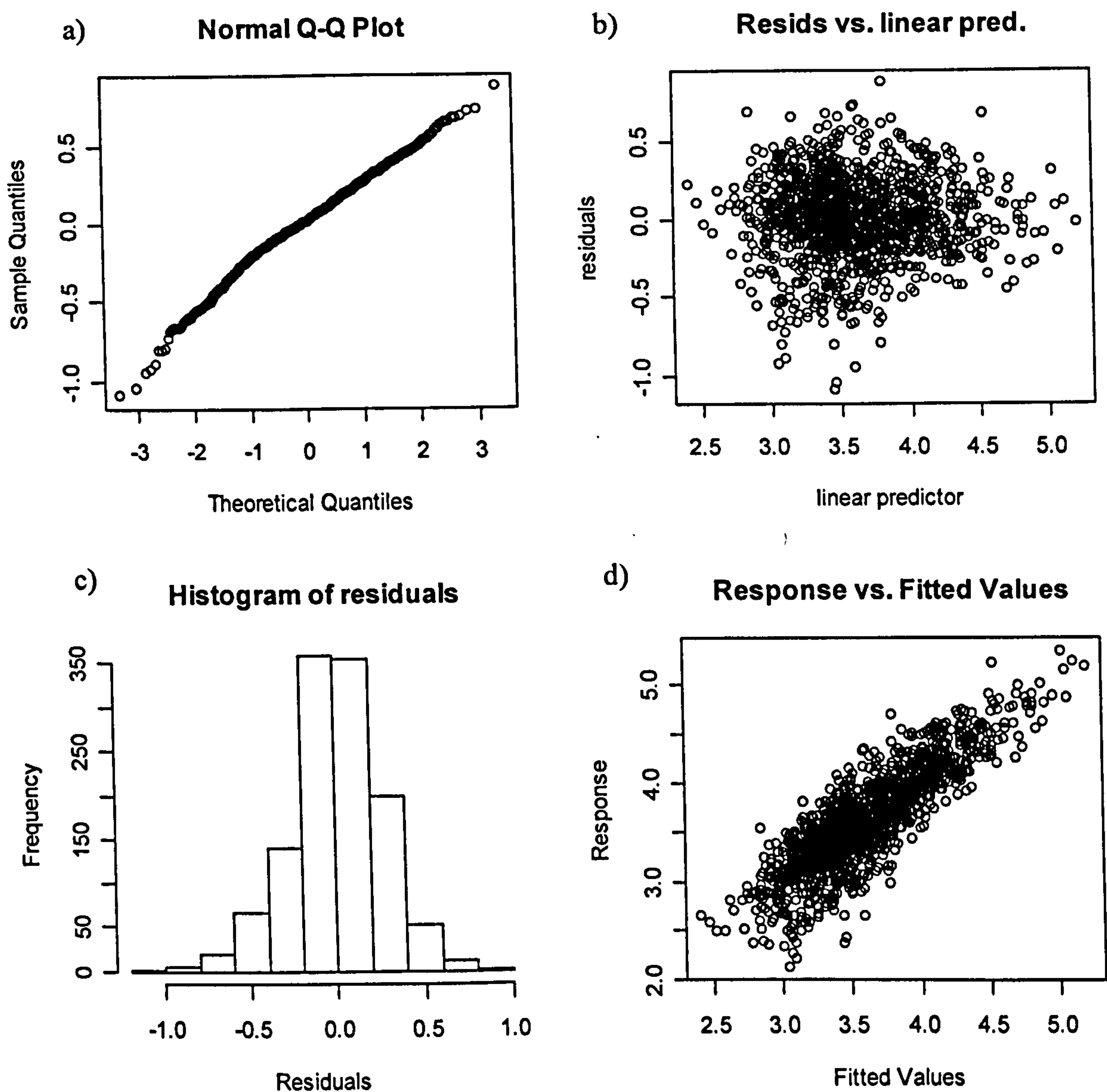


**Figure 60:** Regression diagnostics for the  $\text{NO}_x$  GAM at the Fishergate monitoring site.

#### 6.6.5. ADMS-Urban

The statistical analysis of the predictions made with ADMS-Urban, in the same manner as the monitored data shown in section 6.5, should provide insight into the important drivers of the dispersion model. Also, analysis of the subsequent response curves will illustrate whether the dispersion model assumes similar relationships to those seen between the monitored  $\text{NO}_x$  and  $\text{NO}_2$  concentrations and their driving variables.

ADMS-Urban was used to predict the hourly concentrations of  $\text{NO}_x$  and  $\text{NO}_2$  for the study years (2002 to 2006). This required running 5 separate models, one for each of the study years. The same background and meteorological data were used as those used in the original GAM development. As shown in Chapter 4, the traffic emissions were calculated from a combination of SATURN predictions and survey data. All road links contained within the York emissions inventory (921) were modelled explicitly (see Figure 18). The latest emission factors



provided with ADMS-Urban (known as EURO SCALED 03) were used to calculate the traffic emissions (note, emission factors are not editable). These emission factors are year dependent due to the uptake and effect of new fuels and vehicle technologies. The traffic composition (i.e., proportion of different vehicles using the road network), calculated from the survey data shown in Chapter 4, was held constant for the various years since we had no data from which to adjust for the different years. The ADMS-Urban receptor sites correspond to the co-ordinates of the seven monitoring sites around York.

ADMS-Urban requires the input of background pollution data, and so the predictions made with ADMS for the last two thirds of 2006 are not available since the NO<sub>x</sub> (and NO<sub>2</sub>) monitor at Dunnington was removed in April 2006 (see section 3.5 of Chapter 3). Additionally, the periods where monitoring data were not available (i.e., pre 2004 for the sites of Gillygate, Holgate Road, Lawrence Street and Nunnery Lane and post April 2006 for all sites) have been removed from the ADMS-Urban predictions as this will ensure that the GAMs developed using the ADMS-Urban predictions are constructed with data for the same period (enabling a like for like comparison). The relative contributions of the various explanatory variables are shown in Table 35.

It can be seen that in general the same four explanatory variables were selected for inclusion into the ADMS-Urban GAMs; these variables being (in order of importance, the background NO<sub>x</sub>/NO<sub>2</sub> term, the 'u,v' term, a term for month and finally a trend term. In all instances the inclusion of temperature over month did not significantly improve the model fit. Additionally, the terms for precipitation and cloud cover were not found to have a significant association with the response variable and so neither term was included in the final fitted models. Humidity was found to have an association with the response variable for some sites; however, since it was considered only desirable to include four terms in the GAMs, (so as to be as consistent with those created in the previous section), humidity did not enter the final fitted models.

The univariate contributions highlighted in Table 35 stress the relative importance of the explanatory variables once inside the model. It can be seen that background NO<sub>x</sub>/NO<sub>2</sub> is an important explanatory variable in all models. Indeed, this term was the first variable to enter each of the 14 models created with ADMS-Urban predictions. For some sites, the model containing only the urban background variable (i.e.,  $\log(\text{NO}_x) = s(\text{Bkg NO}_x)$ ) could explain a substantial proportion of the variability in the response NO<sub>x</sub>/NO<sub>2</sub> concentrations (~ 90 %). The wind term (u,v) is also an important driving factor for many of the sites under examination; for example, this term has the largest univariate contribution at the sites of City Centre, Fishergate, Gillygate, Nunnery Lane and Lawrence Street.



**Table 35:** Relative contributions of the various explanatory variables included in the final fitted models. Response variables are ADMS-Urban NO<sub>x</sub> and NO<sub>2</sub> predictions (as opposed to raw monitored data used previously). B = Bootham C = City Centre, F = Fishergate, G = Gillygate, N = Nunnery Lane, H = Holgate Road and l = Lawrence Street.

Explanatory variable	B	C	F	G	N	H	L
<b>NO<sub>2</sub></b>							
Bkgd NO <sub>2</sub>	30.4	17.5	12.7	20.3	12	24	6.6
U,V	7.3	19.2	25.7	21.2	32.3	18	39.2
Temperature							
Month	0.6	1.4	0.4	0.2	0.3	0.1	1.6
Year	0.2	0.5	1.4	0.9	1.1	0.9	1.3
TOTAL	96.3	93.4	90.7	94.8	84.7	93	84
<b>NO<sub>x</sub></b>							
Bkgd NO <sub>x</sub>	27.7	20.2	9.5	15.4	15.1	20	12
U,V	6.4	19.2	23	25.5	18	17.4	32.3
Temperature							
Month	0.8	0.3	1.4	1	1	0.5	0.3
Year	0.1	0.5	1.8	1	1.2	0.9	1.1
TOTAL	97.5	91	92.3	93.6	96	92.1	84.7

It is also of interest to note that the total deviance explained by the GAMs created with the predictions of ADMS-Urban (Table 35), is greater than those models created with monitoring data (Table 34); for example, the mean of the total deviance explained in observed NO<sub>2</sub> concentration for the 7 sites is ~71 %, whereas the mean for the predicted NO<sub>2</sub> concentrations is ~ 91 %.

The smooth response curves for the ADMS-Urban GAMs, created as part of the GAM modelling framework, are displayed in Figure 61. For reasons of consistency the smooth plots for the NO<sub>2</sub> concentrations at Fishergate are shown. It can be seen that there is great similarity in the smooth plots in Figure 54 (monitored data) with those in Figure 61 (ADMS data).

Firstly, the relationship between the target NO<sub>2</sub> concentration (modelled) and background NO<sub>2</sub> concentration shows a distinctly positive association (Figure 61a). Similarly to Figure 54a, the confidence intervals become wider for higher concentrations; this divergence is a result of the lower data capture for these concentrations (see rug plot at the base). The similarity between the two smooth curves (Figure 54a and Figure 61a) indicates that the



dispersion model is adequately representing the relationship between ambient air pollution and background air pollution.

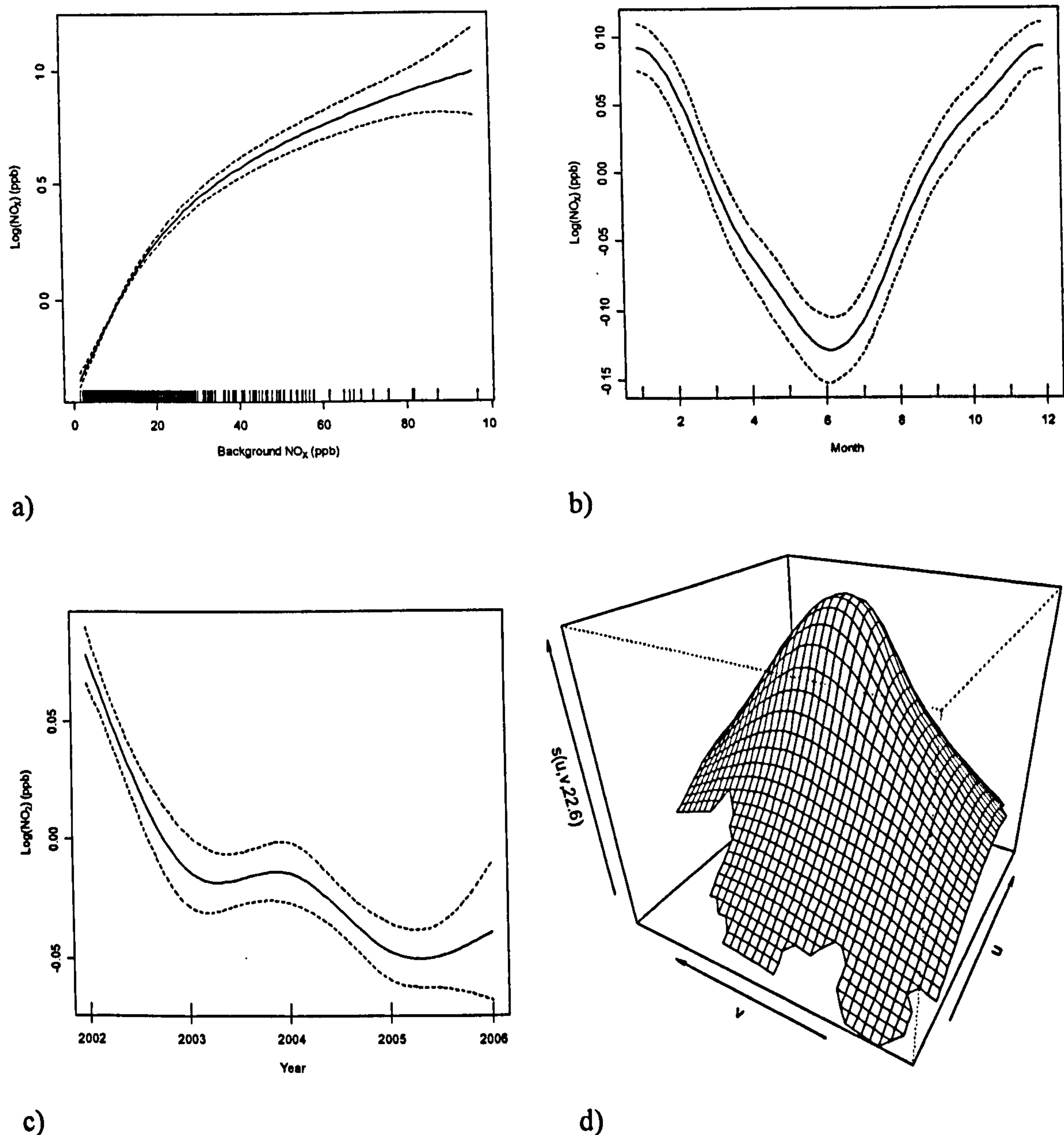


**Figure 61:** Fitted components of the ADMS-Urban NO<sub>2</sub> concentrations at Fishergate: (a) smooth function of  $s(\text{BkgNO}_2)$  (b) smooth function of month,  $s(\text{month})$ , (c) smooth function of trend,  $s(\text{year})$ , (d) bivariate smooth function of wind components,  $s(u,v)$ .

The fitted smooth curve for month (seasonality variable) seen in Figure 61b is also similar to that in Figure 54b. In both plots, the lowest concentrations are found during the summer months and the highest during the colder, winter months. The smooth curve for month using the ADMS-Urban predictions is somewhat more idealistic than that created with monitored data (i.e., the shape of the curve more closely resembles the underlying theory of lower pollutant concentrations in summer months compared to those of winter). This plot therefore indicates that ADMS-Urban does well at reproducing the seasonality in pollutant concentrations.

The smooth curve for trend ( $s(\text{year})$ ) (Figure 61c) shows a different pattern over the study years compared to that created with monitored data (Figure 54c). The trend curve for the



ADMS-Urban predictions shows a steady decline over the study years; whereas the trend curve for the monitored concentrations shows a decline during the first half of the period, but for the years 2005 and 2006 the NO<sub>2</sub> concentrations begin to increase. This is the only smooth plot that shows substantial differences between monitored and predicted data and indicates that the processes represented in ADMS-Urban model are not following those in real life. The evidence in Figure 54 and Figure 61c therefore suggests that at some point over the six-year period the assumptions and processes modelled in ADMS-Urban are diverging from those that occur in the 'real world'.

The smooth plot for the interactive wind flow component (Figure 61d) also shows similarity to the previous plot at Fishergate (Figure 54d). Both the smooth surfaces show the highest concentrations in the centre of the plot (i.e., close to the monitoring site) with concentrations falling off suddenly with increasing distance from the monitor. Figure 62 illustrates the NO<sub>2</sub> smooth plots for the 'u,v' term for all monitoring sites included in the study.

In general, the highest NO<sub>2</sub> (and NO<sub>x</sub> not shown) concentrations are seen at the centre of the plot, close to the monitor. As explained previously, these high NO<sub>2</sub> concentrations occur at low wind speeds and so indicate that all the sites are subject to ground level emissions.

In comparison to the measured smooth plots for the wind term (shown in Figure 57) the ADMS-Urban smooth plots illustrate some quite different relationships between predicted concentration and the 'u,v' term. The site-specific detail shown in the measured data plots is not as strongly reproduced in the corresponding plots made with ADMS-Urban predictions. For example, the band of high NO<sub>2</sub> concentration at Bootham to the southeast shown in Figure 57a is much less pronounced in Figure 62a. Additionally, the high NO<sub>2</sub> to the east of the Gillygate monitoring site (Figure 57d) is totally lacking in the corresponding ADMS-Urban plot (Figure 62d); instead, the lowest NO<sub>2</sub> concentrations are seen when the wind blows from this direction.

Generally speaking, the wind term plots for ADMS-Urban predictions highlight that the underlying principles of dispersion are present (i.e., high concentrations at low wind speeds) but the site-specific detail in the wind-concentration interaction is lacking. This provides strong evidence to suggest that ADMS-Urban is not reproducing the localised wind patterns seen at the monitoring sites.

#### **6.6.6. ADMS-Urban trend estimation**

This section will examine the trends in observed and predicted NO<sub>x</sub> and NO<sub>2</sub> concentration further. Figure 63 illustrates the observed and predicted NO<sub>2</sub> trend plots for the site of Fishergate side by side. The separate jack-knife procedure for the calculation of confidence intervals, outlined in section 6.6.2. did not reveal any further information and so has not been included here. Instead, the finer detail offered by the plots produced directly from the mgcv framework was preferred.



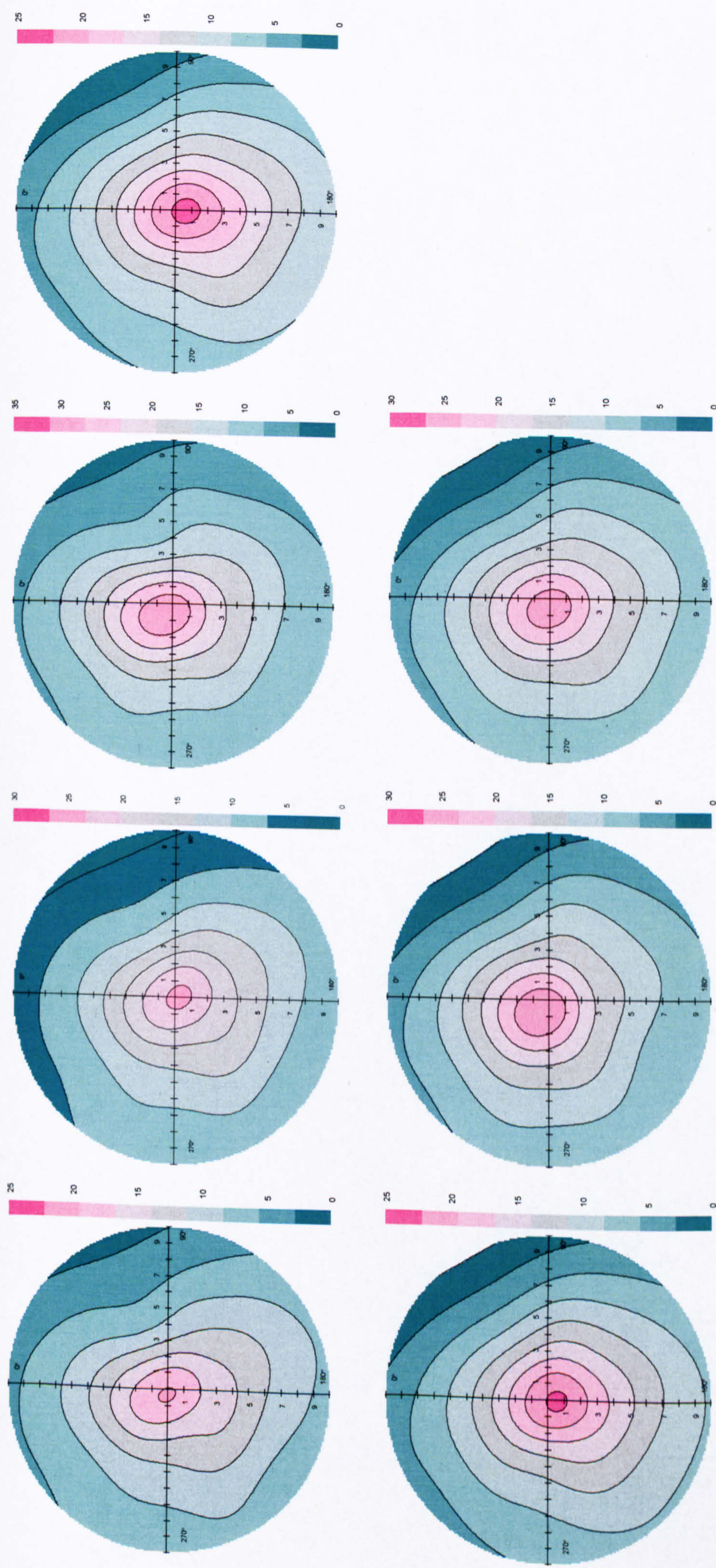


**Figure 62:** 'u,v' response curves for NO<sub>2</sub> concentrations predicted with ADMS-Urban for each of the monitoring sites in York. The plot illustrates a 3D surface since both wind speed and wind direction are taken into account. A) Bootham, b) City Centre, c) Fishergate, d) Gillygate, e) Holgate Road, f) Lawrence Street and g) Nunnery Lane.



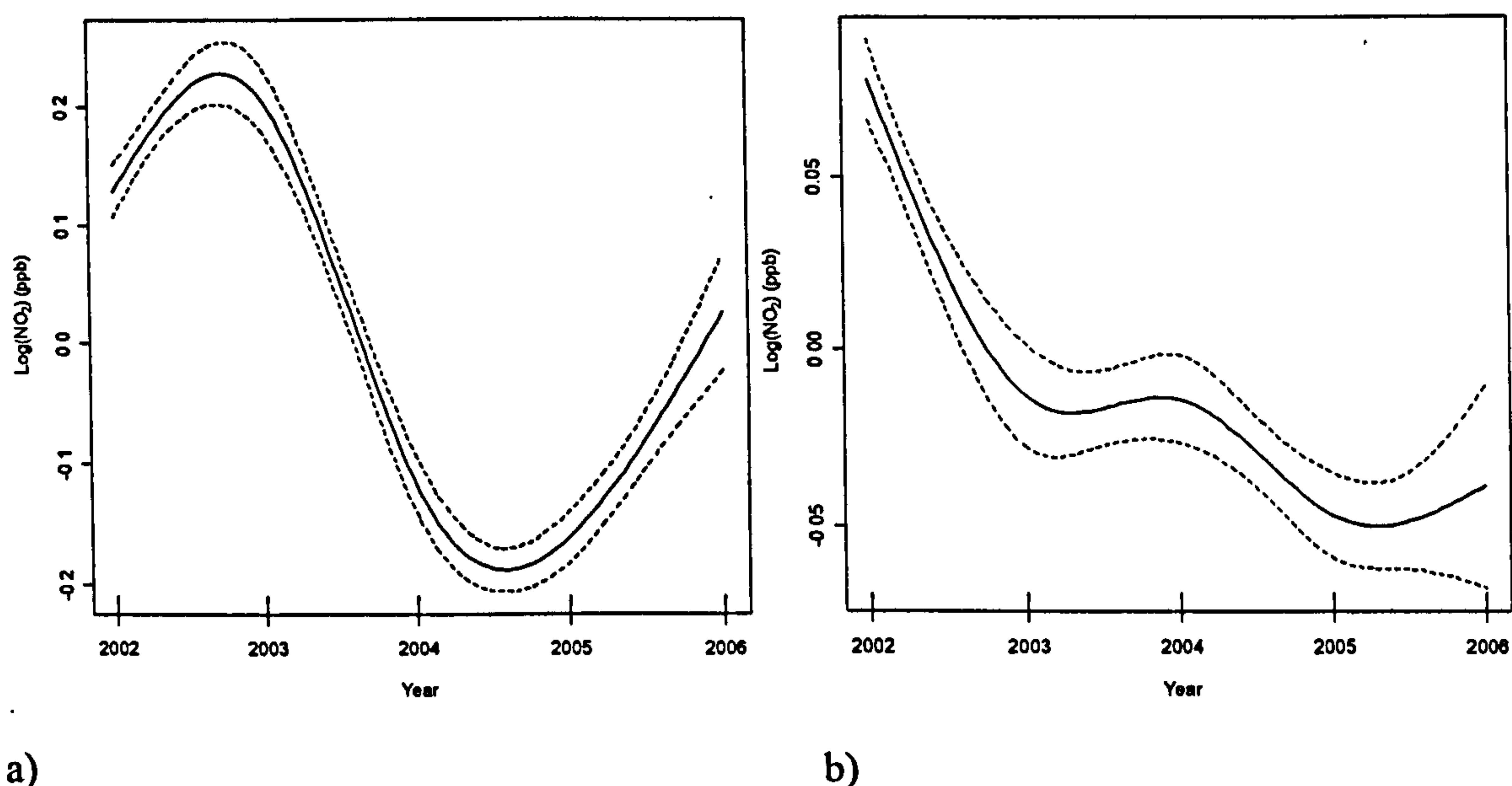


**Figure 63:** Fitted  $s(\text{year})$  smooth curves for monitored (a) and ADMS-Urban predicted (b)  $\text{NO}_2$  concentrations for the site of Fishergate.

As was mentioned previously in the discussion regarding Figure 54, the trend plots more closely resemble the trends in pollutant emissions (rather than ambient concentrations) since the effects of seasonality and meteorology have been removed. The most likely cause of the divergence in the trend plots for predicted and monitored data is therefore the way ADMS-Urban estimates road traffic emissions.

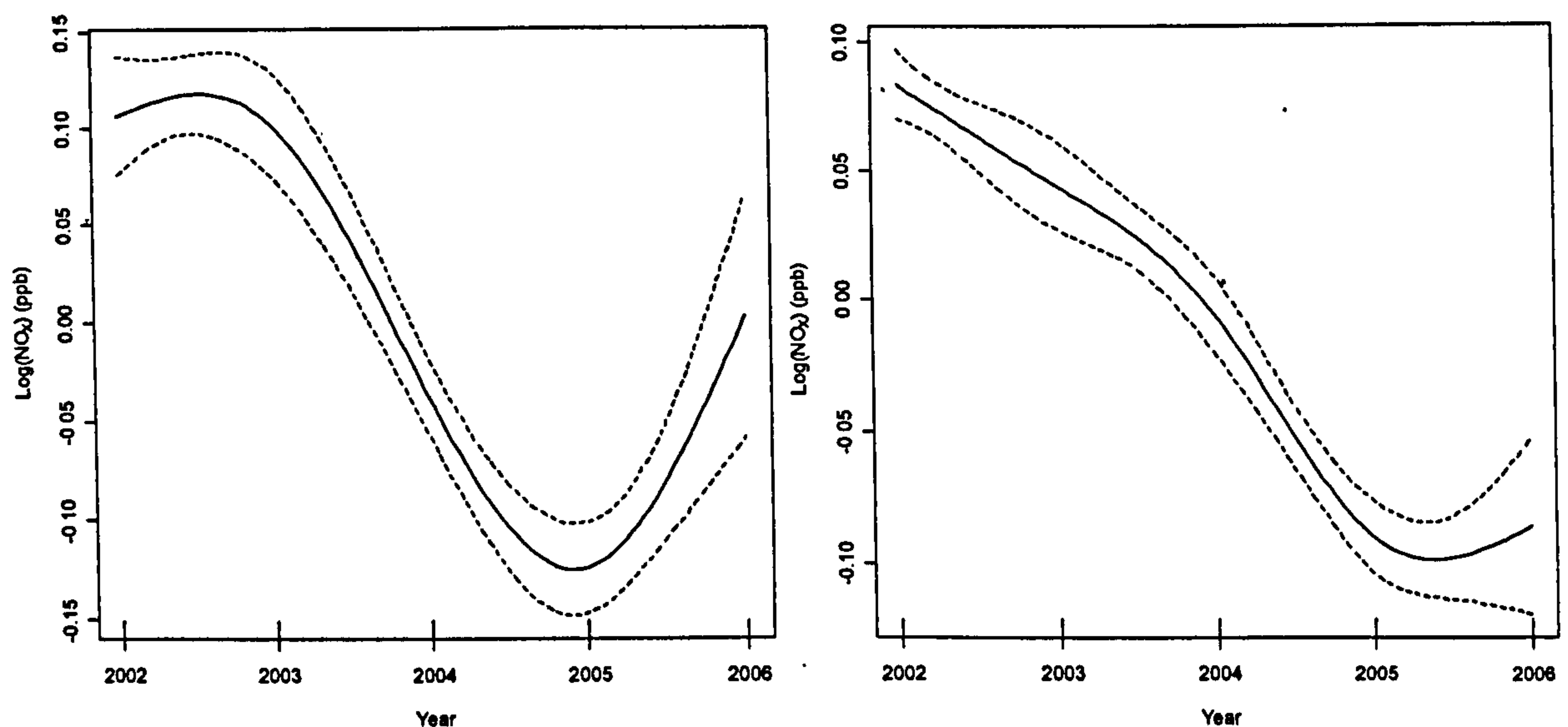
As already highlighted, the emissions factors used to estimate traffic emissions assume a steady decline in transport emissions due to the development of cleaner engines and their associated greater uptake. It is likely, therefore, that these assumptions have not occurred to this extent in real life and thus the steady decline in ambient  $\text{NO}_2$  concentrations predicted by ADMS-Urban, are very different from the real world scenario. Indeed, Figure 63a indicates an increase in pollutant emissions during the latter period of study.

The trends in observed and predicted  $\text{NO}_x$  concentrations at Fishergate are illustrated in Figure 64. The trends in the predicted  $\text{NO}_2$  and  $\text{NO}_x$  concentrations, shown respectively in Figure 63 and Figure 64, are representative of the trends in predicted  $\text{NO}_x$  and  $\text{NO}_2$  concentrations at the remaining long-term sites. Figure 64 shows a similar story to the trends in  $\text{NO}_2$  concentration.

The general decreasing trend in  $\text{NO}_x$  and  $\text{NO}_2$  predictions (seen at all three of the long-term sites) suggests that ADMS-Urban is not accounting for an influential source of  $\text{NO}_x$  (and  $\text{NO}_2$ ) emissions. It seems likely that the projected uptake of cleaner vehicles and the reductions in  $\text{NO}_x$  traffic emissions resulting from technological improvements, which are contained within the emission factors used to calculate traffic emissions, have overestimated the actual figures. The rate of decline in  $\text{NO}_x$  and  $\text{NO}_2$  emissions, and subsequent  $\text{NO}_x$  and  $\text{NO}_2$  predicted



concentrations have therefore not matched those observed and so highlights an important discrepancy in the estimation of vehicular emissions.



a)

b)

**Figure 64:** Fitted  $s(\text{year})$  smooth curves for monitored (a) and ADMS-Urban predicted (b)  $\text{NO}_x$  concentrations for the site of Fishergate.

## 6.7. Discussion and conclusion

A major difficulty faced in this study has been the non-uniformity in the length of datasets for the different sites. Some sites have monitoring data that spans nearly four years (Bootham and Fishergate), whereas other sites only have data for just over two (Gillygate, Holgate Road, Lawrence Street and Nunnery Lane). This difference in data length, especially the shortness in data length at some of the sites, has made it challenging to analyse the change in pollutant concentration over the study years in a consistent fashion. It has also meant that the length of dataset used to create the GAMs at the various sites has not been consistent. Each site has experienced its own unique ‘holes’ in the dataset.

Additionally, a limitation of meteorological and seasonality normalisation is the fact that the models assume the relationships between the various explanatory variables and the response variable remain constant over time. As highlighted by Thompson et al. (2001) it is possible that substantial changes in emissions (the aim of many air pollutant control strategies) could cause a change in the existing relationships between the response variable and meteorology. Therefore, by applying a uniform model to the entire dataset ignores the possibility of dynamic relationships. It may therefore be more suitable to analyse the  $\text{NO}_x$  and  $\text{NO}_2$  concentrations in smaller timeframes (i.e., a single year at a time) so that the risk of changing relationships between response and explanatory variables is reduced. It would be interesting to compare smooth plots created with only the first year of monitoring (and



modelled) against smooth plots created from only the final year of available data. Any subsequent difference in the smooth plots would highlight changes in the processes controlling for ambient pollutant concentrations. However, in this Chapter we have simply assumed that the relationships between response and explanatory variables are constant throughout the six-year period.

A further point that requires discussion is the fact that the meteorological data used in this Chapter are sourced from a single monitoring station. It is likely that meteorological parameters will vary across an urban area and therefore applying data from a single site may be a source of uncertainty in the construction of smooth relationships. Wind flow for example, is unlikely to remain constant across an entire urban area and so it is a possibility that the smooth relationships we have created in this Chapter are misrepresentative to a certain degree. However, since the Church Fenton meteorological data are considered representative for York (according to the Meteorological Office), and given that no other meteorological data are available, it was considered acceptable to apply these same data to all monitoring sites within the urban area of York.

The reduction in annual mean  $\text{NO}_x$  concentrations at Fishergate, section 5.4.2 of Chapter 5, is similar to the reductions reported in this Chapter (Figure 64a). Note only the period 2002 to 2006 has been analysed in the present Chapter due to restrictions on the length of meteorological data. Indeed Figure 34 (Chapter 5) illustrates a slightly higher annual mean  $\text{NO}_x$  concentration in 2003 compared to 2002; a feature consistent in the 24-hr  $\text{NO}_x$  data reported in Figure 64a. However, the upturn in 24-hr  $\text{NO}_x$  concentrations at Fishergate during the latter period of the study years was not seen in the raw annual mean concentrations at this site. This difference could be a consequence of the normalisation procedure (i.e., the fact that the influence of meteorology and season have been removed from the ambient concentrations). The trends in  $\text{NO}_x$  and  $\text{NO}_2$  concentrations at Bootham and City centre are also consistent to the trends in annual mean concentrations analysed previously.

## 6.8. Chapter summary

This Chapter has highlighted the important driving factors in  $\text{NO}_x$  and  $\text{NO}_2$  concentration at the various monitoring sites. The background pollutant concentration and the wind speed-wind direction term have consistently been identified as the most important variables in explaining the variability in  $\text{NO}_x$  and  $\text{NO}_2$  concentration. These terms were also identified as important driving factors for the ADMS-Urban model.

The fact that background pollutant concentration and wind flow have consistently been identified as important driving factors in explaining the variability in  $\text{NO}_x$  and  $\text{NO}_2$  implies that air quality management strategies, aimed at reducing emissions, will only reduce ambient pollutant concentrations to a certain degree. Perhaps a more effective strategy would be aimed at reducing the regional background pollutant concentrations.



Table 36 illustrates the percentage deviance explained for GAMs with solely the background pollutant concentration as an explanatory term (i.e.,  $\log(\text{NO}_x) \sim s(\text{bkg NO}_x)$ ). It can be seen that irrespective of the localised influences of air quality (i.e., localised road traffic emissions), the regional background contribution can explain a high proportion of the variability in  $\text{NO}_x$  and  $\text{NO}_2$  concentrations. It would be interesting to compare the results of Table 36 with those from similar GAMs analysing  $\text{NO}_x$  and  $\text{NO}_2$  concentrations from monitoring sites in other urban areas.

**Table 36:** The contributions to percentage deviance explained for GAMs containing solely the background pollutant data as an explanatory term. B = Bootham C = City Centre, F = Fishergate, G = Gillygate, N = Nunnery Lane, H = Holgate Road and L = Lawrence Street.

	B	C	F	G	N	H	L
<b>Monitored</b>							
NO <sub>2</sub>	62	33	47	38	42	34	35
NO <sub>x</sub>	76	46	55	36	44	37	27
<b>ADMS-Urban</b>							
NO <sub>2</sub>	88	70	57	71	67	72	53
NO <sub>x</sub>	90	71	63	68	74	73	42

During the GAM construction process it became apparent that the predictions made with ADMS-Urban were highly dependant on the background  $\text{NO}_x$  or  $\text{NO}_2$  concentrations. Indeed, it can be inferred from Table 36 that the percentage deviance explained in both  $\text{NO}_x$  and  $\text{NO}_2$  concentrations for the ADMS-Urban GAMs are much higher than that explained by the same GAMs for observed  $\text{NO}_x$  and  $\text{NO}_2$  concentrations. This therefore highlights the importance of background pollutant data when running models since this term alone can explain up to ~90 % of the variability in predicted pollutant concentrations at some sites. It is therefore an extremely important input requirement for the dispersion modelling process.

Finally, the trends in normalised  $\text{NO}_x$  and  $\text{NO}_2$  concentrations have highlighted a possible increase in traffic emissions towards the end of the study years (section 6.6.2), something that would not have been discovered if the analysis concentrated solely on trends in raw measurements (i.e., Chapter 5). The divergence in  $\text{NO}_x$  and  $\text{NO}_2$  concentration trends for predicted and monitored data suggests that the processes used to estimate traffic emissions (emissions factors) in ADMS-Urban do not follow those of 'real life'. Long-term projections made with ADMS-Urban are therefore under-predicting measured data.



## **7. A case study: Comparison of ADMS-Urban and generalised additive modelling**

### **7.1. Chapter preview**

This Chapter compares the statistical modelling technique of generalised additive modelling against the dispersion model, ADMS-Urban, in predicting the hourly  $\text{NO}_x$  and nitrogen dioxide ( $\text{NO}_2$ ) concentrations at a busy street canyon location. Bivariate polar plots will also be used to analyse the models performance at reproducing the wind flow (speed and direction) and pollution data (measured and predicted concentrations) interaction. This work will provide the CYC with a greater understanding of the behaviour of  $\text{NO}_x$  and  $\text{NO}_2$  concentrations in the street canyon of Gillygate.

### **7.2. Introduction**

This Chapter aims to take the comparison of ADMS-Urban and GAMs a step further by undertaking a case study investigation of  $\text{NO}_x$  and  $\text{NO}_2$  concentrations at a single street canyon location in York. The present Chapter uses GAMs and ADMS-Urban to predict the hourly average  $\text{NO}_x$  and  $\text{NO}_2$  concentrations for 2005 in Gillygate, York. The hourly  $\text{NO}_x$  and  $\text{NO}_2$  concentrations at Gillygate were chosen as a case study since the air quality on this street has been investigated before (Boddy et al. 2005a, 2005b; Dixon et al., 2006), and also because the site is included as part of the AQMA of York and so any information gained regarding the air quality (or the workings behind the air quality) at this site will be useful for the CYC. It will also be interesting to see how GAMs and ADMS-Urban perform on a different scale (i.e., hourly concentrations as opposed to the 24-hr average concentrations of the previous Chapter).

### **7.3. Methodology**

#### **7.3.1. Site information**

Gillygate is located to the north of the city, close to where the A19 arterial route meets the inner ring road (see Figure 13, Chapter 3). It is orientated approximately from north-east to south-west ( $\sim 30^\circ$ ) with the monitoring station situated on the west side of the road around two metres from the road edge. Congestion is common and at peak periods, long queues can form stretching the entire length of the street, with queuing more predominant in the inbound lane (Dixon et al., 2006).

Gillygate has street canyon characteristics (i.e. narrow width  $\sim 12$  m, and high building height  $\sim 15$  m) and so pollutant concentrations at this location are often elevated. The street has already been the subject of investigation in the two-part study by Boddy et al. (2005a, 2005b), where the influence of background winds and traffic characteristics were used to explain the



spatial variation in carbon monoxide concentrations. These papers found evidence of an across canyon vortex, where the highest pollutant concentrations were found on the leeward side of the canyon during perpendicular wind flow. In addition, the study also highlighted the presence of complex 3D turbulence patterns such as helical flow regimes and along-canyon channelling. Despite York being a relatively small city, a substantial area of the city centre was declared an AQMA in 2002 as a result of high ambient NO<sub>2</sub> concentrations. Gillygate is included in the AQMA of York and a real time monitoring station has been in operation at the site since October 2003, measuring hourly NO<sub>x</sub>, NO and NO<sub>2</sub> concentrations.

### 7.3.2. ADMS-Urban

ADMS-Urban uses relevant meteorological, emissions and activity (e.g. traffic, industrial) data, to predict the concentrations of pollutants as they disperse from a source. Roads are treated as a series of line sources and emissions are assumed constant along the entire length of each road. For roads with street canyon characteristics, a further street canyon model (based on the OSPM model) is used, to represent the dynamics and dispersion features expected in such locations. Emissions were calculated for the street of Gillygate as outlined in section 4.5. A single line source of 292 metres was created to represent Gillygate. The vehicle specific traffic counts were calculated from SCOOT data (split cycle and offset optimisation technique) and a series of manual traffic surveys recorded at the site. SCOOT is a congestion management tool and its use at Gillygate is outlined by Boddy et al. (2005b). SCOOT measures traffic flow at hourly intervals; these data are primarily used to control the timings of traffic lights in the area in an attempt to keep congestion to a minimum. The emission rates for Gillygate (g/km/s) were exported into ADMS-Urban.

Since only one road is being modelled in isolation, local background concentrations were used as the background pollution input data (see Table 13, section 4.5.4) to account for other emission sources in the area that would not otherwise be included in the model. The local background data are split between Bootham (NO<sub>x</sub>, NO<sub>2</sub> and SO<sub>2</sub>) and Dunnington (O<sub>3</sub>). Measurements are made with commercial instrumentation by standard chemiluminescence (NO<sub>x</sub>, NO and NO<sub>2</sub>), UV absorption (O<sub>3</sub>) and fluorescence (SO<sub>2</sub>) techniques (AQEG, 2004) as described in Chapter 3.

The meteorological data were obtained from the UK Meteorological Office weather station at Church Fenton, 12 km to the south west of the city (see Table 14, section 4.5.4.). These meteorological measurements are made at a height of 10 m above flat terrain. The minimum Monin-Obukhov length was set to 30 m, and the surface roughness to 0.5 m following advice from CERC.

The street canyon module within ADMS-Urban is used to calculate pollutant concentrations in roads where the canyon height exceeds 0.5 m. It is based on the Danish OSPM



model which comprises of simplified dispersion and Gaussian plume models. The canyon height of Gillygate was set to 15 m and the canyon width to 12 m. The street canyon module creates a recirculation vortex in the canyon for all non-parallel wind flows; it reverses the street level wind direction. The vortex varies in width depending on building height and roof level velocity; in some cases it may extend the whole width of the street whereas in others it will be limited to the leeward side (CERC, 2006a). The width of the recirculation region is determined by the following:

$$L_R = 2 r H_B$$

Equation 9

Where  $H_B$  = canyon height  
 $u_t$  = wind speed at roof level  
 and  $r = 1$  ( $u_t \geq 2 \text{ m s}^{-1}$ )  
 $= u_t - 1$  ( $1 < u_t < 2 \text{ m s}^{-1}$ )  
 $= 0$  ( $u_t \leq 1 \text{ m s}^{-1}$ )

The in-canyon pollutant concentrations are thus a balance between the addition of traffic emissions at ground level and a loss of pollutant concentrations at the top of the canyon (CERC, 2006a). All concentrations within the vortex are assumed constant.

ADMS-Urban has been used to predict hourly  $\text{NO}_x$  and  $\text{NO}_2$  concentrations at Gillygate for the year 2005. The receptor point corresponds to the location of the sampling system for the Gillygate real time monitor, just inside the Gillygate street canyon.

### 7.3.3. Generalized additive modelling

There were two stages involved with GAM predictions: model development, and prediction. The R programming language (R Development Core Team, 2006) with package 'mgcv' version 1.3-17 (Wood, 2006) was used throughout.

#### 7.3.4.1. GAM development

The GAMs were developed to estimate the hourly  $\text{NO}_x$  and  $\text{NO}_2$  concentrations at Gillygate based on the variables used to construct the ADMS-Urban model: wind speed, wind direction, temperature, humidity, rainfall, urban background data ( $\text{NO}_x$ ,  $\text{NO}_2$ , and  $\text{O}_3$ ). In addition, hourly SCOOT traffic count and SCOOT traffic occupancy (percentage of time the SCOOT detector was occupied) were also used in the GAM construction process. These covariates are known to have an affect on concentrations of  $\text{NO}_x$  and  $\text{NO}_2$ .

The aim was to find the combination of explanatory variables that describe a high degree of the pollutant concentration variability. The large list of potential variables was



reduced by the manual selection process, outlined in the previous Chapter (section 6.5), until only the most important covariates remained. A total of 7523 hours of data were used to find the important explanatory variables in this GAM construction process.

The final NO<sub>x</sub> and NO<sub>2</sub> models are shown below:

$$\text{Log}(\text{NO}_x) = s_1(\text{bgd NO}_x) + s_2(u,v) + s_3(\text{flow}) \quad \text{Equation 10}$$

$$\text{Log}(\text{NO}_2) = s_1(\text{bgd NO}_x) + s_2(u,v) + s_3(\text{flow}) + s_4(\text{bgd O}_3) \quad \text{Equation 11}$$

Where bgd NO<sub>x</sub> is the urban background NO<sub>x</sub> concentration, flow is the hourly traffic count at Gillygate and bgd O<sub>3</sub> is the background O<sub>3</sub> concentration. The final NO<sub>x</sub> and NO<sub>2</sub> models can explain 80 % and 77 % of the variability in the hourly pollutant concentrations and the fitted model components influence the NO<sub>x</sub> and NO<sub>2</sub> concentrations as expected e.g. an increase in the volume of traffic is associated with an increase in pollutant concentration etc.

It should be noted that the explanatory terms of background NO<sub>x</sub> and background O<sub>3</sub> are somewhat negatively correlated (-0.55). In the previous Chapter the threshold for correlation was set at +/-0.5, and so by strictly repeating the procedure of Chapter 6, these two variables should not be permitted to enter the same GAM. However, since the correlation between these two variables is only marginally over the arbitrarily chosen limit, it was deemed acceptable to include both background NO<sub>x</sub> and O<sub>3</sub> into the NO<sub>2</sub> GAM. To ensure that the model structure was not significantly affected by the inclusion of both these explanatory terms, the smooth curves for all variables were examined after the inclusion of an additional term; if, in this case, the inclusion of O<sub>3</sub> lead to an alteration in the smooth curves for those variables already selected (i.e., background NO<sub>x</sub>, traffic flow and u,v) then the term would not have been used in the final model. Since, inclusion of O<sub>3</sub> did not lead to a change in the smooth plots however, it was accepted. The O<sub>3</sub> term should represent the photochemical processes between NO<sub>x</sub>, NO<sub>2</sub> and O<sub>3</sub>.

#### 7.3.4.2. GAM prediction

GAM predictions were made using a Bootstrap technique. N random samples, equivalent to 75 % of the original input dataset, were randomly selected. The NO<sub>x</sub> and NO<sub>2</sub> GAMs developed in stage 1 were fitted to each sub-sample and then used to predict the remaining 25 % of the input dataset. The final GAM predictions were calculated by taking the mean of each hour predicted for the n samples. All calculations were made with 1000 bootstrap replicates (n = 1000). This procedure ensured that the same data used to construct the model were not used for prediction. All predictions were therefore made using an independent (withheld) sample of data.



## 7.4. Results and discussion

The measured daily concentrations of  $\text{NO}_x$  and  $\text{NO}_2$  have been compared with predictions made through the use of the GAMs and the ADMS-Urban model (Table 37). Both model techniques under predict  $\text{NO}_2$  at Gillygate, particularly the ADMS-Urban model. In terms of  $\text{NO}_x$  concentration, ADMS-Urban performs better than for  $\text{NO}_2$  predictions, predicting an annual mean within 11 % of the measured, compared with 21 % for  $\text{NO}_2$ . For the GAM, annual mean predictions were within 3 % and 5% for  $\text{NO}_2$  and  $\text{NO}_x$ , respectively. Table 37 also shows the root-mean square errors of the hourly deviance for both the GAM and the ADMS-Urban predictions. The results show that the deviance of the GAM predictions from the measured values is considerably lower than that of the ADMS-Urban model.

**Table 37:** Measured and predicted  $\text{NO}_x$  and  $\text{NO}_2$  concentrations (ppb) at Gillygate for 2005 and the root mean square error of the hourly deviance

	Measured		ADMS-Urban		GAM	
	$\text{NO}_x$	$\text{NO}_2$	$\text{NO}_x$	$\text{NO}_2$	$\text{NO}_x$	$\text{NO}_2$
Annual Mean	38	19	34	15	37	18
Root mean square error of hourly deviance	-	-	24.9	9.6	18.1	6.4

Simple pollution roses, where pollution concentration is averaged for various wind direction categories (i.e. 0-10, 10-20° etc.), give an indication as to the location of emission sources at a particular site. Bivariate polar plots, an extension of simple pollution roses, provide a comprehensive picture not only of the direction of influential pollution sources but also of their wind speed dependence (Carslaw et al., 2006). The technique has primarily been used to investigate emission sources in close proximity to international airports (Carslaw et al., 2006). The plots are constructed by averaging pollutant concentration by wind speed categories (0-1, 1-2  $\text{m s}^{-1}$  etc.) as well as wind direction (0-10, 10-20° etc.). The work by Carslaw et al. (2006), an extension of work carried out by Yu et al. (2004), provides a detailed discussion into the bivariate polar plot technique. This paper also identifies the suitability of this technique for investigating the complex wind-flow interactions often experienced in urban street canyons.

Bivariate polar plots have been used to analyse the monitored  $\text{NO}_x$  and  $\text{NO}_2$  concentrations recorded at Gillygate (Figure 65a and b). The centre of the plot (receptor point) corresponds to 0  $\text{m s}^{-1}$ ; Gillygate is orientated approximately 30° from north.



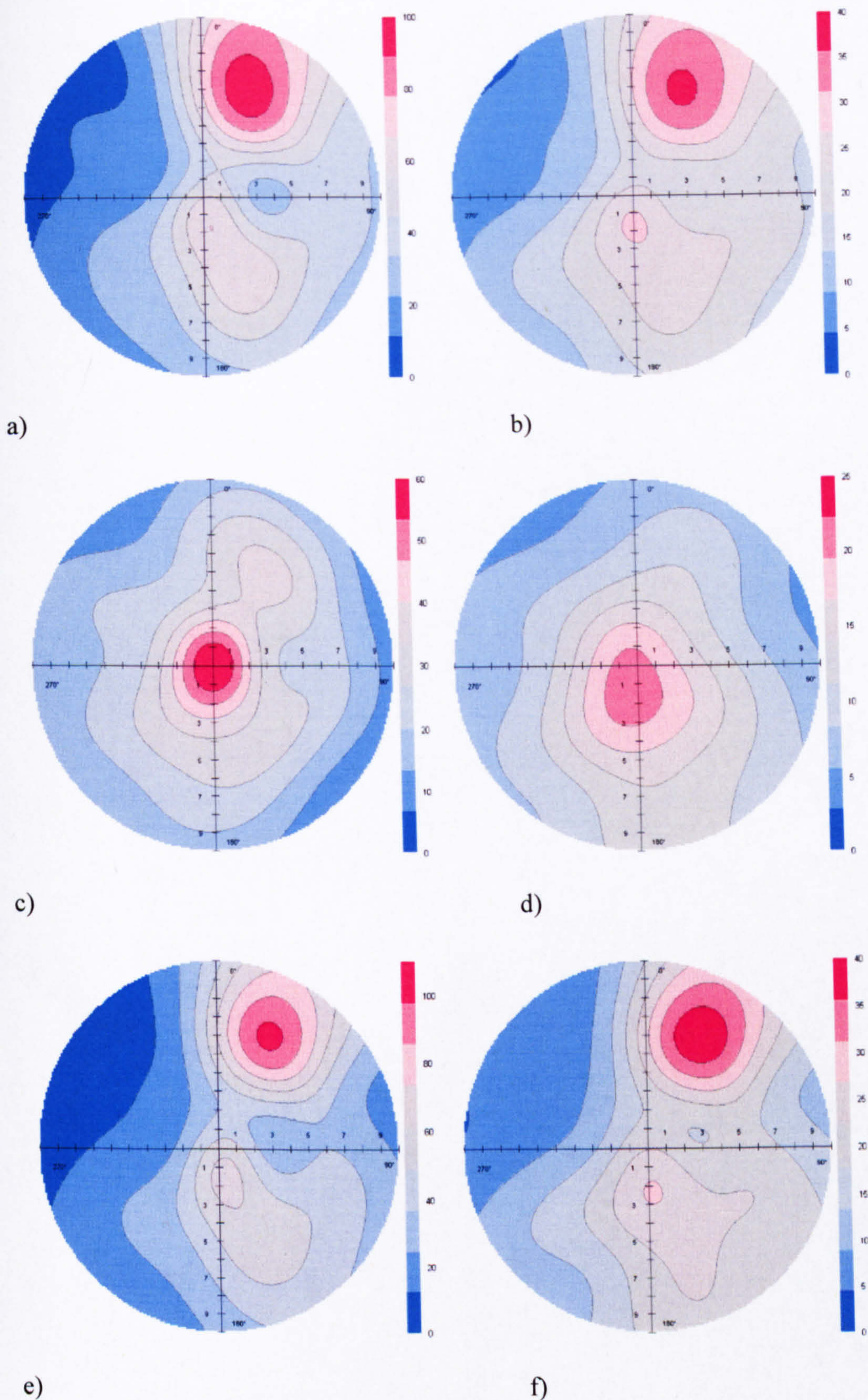


**Figure 65:** Smoothed bivariate wind-pollution roses for measured and predicted  $\text{NO}_x$  and  $\text{NO}_2$  concentrations at Gillygate. a) Measured  $\text{NO}_x$ , b) Measured  $\text{NO}_2$ , c) ADMS-Urban  $\text{NO}_x$ , d) ADMS-Urban  $\text{NO}_2$ , e) GAM  $\text{NO}_x$ , f) GAM  $\text{NO}_2$ . Note that the scale for the ADMS plots (c and d) are different to the others to accommodate the difference in the predictions without losing detail. The centre of each plot is at  $0 \text{ ms}^{-1}$  and the circumference at  $10 \text{ ms}^{-1}$ .



There are several interesting elements that should be noted. Firstly, the highest concentrations are recorded when the wind blows at angles parallel to, or near parallel to, the axis of Gillygate (Figure 65a and b). Secondly, the  $\text{NO}_x$  and  $\text{NO}_2$  concentrations generally decrease as wind speeds increase (inverse relationship). High pollutant concentrations at low wind speeds is suggestive of a local ground level source, as an increase in wind speed will result in greater turbulence and dilution of the plume. The results therefore suggest that the  $\text{NO}_x$  and  $\text{NO}_2$  concentrations at Gillygate are heavily dominated by traffic emissions from vehicles using the street.

The region of high  $\text{NO}_x$  and  $\text{NO}_2$  to the NE of the plot (approximately  $30^\circ$ ) can be indicative of an elevated source e.g. a chimneystack, since at high wind speeds the plume is more likely to reach ground level locally. However, an investigation of the vicinity around Gillygate showed that no such sources were present. A closer examination of the  $\text{NO}_x$  and  $\text{NO}_2$  concentrations for these points (wind speed  $> 3 \text{ m s}^{-1}$ , wind direction from  $0$ - $50^\circ$ ) shows that the source displays characteristics of strong traffic emissions (Figure 66). It is likely that during parallel, or near parallel wind directions, the traffic emissions along the road are channelled down the street, as found previously by Boddy et al. (2005a).

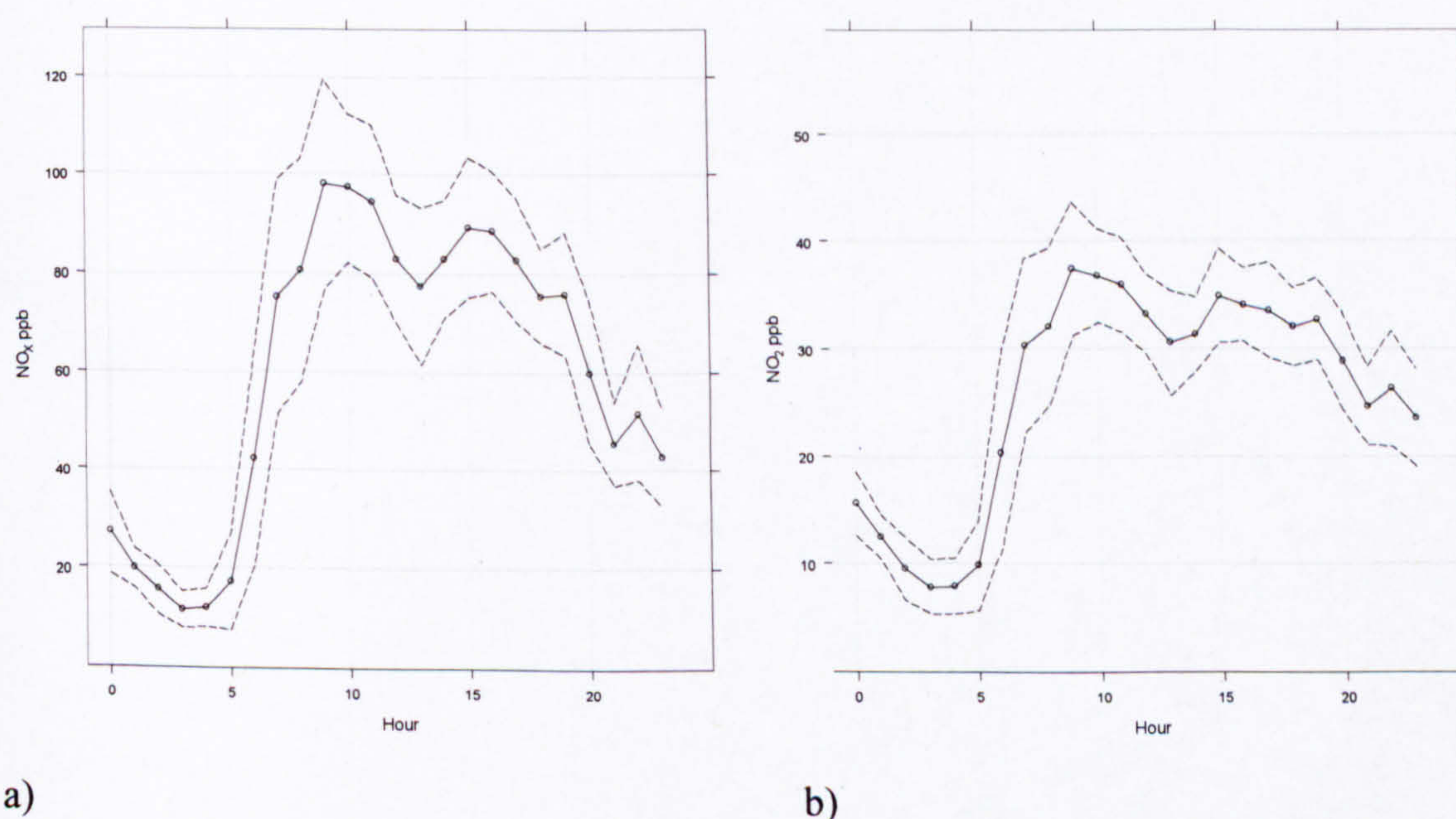


**Figure 66:** Diurnal profile of  $\text{NO}_x$  (a) and  $\text{NO}_2$  (b) concentrations for wind speeds greater than  $3 \text{ m s}^{-1}$  and between  $0^\circ$  and  $50^\circ$ . The dashed lines show the 95% confidence intervals.

In a typical street canyon, the highest pollutant concentrations are seen at the leeward side of the canyon in the presence of perpendicular winds. Under such conditions, an across canyon vortex effectively reverses the wind flow at street level, so vehicular emissions released in the street are channelled towards the leeward side. Marylebone Road in London provides a good example of an urban street canyon and the associated across canyon vortex. Orientated in an approximately east-west direction, with the monitor being on the south side of the canyon, the highest



concentrations at Marylebone Road are observed when winds blow from the south (Figure 67). The evidence presented in Figure 65a and b therefore suggest that the pollutant-wind interaction at Gillygate is complex since it does not follow this idealised street canyon characteristic.

Bivariate plots have also been produced from the input wind flow (speed and direction) and model output ( $\text{NO}_x$  and  $\text{NO}_2$  predictions) for both ADMS-Urban (Figure 65c and d) and the two GAMs (Figure 65e and f), which can be compared with Figure 65 (a) and (b) to illustrate whether the models can reconstruct the complex wind flow-pollutant interactions that occur in a street canyon.

The scales used to plot the ADMS-Urban predictions are considerably smaller than those of the measured concentrations reflecting the under-estimation of the model predictions seen in Table 37.

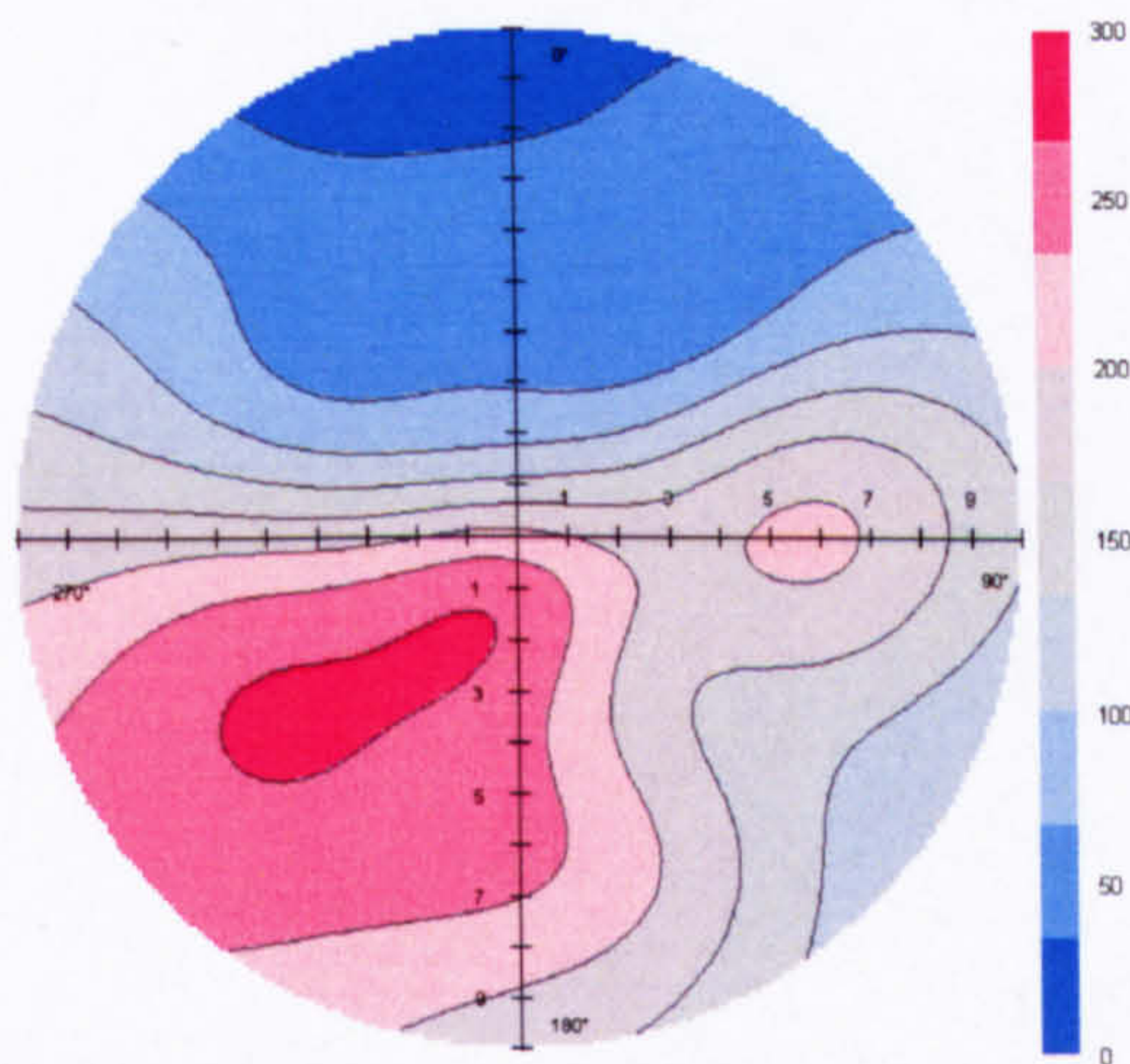


**Figure 67:** Bivariate wind-pollution rose for measured  $\text{NO}_x$  concentrations at the Marylebone Road, London. The centre of each plot is at  $0 \text{ ms}^{-1}$  and the circumference at  $10 \text{ ms}^{-1}$ .

The ADMS-Urban bivariate plots for  $\text{NO}_x$  (Figure 65 c) and  $\text{NO}_2$  (Figure 65 d) show little resemblance to those of the measured concentrations (Figure 65a and b), suggesting that the model is not representing the complex local wind flow interactions found in the Gillygate street canyon. There is no evidence of the high  $\text{NO}_2$  region to the NE of the site and the higher band of  $\text{NO}_2$  aligned with the orientation of the street is relatively less pronounced. Instead, the ADMS-Urban  $\text{NO}_2$  plot displays the highest pollutant concentrations at extremely low wind speeds from all directions. In the ADMS-Urban  $\text{NO}_x$  plot, there is greater evidence of the peak in pollution when winds blow from  $30^\circ$ , albeit at concentrations of 30 to 40 ppb (not the 80 to 100 ppb seen in the measured concentrations). Again, the highest  $\text{NO}_x$  concentrations are found at low wind speeds from all directions (centre of the plot).

The GAM results (Figure 65e and f) show clear similarities to the measured concentrations (Figure 65a and b). Both the region of high pollutant concentrations to the NE of the site and the road emission region can be clearly seen, which suggests that the GAM can



better reconstruct the localised interaction between wind speed, wind direction and traffic emissions in Gillygate, compared to the dispersion model.

A sensitivity study has been carried out to investigate whether the magnitude and spatial variation of the observed NO<sub>x</sub> and NO<sub>2</sub> concentrations could be reproduced in the ADMS-Urban model predictions (such as by doubling the traffic flows, inclusion of additional road sources etc.). The results are shown in Table 38.

**Table 38:** Annual mean predictions (2005) of NO<sub>x</sub> and NO<sub>2</sub> concentrations for various scenarios. \* Only one road source representing Gillygate is modelled.

Description	Model scenario	Annual mean		NO <sub>x</sub> : NO <sub>2</sub>
		NO <sub>x</sub> (ppb)	NO <sub>2</sub> (ppb)	
Measured	-	38.3	18.6	0.49
Base case (one road source representing Gillygate) *	1	33.8	14.7	0.44
Double traffic flow on Gillygate *	2	50.7	18.3	0.36
Canyon height of Gillygate adjusted to 20m *	3	36.1	15.9	0.44
Canyon height of Gillygate adjusted to 30m *	4	37.4	17.3	0.46
Increased primary NO <sub>2</sub> emissions to 15% *	5	33.8	15.4	0.46
Increased primary NO <sub>2</sub> emissions to 20% *	6	33.8	17.5	0.52
3 road sources representing the northern 3-way junction	7	33.9	14.8	0.44
All roads in the city. Background site = Dunnington	8	33.4	15.7	0.47
Monin Obukhov length of 10 m (small towns of less than 50 000) *	9	36.0	15.4	0.43
Monin Obukhov length of 100 m (large conurbations of 1 million) *	10	33.6	14.6	0.44
Surface roughness of 0.3 m (recommended for agricultural land) *	11	33.0	14.7	0.45
Surface roughness of 1 m (recommended for cities and woodlands) *	12	33.7	14.6	0.43



Doubling the Gillygate traffic volume (scenario 2) has a large effect on the predicted  $\text{NO}_x$  concentration, leading to an increase of around 50 % compared to the base case. This scenario also resulted in a 24 % increase in the  $\text{NO}_2$  predictions, with the predicted annual mean resembling that measured.

Scenarios 3 and 4 illustrate how the dimensions of a street canyon can influence the predicted concentrations within it. Canyon height affects the size of the across canyon vortex which is established in the street (Equation 8) and so in turn affects the concentrations predicted by the model. Increasing the canyon height from 15 m to 20 (30 m) has the effect of increasing the  $\text{NO}_x$  concentration by 7 % (11 %) and that of  $\text{NO}_2$  by 8 % (18 %). Although the canyon height is not a constant 15 m along the whole length of Gillygate (an area of model uncertainty), it is unlikely to be as much as 20-30 m. However, these tests do illustrate that the model predictions are particularly sensitive to the canyon dimensions.

Scenarios 5 and 6 were concerned with primary  $\text{NO}_2$  emissions, since recent studies suggest primary  $\text{NO}_2$  emissions are of greater importance than previously thought (AQEG, 2006). The primary  $\text{NO}_2$  fraction was adjusted from the model default 10% of  $\text{NO}_x$  emissions to 15% (scenario 5) and 20% (scenario 6). In both of these scenarios, the  $\text{NO}_x$  concentration remained invariant, whilst the  $\text{NO}_2$  concentration increased. Consequently, the  $\text{NO}_2$ :  $\text{NO}_x$  ratio more closely resembled that measured. The measured  $\text{NO}_2$ :  $\text{NO}_x$  ratio was 0.49, for the baseline scenario it was 0.44, and for the 15 % and 20 % primary  $\text{NO}_2$  emissions assumptions was 0.46 and 0.52 respectively. To reproduce the observed  $\text{NO}_2$ :  $\text{NO}_x$  ratio, the primary  $\text{NO}_2$  emissions proportion would need to be of the order of 17-18 %, in agreement with the observed ratio for many UK regions (AQEG, 2006). In London, this increase is thought to be due to the increased use of certain after-treatment devices fitted to light and heavy duty vehicles. In York, it is thought that the relatively high numbers of diesel buses (not fitted with particle traps) and the increasing use of diesel engines in all vehicles types (derived from local traffic surveys) could contribute to a high primary  $\text{NO}_2$  fraction.

Scenarios 7 and 8 include, firstly some of the other roads connected to Gillygate (scenario 7) and secondly, all other road sources in the City of York (scenario 8), rather than just Gillygate itself. The traffic activity data for the additional road sources came from the SATURN traffic model (Van Vliet, 1982). The SATURN model provides an estimate of the annual average daily traffic flow and average speed for every major road in the city. These activity data were combined with emission factors and the total road traffic emissions calculated for the additional scenarios (explained previously). It should be noted that for scenario 8 the background data were changed from the urban background station (Bootham) to the background station located outside the city centre (Dunnington) so as to avoid double counting of emission sources.

Scenario 7 made only a minor difference for both pollutants and for scenario 8, there was a slight decrease in  $\text{NO}_x$  of around 1 % and a small increase (~7 %) in  $\text{NO}_2$  concentrations.



The inclusion of all roads in the city (scenario 8) resulted in a slightly more pronounced region along the alignment of the road for predicted NO<sub>2</sub> concentrations compared to the base case (not shown for brevity); however the highest concentrations were still concentrated at the receptor point. The predicted NO<sub>x</sub> concentrations showed a less defined region to the NE than the original base case scenario, and in fact displayed higher concentrations at the receptor point (not shown). It is likely that the change in background data (i.e., from Bootham to Dunnington) had a profound effect on the ambient NO<sub>x</sub> and NO<sub>2</sub> concentrations predicted at Gillygate with the ADMS-Urban model.

Finally, scenarios 9-12 vary the base case values for the Monin-Obukhov length (9 and 10) and the surface roughness (11 and 12) of 30 m and 0.5 m respectively, to investigate the sensitivity of the model to these parameters. Setting the Monin-Obukhov length to 30 m (lower limit threshold) was selected as it is a value recommended for a city of York's size. By setting the lower limit to 10 m (typical for a city with < 50,000 inhabitants, much smaller than York), the NO<sub>2</sub> and NO<sub>x</sub> concentrations become more closely aligned with the measurements, although the NO<sub>2</sub>: NO<sub>x</sub> ratio is still very similar to the base case. Increasing this parameter to a minimum of 100 m (typical for a city with ≥ 1 million inhabitants) has a very minor effect on both concentrations. Similarly, altering the surface roughness variable has only a minor effect on the prediction of both NO<sub>x</sub> and NO<sub>2</sub> concentrations.

Despite some of these scenarios producing annual mean predictions more in line with measured concentrations and the observed NO<sub>2</sub>: NO<sub>x</sub> ratio, the high measured concentrations of NO<sub>x</sub> and NO<sub>2</sub> to the NE of the receptor point (~ 68 and 29 ppb, respectively) were not reproduced through any of these scenarios. This is most likely because the conditions seen at Gillygate (Figure 65 a and b) are specific to that site, and the processes used to reconstruct the concentrations in ADMS-Urban are idealistic. It is somewhat unfair to expect ADMS-Urban to reproduce extremely localised conditions, which do not follow the fundamental ideas of what a street canyon should behave like.

There are several important differences between ADMS-Urban and the GAM technique which should be noted. Firstly, ADMS-Urban can more easily predict a variety of pollutant concentrations (NO<sub>x</sub>, NO<sub>2</sub>, PM<sub>10</sub>, SO<sub>2</sub> and O<sub>3</sub>) in a range of different locations. ADMS-Urban could also predict concentrations for the whole of York itself in the form of contour maps. This latter task is difficult for GAMs where a model is developed to predict a single pollutant at a specific location; several different models would be required to cover various locations and pollutants.

Secondly, the GAMs created for this study are restricted to sites where traffic counts are available (which are limited in York). ADMS-Urban, however, can be applied to wide areas since it uses SATURN model predictions as traffic inputs (available for the majority of streets in York city centre). Further, GAMs are less useful for predictive purposes as emissions characteristics will change over time; it would be necessary to add a further explanatory variable



to the GAM model to explain such changes in relationships over time (such as, a decrease in NO<sub>x</sub> emissions associated with new technology for petrol cars).

Also, since only a single road source had been modelled, the run times for ADMS-Urban were kept low (i.e. couple of minutes). However, as the complexity in the input data increases (i.e. multiple sources such as scenario 8) the run times for this model can reach two to three days. GAMs, once they have been developed take around an hour to process the 1000 iterations (without the bootstrap procedure the prediction process only takes several minutes).

A limitation of the current work is that residual autocorrelation was not accounted for in the GAMs. As a consequence, the prediction uncertainties for the GAMs may be optimistic (Wood, 2006). However, previous work also in a street canyon setting using Generalized Additive Mixed Models, which can account for the correlation structure of the data, showed that accounting for the autocorrelation only had a minor effect on the prediction uncertainties (Carslaw et al., 2007). Furthermore, all reported model uncertainties in this study were based on model predictions using data sets independent of those used to build the models. Accepting this limitation, the GAM technique does well in reproducing the observed NO<sub>x</sub> and NO<sub>2</sub> concentrations and shows the strength of such a technique for specific applications where appropriate input data are available. The GAM approach is also of use as an explanatory tool in this context.

## 7.5. Chapter summary

This work has highlighted that GAMs and bivariate polar plots can offer detailed information regarding the complex wind-concentration interaction in a street canyon setting. The non-parametric GAMs developed in this paper predict the annual mean NO<sub>x</sub> and NO<sub>2</sub> concentrations observed at Gillygate with high accuracy. An important finding is that GAMs reproduce the wind speed – wind direction dependence of concentrations shown in the measured bivariate polar plots (Figure 65 a and b), thus suggesting that this technique has the ability to capture the complex interaction between winds and the ambient pollutant concentrations in a complex urban environment.

The sensitivity study (Table 38) showed that the ADMS-Urban model predictions could be improved through changes to some of the input parameters. In particular, altering the proportion of primary NO<sub>2</sub> emissions significantly improved the predicted NO<sub>2</sub>: NO<sub>x</sub> ratio when the value was set to that observed in many UK regions (AQEG, 2006). This observation demonstrates the importance of using the correct input parameters relevant to a specific location to initialise such a dispersion model. The sensitivity study also illustrated how the model could be used to investigate variations in pollutant concentrations as a result of proposed changes in air quality management strategies. This type of information is extremely important to local authorities and other organisational bodies.



The findings of this Chapter have therefore potentially highlighted the differing air quality management roles of the two modelling techniques; the use of GAMs over ADMS-Urban if the aim of study is to understand and reproduce localised air quality in complex urban environments, and the use of ADMS-Urban over GAMs when the user is more concerned with the relative changes in air quality (i.e. the impact of various management strategies). Since only one street canyon has been investigated here, it would be of interest to analyse the two modelling techniques in other urban environments, both where the typical effects of a street canyon are thought to exist, and also in areas that are not heavily influenced by complex wind-flow interactions.

The studies carried out by ITS in the street of Gillygate provide evidence of canyonisation in the street of Gillygate (Boddy 2006a, 2006b, Dixon 2006). However, the wind speed – wind direction plot for Gillygate in this Chapter (Figure 65 a and b) shows that the  $\text{NO}_x$  and  $\text{NO}_2$  concentrations recorded at this monitoring site do not display street canyon characteristics. This concept was also suggested in Chapter 6, Figure 57d. Indeed Figure 57d in particular illustrates the reverse situation as what would be expected in a street canyon. This discrepancy between studies is interesting. However, since the analysis of these studies have been carried out at separate locations along Gillygate the discrepancy could be a consequence of differing relationships between wind flow and pollutant concentration along the street. It would be interesting to simultaneously monitor the  $\text{NO}_x$  and  $\text{NO}_2$  concentrations at multiple locations along Gillygate so that a more complete understanding can be achieved.

It would be reasonable to expect the two wind interactive plots produced within this thesis for the site of Gillygate (Figure 57 and Figure 65) to be similar. However, there are striking differences. Firstly, the peak in  $\text{NO}_x$  and  $\text{NO}_2$  concentrations to the NE of Gillygate seen in Figure 65a and b, believed a consequence of the road junction in this direction, is not reproduced in the long-term plot (Figure 57d). Moreover, Figure 57d shows the highest  $\text{NO}_2$  concentrations from a southeasterly direction, a fact that is not reproduced in the plot containing the hourly 2005 data (Figure 65 a and b).

It is possible that the case study year of 2005, chosen since this was the latest full year of monitoring data available at the time of study, was subject to unusual conditions and the consequent NE peak caused by an isolated event. Equally, it could also be the case that the difference in temporal scale used to create the plots (24-hour mean concentrations for Figure 57d and hourly mean concentrations for Figure 65) has highlighted different relationships. To investigate this latter point further, a new plot (Figure 68) using 24-hr  $\text{NO}_x$  and  $\text{NO}_2$  concentrations has been produced from the hourly data used to create Figure 65.



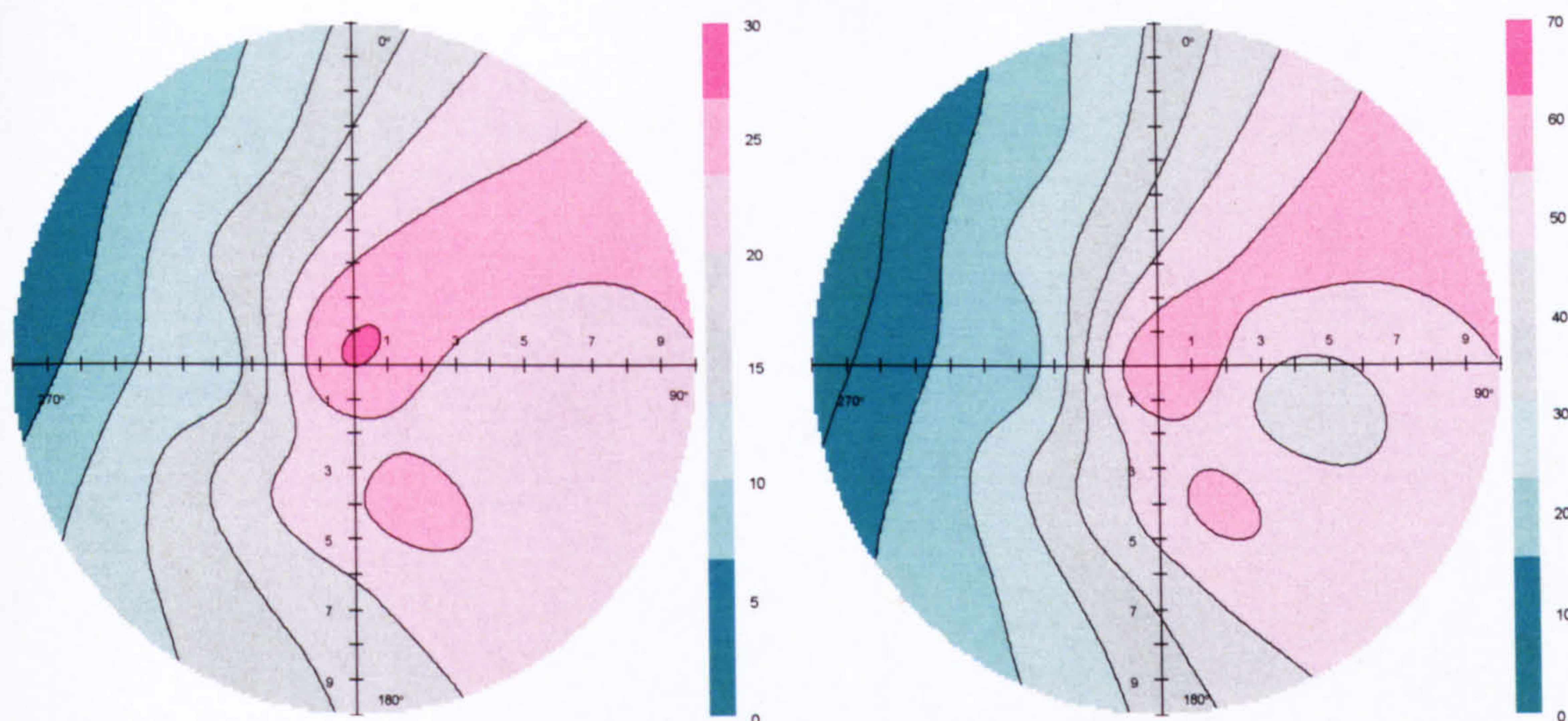


**Figure 68:** Observed 24-hr mean (a)  $\text{NO}_2$  and (b)  $\text{NO}_x$  concentrations recorded at Gillygate for the year 2005. 24-hr means are calculated from the hourly  $\text{NO}_x$  and  $\text{NO}_2$  observations used to create Figure 65.

It can be seen in Figure 68 that the change in scale for the  $\text{NO}_x$  and  $\text{NO}_2$  concentrations has quite substantially altered the shape of relationship between pollutant concentration and the wind flow. The NE peak in  $\text{NO}_x$  and  $\text{NO}_2$  concentration has been removed, with the highest concentrations now occurring during easterly wind flow. The relationships illustrated in Figure 68 are much similar to those seen in Chapter 6 (Figure 57d) and so indicate that the choice of temporal scale used to analyse ambient pollutant concentrations is important.

Also the discrepancy between the annual mean  $\text{NO}_x$  and  $\text{NO}_2$  concentrations predicted for 2005 in Chapter 4 with those for this Chapter can be explained by a difference in traffic counts used to calculate the traffic emissions. Chapter 4 used the SATURN model predictions as AADT inputs for each of the roads included in the analysis. However, for the purpose of this Chapter, the AADT estimations used as input for ADMS-Urban came from the SCOOT traffic management system. These SCOOT data could not be used in Chapter 4 since they are only available for Gillygate. Since multiple sites are analysed in Chapter 4 it was considered more appropriate to use the SATURN traffic data as this is available for all road sources in York. Moreover, in this Chapter only the traffic survey data for Gillygate was used to estimate the breakdown of vehicle type in the calculation of traffic emissions; in the previous Chapter the results from all sites were combined to estimate the overall vehicle breakdown for York. Finally, differences in background pollution data will also contribute to the differences in annual mean  $\text{NO}_x$  and  $\text{NO}_2$  concentrations predicted for Gillygate in this Chapter and those in Chapter 4.



## 8. Conclusions

Since the funding for this PhD was jointly provided by NERC and the CYC (a CASE studentship) an important focus of the project was to update or 'fine-tune' the dispersion modelling procedure with regards to the urban area of York. Indeed, much of the work carried out in Chapter 4 is used regularly by the CYC in their day-to-day air quality modelling work. This work is of great value to the CYC air quality department since it is important to use up-to-date emission inventories in dispersion modelling, thus ensuring the models are initialised with locally relevant data. Importantly, the results of dispersion modelling work carried out by CYC are frequently used to aid management decisions and so it is vital that the input emissions estimated for York are as representative of 'true' emissions as possible.

The extensive traffic surveys carried out across the city characterised the traffic fleet using the York road network. The results of this survey will aid in quantifying and understanding air quality across the city of York. It was seen that the traffic fleet (composition) using the road network in York is actually newer than that which is estimated from national transport statistics. As section 4.5 showed, much of the discrepancy between York and the national traffic composition derives from the larger vehicle categories, such as buses and HGVs. The York bus fleet for example, is considerably newer than the national average, with 80 % of all buses surveyed falling into the EURO 3 category as opposed to 50 % nationally. As a consequence, the estimated vehicular emissions for the York area were lower than those estimated using national transport statistics (24 % reduction in NO<sub>2</sub> and NO<sub>x</sub> emissions compared to base case estimates using national statistics). The modified traffic emission data were subsequently used in the dispersion modelling process and resulted in lower ambient NO<sub>x</sub> and NO<sub>2</sub> concentration estimates (section 4.5.4); on average the NO<sub>2</sub> concentrations predicted at the five-receptor sites fell by 1.6 % (3.9 % for NO<sub>x</sub>).

It should be noted that the traffic survey results would need regular updates so that changes to the traffic fleet over time are taken into consideration. The methodology created as part of Chapter 4 could therefore be used as a template for future surveys.

Chapter 4 also investigated the sensitivity of ADMS-Urban to its basic input parameters. Following the recent scientific work regarding primary NO<sub>2</sub> emissions (Carslaw and Beevers, 2004 a, 2004b; Carslaw, 2005), it was considered important to increase the fixed value of the NO<sub>2</sub>: NO<sub>x</sub> ratio used in the modelling framework. A fixed value of 18 % was chosen as the new default value (since this produced an NO<sub>2</sub>: NO<sub>x</sub> ratio more in line with that from observed data) and the subsequent model results highlighted the impact that increased NO<sub>2</sub> emissions had on ambient predictions (NO<sub>2</sub> concentrations increased by around 3 % compared to the base case). It would be desirable to more accurately calculate the NO<sub>2</sub> to NO<sub>x</sub> emissions ratio for the York area since the work carried out as part of this thesis has highlighted its importance in terms of reproducing the ambient NO<sub>x</sub> and NO<sub>2</sub> concentrations.



The work carried out in Chapter 4 was the basis for the ADMS-Urban modelling work contained in the subsequent Chapters. The new base case will be used by the CYC in ensuing air quality studies since it incorporates both the updated transport emissions, increased primary NO<sub>2</sub> factor, and also the most locally relevant Monin-Obukhov and surface roughness lengths. Chapter 5 summarises recent air quality data in York. Unsurprisingly, the highest NO<sub>x</sub> concentrations recorded at the various monitoring sites in York are found at the roadside sites; and from these roadside sites those with the heaviest traffic flows record the highest NO<sub>x</sub>. Interestingly, the highest NO<sub>2</sub> concentrations recorded in York occur at the urban centre site some distance away from the influence of roads. Therefore, despite much of the centre of York being pedestrianised, there is still a risk of public exposure to relatively high NO<sub>2</sub> concentrations. This Chapter also likens the air quality in York to that of suburban sites on the outskirts of major urban areas (e.g. Hillingdon, London) rather than the air quality seen in other, larger, urban areas (e.g. London).

The analysis within Chapter 5 also contains a thorough investigation of the long-term trends in NO<sub>x</sub> and NO<sub>2</sub> concentrations recorded at some of the monitoring sites in York. Preliminary analysis (Table 26) revealed an overall decrease in NO<sub>x</sub> and NO<sub>2</sub> concentrations at all four long-term sites. For example, the overall spread of NO<sub>x</sub> concentrations (inter quartile range) at Fishergate has fallen by around 10 ppb over the period 1999 to 2006. Subsequent linear regression analysis revealed a negative slope coefficient (trend) in NO<sub>x</sub> concentrations at all four of the monitoring sites under study, but only the negative trend in NO<sub>x</sub> at Fishergate was found to be statistically significant. Linear regression using the NO<sub>2</sub> concentrations at the four long-term sites also suggested a negative trend, although none of the slope coefficients were statistically significant. Concentrating on Fishergate, this difference in NO<sub>x</sub> and NO<sub>2</sub> concentration trends indicates a distinct difference in the behaviour of these two pollutants: the NO<sub>2</sub>: NO<sub>x</sub> ratio has significantly increased at this site over the study years.

Interestingly, the analysis in Chapter 5 revealed an increase in the annual maximum NO<sub>x</sub> and NO<sub>2</sub> concentrations at the sites of Bootham, Fishergate and City Centre (only City Centre slope coefficient was statistically significant, see Figure 36). This increase in maximum concentrations is perhaps indicative of an increase in sporadic or episodic NO<sub>x</sub> and NO<sub>2</sub> events given that the NO<sub>x</sub>, and to some extent NO<sub>2</sub>, concentrations generally appear to be declining over the period. In light of this result the hourly NO<sub>2</sub> objective may in the future become increasingly tougher to meet, and the annual mean objective easier.

Section 5.4.2 provides evidence to suggest that the change in the ratio of NO<sub>2</sub>: NO<sub>x</sub> concentrations observed at a number of sites in York may be a response to increased O<sub>3</sub> concentrations (measured at Dunnington). Other investigations regarding the changing NO<sub>x</sub>, NO<sub>2</sub> and NO<sub>2</sub>: NO<sub>x</sub> ratio have concluded that increasing primary NO<sub>2</sub> emissions are the cause. It is likely, therefore, that both increases in primary NO<sub>2</sub>, alongside increases in O<sub>3</sub> concentrations are working in tandem to increase/influence the NO<sub>2</sub>: NO<sub>x</sub> ratio.



Subsequent analysis of NO<sub>x</sub> and NO<sub>2</sub> concentrations at other cities across the UK revealed similar patterns in the behaviour of these pollutants. 35 out of 38 sites showed a negative trend in NO<sub>x</sub> concentration over the eight year period, whereas, only 26 of 38 sites have a negative trend in NO<sub>2</sub>. This evidence therefore, crudely suggests a greater decline in NO<sub>x</sub> compared to NO<sub>2</sub> across the UK monitoring sites.

Further analysis was carried out to reveal whether the rate of change in NO<sub>x</sub> and NO<sub>2</sub> concentrations was related to the size of urban area (indicated by population) but no statistical evidence was found (Figure 40 and Figure 41). Additionally, analysis designed to reveal patterns/similarities in trends at the different types of monitoring sites also revealed little information and so provided no evidence to indicate similarities in the behaviour of NO<sub>x</sub> (and NO<sub>2</sub>) at similar site types (Figure 42).

Finally, the analysis of Chapter 5 explored monthly mean NO<sub>x</sub> and NO<sub>2</sub> concentrations as opposed to annual means. Despite some large variability in results, section 5.4.4 (Figure 46 and Figure 47) showed significant negative trends in monthly NO<sub>x</sub> concentrations at Fishergate for the months of March, May, June, July and August. The NO<sub>x</sub> concentrations at Bootham also displayed a significant reduction for the month of August. These significant reductions in pollutant concentrations coincide with busy tourism months. The reductions in NO<sub>x</sub> and NO<sub>2</sub> concentrations, highlighted in the Chapter 5 analysis, are an indication of successful air quality management strategies implemented by the CYC.

The analyses contained within Chapters 6 and 7 use the statistical technique of GAMs to investigate the non-linear behaviour of NO<sub>x</sub> and NO<sub>2</sub> concentrations. These analyses have provided a greater understanding of the behaviour of NO<sub>x</sub> and NO<sub>2</sub> concentrations at the various study sites in York compared to the linear regression applied in Chapter 5.

The ability of GAMs to incorporate non-linear structure in their calculations served especially useful in terms of defining the site-specific relationships between pollutant concentrations and wind flow. Figure 57 illustrated the unique interaction between wind flow and pollutant concentration at each of the monitoring sites. In each case, the influences of local emission sources were shown in the polar plots and in the majority of cases, the pollutant concentrations were influenced strongly by neighbouring roads.

The GAM analysis in Chapter 6 also revealed the importance of background pollutant concentrations in reproducing/explaining the NO<sub>x</sub> and NO<sub>2</sub> concentrations recorded in York. Indeed, GAMs containing solely the background pollutant concentrations as an explanatory term ( $\text{Log}(\text{NO}_x) \sim s(\text{bkg NO}_x)$ ) could explain in excess of around 40 % of the total variability in observed NO<sub>x</sub> concentrations at all monitoring sites (Table 36), which provides strong evidence to suggest that the urban air quality in York is highly influenced by that of the wider area. Such evidence is interesting in terms of air quality strategy and management since it seems unlikely that hot spot or extremely localised emission control strategies would be completely successful in terms of reducing the ambient pollutant concentrations found in York. It would be more



desirable for the CYC to work in tandem with other local and district authorities in the Yorkshire area (or north east) to reduce the overall regional pollutant concentrations and also for there to be a greater emphasis on tackling the problem of air quality at a national scale.

Chapter 6 also investigated the long-term  $\text{NO}_x$  and  $\text{NO}_2$  concentrations made with ADMS-Urban. The same methodology that was applied to the monitored data (section 6.5) was applied to the predictions made with ADMS-Urban thus enabling similarities/differences in the GAM results to be highlighted. This analysis revealed that on the whole, the same explanatory variables were selected for both the monitored and predicted data. As found for monitored pollutant concentrations, the ADMS-Urban GAM analysis revealed the importance of background pollutant data in terms of reproducing the ADMS-Urban predictions. Indeed, background  $\text{NO}_x$  alone could explain around 90 % of the variability in predicted  $\text{NO}_x$  concentrations for a range of receptor sites (Table 36). This high dependence of ADMS-Urban predictions on background pollutant data suggests that a great deal of emphasis is placed on this variable in terms of the internal dispersion modelling procedure. It highlights the extreme importance of using locally relevant background input data.

The greatest difference between the GAMs created with monitored data and those created with ADMS-Urban predictions was for the trend term. The trends in  $\text{NO}_x$  and  $\text{NO}_2$  concentration for ADMS-Urban predictions showed a steady decline over the study years. The trend for observed  $\text{NO}_x$  and  $\text{NO}_2$  concentrations however showed an increase towards the end of the period. This difference in the trend curve could represent a fundamental change in the volume of emissions released in the urban area of York – something that has not been accounted for in the estimation of traffic emissions used as inputs for ADMS-Urban.

Finally, the case study comparison at Gillygate (Chapter 7), illustrated the predictive power of GAMs. The bootstrap procedure provided a method of prediction for the GAMs without over fitting. The study illustrated the inadequacies of ADMS-Urban at reproducing the complex wind speed- wind direction interaction with ambient pollutant concentrations at the site of Gillygate. This Chapter also used traffic count as an explanatory variable with some success; the crude relationship between traffic numbers and ambient  $\text{NO}_x$  and  $\text{NO}_2$  concentrations was as expected (positively associated).

An interesting aspect of the work carried out in Chapters 6 and 7 is the difference in the interactive wind term plots for the site of Gillygate. A closer examination of these data revealed that changing the scale of measurement data from hourly to 24-hr concentrations resulted in a substantial change in the relationship between wind flow and concentrations (Figure 68). For example, the large peak in  $\text{NO}_2$  (and  $\text{NO}_x$ ) concentrations seen to the NE of Gillygate (believed to be caused by a busy road junction in this area) was not as prominent when the same data were analysed on a different time scale (Figure 68). This analysis has therefore highlighted the importance of carrying out data analysis on a range of different time scales if a true understanding of  $\text{NO}_x$  and  $\text{NO}_2$  concentrations are to be gained.



Future studies could extend the detailed investigation of urban air quality ( $\text{NO}_x$  and  $\text{NO}_2$ ) concentrations in York to other urban areas of the UK. Chapter 5 provided a brief introduction to the trends in air quality in other cities across the UK but the analysis was not as detailed as that carried out for York in the subsequent Chapters. Much work has been carried out investigating the London area but the provincial towns around the UK are less well investigated. Norwich or other similar sized cities to York would be interesting to investigate, since there may well be similarities in the behaviour of  $\text{NO}_x$  and  $\text{NO}_2$  concentrations in comparison to York. The analysis within this thesis has highlighted the danger of assuming a similar behaviour of  $\text{NO}_x$  and  $\text{NO}_2$  concentrations in all urban areas.

It would also be interesting to carry out a comparison of GAMs with other dispersion models e.g. AERMOD, CALPUFF, CALINE3. For example, the Environmental Research Group at Kings College London have developed an air pollution toolkit to model a range of pollutants across the Greater London Area. It would therefore be of interest to carry out a similar cross comparison with this toolkit and/or other commercially available dispersion models.

Furthermore, it will also be interesting to study other air pollutants. The work carried out in this thesis has focused on  $\text{NO}_x$  and  $\text{NO}_2$  concentrations; however, there is a range of pollutants included in the NAQS (section 2.2.2) that are of particular threat to human health and/or the environment. The literature surrounding the use of GAMs in an air quality setting is not restricted to  $\text{NO}_x$  and  $\text{NO}_2$ , for example the Riess (2006) study used GAMs to investigate benzene and butadiene concentrations. It may therefore be a good idea to extend the investigations of Chapters 5, 6 and 7 to other notorious airborne pollutants; namely  $\text{PM}_{10}$ ,  $\text{PM}_{2.5}$  or  $\text{O}_3$  and so provide a more complete understanding of air pollution in the City of York.

The work carried out in this thesis was to a large degree dependant on the availability of monitoring data collected by the CYC and the Meteorological Office. The linear regression analysis in Chapter 5 is therefore limited to the 4 long-term monitoring sites. Indeed, the long-term trends analysis (Chapter 6) could not extend beyond April 2006 since the chemiluminescence analyser at Dunnington was removed. It would be interesting to apply some of the techniques developed in this thesis to longer running time series datasets, for example, the  $\text{NO}_2$  concentrations at the monitoring site in Glasgow Hope Street where data are available from 1982, or at London Harrow where the  $\text{NO}_2$  concentrations have been recorded since 1980 ([www. http://www.airquality.co.uk/archive/index.php](http://www.airquality.co.uk/archive/index.php)).

In conclusion, this thesis has provided valuable information regarding the  $\text{NO}_x$  and  $\text{NO}_2$  concentrations in and around the City of York (both spatially and temporarily). The study has shown that the use of relatively simple statistical techniques can be used to successfully investigate the behaviour of  $\text{NO}_x$  and  $\text{NO}_2$  concentrations and also to reproduce  $\text{NO}_x$  and  $\text{NO}_2$  concentrations with relative success.  $\text{NO}_2$  is one of three pollutants ( $\text{PM}_{10}$ ,  $\text{NO}_2$  and  $\text{O}_3$ ) that have been highlighted as essential pollutants to study by the draft NCAS composition report.



Furthermore, the increase in primary NO<sub>2</sub> concentrations seen at numerous sites across the UK has started to place even greater emphasis on the importance of understanding the behaviour of NO<sub>x</sub> and NO<sub>2</sub> concentrations in an urban setting in the hope that a more refined approach to NO<sub>x</sub> reduction strategy can be achieved. The information regarding the influence of regional air pollution contained within this thesis therefore sits within a very topical scientific setting and the general findings are highly important in terms of the general understanding of NO<sub>x</sub> and NO<sub>2</sub> behaviour in an urban environment.

A primary aim of this thesis was to establish the importance of regional air quality (NO<sub>2</sub> concentrations) in terms of explaining observed NO<sub>2</sub> concentrations in an urban area. Table 36 indicated that as much as 47 % of the NO<sub>2</sub> concentrations at roadside sites are a consequence of background or regional NO<sub>2</sub> concentrations. The fraction exceeds 69 % for the NO<sub>2</sub> concentrations recorded at the urban background monitoring site in York. This investigation has therefore highlighted the overall importance of regional air quality in explaining the behaviour of NO<sub>x</sub> and NO<sub>2</sub> concentrations in an urban area the size of York. As a result, it may be more productive to focus management strategies on the reduction of regional pollution levels as opposed to concentrating on smaller, hotspot locations.

This thesis has also highlighted the fact that the NO<sub>x</sub> and NO<sub>2</sub> concentrations observed at a roadside monitoring site in York behave quite differently from the those observed at a similar site type in London. Such observations warrant further investigation, but highlight the fact that universal management strategies applied to combat air pollution at specific site types in cities across the UK would most likely not result in universal improvements in air quality.

In terms of wider scientific context this study has highlighted the use of the statistical technique of generalised additive modelling in terms of analysing air quality data. GAMs provide a method of quantifying the contribution of background/regional air quality in explaining the roadside or urban centre air quality concentrations. This is a technique that can thus be applied to other urban areas and so enhance the general understanding of ambient air pollution and also the role of regional air pollution in an urban setting.

Finally, this study has also highlighted the value of using bivariate pollution roses in an urban air quality context. Previous studies have solely applied this graphical tool to airport air quality. The work contained within this thesis has confirmed the importance of bivariate pollution roses in an urban environment.



## 9. References

- Air Quality Expert Group (AQEG). 2004. Nitrogen Dioxide in the United Kingdom, Report prepared by the Air Quality Expert Group for the Department for Environment, Food and Rural Affairs; Scottish Executive; Welsh Assembly Government; and Department of the Environment in Northern Ireland. HMSO. The report can be found at: <http://www.defra.gov.uk/environment/airquality/aqeg/nitrogen-dioxide/index.htm>
- Air Quality Expert Group (AQEG). 2006. Trends in Primary Nitrogen Dioxide in the UK. Draft report for comment. Prepared for: Department for Environment, Food and Rural Affairs; Scottish Executive; Welsh Assembly Government; and Department of the Environment in Northern Ireland. HMSO. The report can be found at: <http://www.defra.gov.uk/environment/airquality/publications/primaryno2-trends/pdf/primary-no-trends.pdf>
- Aleksic, N., Boynton, G., Sistla, G., Perry, J. 2005. Concentrations and trends of benzene in ambient air over New York State during 1990-2003. *Atmospheric Environment* 39, 7894 – 7905
- Aldrin, M., Haff, I.H. 2005. Generalised additive modelling of air pollution, traffic volume and meteorology. *Atmospheric Environment* 39, 2145 – 2155
- Baccini, M., Biggeri, A., Lagazio, C., Lertxundi, A., Saez, M. 2007. Parametric and semi-parametric approaches in the analysis of short-term effects of air pollution on health. *Computational Statistics and Data Analysis* 51, 4324 – 4336
- Boddy, J.W.D., Smalley, R.J., Dixon, N.S., Tate J.E., Tomlin, A.S. 2005a. The spatial variability in concentrations of a traffic-related pollutant in two street canyons in York, UK–Part I: The influence of background winds. *Atmospheric Environment* 39, 3147 – 3161
- Boddy, J.W.D., Smalley, R.J., Goodman, P.S., Tate, J.E., Bell, M.C., Tomlin, A.S. 2005b. The spatial variability in concentrations of a traffic-related pollutant in two street canyons in York, UK–Part II: The influence of traffic characteristics. *Atmospheric Environment* 39, 3163 – 3176
- Bown, W. 1994. Deaths linked to London smog. *New Scientist* 142, 4
- Bower, J.S., Broughton, G.F.J., Stedman, J.R., Williams, M.L. 1994. A winter NO<sub>2</sub> smog episode in the UK. *Atmospheric Environment* 28, 461 – 475
- Brauer, M., Hoek, G., van Vliet, P., Meliefste, K., Fischer, P.H., Wijga, A., Koopman, L.P., Neijens, H.J., Gerritsen, J., Kerkhof, M., Heinrich, J., Bellander, T., Brunekreef, B. 2002. Air pollution from traffic and the development of respiratory infections and asthmatic and allergic symptoms in children. *American Journal of Respiratory and Critical Care Medicine* 166, 1092 – 1098
- Brimblecombe, P. 1986. Air composition and chemistry. Cambridge University Press
- Brimblecome, P., Bowler, C. 2002. The history of air pollution in York, England. *Journal of Air and Waste Management Association* 42, 1562 – 1566
- Brimblecombe, 1988. The big smoke: A history of air pollution in London since mediaeval times. Routledge, London
- Carpenter, L. J. Clemitshaw, K. C., Burgess, R. A., Penkett, S. A., Cape, J. N., McFadyen, G. G. 1998. Investigation and evaluation of the NO<sub>x</sub>/O<sub>3</sub> photochemical steady state. *Atmospheric environment* 32, 3353 – 3365
- Carruthers, D.J. Holroyd, R.J., Hunt, J.C.R., Weng, W.S., Robins, A.G. Apsley, D.D., Thompson, D.J., Smith, F.B. 1994. UK-ADMS: A new approach to modelling dispersion in the earth's boundary layer. *Journal of Wind Engineering and Industrial Aerodynamics* 52, 139 – 153
- Carruthers, D.J., Edmunds, H., Lester, A.E., McHugh, C.A., Singles, R.J. 1997. Use and validation of ADMS-Urban in contrasting urban and industrial locations. 5<sup>th</sup> International Conference on Harmonisation within Atmospheric Dispersion Modelling for regulatory purposes, 360 – 367



- Carruthers, D.J., Edmunds, H.A., Lester, A.E., McHugh, C.A., and Singles, R.J. 1998. Use and Validation of ADMS-Urban in contrasting Urban and Industrial Locations. *International Journal of Environment and Pollution*, 14, Nos. 1 – 6
- Carslaw, N., Carpenter, L.J., Plane, J.M.C., Allan, B.J., Burgess, R.A., Clemitshaw, K.C., Penkett, S.A. 1997. The simultaneous observation of nitrate and peroxy radicals in the marine boundary layer at night. *Journal of Geophysical Research-Atmospheres* 102, 18917 – 18933
- Carslaw, N., Carslaw, D. 2001. The Gas phase chemistry of urban atmospheres. *Surveys in Geophysics* 22, 31 – 53
- Carslaw, D.C., Beevers, S.D. 2004a Investigating the potential importance of primary NO<sub>2</sub> emissions in a street canyon. *Atmospheric Environment* 38, 3585 – 3594
- Carslaw, D.C., Beevers, S.D. 2004b New Directions: Should road vehicle emissions legislation consider primary NO<sub>2</sub>? *Atmospheric Environment* 38, 1233 – 1234
- Carslaw, D.C. 2005. Evidence of an increasing NO<sub>2</sub>/NO<sub>x</sub> emissions ratio from road traffic emissions. *Atmospheric Environment* 39, 4793 – 4802
- Carslaw, D.C., Beevers, S.D. 2005a Estimations of road vehicle primary NO<sub>2</sub> exhaust emission fractions using monitoring data in London. *Atmospheric Environment* 39, 167 – 177
- Carslaw, D.C., Beevers, S.D. 2005b. Development of an urban inventory for road transport emissions of NO<sub>2</sub> and comparison with estimates derived from ambient measurements. *Atmospheric Environment* 39, 2049 – 2059
- Carslaw, D.C., Beevers, S.D., Ropkins, K., Bell, M.C. 2006. Detecting and quantifying aircraft and other on-airport contributions to ambient nitrogen oxides in the vicinity of a large international airport. *Atmospheric Environment* 40, 5424 – 5434
- Carslaw, D. C., Beevers, S. D., Tate, J. E., 2007. Modelling and assessing trends in traffic-related emissions using a generalized additive modelling approach. *Atmospheric Environment* 41, 5289 – 5299
- Carslaw, D.C., Carslaw, N. 2007. Detecting and characterising small changes in urban nitrogen dioxide concentrations. *Atmospheric Environment* 41, 4723 – 4733
- Cambridge Environmental Research Consultants (CERC). 2006a. ADMS-Urban: An urban air quality management system. User Guide. Cambridge Environmental Research Consultants Ltd. <http://www.cerc.co.uk>
- Cambridge Environmental Research Consultants (CERC). 2006b. EMIT: Atmospheric emissions inventory toolkit user guide. Version 2.2. Cambridge Environmental Research Consultants Ltd. <http://www.cerc.co.uk>
- Clench-Aas, J., Bartonova, A., Klaeboe, R., Kolbenstvedt, M. 2000. Oslo traffic study-part 2: quantifying effects of traffic measures using individual exposure modelling. *Atmospheric Environment* 34, 4737–4744.
- Davis, J.M., Speckman, P. 1999. A model for predicting maximum and 8h average ozone in Houston. *Atmospheric Environment* 33, 2487 – 2500
- Department of Health. 1997. Air and Health. Department of Health and WHO
- Department of the Environment. 1995. Expert Panel on Air Quality Standards: Particles. HMSO
- DETR, 2000. The Air Quality Strategy for England, Scotland, Wales and Northern Ireland. HMSO
- Department for Environment, Food and Rural Affairs. 2003. The Air Quality Strategy for England, Scotland, Wales and Northern Ireland: Addendum, 2003. HMSO
- Department for Environment, Food and Rural Affairs, 2004. An evaluation of the air quality strategy. HMSO



- Department for Environment, Food and Rural Affairs. 2006. The Air Quality Strategy for England, Scotland, Wales and Northern Ireland. A consultation document on options for further improvements in air quality. HMSO
- Derwent, R.G., Jenkin, M.E., Saunders, S.M., 1996. Photochemical ozone creation potentials for a large number of reactive hydrocarbons under European conditions. *Atmospheric Environment* 30, 181 – 199
- Derwent, R. G. and D. R. Middleton. 1996. An empirical function for the ratio of  $\text{NO}_x$ :  $\text{NO}_2$ . *Clean Air* 26, 57 – 59
- Dixon, N.S., Boddy, J.W.D., Smalley R.J., Tomlin. A.S. 2006. Evaluation of a turbulent flow and dispersion model in a typical street canyon in York, UK. *Atmospheric Environment* 40, 958 – 972
- Emmerson K.M., Carslaw, N., Carpenter, L.J., Heard, D.E., Lee, J.D., Pilling, M.J. 2005. Urban Atmospheric Chemistry during the PUMA campaign 1: Comparison of modelled OH and  $\text{HO}_2$  concentrations with measurements. *Journal of Atmospheric Chemistry* 52, 143 – 164
- Fujita, E.M., Stockwell, W.R., Campbell, D.E., Keislar, R.E. 2003. Evolution of the magnitude and spatial extent of the weekend ozone effect in California's South Coast air basin, 1981-2000. *Journal of Air and Waste Management Association* 53, 802 – 815
- Fenger, J. (1999). Urban air quality. *Atmospheric Environment* 33, 4877 – 4900
- Ferrari, C.P., Kalunzy, P., Roche, A., Jacob, V., Foster, P. 1998. Aromatic hydrocarbons and aldehydes in the atmosphere of Grenoble, France. *Chemosphere* 37, 1587 – 1601
- Fewster, R.M., Buckland, S.T., Siriwardena, G.M., Baillie, S.R., Wilson, J.D. 2000. Analysis of population trends for farmland birds using generalised additive models. *Ecology* 81, 1970 – 1984
- Fiester, U., Balzer K. 1991. Surface ozone and meteorological predictors on a subregional scale. *Atmospheric Environment* 25, 1781 – 1790
- Fiore, A.M, Jacob, D.J., Logan, J.A. and Yin, J.H., 1998. Long-term trends in ground level ozone over the contiguous United States, 1980–1995. *Journal of Geophysical Research* 103, 1471 – 1480
- Finlayson-Pitts, B.J., Pitts, J.N. 1997. Tropospheric air pollution: ozone, airborne toxics, polycyclic aromatic hydrocarbons and particles. *Science* 276, 1045 – 1051
- Finlayson-Pitts, B.J., Pitts, J.N. 2000. Chemistry of the upper and lower atmosphere. Academic Press Inc. (London) Ltd
- Gardner, M.W., Dorling, S.R. 1999. Neural network modelling and prediction of hourly  $\text{NO}_x$  and  $\text{NO}_2$  concentrations in urban air in London. *Atmospheric Environment* 33, 709 – 719
- Gardner, M.W., Dorling, S.R. 2000. Meteorologically adjusted trends in UK daily maximum surface ozone concentrations. *Atmospheric Environment* 34, 171 – 176
- Gardner, M.W., Dorling, S.R. 2000. Statistical surface ozone models: an improved methodology to account for non-linear behaviour. *Atmospheric Environment* 34, 21 – 34
- Gerboles, M., D. Rembges, C. Brun and F. Lagler 2002. Uncertainty of  $\text{NO}_2$  measurements by chemiluminescence: a case study at the JRS AIRMON station and discussion of the quality objective of the  $\text{NO}_2$  European Directive: EUR 20381 EN
- Grosjean, D. and J. Harrison. 1985. Response Of Chemi-Luminescence  $\text{NO}_x$  Analyzers And Ultraviolet Ozone Analyzers To Organic Air-Pollutants. *Environmental Science & Technology* 19, 862 – 865
- Guardani, R., Nasciemento, C.A.O., Guardani, M.L.G., Martins, M.H.R.B., Romano, J. 1999. Study of atmospheric ozone formation by means of neural network-based model. *Journal of Air and Waste Management Association* 49, 1342-1346



Greater London Authority. 2002. 50 years on: The struggle for air quality in London since the great smog of December 1952. Great London Authority

Hall, D.J., Spanton, A.M., Dunkerley, F., Bennett, M., Griffins, R.F. 2000. An inter-comparison of the AERMOD, ADMS and ISC Dispersion Models for Regulatory Applications. R&D Technical Report. Environment Agency

Hanna, S.R., Egan, B.A., Purdum, J., Wagler, J. 1999. Evaluation of ISC3, AERMOD and ADMS dispersion models with the Optex, Duke Forest, Kincaid, Indianapolis and Lovett Field data sets. Proceedings of the 6<sup>th</sup> International Conference on harmonisation within atmospheric dispersion models. Rouen, France 11-14 October, 1999

Harrison, R.M. 2001. Pollution: cause, effects and control. The Royal Society of Chemistry.

Harrison, R.M. 2006. An introduction to pollution science. The Royal Society of Chemistry.

Hastie, T.J., Tibshirani, R.J. 1990. Generalised additive models. London, Chapman and Hall.

Heikkinen, R.K., Luoto, M., Kuussaari, M., Toivonen, T. 2007. Modelling the spatial distribution of a threatened butterfly: Impacts of scale and statistical technique. *Landscape and Urban Planning* 79, 347 – 357

Hoek, G., Brunekreef, B., Goldbohm, S., Fischer, P., van den Brandt, P.A. 2002. Association between mortality and indicators of traffic-related air pollution in the Netherlands: a cohort study. *Lancet* 360, 1203 – 1209

Holland, D.M., De Oliveria, V., Cox, L.H., Smith, R.L., 2000. Estimation of regional trends in sulphur dioxide over the Eastern United States. *Environmetrics* 11, 373 – 393

Huang, L., Smith, R. 1999. Meteorologically-dependent trends in urban ozone. *Environmetrics* 10, 103 – 118

Jacobson, M.Z. 1999. Fundamentals of atmospheric modelling. Cambridge University Press.

Jenkin, M. E., Clemitshaw, K.C. 2000. Ozone and other secondary photochemical pollutants: chemical processes governing their formation in the planetary boundary layer. *Atmospheric Environment* 34, 2499 – 2527

Jenkin, M. E. 2004a. Analysis of sources and partitioning of oxidant in the UK-Part 1: the NO<sub>x</sub> - dependence of annual mean concentrations of nitrogen dioxide and ozone. *Atmospheric Environment* 38, 5117 – 5129

Jenkin, M. E. 2004b. Analysis of sources and partitioning of oxidant in the UK--Part 2: contributions of nitrogen dioxide emissions and background ozone at a kerbside location in London. *Atmospheric Environment* 38, 5131 – 5138

Jo, W.K., Yoon, I.H., Nam, C.W. 2000. Analysis of air pollution in two major Korean cities: trends, seasonal variations, 1-hour maximum versus other hour-based concentrations and standard exceedences. *Environmental Pollution* 110, 11 – 18

Kan, H., London, S.J., Chen, G., Zhang, Y., Song, G., Zhao, N., Jiang, L., Chen, B. 2007. Differentiating the effects of fine and coarse particles on daily mortality in Shanghai, China. *Environment International* 33, 376 – 384

Klemm, O., Ziomas, I.C., Balis, D., Supan, P., Slemr, J., Romero, R., Vyras, L.G. 1998. A summer air-pollution study in Athens, Greece. *Atmospheric Environment* 32, 2071 – 2087

Kunzli, N., Kaiser, R., Medina, S., Studnicka, M., Chanel, O., Filliger, P., Herry, M., Horak Jr., F., Puybonnieux-Textier, V., Quenel, P., Schneider, J., Seethaler, R., Vergnaud, J.-C., Sommer, H. 2000. Public-health impact of outdoor and traffic-related air pollution: a European assessment. *The Lancet* 356, 795 – 801



- Kurtenbach, R., K. H. Becker, J. A. G. Gomes, J. Kleffmann, J. C. Lorzer, M. Spittler, P. Wiesen, R. Ackermann, A. Geyer and U. Platt 2001. Investigations of emissions and heterogeneous formation of HONO in a road traffic tunnel. *Atmospheric Environment* 35, 3385 – 3394
- Larrieu, S., Jusot, J-F., Blanchard, M., Prouvost, H., Declercq, C., Fabre, P., Pascal, L., Tertre, A. L., Wagner, V., Rivière, S., Chardon, B., Borrelli, D., Cassadou, S., Eilstein, D., Lefranc, A. 2007. Short term effects of air pollution on hospitalizations for cardiovascular diseases in eight French cities: The PSAS program. *Science of the Total Environment* 387, 105 – 112
- Leighton, P. A. 1961. *Photochemistry of Air Pollution*. New York, Academic Press
- Monks, P. 2000. A review of the observations and origins of the spring O<sub>3</sub> maximum. *Atmospheric Environment* 34, 3545 – 3561
- Naess, Ø., Nafstad, P., Aamodt, G., Claussen, B., Rosland, P. 2006. Relation between concentration of air pollution and cause-specific mortality: Four-year exposures to Nitrogen dioxide and particulate matter in 470 neighbourhoods in Oslo, Norway. *American Journal of Epidemiology* 165, 435 – 443
- NSCA 1999. *Pollution Handbook*. National society for Clean Air and Environmental Protection.
- NSCA 2002. *Clean Air Revolution: 1953-2025. Marking 50 years since the great London Smog*. Clean Air and Environmental Protection 32, No 4
- O'Neill, M.S., Loomis, D., Borja-Aburto, V.H. 2004. Ozone, area social conditions, and mortality in Mexico City. *Environmental Research* 94, 234 – 242
- Paramesh, H. 2002. Epidemiology of asthma in India. *Indian Journal of Paediatrics* 69, 309 – 312
- Pope III, C. A., Burnett, R.T., Thun, M.J., Calle, E.E., Krewski, D., Ito, K., Thurston, G.D. 2002. Lung Cancer, Cardiopulmonary Mortality, and Long-term Exposure to Fine Particulate Air Pollution. *The Journal of the American Medical Association* 287, 1132 – 1141
- PORG, 1997. *Ozone in the United Kingdom. Fourth report of the UK photochemical oxidants review group*. London, Department of the Environment, Transport and the Regions
- Qian, Z., He, Q., Lin, H., Kong, L., Liao, D., Dan, J., Bently, C.M., Wang, B. 2007. Association of daily cause-specific mortality with ambient particle air pollution in Wuhan, China. *Environmental Research* 105, 380 – 389
- R Development Core Team. 2006. *R: A language and environment for statistical computing*. R Foundation for Statistical Computing, Vienne, Austria. URL <http://www.R-project.org>
- Reiss, R. 2006. Temporal trends and weekend-weekday differences for benzene and 1,3 butadiene in Houston, Texas. *Atmospheric Environment* 40, 4711 – 4724
- Samoli, E., Aga, E., Touloumi, G., Nisiotis, K., Forsberg, B., Lefranc, A., Pekkanen, J., Wojtyniak, B., Schindler, C., Niciu, E., Brunstein, R., Dodic Fikfak, M., Schwartz, J., Katsouyanni, K. 2006. Short-term effects of nitrogen dioxide on mortality: an analysis within the APHEA project. *European Respiratory Journal* 27, 1129 – 1138
- Schlink, U., Herbarth, O., Richter, M., Dorling, S., Nunnari, G., Cawley, G., Pelikan, E. 2006. Statistical models to assess the health effects and to forecast ground-level ozone. *Environmental Modelling and Software* 21, 547 – 558
- Schreffler, J.H., Barnes, H.M. 1996. Estimation of Trends in Atmospheric Concentrations of Sulfate in the Northeastern United States. *Journal of the Air & Waste Management Association* 46, 621 – 630
- Schwartz, J., 1994. Air pollution and daily mortality: A review and Meta Analysis. *Environment Research* 64, 36 – 52
- Segala, C., Poizeau, D., Mesbah, M., Willems, S., Maidenbergh, M. 2008. Winter air pollution and infant bronchiolitis in Paris. *Environmental Research* 106, 96 - 100



- Shi, J.P., Harrison, R.M. 1997. Rapid NO<sub>2</sub> formation in diluted petrol-fuelled engine exhaust – a source of NO<sub>2</sub> formation in winter smog episodes. *Atmospheric Environment* 31, 3857 – 3866
- Siriwardena, G.M., Baillie, S.R., Buckland, S.T., Fewster, R.M., Marchant, J.H., Wilson, J.D. 1998. Trends in the abundance of farmland birds: a quantitative comparison of smoothed Common Birds Census indices. *Journal of Applied Ecology* 35, 24 – 43
- Smith, N., Plane, J.M.C., Nien, C-F., Solomon, P. 1995. Nighttime radical chemistry in the San Joaquin Valley. *Atmospheric Environment* 29, 2887 – 2897
- Solomon, G.M., Balmes, J.R. 2003. Health effects of diesel exhaust. *Clinics in Occupational and Environmental Medicine* 3, 61 – 80
- Sommariva, R., Haggerstone, A.-L., Carpenter, L. J., Carslaw, N., Creasey, D. J., Heard, D. E., Lee, J. D., Lewis, A. C., Pilling, M. J., Z'ador, J. 2004. OH and HO<sub>2</sub> chemistry in clean marine air during SOAPEX-2. *Atmosphere Chemistry Physics* 4, 839 – 856
- Suárez-Seoane, S., Osborne, P.E., Alonso, J.C. 2002. Large-Scale Habitat Selection by Agricultural Steppe Birds in Spain: Identifying species-habitat responses using generalized additive models. *The Journal of Applied Ecology* 39, 755 – 771
- Thompson, M.L., Reynolds, J., Cox, L.H., Guttorpl, P., Sampson, P.D. 2001. A review of statistical methods for the meteorological adjustment of tropospheric ozone. *Atmospheric Environment* 35, 617 – 630
- Van Vliet, D. 1982. SATURN – a modern assignment model. *Traffic Engineering and Control* 23, 578 – 581
- Venkatram, A., P. Karamchandani, P. Pai and R. Goldstein 1994. The Development And Application Of A Simplified Ozone Modelling System (Soms). *Atmospheric Environment* 28, 3665 – 3678
- Winor, A. M., J. W. Peters, J. P. Smith and J. N. Pitts. 1974. Response Of Commercial Chemiluminescence NO-NO<sub>2</sub> Analyzers To Other Nitrogen-Containing Compounds. *Environmental Science & Technology* 8, 1118 – 1121
- World Health Organisation (WHO). 1997. World Health's Organisation's Environmental Health Criteria 188. Nitrogen Oxides, WHO
- Wood, S.N., Augustin, N. H., 2002. GAMs with integrated model selection using penalised regression splines and applications to environmental modelling. *Ecological modelling* 157, 157 – 177
- Wood, S.N. 2006. Generalised additive models: An introduction with R. Chapman and Hall/CRC
- Yu, K.N., Cheung, Y.P., Cheung, T., Henry, R.C. 2004. Identifying the impact of large urban airports on local air quality by nonparametric regression. *Atmospheric Environment* 38, 4501 – 4507
- Zheng, J., Swall, J.L., Cox, W.M., Davis, J.M., 2007. Inter-annual variation in meteorologically adjusted ozone levels in the eastern United States: a comparison of two approaches. *Atmospheric Environment* 41, 705-716